NAS 9-12083
DRL-12, DRD-MA-129T
LMSC-D152738

VOLUME I
FINAL REPORT

SPACE SHUTTLE THERMAL PROTECTION SYSTEM DEVELOPMENT

17 January 1972

National Aeronautics and Space Administration
Manned Spacecraft Center
Houston, Texas

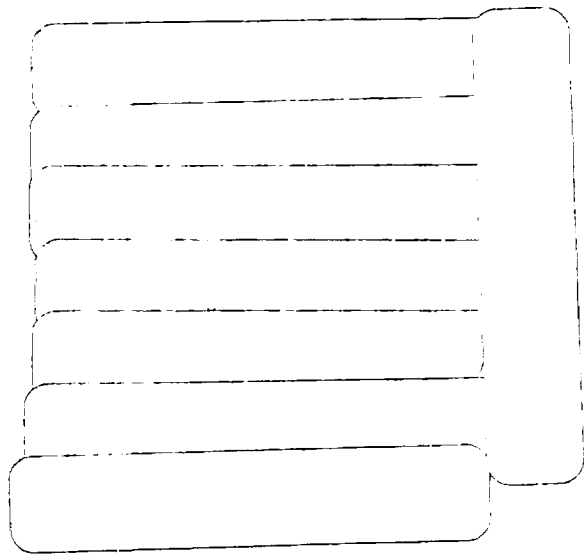

LOCKHEED MISSILES & SPACE COMPANY

ABSTRACT/FOREWORD

This final report presents the results of NASA Contract NAS 9-12083, "Space Shuttle Thermal Protection System Development" performed by Lockheed Missiles and Space Company, Inc. for the National Aeronautics and Space Administration, Manned Spacecraft Center, under the direction of the Thermal Technology Branch of the Structures and Mechanics Division, D. J. Tillian, COR.

The contract objective was to establish materials and design technology of the LMSC all-silica LI-1500 rigid surface insulation (RSI) thermal protection system (TPS) concept for the Shuttle spacecraft. All results of contract development efforts to satisfy this objective are documented. Descriptions and results of mechanical, thermophysical, and environmental testing are reported. Various concepts of attachment and strain isolation are presented. Descriptions of analytical sizing and design procedures are presented in a manner formulated to allow competent engineering organizations to perform rational design studies. Results of parametric studies involving material and system variables are reported. Design criteria, detail analysis, and resulting designs are shown for specific TPS point design problems. Descriptions of test hardware delivered to NASA/MSC for test evaluation are provided. Material performance and design data are also delineated.

Areas requiring additional development effort are discussed and the conclusion drawn that no problems are foreseen that cannot be solved within the present NASA Shuttle time span. Based on the results of this contract effort, LMSC considers the LI-1500 TPS to be sufficiently well developed to warrant consideration of being used on the first shuttle flight vehicle.

Pages ii, iii, and iv are blank.

CONTENTS

Preceding page blank

ESTABLISHED MAJOR LI-1500 ATTRIBUTES

- LOW CONDUCTIVITY
- LOW COEFFICIENT OF THERMAL EXPANSION
- THERMAL SHOCK PROOF
- IMPROVED HIGH EMITTANCE COATING
- OVERSHOOT CAPABILITY TO 3000°F
- ONE-HUNDRED 2500°F MISSION CAPABILITY, DOUBLY PERTURBED 1100-NM CROSSRANGE TRAJECTORY
- ON-LINE MANUFACTURING, READILY AVAILABLE RAW MATERIAL
- LOWEST WEIGHT REUSABLE TPS
- LOWEST SHUTTLE PROGRAM COST TPS

SUMMARY

The basic objectives of this contract were to establish materials and design technology of the LMSC all-silica LI-1500 rigid surface insulation TPS concept for the Shuttle spacecraft. These objectives have been satisfied through implementation of the Program Plan (LMSC-A991130) submitted to NASA/MSC on 16 July 1971.

An extensive effort was performed to develop the design methodology required for Shuttle TPS design. Parametric investigations were performed and sensitivities to material and geometrical variables were established. These relationships were used in a parametric approach to specific design problems. An existing two-dimensional finite element program was modified to improve accuracy and perform design analysis. Capability was established to analyze both isotropic and orthotropic materials. A three-dimensional finite element program was used to verify the 2-D analysis and perform specific design analyses. The 3-D program results were used to modify the 2-D modeling techniques, and close correlation has been established. The 3-D program was also used to evaluate the coating stresses along tile sides with large thermal gradients. As predicted, the LI-1500 low coefficient of thermal expansion precludes high stresses due to such gradients. Numerous variations in attachment schemes were evaluated for LI-1500 and yielded promising results.

The majority of the design effort was oriented to provide designs of four prototype panels to specific requirements provided by NASA/MSC. A non-linear beam-column computer analysis has been perfected for optimum weight design. Thermal/structural optimizations, including the heat sink effect of the bond, have been performed for 16 separate designs. The resulting designs are approximately the same weight as an ablative TPS but total shuttle program costs are reduced by a minimum of $200 million. These designs have also been compared with metallic heat shields, and the results indicate both substantial weight savings and reduced costs with the use of the LI-1500.

A new coating that was developed under the Material Improvement Contract (NAS 9-12137) was baselined for the LI-1500 system in October. This coating utilizes a Silicone Carbide emittance agent and has been designated 0042. A series of 100 radiant test cycles was successfully performed; each 2800-second cycle included a 150-second dwell at 2500°F. During the entire 100 test cycles, the coating surface was exposed to 2500°F for 4 hours, temperatures above 2300°F for 14 hours, and temperatures above 2000°F for 28 hours. Repeatability of the measured in-depth thermocouple data during this test series verified the thermal stability of LI-1500.

A failure theory that is based on linear interaction of biaxial stresses has been partially developed by test.

Various attachment schemes have been investigated to develop strain isolation techniques. LMSC has currently baselined direct bonding with the use of commercially available RTV-560 adhesive. The unique properties of LI-1500 allow sufficient strain isolation with a 0.090-in. bondline thickness for the prototype panels.

Thermophysical and mechanical tests have been performed on as-fabricated and oven-cycled material. Thermal conductivity measurements have been made at various temperatures and pressures. The conductivity is essentially the same as previously reported and the adequancy of design values have been established by data correlations in 1-atmosphere radiant tests and in low-pressure arc-jet tests. The thermal coefficient of expansion was determined to be 3×10^{-7} in./in/°F as reported in previous evaluations. Specific heat values are also unchanged. Emittance tests on the 0042 coating indicated total normal emittance of 0.89 at room temperature and 0.93 at 2000°F. Measurements of the 0042 coating thermal coefficient of expansion indicate values compatible with those of LI-1500, about 4×10^{-7} in./in./°F at 1100°F.

Tension, compression, and shear properties were measured in the parallel- and normal-to-fiber orientation direction. The material exhibits orthotropic properties, the tension modulus being ten times greater in the parallel-to-fiber direction than the normal-to-fiber orientation. Tests on thermally cycled materials indicated some decrease in strength, which does not influence design. High temperature tests have indicated that a brittle-ductile transition point occurs at about 2160°F. Mechanical properties of both the 0025 and 0042 coatings have been measured. Current strengths are more than adequate for rational designs of the Space Shuttle TPS.

Radiant heat in combination with low pressures on a 6 x 24 in. panel have been successfully performed. Radiant tests of three joint concepts were inconclusive. Joint concepts must be evaluated in a convective environment. Instrumented joint gap and mismatch models have been tested by NASA/MSC, but resulting data are not yet available. Thirty days of hard vacuum exposure had no effect on LI-1500. Infrared transmittance tests indicate that there is no transmission greater than 0.1 percent on both the 0042 coating and LI-1500 from wavelengths of 1.5 to 20 microns.

Coated LI-1500 specimens have been subjected to various moisture environments and then frozen and thawed at temperatures up to 1000°F with no discernible damage. Specimens cooled to -150°F and subjected to a radiant heat reentry environment showed no detectable damage. Rain erosion tests at 10° angle of attack and 350 mph experienced no detectable damage. Specimens with and without waterproofing exposed to 50-, 75- and 95-percent relative humidity showed minimal moisture pickup and no detectable degradation after ascent/entry thermal/pressure tests. Specimens exposed to rain performed equally well, with the exception of one specimen (without waterproofing) that absorbed a large amount of water through the uncoated sides. During an ascent/entry thermal/pressure test, small areas of the coating were lost. These failures, however, were not of a magnitude that would affect reentry thermal performance.

Specimens were exposed to 3000°F surface temperature radiant tests to evaluate overshoot capability. Although some surface slumping occurred, the coating integrity and basic heat shielding capability was retained. This test demonstrated that one reentry with lower surface temperatures reaching 3000°F could be sustained by the system without catastrophic failure of the orbiter vehicle. (Analysis indicates the structural temperature would not exceed 310°F at touchdown.)

A newly developed (NAS 9-12137) all-silica closure strip material, FI-600 (flexible insulation- 6 pcf), was tested in both thermal and acoustic environments. This material showed no discernible degradation and has been incorporated in the deliverable prototype panels.

Four prototype panels have been designed, fabricated, and delivered to NASA/MSC for test and evaluation. The first panel is a beryllium subpanel with 12 x 12 x 1.25-in. tiles. Two aluminum panels have been delivered with 6 x 6 x 2.50-in. tiles and 6 x 6 x 1.4-in tiles for separate vehicle primary structure applications. The fourth panel is a titanium primary structure panel with 6 x 6 x 1.35-in. tiles.

A total of 83 acceptable 12 x 12 x 2-in. tiles were fabricated under this program. These tiles have been used for contract testing, for deliverable test specimens to various agencies, and for the prototype panels.

CONCLUSIONS

GENERAL

- Based on LMSC tests and analysis, LI-1500 is sufficiently well developed to be baselined as the thermal protection system for the first Shuttle vehicle.
- LI-1500 TPS is indicated to be the lightest reusable system for the Shuttle.
- LI-1500 TPS is indicated to be the most economical system for the Shuttle.

MATERIAL

- A new improved waterproof coating system (0042) has been developed.
- A new flexible joint material (FI-600) has been developed.

TESTING

- Based on thermal tests, LI-1500/coating system has 100-mission reuse capability to 2500°F.
- LI-1500/coating system has overshoot capability to 3000°F.
- Thermal performance of LI-1500 does not degrade with reuse.
- LI-1500 is thermal shock resistant.
- LI-1500 has lowest RSI conductivity.
- Thermal conductivity is pressure dependent.
- Thermal conductivity design curves for high and low pressure have been validated.
- LI-1500 has the lowest RSI thermal expansion $\sim 3 \times 10^{-7}$ in./in./°F.
- 0042 coating thermal expansion is compatible with LI-1500 thermal expansion.
- 0042 coating emittance is high ~0.90 total normal.
- LI-1500 is orthotropic.
- Strength reduced slightly near heated surface with reuse – no design impact.
- Strength increases with temperature to brittle-ductile transition point.
- Long term vacuum has no effect.
- Freeze-thaw cycles have no effect.

- Cold soak (-150°F) followed by reentry heat pulse has no effect.
- Less than 0.1 percent infrared transmission (1.5 to 20 microns).
- No rain erosion – 10° angle of attack, 350 mph, 5 min. at 1.1 in. rain/hr.
- High water content on non-waterproofed tiles during ascent/reentry thermal/pressure environment can cause minor coating loss - no effect on heat shielding capability.

DESIGN

- LMSC has developed a rational design methodology.
- Fine-mesh, double-precision finite element codes utilizing orthotropic solid elements are required for RSI stress analysis.
- Orthotropic LI-1500 properties should be incorporated for rational design/analysis.
- Possibility of combined stress failure mode of RSI recognized.
- Experimental results validate analysis techniques.
- Substrate should be designed for no skin buckling in absence of valid test data on effect of buckled skin design on RSI.
- Heat sink effect of bond results in lower TPS system weight than mechanical fasteners.
- Bond weight not a significant driver on lower surface.
- Bond weight is a major driver on upper surface.
- Mechanical fasteners show promise.
- Primary panel structure optimized with non-linear beam-column analysis.
- Z-stiffeners optimum for panel designs compared with other configurations of similar cost/manufacturing complexity.
- Panel designs should be based on thermal/structural optimization.
- Strain arrestor plate can offer strain isolation at -200°F orbital cold soak condition as well as allowing use of larger tiles.
- Coating stresses well within allowables, even on sides of tile.
- Discontinuous bond between tiles keeps LI-1500 stress levels down.
- Low density filler block in baseline joint does not perturb LI-1500 temperature distribution appreciably.

- Preliminary analysis indicates lightweight core concept shows no advantage.
- Textured and discontinuous coatings offer no advantage.
- Beryllium subpanel concept with direct-bonded LI-1500 leads to largest (12 x 12 in.) tile size.
- LMSC has feasible refurbishment scheme for bonded tiles.
- Reduced conductivity of LI-1500 under reentry pressure environment results in lighter TPS system than competitive materials.
- Low LI-1500 coefficient of expansion limits thermal stresses and reduces required external gaps.

RECOMMENDATIONS

LMSC considers the LI-1500 TPS sufficiently well developed to be baselined for the first orbital Shuttle vehicle. This contract has demonstrated the potential capability of LI-1500 to satisfactorily operate within the Shuttle environment. However, numerous questions remain to be answered prior to application to the first vehicle. LMSC recommends that NASA immediately proceed with the RSI Phase III development effort with particular emphasis on the following:

- Prepare a definitive program plan to ensure proper interface and consistent data requirements schedule with the Shuttle Phase C/D Orbiter contractor.
- Develop and test alternate attachment methods with emphasis on reliability, ease/cost of application and replacement, and ability to survive cold soak conditions (-200°F).
- Develop refined mechanical test methods and generate statistical design properties including development of a failure theory through combined property testing.
- Perform convective testing and analytical evaluation of gaps and joints including use of calorimeter models to assess the resulting effects. Convective tests should also be performed on models containing both LI-1500 and upstream units of leading edge materials to assess any adverse effects.
- Continue definition of thermophysical properties under cyclic heating and environmental conditions.
- Continue evaluation of environmental effects on RSI performance such as salt, atmospheric conditions, and propellant contamination.
- Further define expected Shuttle environment based on final Phase B efforts, including various planned missions and abort conditions.
- Continue material improvement efforts with emphasis on coatings, waterproofing, and in-place refurbishment capability.
- By test and analysis, define RSI failure modes, damage tolerance, and accept/reject criteria for application and refurbishment.
- Update design criteria as influenced by Phase B studies and planned Shuttle missions.
- Perform arc-jet tests to establish ultimate temperature capability.
- Continue design methods development and prepare a "preliminary design" handbook.

- By analysis and test, define the interaction between the RSI and structural components.
- Continue non-destructive evaluation (NDE) investigations with emphasis on scale-up required for Shuttle turnaround requirements.
- Perform detail designs of non-configuration dependent vehicle areas – doors, cutouts, chines.
- Continue cost evaluation to define funding required for the Shuttle TPS program.
- Formulate a definitive plan to manrate the LI-1500 TPS prior to first orbital flight.

LMSC also recommends that NASA initiate a separate effort to review existing flight vehicles to determine the feasibility of performing flight tests. A plan should be generated for obtaining "piggy back" flight test experience (or other economical measures) with LI-1500 which would provide simulation of one or more of the following characteristics of the Shuttle design reentry aerodynamic heating environment:

- Convective heat rate vs time
- Convective heat rate vs Mach number and Reynolds number
- Laminar boundary layer heating pulse
- Turbulent boundary layer heating pulse
- Boundary layer thickness vs gap and joint mismatch dimensions
- Flight heat rate and enthalpy with and without candidate leading edge materials upstream of LI-1500.

INTRODUCTION

The basic objective of this contract was to establish materials and design technology of LI-1500 rigidized surface insulation. LMSC's approach to accomplishing this program objective was based on executing the following tasks as specified in the negotiated contract statement of work:

- Task 1.0 - Program Plan
- Task 2.0 - Design
  - 2.1 - Design Criteria, Environments and Requirements
  - 2.2 - Design Applications
- Task 3.0 - Material Optimization
- Task 4.0 - Property Characteristics
- Task 5.0 - Environmental Response Behavior
  - 5.1 - Material Substrate Evaluation
  - 5.2 - Design Details Evaluation
  - 5.3 - Specialized Environmental Tests
- Task 6.0 - Prototype Panels and Specimen Deliverables
  - 6.1 - Prototype Panels
  - 6.2 - Material Samples

Significant progress has been made under this contract in bringing the LI-1500 TPS into maturity. The contract objectives have been satisfied through design, analysis, test, and fabrication efforts under the respective tasks.

Per agreement with the COR, this document is being published in two volumes. Volume II reports the results of Task 2.0 - Design and presents the design methodology evolved for TPS design application. Volume I presents the results from the remaining tasks, including a summary of Task 2.0.

Personnel from all three LMSC divisions have contributed to the success of this program. The following individuals deserve special recognition in accomplishing the program objectives:

J. A. DeRuntz	- Task 2.0 Leader
R. P. Banas	- Task 4.0 Leader
D. R. Elgin	- Task 5.0 Leader
J. O. Donaldson	- Thermodynamics Testing
G. R. Cunnington, Jr.	- Thermophysical Tests
A. M. C. Holmes	- Mechanical Testing
Roger Perkins	- Mechanical Testing

Special recognition must be given to all members of the LI-1500 manufacturing facility and the Material Sciences Composite Laboratory under the direction of R. M. Beasley. In accomplishing the many testing activities, excessive demands were satisfied as to schedule and quantity of specimens. The related Material Improvement Program (NAS 9-12137) has contributed significantly to the success by providing the improved 0042 coating system and the FI-600 joint material. This program is directed by R. M. Beasley and Y. D. Izu.

Section 1

PROGRAM PLAN

LMSC presented the contractually required Program Plan (LMSC-A991130) to NASA/MSC on 16 July 1971. This plan conformed with the contract Data Requirements List (DRL) and the Data Requirements Description (DRD, MA-020T). The major topics presented in detail were:

- Program Description
- Management Procedures, Organization, and Facilities
- Detail Task Description and Related Manpower
- Program Phasing
- Technical Statement of Work
- Submittal of Data

LMSC's master schedule (Fig. 1-1) has been updated to reflect the actual delivery dates approved by the NASA/MSC COR through 17 February. All program milestones were met on the original schedule, prior to 4 October. At that time, LMSC exercised the option of extending the Midterm Report and prototype panel Critical Design Review (CDR) 1 month, as prescribed in the NASA twx received 29 September. This extension was offered to provide a maximum technology interchange between concurrent Development and Improvement Programs. As noted in the various sections of this report, a new improved coating system resulted from this extension.

Tasks related to the prototype panels were extended to reflect the 5-week period between 4 October and 12 November. Approval by NASA/MSC to proceed with fabrication of the panels was received 1 December 1971. Accordingly, delivery of the two aluminum panels has been extended to 17 February, and the titanium and

beryllium panel delivery has been extended to 28 February. The TPS cost report also has been extended to 28 February to reflect the requirement of accumulating actual panel fabrication costs. The final oral report has been extended to 17 February to coincide with first panel delivery. Per NAS/MSC directions, the final material sample delivery date has been extended to 1 March. Per agreement with the contract COR, the Design Methods Report is being published as Volume II of this report.

The Organization Chart (LMSC-A991223) required under this task was submitted to NASA/MSC under a separate cover on 30 July. LMSC'c management policy is to assign executive management responsibility for all programs to "line-of-business" managers reporting directly to a division General Manager. Because the thermal protection system is a critical subsystem for manned reentry vehicles, TPS work is managed as a major subsystem program within the Manned Space Program line-of-business. LMSC assigned prime responsibility for the NAS 9-12083 development program to the Thermal Protection Systems organization in the Manned Space Programs Office of the Space Systems Division. This organization has participated in all phases of LMSC'c Space Shuttle efforts and is intimately familiar with the requirements of the TPS. Individuals assigned to this project have assisted in both the development of LI-1500 and the past related contract activities. The key individuals continue to support the LI-1500 efforts under current LMSC Independent Development activities. The project organization and its position in the overall LMSC organization, including the line departments furnishing project support, have been shown in the Organization Chart document.

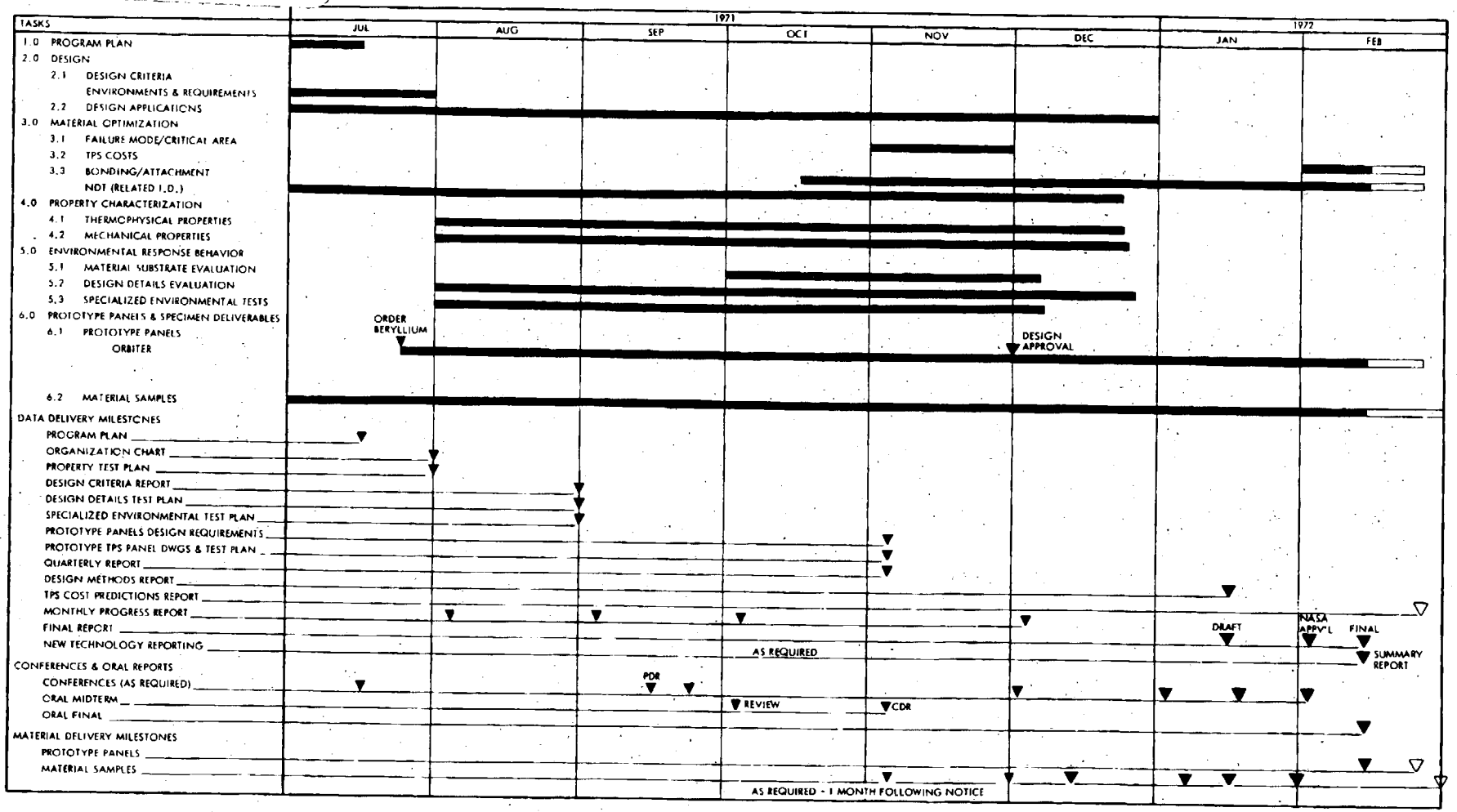

Fig. 1-1 Revised Master Schedule

Section 2
DESIGN

The development of rigidized surface insulation for shuttle application includes the establishment of rationale, methods of analyses, techniques, and design. This key contract task defines the criteria/methodology required for shuttle usage of LI-1500 RSI. The importance of this task and the magnitude of effort has caused LMSC to publish this final report in two volumes. Volume II concentrates on this task and provides a logical separation of the data presented in this final report. The contract specifies limited distribution of a Design Methods Report. With agreement of the COR, LMSC has elected to present this as Volume II, with the resulting larger distribution.

Design methodology developed by LMSC for the shuttle TPS, including analysis, verification, and design techniques, allows detailed definition of design applications of LI-1500. Although such methodology is applied to LMSC-developed RSI material in the design of four deliverable prototype panels, the design/analysis logic applies to other RSI material systems as well. This study has considered RSI for application to primary structure as well as subpanels. Optimization methods have been developed which result in minimum weight/cost systems that are refurbishable. Strength/stiffness requirements and failure criteria are identified for LI-1500 RSI system components and metallic substrate materials and configurations. Fastener concepts as well as tile bonding methods have been studied and textured coating systems evaluated.

Table 2-1 presents the LI-1500 design property values resulting from the work of this contract and used for the design of the prototype panels. Stress allowables shown are average values from a limited number of tests (generally four specimens, see Section 4 of this volume) which preclude a statistical interpretation of the data. In addition, since there is no clear precedent to follow in the mechanical testing of RSI materials used here, experimental techniques are still in a state of development. Hence this in itself is a source of scatter in the data. Since ultimate allowable stresses are used in conjunction with ultimate design loads, LMSC believes the approach of using average values

Table 2-1

LI-1500 INSULATION SYSTEM DESIGN PROPERTIES

(ROOM TEMPERATURE UNLESS OTHERWISE NOTED)

PROPERTY (ULTIMATE)		LI-1500 STRONG DIRECTION	LI-1500 WEAK DIRECTION	RTV-560 BOND	LI-0042 COATING	LI-0025 COATING
TENSION (PSI)		70	15	800	>2000	600
TENSILE MODULUS (PSI)		60,000	6,000	300	$<9.1 \times 10^6$*	3.5×10^6
COMPRESSION (PSI)		150	40	-	>2000	>>600
COMPRESSION MODULUS (PSI)		50,000	5,000	-	$<9.1 \times 10^6$*	3.5×10^6
SHEAR (PSI)		40	25	400	-	
SHEAR MODULUS (PSI)		20,000	4,000	100	$<3.7 \times 10^6$	1.4×10^6
		PARALLEL TO FIBER	PERPENDICULAR TO FIBER			
THERMAL EXPANSION (IN./IN./°F)		3.0×10^{-7}	3.0×10^{-7}	1.14×10^{-4}	2.0×10^{-7}**	2×10^{-7}
HEAT CAPACITY (BTU/LB-°F)	(RT)	0.15	0.15	0.30	-	
	(2000°F)	0.32	0.32	-		
THERMAL CONDUCTIVITY (BTU-IN./FT^2-HR-°F) ~1 ATMOSPHERE	(RT)	0.58	0.35	2.16	6.5	
	(2000°F)		1.56	-	14.2	
THERMAL CONDUCTIVITY (BTU IN./FT^2 HR-°F) ~ VACUUM	(RT)	0.31	0.17	-	6.5	
	(2000°F)		0.67		14.2	
EMITTANCE	(RT)	-	-	-	0.89	0.85
	(2000°F)	-	-	-	0.93	0.63

* LATEST TEST DATA INDICATE MODULUS VALUES OF APPROXIMATELY 1.9×10^6 PSI. VALUES IN TABLE USED IN ANALYSIS.

**LATEST TEST DATA INDICATE THERMAL EXPANSION COEFFICIENT OF APPROXIMATELY 4.0×10^{-7} IN./IN./°F VALUES IN TABLE USED IN ANALYSIS, EXCEPT WHERE NOTED

D05165

is acceptable, particularly in view of experimental verification testing reported in Section 2 of Volume II which indicates a measure of conservatism in the analyses.

Design methods and groundrules were established to carry out parametric studies and evaluate alternate design concepts. The impact of unique LI-1500 thermophysical properties on RSI panel design was ascertained and conclusions as to design validity have been drawn. Finally, cost and weight comparisons with competing TPS concepts have been made. These items are discussed in detail in Volume II of this report and are summarized here for continuity.

Design/Analysis Methods:

- RSI stress analysis requires fine-mesh, double-precision finite element codes.
- TPS design should utilize sophisticated 2-D and 3-D analysis techniques developed or modified specifically for RSI panels.
- Rational design/analysis should incorporate orthotropic LI-1500 properties.
- Combined stress-failure mode of RSI is recognized as a possibility.
- Experimental results validate analysis techniques.
- Design of substrate should incorporate no skin buckling in lieu of test data.

Optimization Studies:

- Heat sink effect of bond indicates lower TPS system weight than mechanical fasteners.
- Bond weight is not a significant driver on lower surface.
- Bond weight is a major driver on upper surface.
- Primary panel structure should be optimized, using nonlinear beam-column analysis.

- Zee-stiffeners are optimum for panel designs compared with other configurations of similar cost/manufacturing complexity.
- Panel designs should be based on thermal/structural optimization.

Design Details Evaluation:

- Orbital cold soak condition (-200^{o}F) negates strain isolation properties of RTV-560 leading to unacceptable LI-1500 stress levels.
- Strain arrestor plate can offer strain isolation at -200^{o}F orbital cold-soak condition as well as allowing use of larger tiles.
- Coating stresses are well within allowables, even on sides of tile.
- Discontinuous bond between tiles keeps LI-1500 stress levels down.
- Low-density filler block in baseline joint does not appreciably perturb LI-1500 temperature distribution.
- Based on preliminary studies, lightweight core concept shows no apparent advantage.
- Textured and discontinuous coatings offer no advantage.

Attachment Studies:

- Beryllium subpanel concept with direct-bonded LI-1500 leads to largest (12 in. x 12 in.) tile size.
- Mechanical fasteners show promise.
- LMSC has feasible refurbishment scheme for bonded tiles.

LI-1500 Advantages:

- Reduced conductivity of LI-1500 under reentry pressure environment results in lighter TPS system than competitive materials.
- Low LI-1500 coefficient of expansion limits thermal stresses and reduces required external gaps.
- Degradation effects on resulting RSI stress levels due to repeated thermal cycling of LI-1500 offer no problem.

Cost/Weight Comparisons:

- LI-1500 TPS system is indicated to be lighter and less costly than comparable metallic heatshield.
- LI-1500 TPS system is indicated to be less costly than ablative heat shield.

Section 3

MATERIALS OPTIMIZATION

Basic improvements and development of both the coating system and basic LI-1500 material are currently being pursued under the RSI Material Improvement Contract (NAS 9-12137). The results of this effort will be reported to NASA/MSC following contract completion in March of this year. Specific data from this improvement effort have been available for use under this contract, as reported in this and other sections. LMSC has demonstrated the reproducibility of the LI-1500/coating system by manufacturing a total of eighty-three 12 x 12 x 2 in. tiles under this contract. These tiles have been used in the various tasks as test specimens and NASA deliverable items. The remaining efforts under this task are discussed under the appropriate subsections. The costing effort has not been completed to date, since the prototype panel fabrication (Task 6.1) is still in process. As discussed in Section 1, the TPS Cost Report will be published separately, following completion of fabrication, cost data accumulation, and delivery to NASA/MSC.

3.1 COATING EVALUATION

At the start of this contract, the baseline coating was the 0025 Cr_2O_3 system used on tile No. TT-14B (delivered under Contract NAS 9-11222), which was tested by Battelle Memorial Institute. This interim coating system exhibited many undesirable qualities including apparent low emissivity, degradation with time, porosity, and cracking tendencies. Under NASA Contract NAS 9-12137, LMSC has developed an improved coating system, 0042. The most promising coating systems developed to date were subjected to an accelerated 100-cycle test program to evaluate possible usage on this contract.

3.1.1 Specimen Description

A 100-cycle test program was performed at LMSC to demonstrate the reusability and integrity of three improved surface coatings. Six specimens, two of each

surface coating, were tested. The specimens were nominally 4 x 4 x 2.45 in. and were coated on the top (heated) surface. The coatings were identified as follows: (1) an improved 0025 consisting of a borosilicate coating with a chrome oxide emittance agent and overglaze applied to specimens TT 42-1 and TT 42-2, (2) 0042 consisting of a borosilicate coating with a silicon carbide emittance agent and overglaze applied to specimens TT 42-5 and TT 42-6, and (3) an integral coating with a silicon carbide emittance agent applied to specimens TT 42-3 and TT 42-4.

3.1.2 Instrumentation

One specimen with each coating was instrumented with six thermocouples (one surface, three in-depth, and two substrate) and bonded with RTV 560 to a 0.125-in. aluminum substrate. Instrumentation locations are shown in Fig. 3.1-1. A pretest photograph of the test specimens is shown in Fig. 3.1-2.

3.1.3 Test Pulse

The testing was performed in LMSC's 1-ATM pressure radiant facility (HIRAD) shown in Fig. 3.1-3. This radiant facility can impose radiant heat rates up to 50 Btu/ft^2 sec on an area of 15 x 15 in.

The test environment imposed on the specimens is shown by the surface temperature history in Fig. 3.1-6. The test pulse simulates the surface temperature for Area 2 shown in Fig. 6.3-5,* with a 200°F temperature overshoot to 2500°F. This corresponds to an 1100-nm crossrange trajectory with a peak temperature perturbation from 2050°F to 2500°F. The heating duration is 50 min with 2.5 min at 2500°F.

The peak surface temperature was intentionally perturbed to 2500°F to evaluate the overshoot capability of the coatings and the LI-1500. The 0042 surface coating was designed to remain waterproof at peak temperatures up to 2300°F.

*Volume II of this report

THERMOCOUPLE LOCATION FOR LI-1500 TEST SPECIMENS

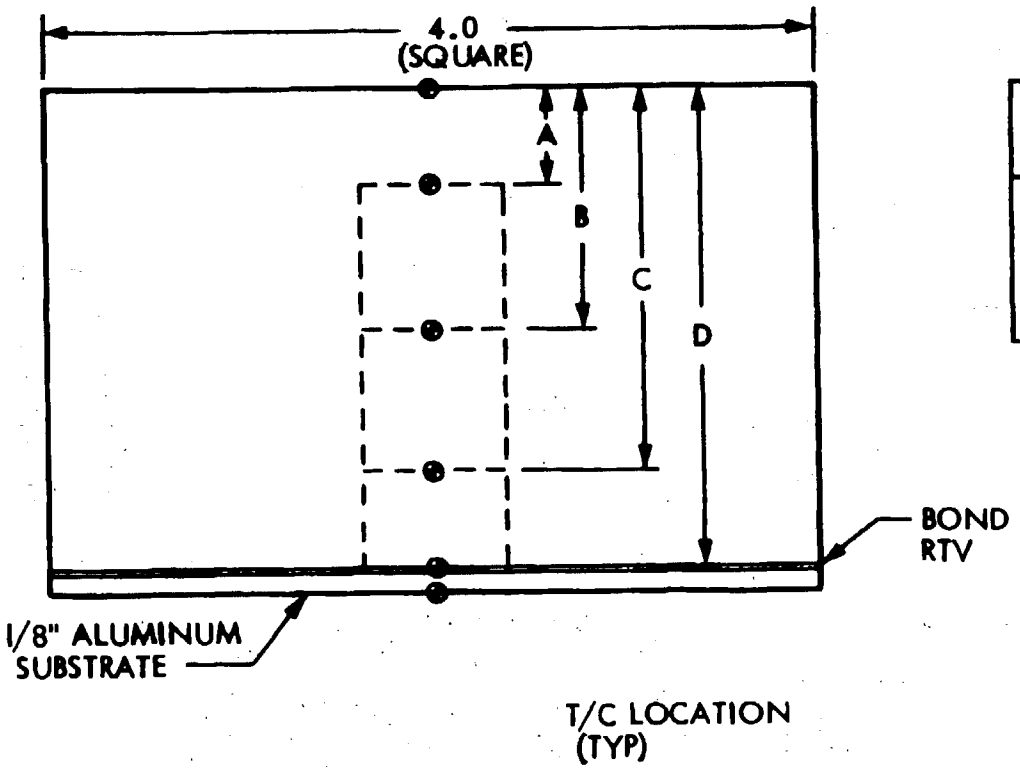

PANEL NO.	A IN.	B IN.	C IN.	D IN.
42-2	.56	1.32	2.07	2.42
42-4	.51	1.25	1.98	2.26
42-6	.59	1.32	2.09	2.45

Fig. 3.1-1

PRETEST PHOTO OF 100 CYCLE LI-1500 TEST SPECIMENS

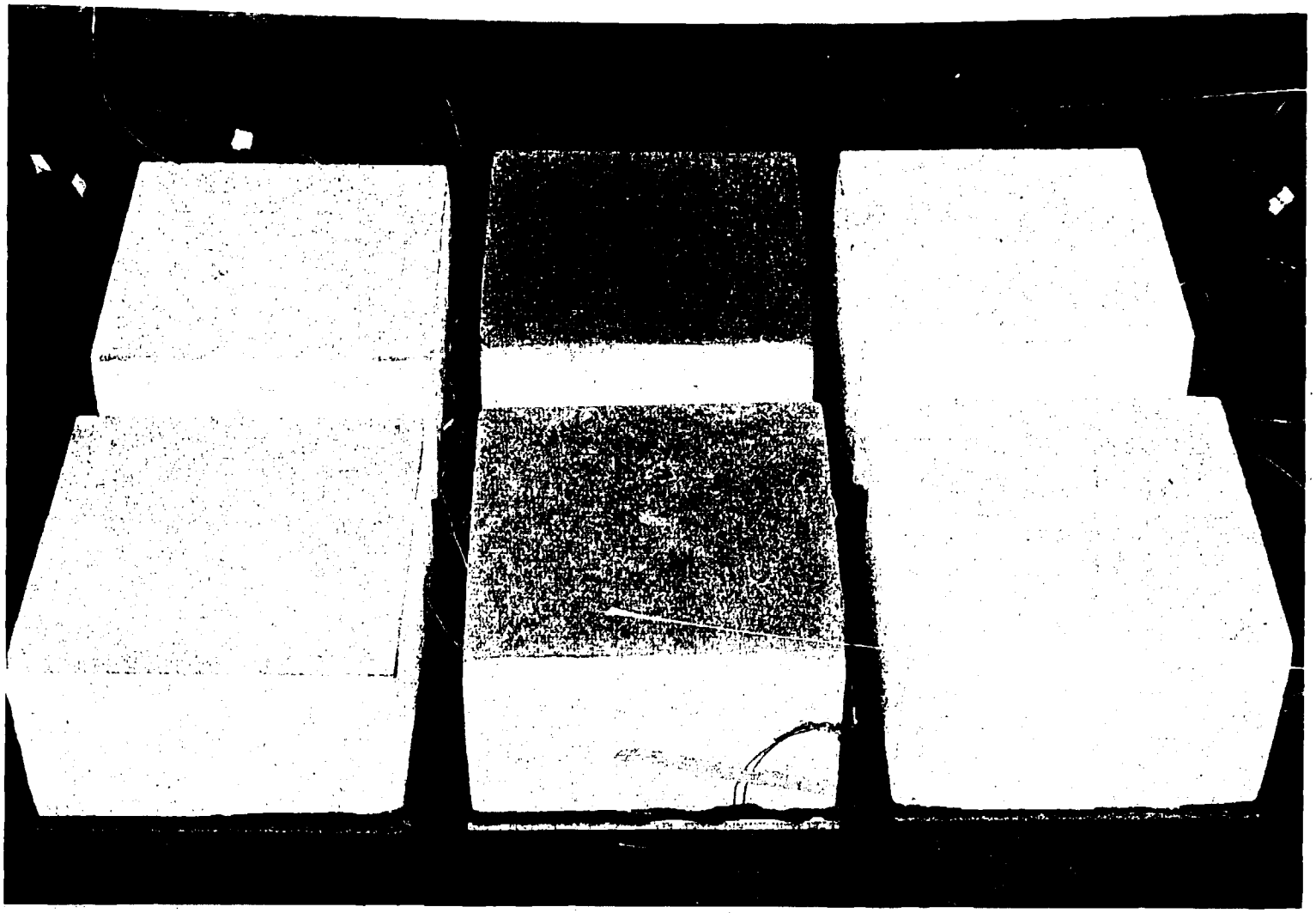

INTEGRAL COATING Cr_2O_3 + OVERGLAZE 0042

DO6145 (1)

Fig. 3.1-2

LMSC 1 ATM RADIANT HEAT FACILITY (HIRAD)

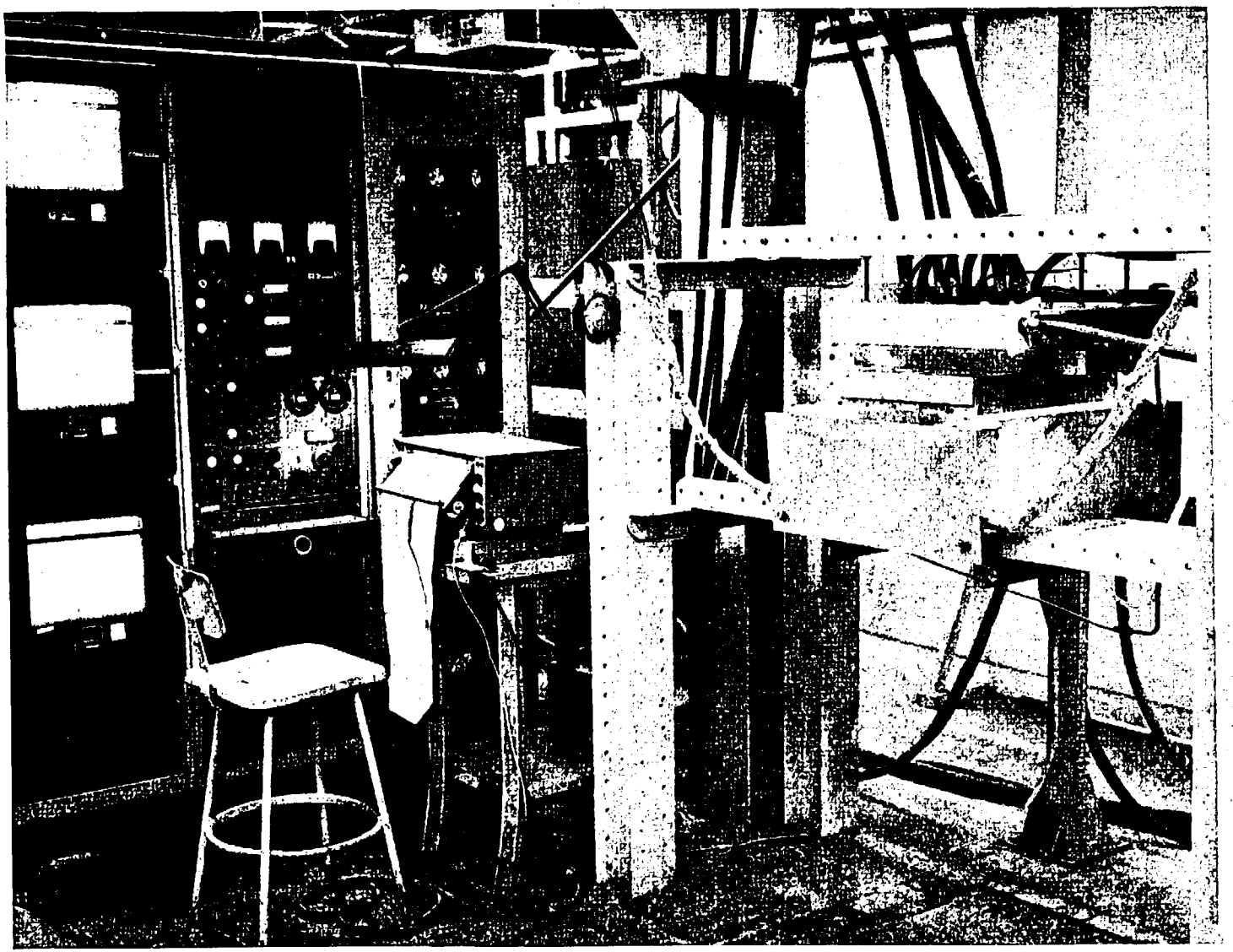

Fig. 3.1-3

The test pulse was controlled by the surface thermocouple and monitored by a calorimeter during the entire 100 cycles. To reduce the cool-down time between cycles (2-1/2 hr initially) a water-cooled copper plate was placed under the specimens. The water was turned on at about 55 min into the run or 5 min after the end of a cycle.

3.1.4 Qualitative Results

Visible inspection of the specimens during and after the 100 cycles at 2500°F indicated the following:

a. The uninstrumented 0042 coating sustained no damage after 100 cycles.

b. The instrumented 0042 coating had hairline cracks in the surface; these emanated from the position where the surface thermocouple was installed below the coating. These cracks appeared to close during the high temperature portions of the test pulse.

c. The integral coating specimens with a silicon carbide emittance agent had hairline cracks.

d. The 0025 coating developed cracks in the surface early in the test program and was removed after the forty-second cycle.

e. The chip in the surface coating on the corner of specimen TT 42-5 occurred during handling and is not attributed to the tests.

The 0042 was developed to be used at 2300°F and, although thermal performance at 2500°F for 100 cycles was demonstrated, the coating did not remain waterproof. Related efforts under the Improvement Contract (NAS 9-12137) are developing the capability of the 0042 coating to remain waterproof at 2500°F. Post-test photos of the specimens after 100 cycles are shown in Figs. 3.1-4 and 3.1-5. The 0025 coated specimens are not shown.

3.1.5 Quantitative Results

Temperature predictions were performed for the 100 cycle LI-1500 tests, using the following groundrules and assumptions:

a. THERM computer code (See Volume II, Section 2.1)

b. One-dimensional thermal model

c. Variation of thermal conductivity and specific heat from Tables 4.1-4 and -5, density = 15 lb/ft^3

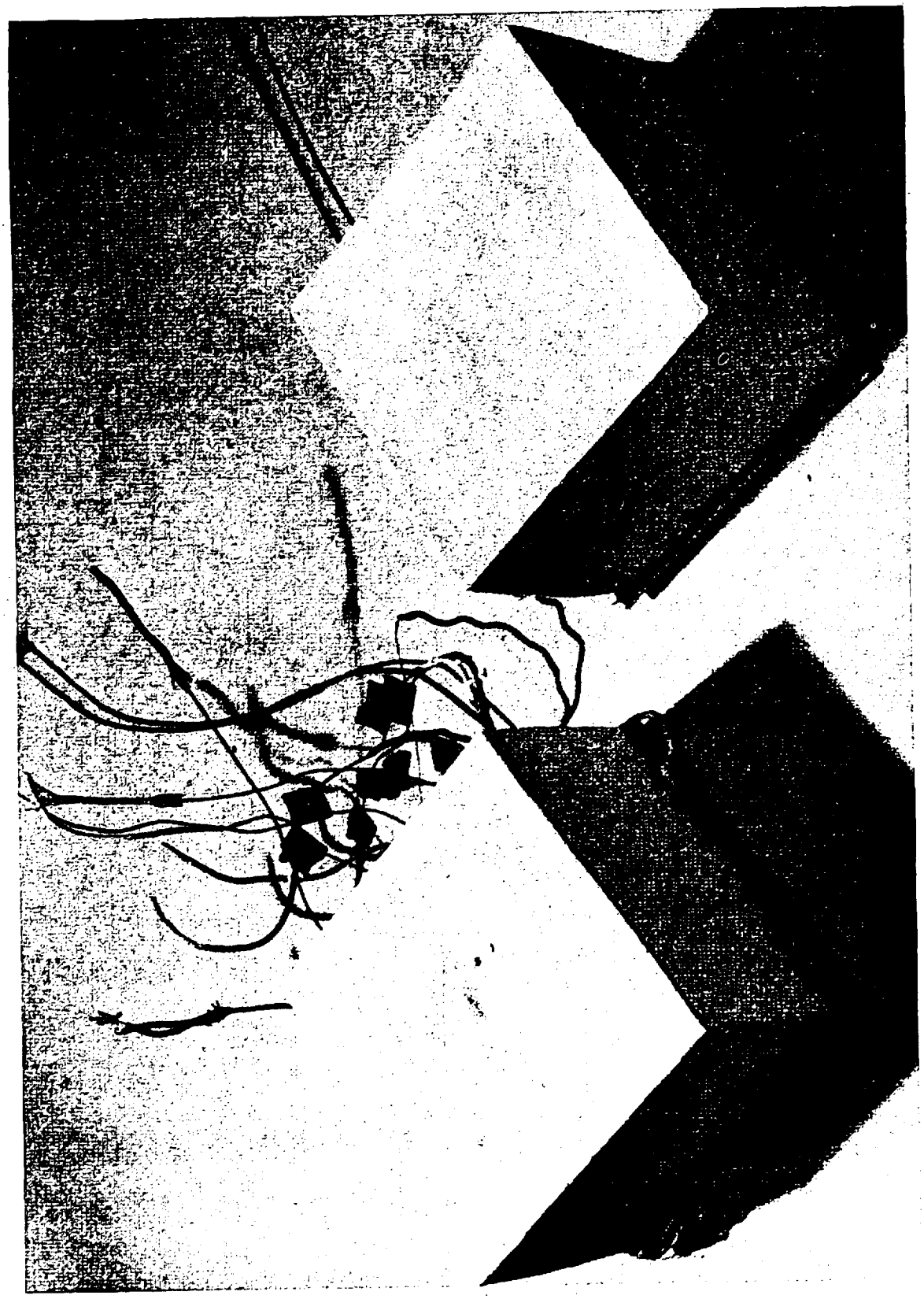

Fig. 3.1-4 LI-1500 Specimens With 0042 Coating After 100 Thermal Cycles

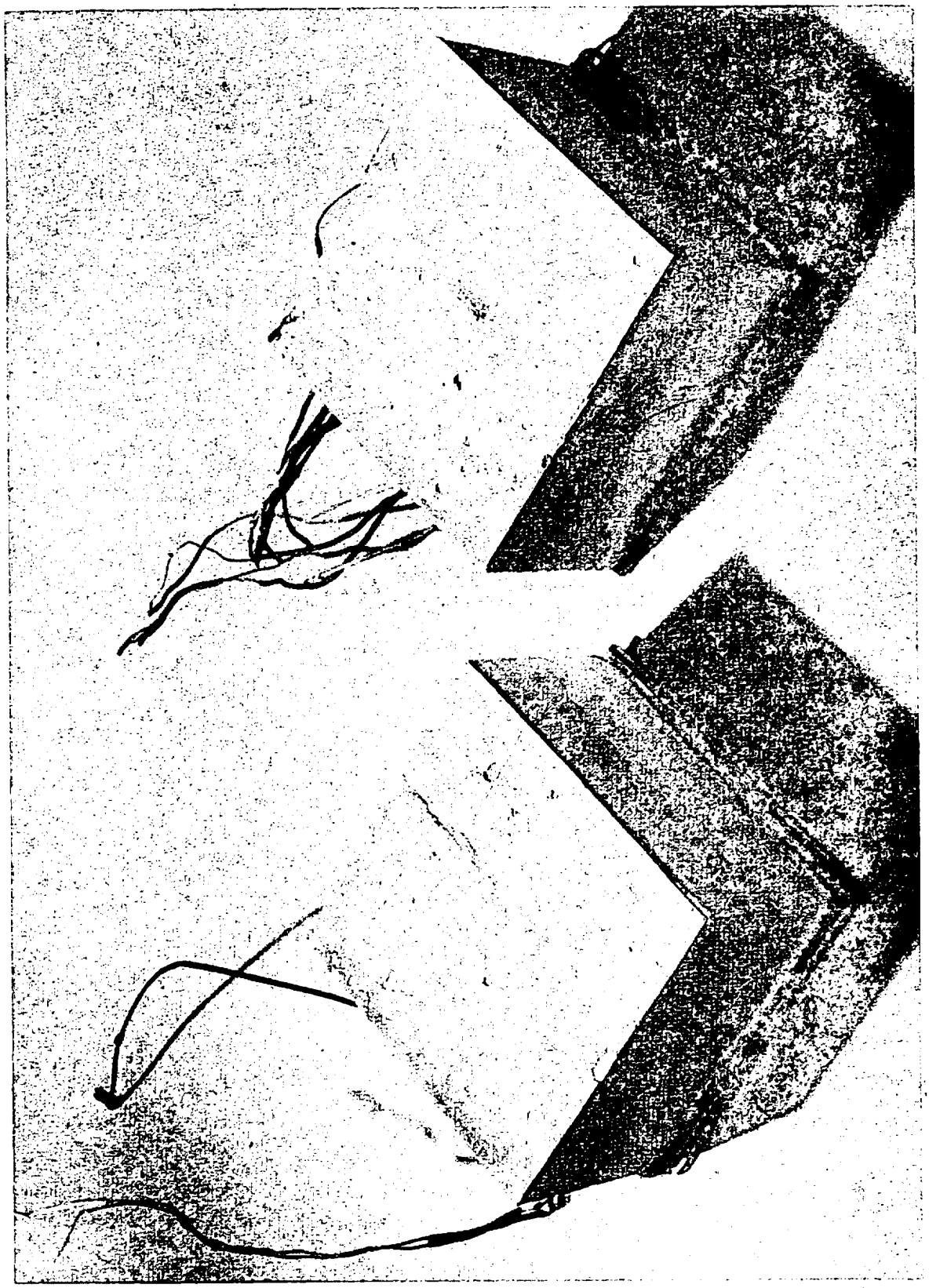

Fig. 3.1-5 LI-1500 Specimens With Integral/Silicon Carbide Coating After 100 Thermal Cycles

d. Input measured surface temperature as boundary condition

e. Adiabatic substrate

f. 0.030-in. RTV 560 adhesive between LI-1500 and aluminum substrate

The measured temperature histories are shown in Figs. 3.1-6a, b, c, and d for the instrumented LI-1500 specimen with the 0042 coating (TT 42-6). Data are plotted for the 4th, 47th, 75th and 100th thermal cycles.

The consistency and repeatability of the measured temperature data are shown in Fig. 3.1-6. The repeatability demonstrates the thermal stability of the LI-1500.

Figure 3.1-6a shows a comparison of measured and predicted temperatures at various locations within the LI-1500. Since the specimens were bonded to 0.125-in. aluminum substrates which were placed on a second piece of 0.125-in. aluminum, the predictions were made for two substrate thicknesses. As shown, the effect of the substrate upon the predicted temperature becomes negligible at depths between 1.3 and 2.09 in. The temperature difference is less than $50^{o}F$ at a depth of 2.09 in. The predictions were also complicated by the fact that the contact resistance between the two 0.125-in. aluminum plates was not known and, also, the adiabatic boundary condition was not met.

A summary of the peak predicted and measured temperatures for the 4th, 47th, 75th, and 100th cycles is shown in Fig. 3.1-7.

Figure 3.1-8 shows measured temperature histories for specimen TT 42 4, the integral silicon carbide coated specimen, for the 4th, 47th, 75th, and 100th cycles. The first thermocouple failed sometime after the 47th cycle, and no data are shown for the 75th and 100th cycles.

The excellent repeatability of the measured data is also shown in Fig. 3.1-9, where the peak measured temperatures for the 4th, 47th, 75th, and 100th cycles are compared to the predicted values.

TEMPERATURE HISTORIES FOR SPECIMEN TT 42-6 DURING 100 CYCLE TESTS

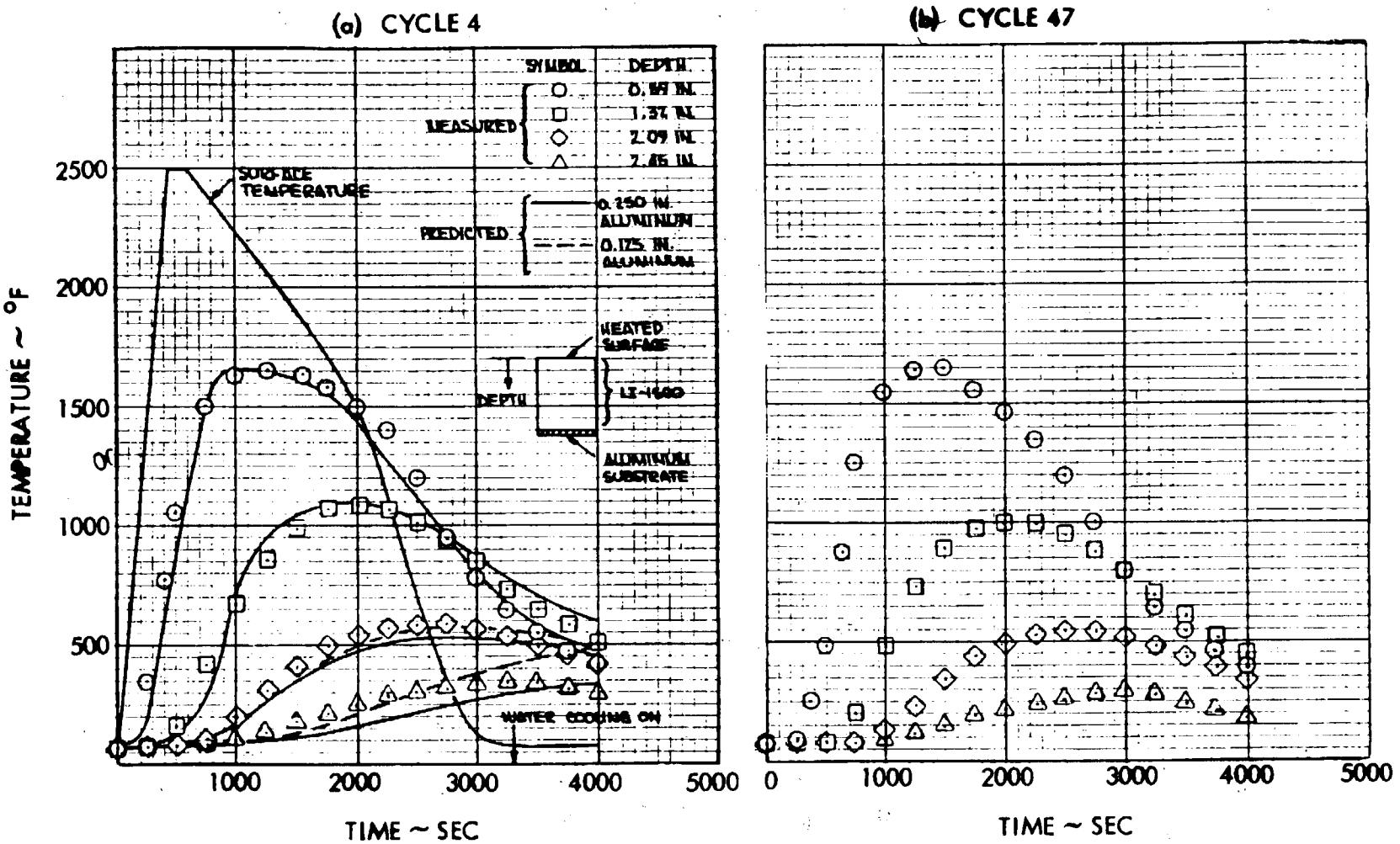

DO6156

Fig 3.1-6

TEMPERATURE HISTORIES FOR SPECIMEN TT 42-6 DURING 100 CYCLE TESTS

(c) CYCLE 75

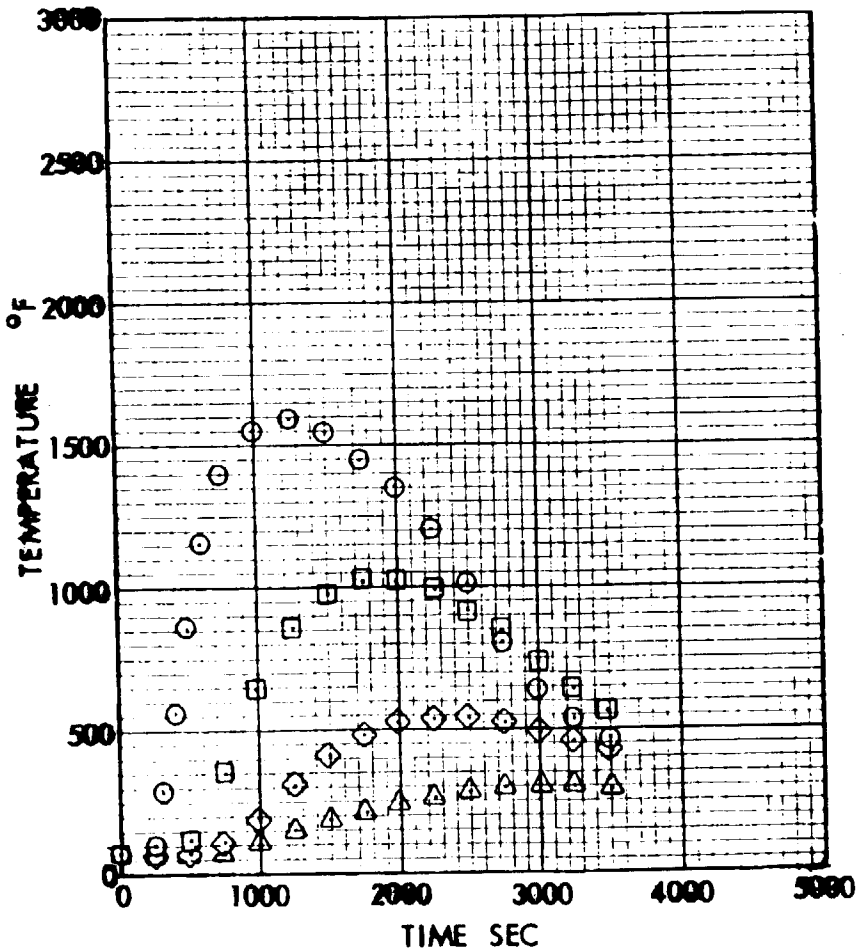

(d) CYCLE 100

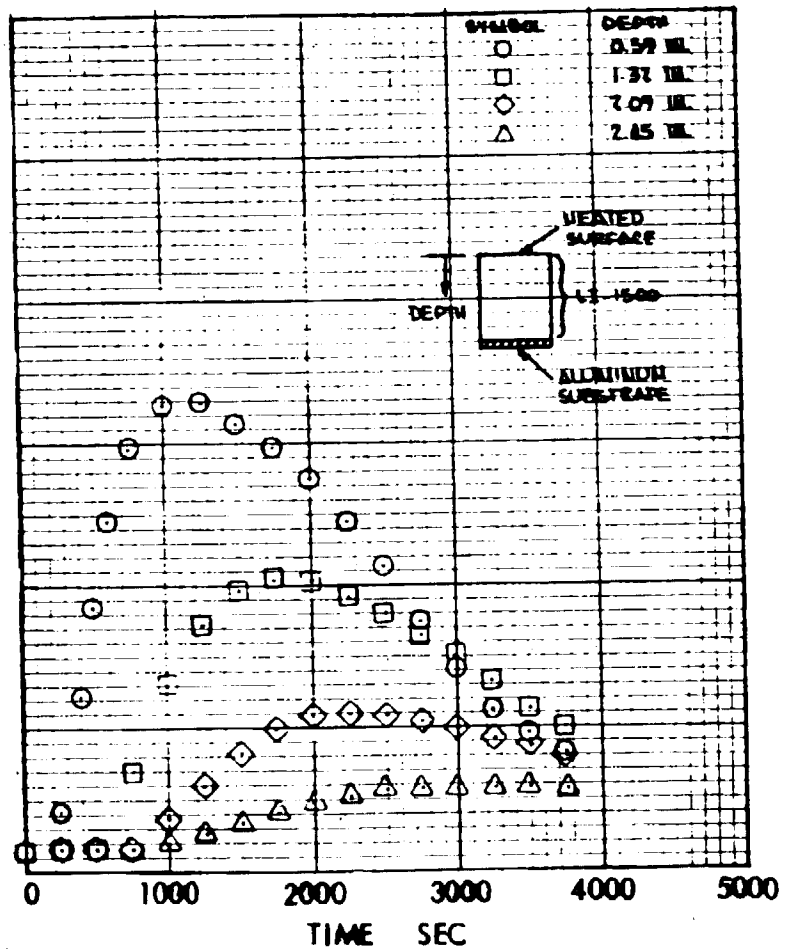

DO6160

Fig. 3.1-6 (Cont)

COMPARISON OF MEASURED AND PREDICTED PEAK TEMPERATURES FOR 100 CYCLE TESTS - SPECIMEN TT 42-6

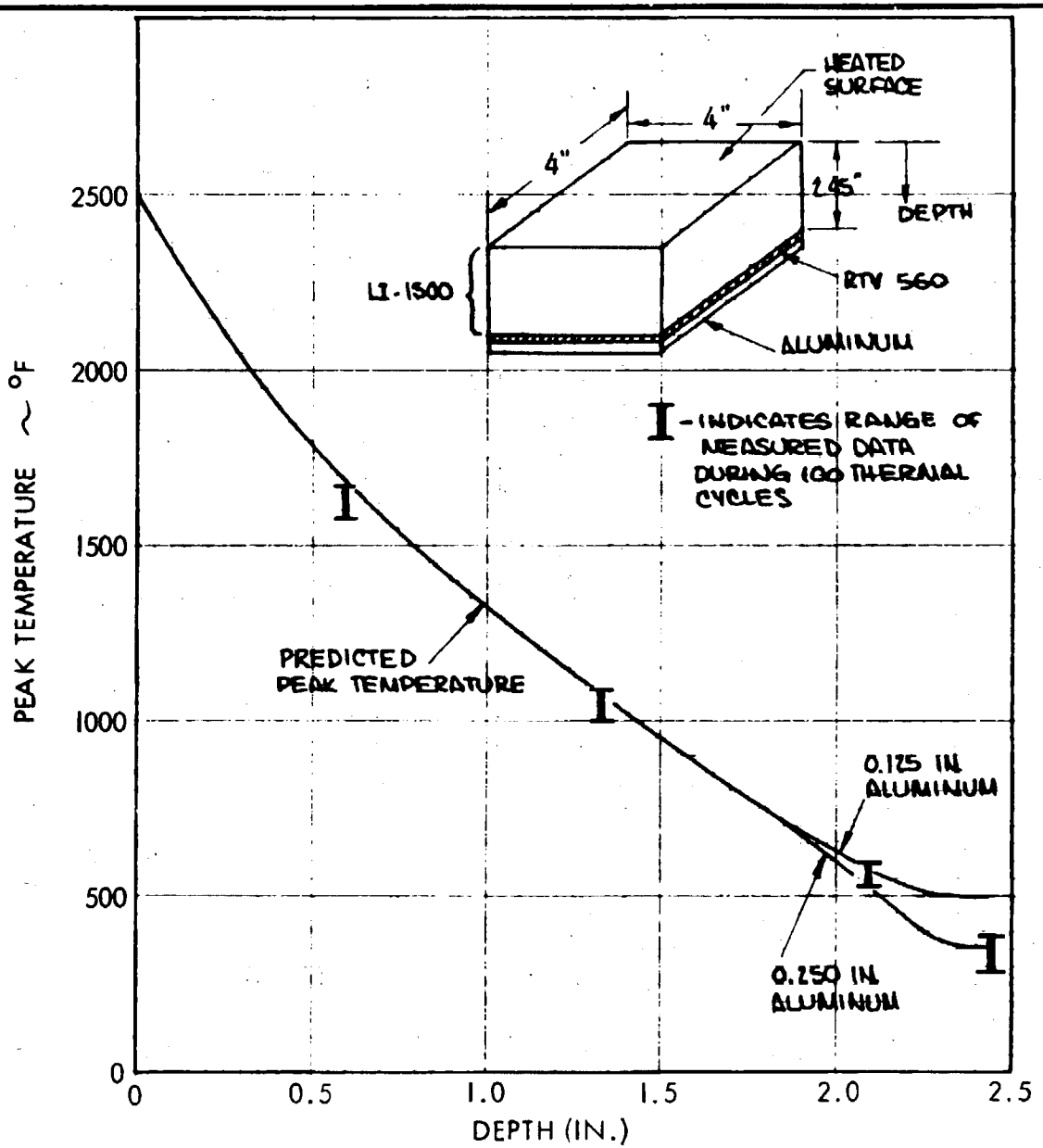

Fig. 3.1-7

TEMPERATURE HISTORIES FOR SPECIMEN TT 42-4 DURING 100 CYCLE TESTS

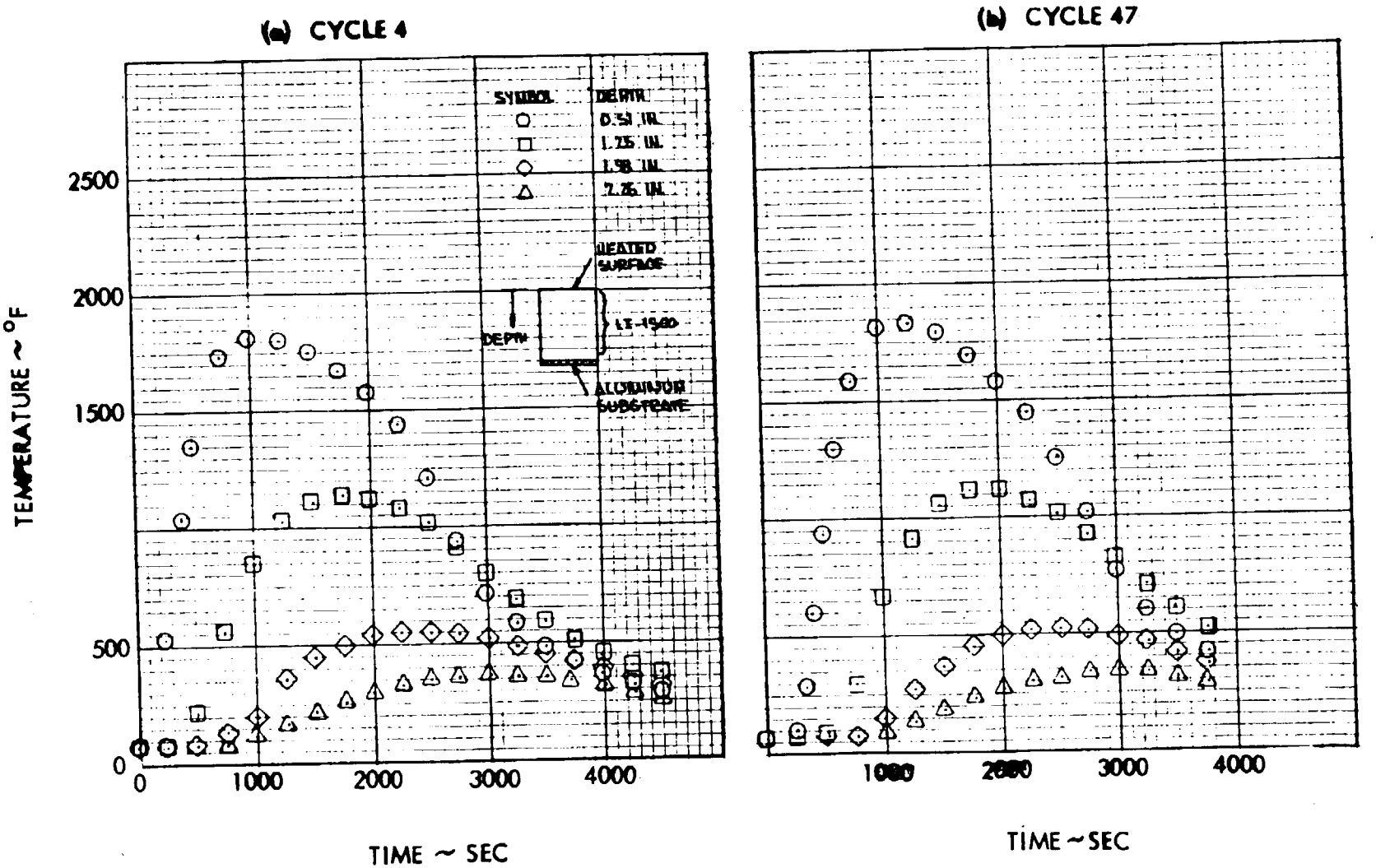

DO6154

Fig. 3.1-8

TEMPERATURE HISTORIES FOR SPECIMEN TT 42-4 DURING 100 CYCLE TESTS (CONTINUED)

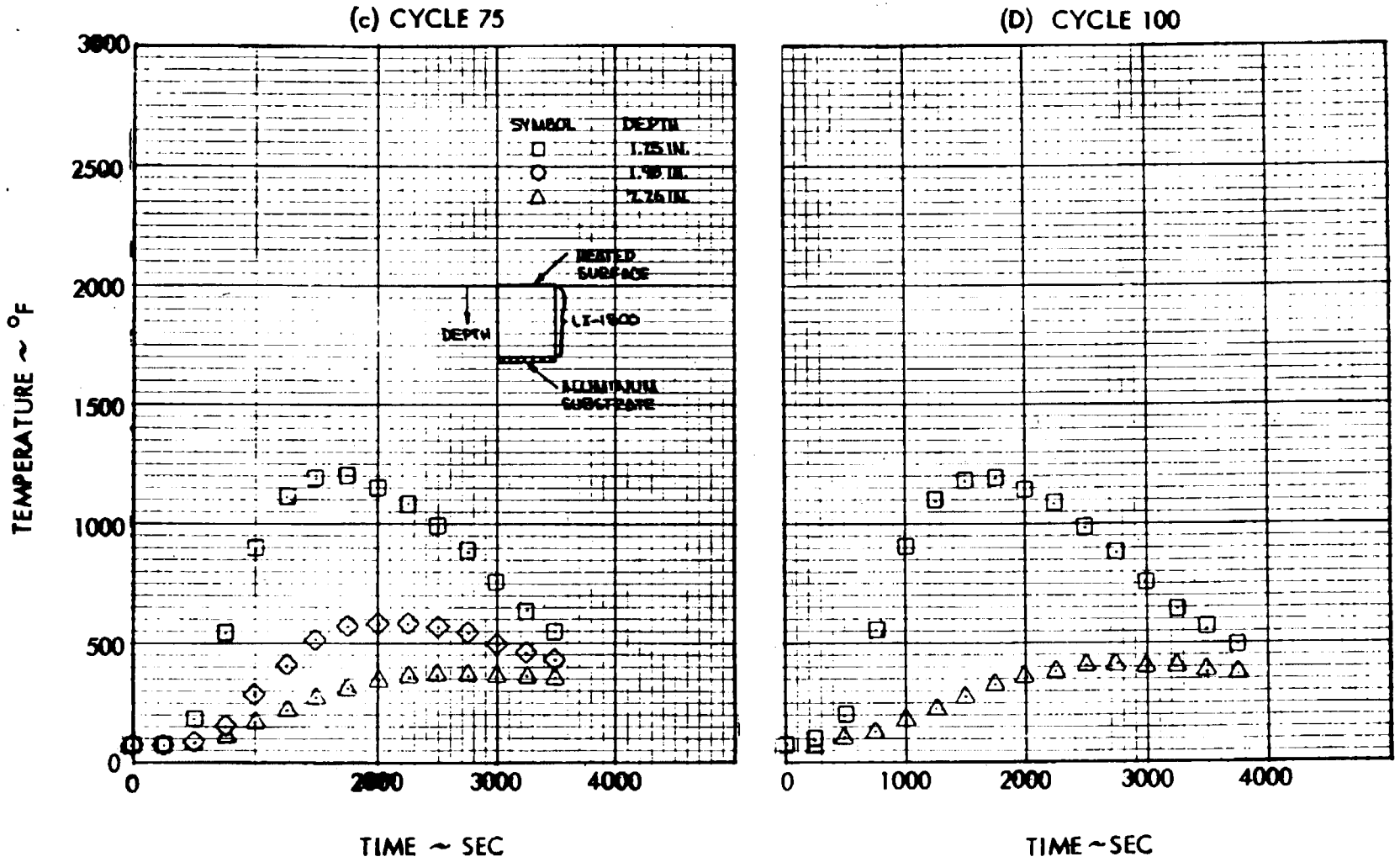

DO6155

Fig. 3.1-8 (Cont)

COMPARISON OF MEASURED AND PREDICTED PEAK TEMPERATURES FOR 100 CYCLE TESTS - SPECIMEN TT42-4

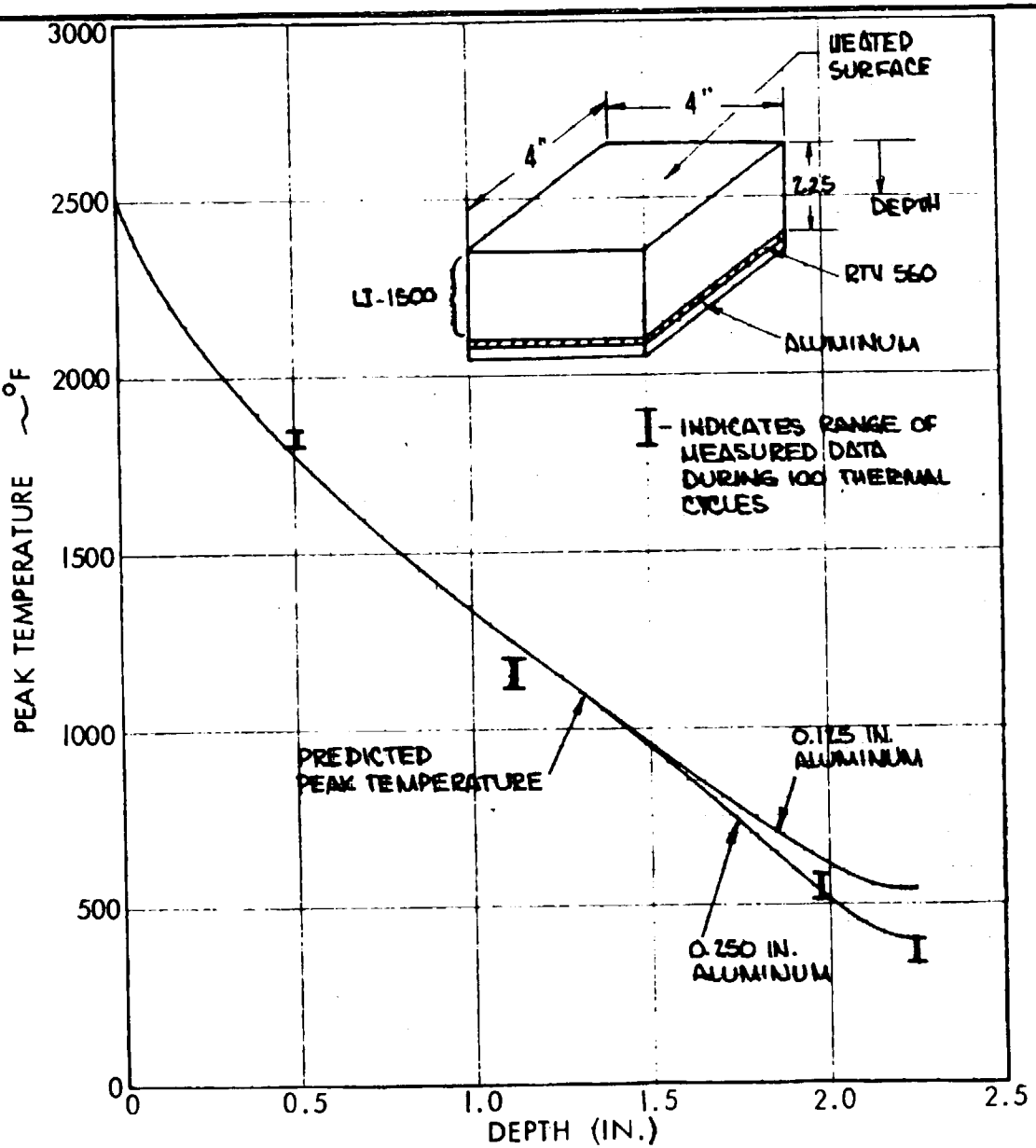

Fig. 3.1-9

Hence even after 83.3 hr of accumulated thermal exposure with about 4.17 hr at the peak temperature of 2500°F and 14 hr above 2300°F, the use of as-fabricated thermal conductivity values results in good agreement between the measured and predicted temperatures for both instrumented specimens TT 42-4 and TT 42-6.

Specimen pre-test and post-test dimensional weight data are shown in Table 3.1-1. The dimensional change of the specimens varied from 1.4 to 3 percent. A 3-percent thickness change is considered minimal for a specimen that has experienced 100 thermal cycles corresponding to 100 entries on an 1100-nm crossrange trajectory.

X-ray diffraction studies of samples taken from various locations on the surface and in-depth from specimens (TT 42-5 and TT 42-6) indicated a crystalline phase change occurred to a depth of about 0.074 in. Samples at depths of 0.116 and 0.164 in. from the surface indicated no phase change transformations. According to the calculated peak temperature in Fig. 3.1-7, peak temperature at a depth of 0.074 in. is about 2375°F. At a depth of 0.052 in., corresponding to a peak temperature of 2400°F, about 6-percent cristobalite was detected. At a depth of 0.014 in., corresponding to about 2480°F, about 59-percent cristobalite was detected. More details on the post-test inspection and analysis of these specimens will be contained in the final report of the Materials Improvement Contract, NAS 9-12137.

The thermal test cycle used for the 100-cycle test is compared with the NASA design surface temperature history for Area 2, and the surface temperature histories for an NAR 1350-nm trajectory and an NASA/MSC 1100-nm trajectory in Fig. 3.1-10. The test cycle used by LMSC remained at 2500°F for 2.5 min and was above 2300°F for 8.3 min.

Although the shape of the test cycle follows the NASA design temperature history, except for the time when it exceeds 2300°F, an actual overshoot trajectory with a peak surface temperature of 2500°F would penetrate to a lower altitude than the design trajectory. Therefore, the vehicle would reenter in a shorter time, since the aerodynamic drag is greater at lower altitudes. This would cause the cooling portion of an overshoot temperature history to reach 100°F in a shorter time than that shown on the figure.

Table 3.1-1

DIMENSIONAL DATA FOR 100 CYCLE TEST PROGRAM

SPECIMEN NO.	SURFACE COATING	LENGTH (IN.)		WIDTH (IN.)		THICKNESS (IN.)	
		PRE-TEST	POST-TEST	PRE-TEST	POST-TEST	PRE-TEST	POST-TEST
TT42-3	INTEGRAL BOROSILICATE WITH SILICON CARBIDE EMITTANCE AGENT	3.933	3.930	3.930	3.917	2.270	2.164
TT42-4	INTEGRAL BOROSILICATE WITH SILICON CARBIDE EMITTANCE AGENT	3.957	3.946	3.940	3.922	2.407	2.150
TT42-5	OO42 - BOROSILICATE WITH SILICON CARBIDE EMITTANCE AGENT	3.932	3.932	3.914	3.914	2.450	2.376
TT42-6	OO42 - BOROSILICATE WITH SILICON CARBIDE EMITTANCE AGENT	3.924	3.924	3.920	3.918	2.445	2.411

040A ORBITER SURFACE TEMPERATURE HISTORY COMPARISON

LOWER SURFACE CENTERLINE, X/L = 0.5

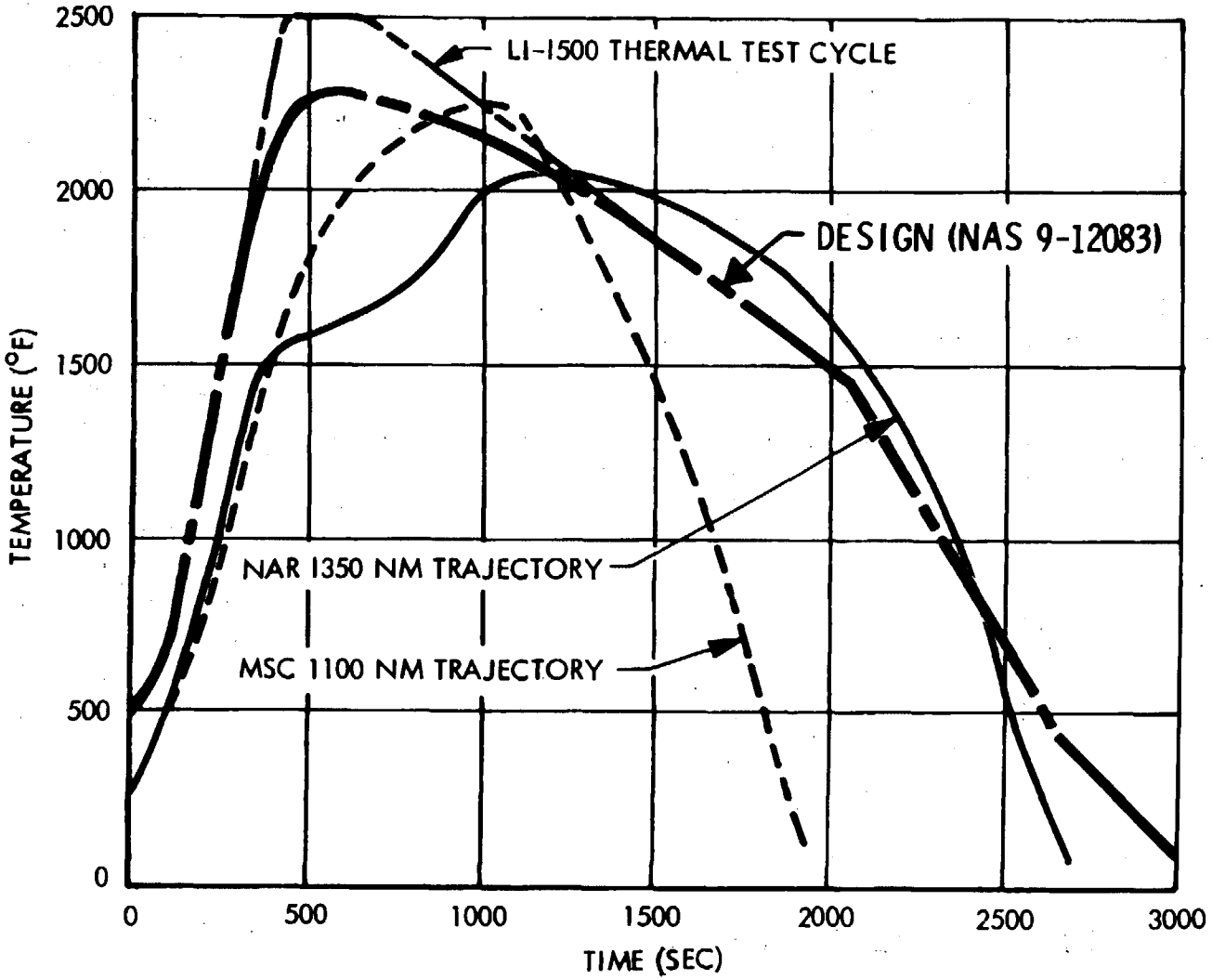

DO6088

Fig. 3.1-10

Hence, the 100-cycle test temperature pulse is an overshoot in terms of time at temperature and in terms of total energy input to the LI-1500. Figure 3.1-10 also indicates two other trajectories that attain 1100-nm crossrange while restricting the surface temperature at the 50-percent length location on the orbiter to less than 2300°F and achieving a reentry in a shorter time than the design pulse.

According to the results of the X-ray diffraction studies on the 100-cycle specimens, limiting the peak temperature to 2300°F for 100 reentries would apparently result in no phase change at the surface.

In summary, the Material Improvement Program NAS 9-12137 has produced a surface coating capable of withstanding 83.3 hr of accumulated thermal exposure with 14 hr at temperatures greater than 2300°F and 4 hr at 2500°F. This environment corresponds to 100 consecutive overshoot reentries representative of an 1100-nm crossrange mission.

3.2 VERIFICATION OF THERMODYNAMIC SIZING METHODS

The adequacy of the thermodynamic sizing methods is illustrated in this section by presenting predictions of measured temperature data for various test specimens and test environments. All predicted temperatures were obtained by using the THERM computer code and the LI-1500 thermophysical properties (thermal conductivity and specific heat) listed in Tables 4.1-6 and 4.1-7. A surface temperature boundary condition that matched the data obtained from the surface thermocouple was used.

3.2.1 Beryllium Fuselage Panel Test At 1-Atm Pressure

NASA/MSC has performed numerous tests at 1-atm pressure on the beryllium fuselage panel supplied by LMSC under NAS 9-11222. Data correlations were accomplished for the full temperature cycle test with zero differential pressure performed on 5 Aug 1971.

A two-dimensional thermal model was used to predict the temperature response of beryllium face sheet and stiffeners. The thermal model, divided into 34 nodes and shown in Fig. 3.2-1, includes nodes for the adhesive used to bond LI-1500 to the beryllium face sheet. The 1.5-in. width of the model corresponds to the distance between stiffeners. The 1.3 in. of LI-1500 was sized for a 500^{o}F maximum temperature with a 0.020-in. bond for an adiabatic backface.* Since the zee-stiffeners were riveted to the face sheet with 3/32-in. diameter monel rivets, a range of contact resistances was investigated based on values used for aluminum sheets with the same rivet diameter and rivet spacing. A contact conductance value of 50 Btu/ft^{2}-hr was chosen for the data correlations. Other assumptions were: (1) thermal conductivity was assumed isotropic and the value from Table 4.1-6 was used; (2) radiation and convection to a 0.375-in. aluminum plate, which was used to represent the bottom of the test fixture; (3) an emittance of 0.2 was assumed for both the beryllium and the aluminum TPS fixture; and (4) since the exact adhesive thickness at the location of the thermocouples was not known, values of 0.042 in. and 0.062 in. were used on the basis of weight calculations of the test panel before and after bonding of the LI-1500 tiles.

---

* "Development of a Rigidized, Surface Insulative Thermal Protection System for Shuttle Orbiter," LMSC-A984200, 16 Feb 1971

TWO-DIMENSIONAL (2-D) THERMAL MODEL OF LI-1500/Be TPS PANEL

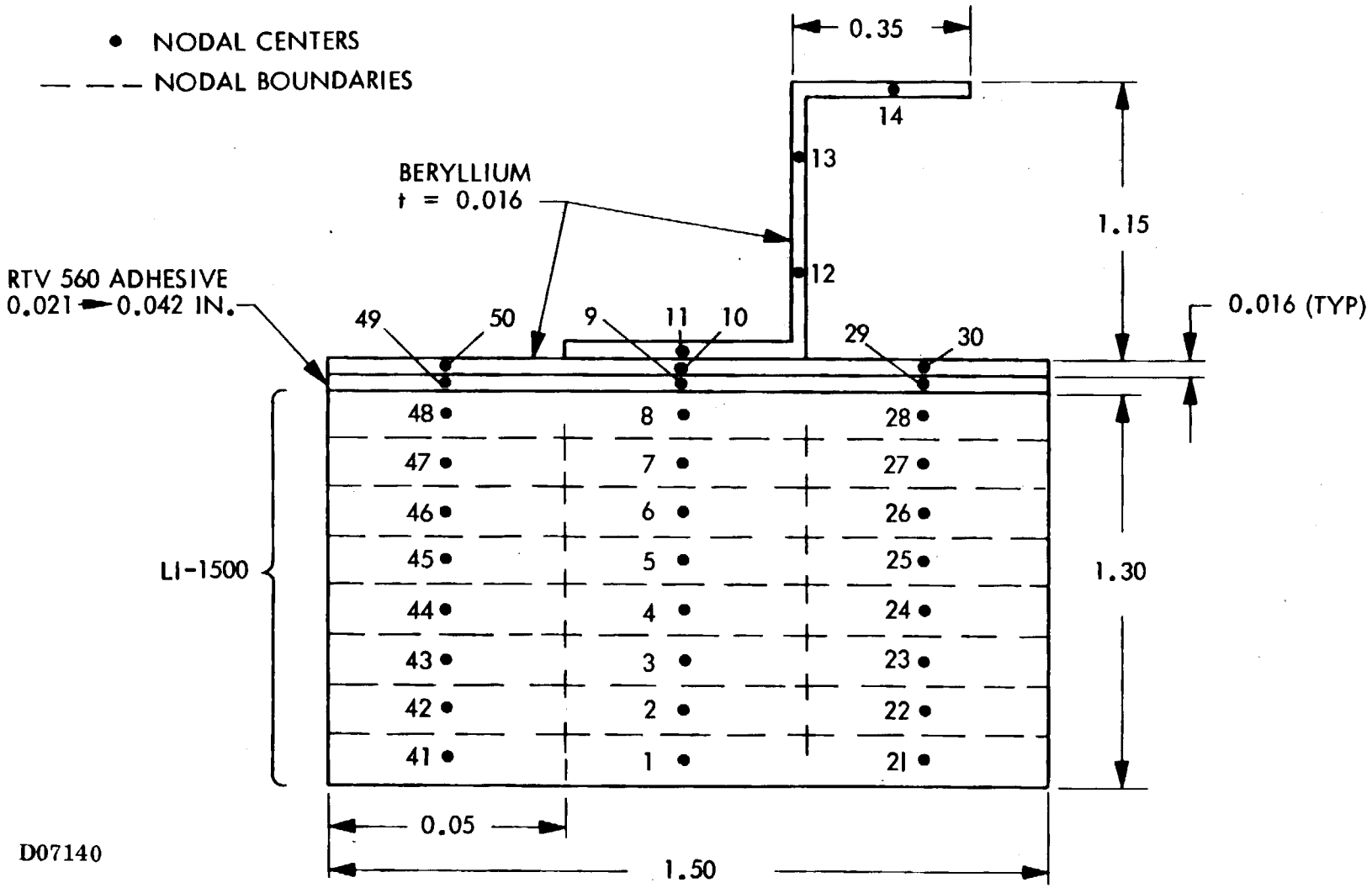

The measured surface temperature is shown in Fig. 3.2-2. This pulse of 900-sec duration is representative of a 200-nm crossrange entry.

Comparisons of measured and predicted temperatures for top and bottom of the zee-stiffener and the face sheet adjacent to the zee-stiffener are shown in Figs. 3.2-3 and 3.2-4, respectively, for 0.042 in. of RTV 560. Similar comparisons for 0.062 in. of RTV 560 are shown in Figs. 3.2-5 and 3.2-6. Both the measured and predicted values for the face sheet adjacent to the stiffener, Thermocouple 51, are higher than the measured or predicted values for the top of the zee-stiffener, Thermocouple 54.

The good agreement between predicted and measured temperatures demonstrates the degree of characterization of LI-1500 thermal properties and the adequacy of LMSC's thermal design techniques for an atmospheric pressure thermal test.

The greater decrease in slope of the measured data during the cooling is attributed to the blowing of air into the test fixture at about 3 min after the end of the surface temperature pulse. This cooling was not accounted for in the predicted temperatures.

Tests of LMSC's second beryllium panel (TP 1006-501), supplied under Contract NAS 9-11222, were performed on 10 December 1971. Preliminary results indicate response of the panel to the full 900-sec heat pulse resulted in a maximum beryllium face sheet temperature of about 360°F. This is essentially the same as the results of panel TP 1006-503 and indicates the repeatability and stability of the thermal properties of the LI-1500. These test results are summarized in the following table. The results for Panel TP 1006-501 are considered preliminary.

Note that even a time span of about 10 months between the time of LI-1500 fabrication and testing of Panel 501 had no effect on its thermal performance. This is worthy of mention on Panel 501, since it was shipped to NASA in January 1971 and returned to LMSC for test fixture modification when the first panel 503, was inadvertently cracked during an improper test situation. Hence, after a year of exposure to different atmospheric conditions, the thermal performance appears stable.

COMPARISON OF MEASURED AND PREDICTED TEMPERATURE FOR TWO LI-1500/BERYLLIUM PROTOTYPE PANELS

PANEL TP 1006-503 Fabricated Dec 1970; Tested 5 Aug 1971			PANEL TP 1006-501 Fabricated Feb 1971; Tested 9 Dec 1971		
T/C No.	Measured Peak Temp (^{O}F)	Predicted Peak Temp (^{O}F)	T/C No.	Measured Peak Temp (^{O}F)	Predicted Peak Temp (^{O}F)
51	370	380–390	51	360	380–390
53	365	370–380	53	345	370–380
54	338	350–360	54	330	350–360

During the test of Panel 503, the radiant lamps were emitting energy directly to one end of the beryllium face sheet and this resulted in a small crack on the beryllium face sheet and on a stiffener. A failure report was written on this panel.*

At the time of fabrication of these panels, the current surface coating was the 0025 borosilicate with a chrome oxide emittance agent. This coating system has since been abandoned due to its cracking tendencies and its semiporous nature. During the full cycle test pulse, with a peak temperature of 2300^{O}F, both panels (503 and 501) developed cracks in the 0025 surface coatings. However, these cracks apparently did not jeopardize the thermal performance of the LI-1500 TPS.

3.2.2 Arc-Jet Test At Low Pressure

LI-1500 Specimen TT5C was supplied to NASA/Ames Research Center for testing in their 3-MW arc-jet facility. The specimen was a flat-faced cylinder with a 4-in. diameter and a thickness of 1.8 in. It was instrumented with three 0.005-in. chromel alumel thermocouples located at distances of 0.5 in., 1.0 in., and 1.5 in. from the surface at the center of the specimen and three thermocouples at the same depths, 1-in. from the center.

*"Failure Report of LI-1500/RTV-560/Beryllium Fuselage Panel TP-1006-503," LMSC-A993382, 24 Sep 1971

SURFACE TEMPERATURE HISTORY FOR BERYLLIUM TPS PANEL TEST

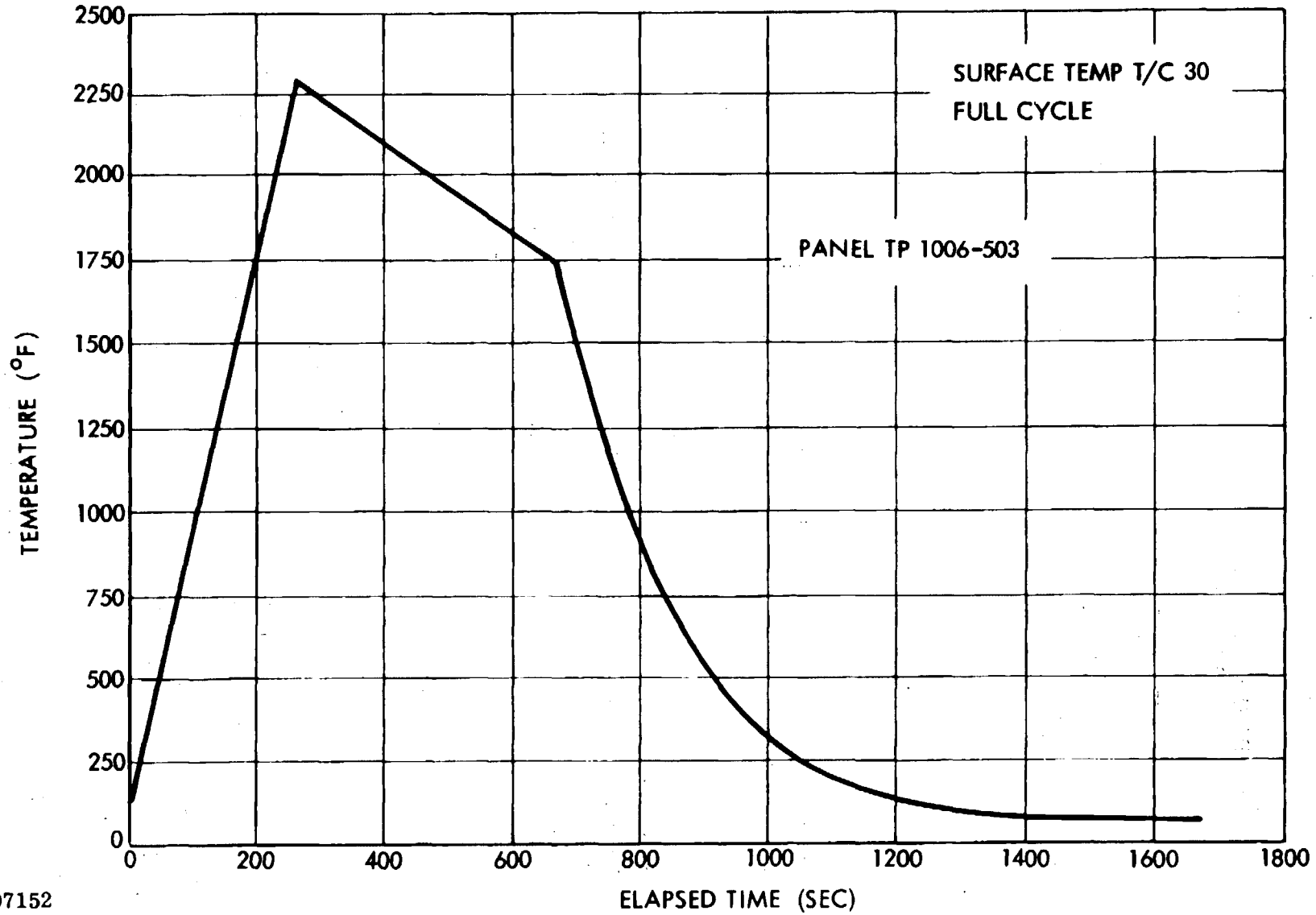

D07152

Fig. 3.2-2

COMPARISON OF MEASURED AND PREDICTED TEMPERATURES FOR Be/LI-1500 PANEL TP 1006-503

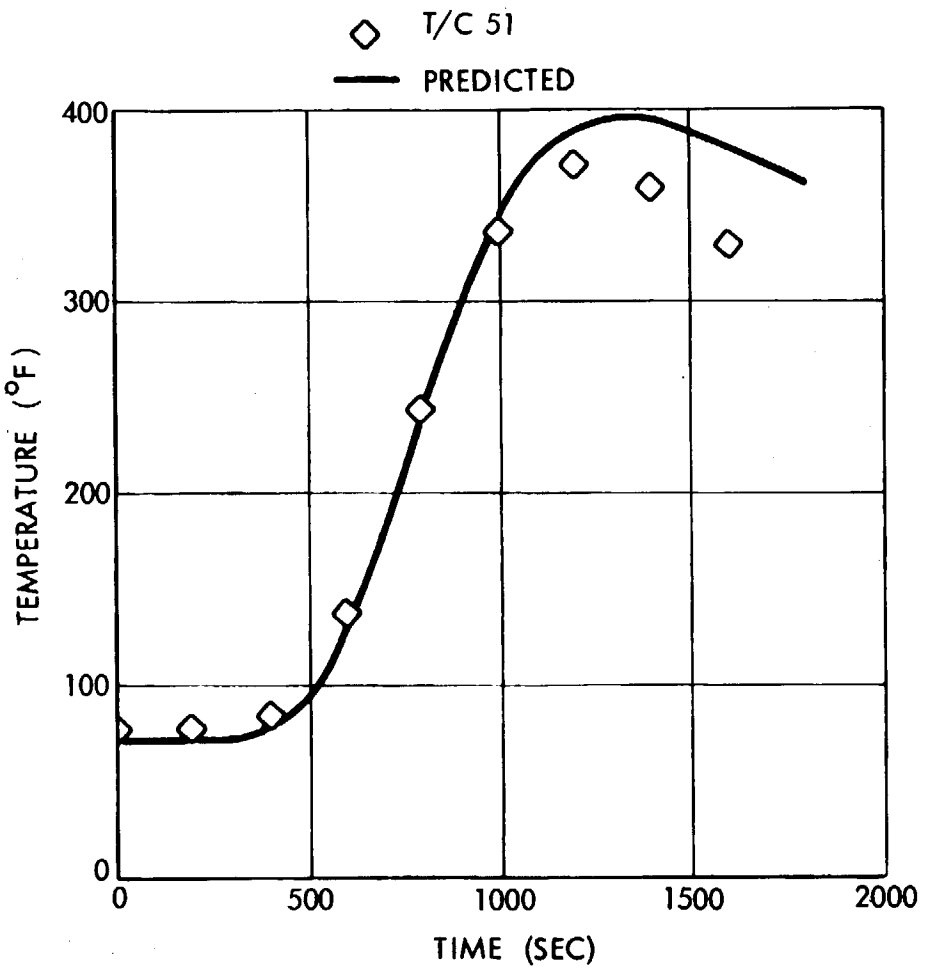

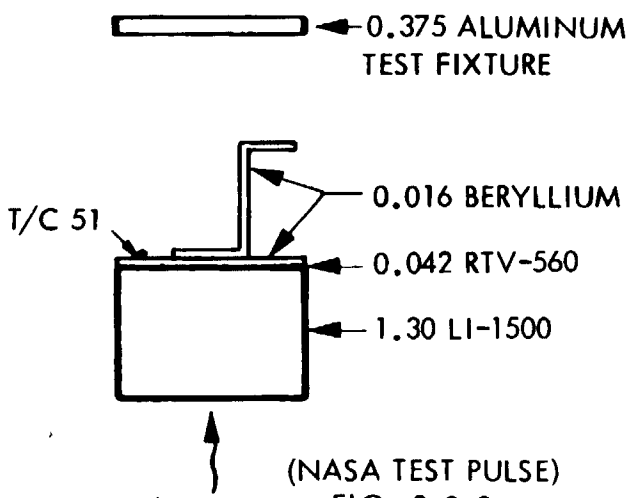

FIG. 3.2-2

D07151

Fig. 3.2-3

COMPARISON OF MEASURED AND PREDICTED TEMPERATURES FOR Be/LI-1500 PANEL TP 1006-503

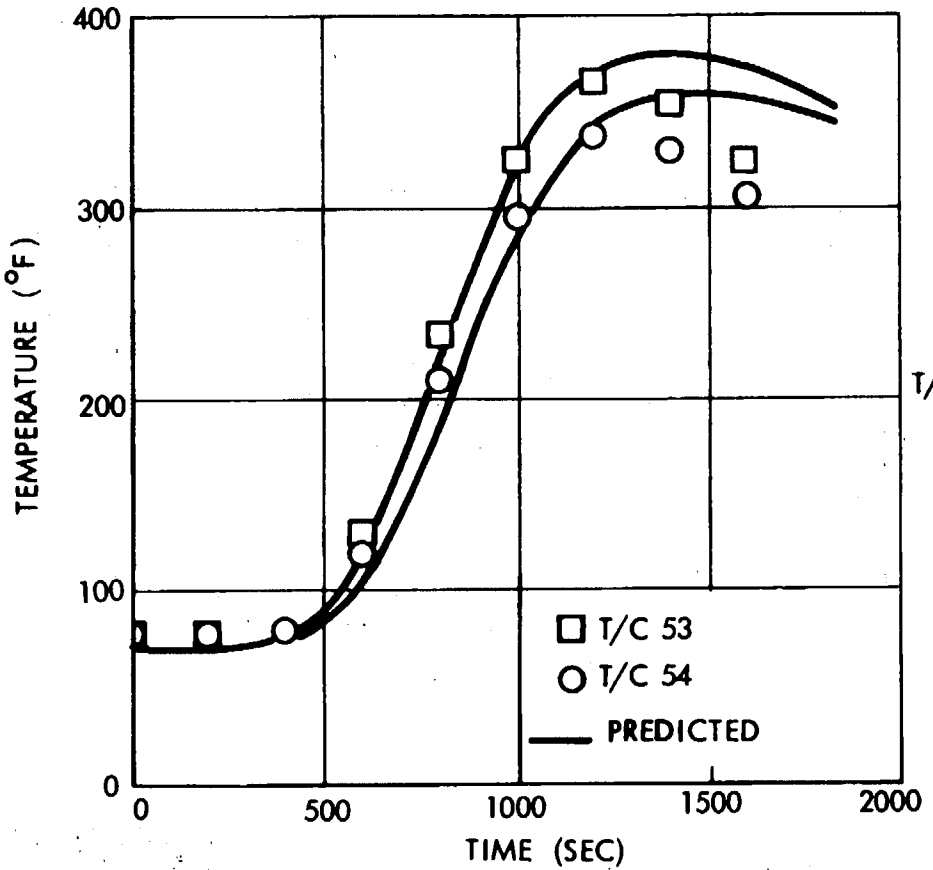

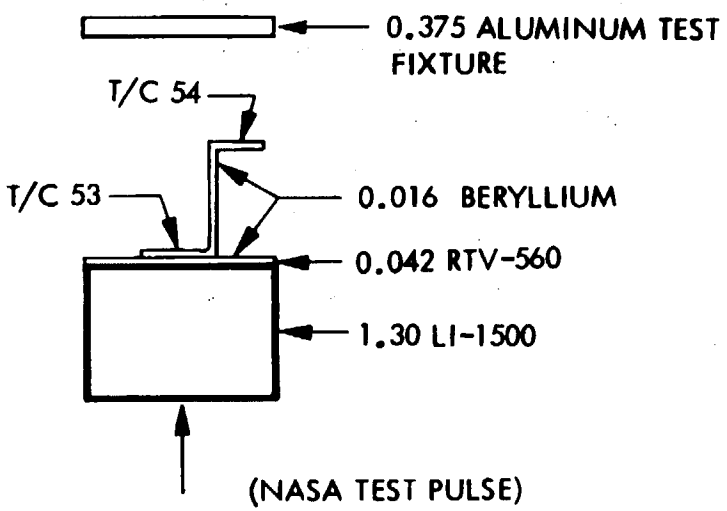

D07139

Fig. 3.2-4

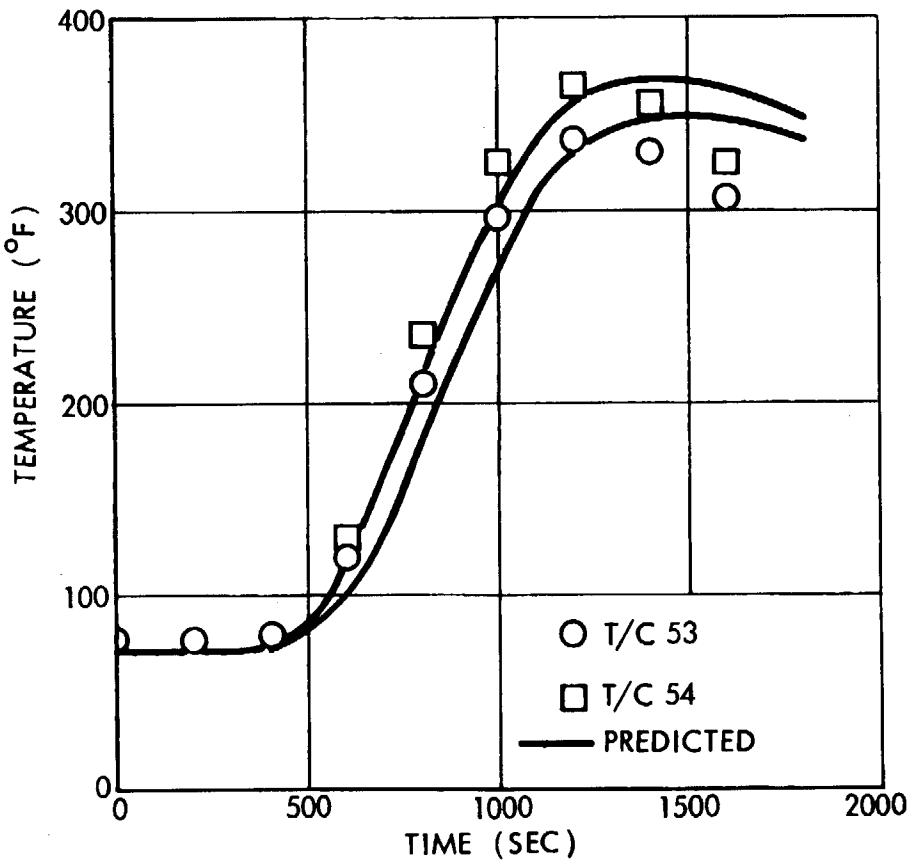

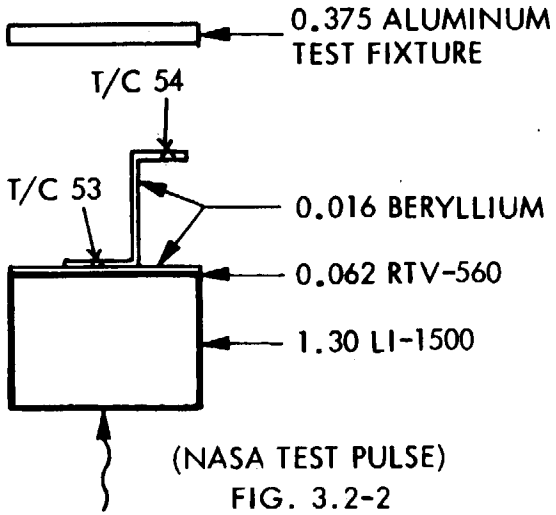

FIG. 3.2-2

Fig. 3.2-5

COMPARISON OF MEASURED AND PREDICTED TEMPERATURES FOR Be/LI-1500 PANEL TP 1006-503

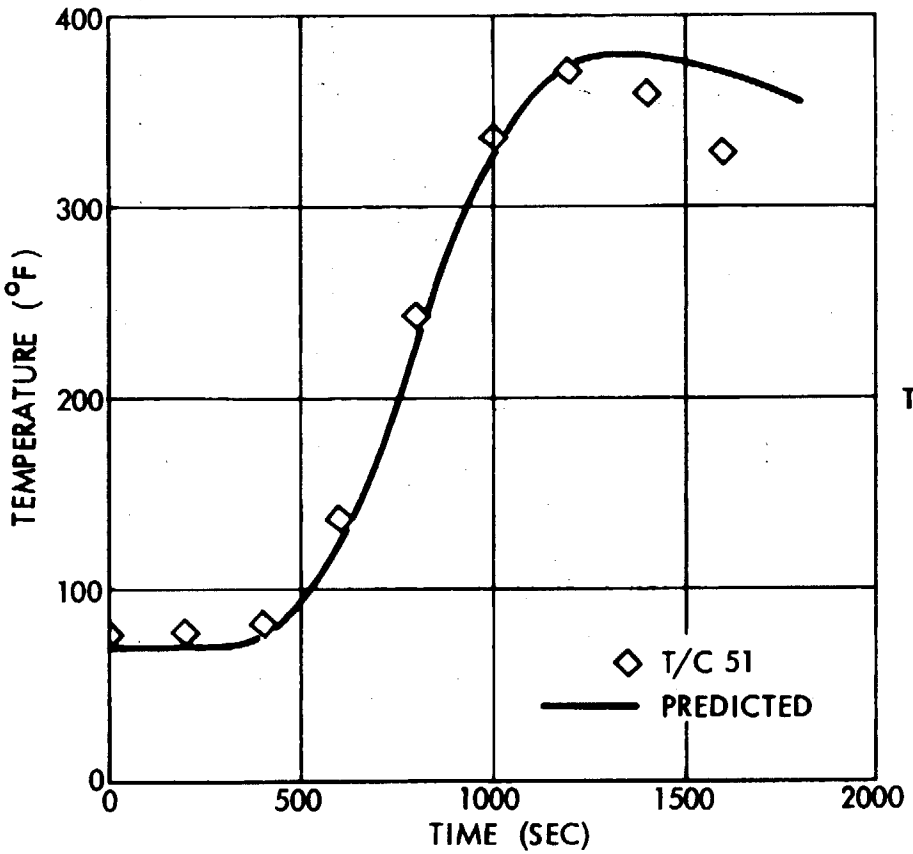

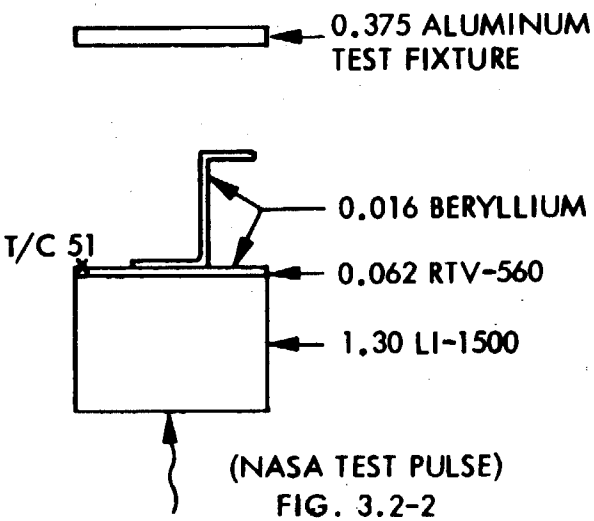

FIG. 3.2-2

D07153 (1)

Fig. 3.2-6

The specimen was placed in the center cavity of an 8-in. diameter, water-cooled copper flat-faced cylinder 3 in. thick. The cavity was 4 in. in diameter and 2 in. deep. The model holder with an LI-1500 specimen in place is shown in Fig. 3.2-7. Three pressure ports, located at 120 deg apart, along with a calorimeter are also shown in Fig. 3.2-7.

To predict the temperature response of LI-1500, a two-dimensional thermal model consisting of 90 nodes was constructed for use with the LMSC THERM computer code. Since the heating distribution over the specimen portion of the model holder was assumed symmetrical, only one-half of the specimen and holder was modeled. Nodes were included to represent the water-cooled copper portions of the holder. Convection and radiation from the edge of the specimen to the water-cooled copper was included. The thermal model, with the thermocouple locations, is shown in Fig. 3.2-8.

Predictions of a test with a reported surface temperature of 2300^{o}F are shown in Fig. 3.2-9, along with measured data. The test pressure on this model surface was about 7 mm of mercury. The model was in the stream for 30 min. The thermal conductivity and specific heat values for LI-1500 are the interim design values reported in LMSC-A984200 (the final report for NAS 9-11222). For this correlation, the thermal conductivity values at 0.1 mm Hg were used (these are lower than the 7 mm values - see Fig. 4.1-12).

Good agreement between predicted and measured temperatures is shown in Fig. 3.2-9, the predicted data are slightly higher than the measured near the end of the test. This correlation suggests that the actual low-pressure thermal conductivity may be lower than the current design values, and more effort is required to define the low-pressure thermal conductivity.

PRETEST PHOTOGRAPH OF LI-1500 IN MODEL HOLDER FOR TEST AT NASA/ARC

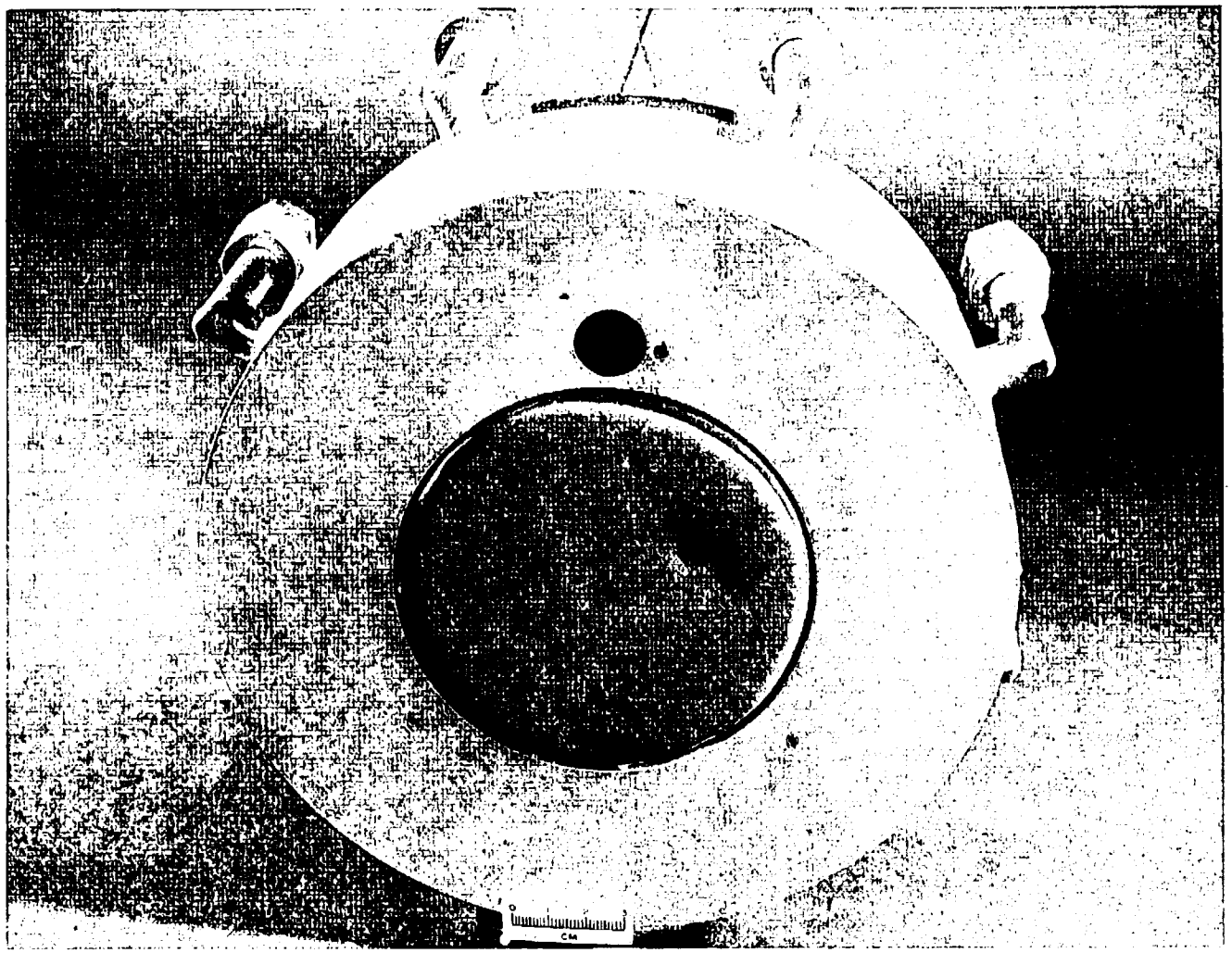

Fig. 3.2-7

SKETCH OF THERMAL MODEL AND INSTRUMENTATION FOR SPECIMEN TT5C

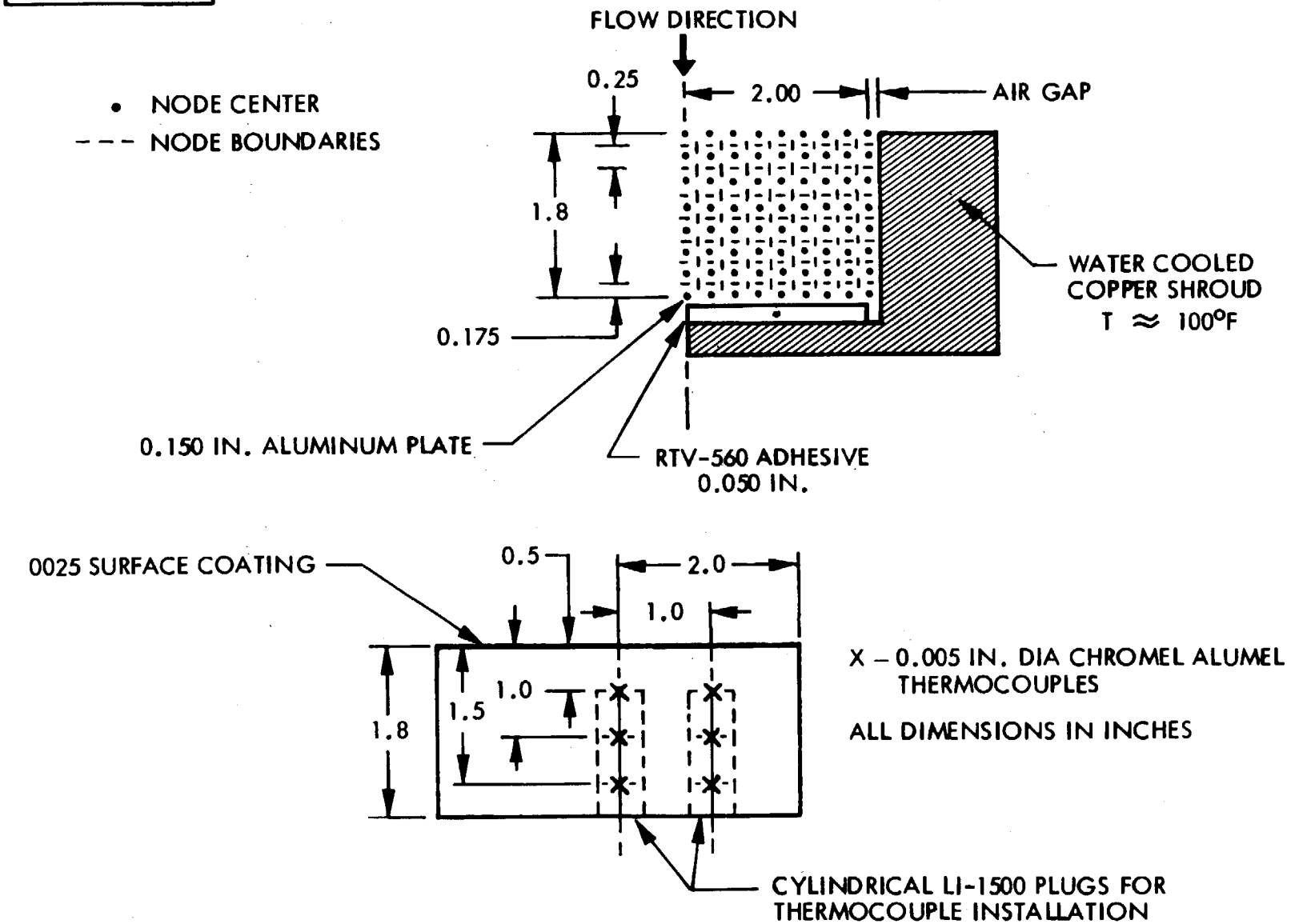

Fig. 3.2-8

COMPARISON OF MEASURED AND PREDICTED TEMPERATURE HISTORIES FOR CENTERLINE OF SPECIMEN TT5C

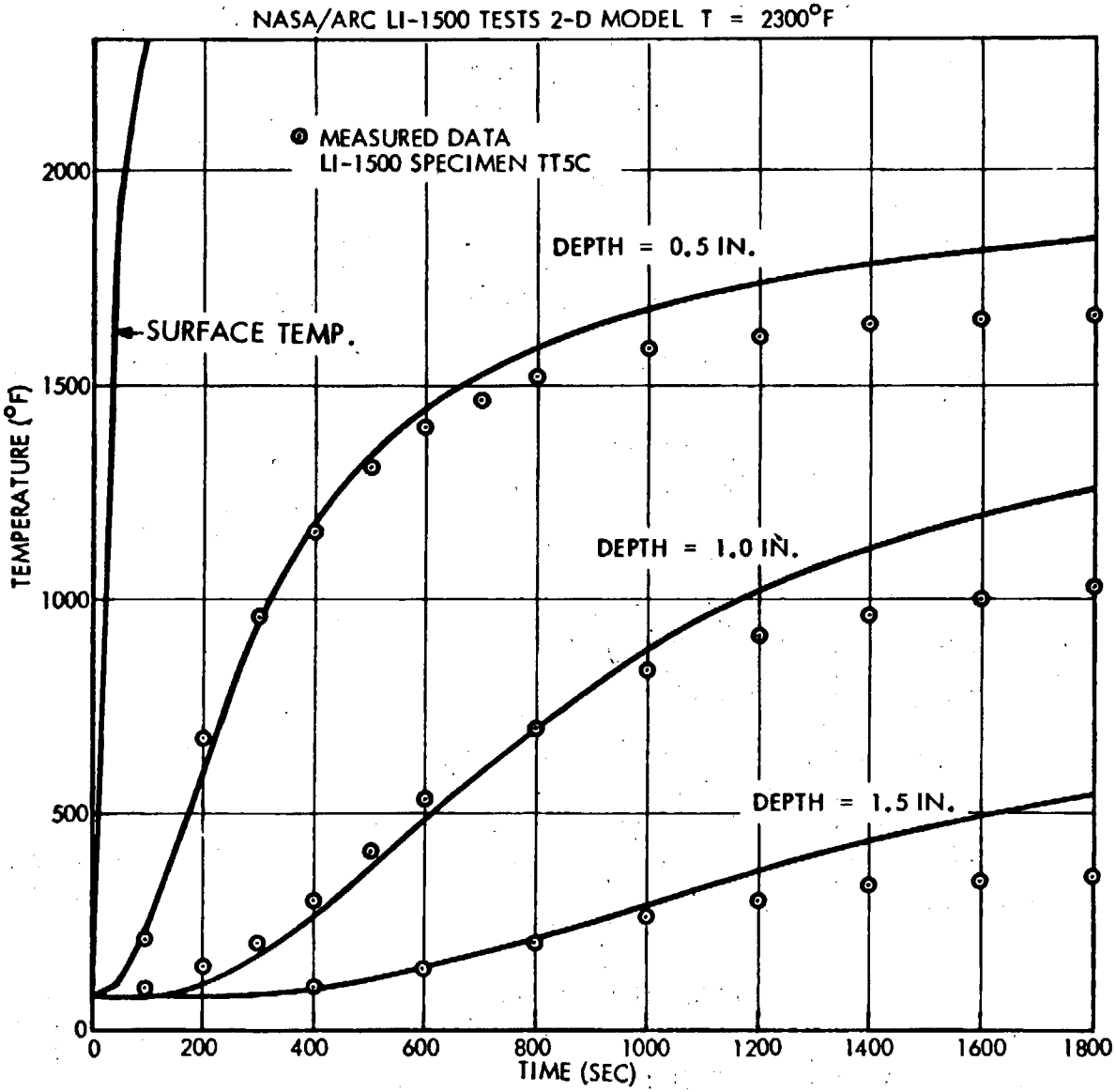

Fig. 3.2-9

3.3 POTENTIAL FAILURE MODES

Throughout the testing and analytical investigations, an effort has been made to identify the possible failure modes of an RSI system in general and to estimate the potential of LI-1500 performance in relation to these failure modes. Failure modes can be regarded at various levels in relation to the total Shuttle design (i.e., one failure mode for the orbiter would be loss of a sufficient quantity (area) of the RSI so that an entry phase overheating failure* occurs, whereas the corresponding failure mode for the RSI might be a bond/attachment failure). With respect to the RSI, the orbiter failure modes would be related to either a loss of a significant quantity of the RSI or a degradation of the properties of the RSI which serve to protect the orbiter from the entry heating (i.e., the thermal conductivity, and the surface emittance). Thus, the failure modes for the RSI would consist of those conditions/mechanisms that result in such a loss of the RSI (i.e., structural/bond/attachment failures and/or undetected degradation from flight to flight) and degradation of thermal properties resulting from the spectrum of Shuttle environments (storage, flight preparation, on pad, launch, orbit, entry, landing).

From this viewpoint, the inevitable occurrences of rock damage during landing, foreign body impact during ground and pad operations (wrenches, etc.), and bird impact during low altitude flight (after entry), would not be considered failure modes for the orbiter (even though they might result in significant RSI failure/degradation) because with proper flight preparation procedures, the effect of such occurrences would be detected and appropriate refurbishment/repair made to preclude subsequent orbiter failure.

LMSC presently considers the major potential RSI failure mode for the orbiter to be the loss of a tile/section of the RSI prior to or early in the reentry. Since the Shuttle reentry environment cannot readily be duplicated by ground testing, it is not possible at this time to completely answer the questions raised regarding this failure mode. However, development of nondestructive evaluation methods will reduce the loss probability. In general, loss of an RSI tile could result from any one of many conditions such as:

*Such a failure could be quantified in terms of a reduced probability of a safe entry and landing.

- Bond/attachment failure
- Undetected RSI cracks from previous flights
- Overstress condition
- Overtemperature condition
- Large amplitude buckles in the structure
- Orbital operation

A sound efficient detailed design of the RSI/TPS will preclude tile loss due to the normal operating environment. Such a design relies in part on accurate definition of material properties and a failure mode theory upon which to base the analytical efforts. LMSC has conducted combined stress tests on LI-1500 in weak shear and normal tension as the first step in establishing a failure theory. A linear interaction is indicated by the results of these tests (and this theory has been considered in the design of the prototype panels for delivery to NASA/MSC). Consequently, treating only uniaxial stresses with full allowable stress would result in design failure. In the absence of biaxial data, the safe design approach would be to reduce uniaxial stress allowables by 50 percent (this would be equivalent to a rectangular stress envelope with a corner on the linear interaction curve). The resulting design would be lacking in efficiency, because 50 percent of the possible stress combinations under the linear interaction curve fall outside of this reduced allowable rectangle. LMSC's development of this failure theory, testing, and design impact is discussed in detail in Vol II, Sections 2.5 and 6.7.

The expected performance of LI-1500 in relation to the potential failure inducing conditions cited above is discussed below.

LMSC is considering RTV 560 as a baseline bond primarily because of the quantity of successful testing that has been accomplished and positive analytical results that have been obtained with this bond. However, it is felt that this bond is not suitable under cold soak conditions where the bond would be at low temperatures around -200°F. Therefore, LMSC has considered other means of installation to preclude imposition of mission constraints. LMSC has developed a strain arrestor concept which shows considerable promise and is also looking into foam bonds as part of a related effort.

Thus, with regard to bond/attachment failures, LMSC feels that more effort is required to determine the optimum approach.

In the past, failure of the coating and LI-1500 due to overshoot surface temperatures has been considered a potential failure node. LMSC has conducted radiant tests to 3000°F. These tests have shown that no catastrophic failure would occur for such a condition.

Since LI-1500 is an amorphous all-silica material system, concern has been expressed that a phase change near the surface could take place after many cycles. The postulated failure states that with volumetric change crystallization could result in layered cracking near the surface. If such a failure occurred, the coating and a portion of LI-1500 could be lost during flight. LMSC does not consider phase change a problem. In all development testing performed on the LI-1500 system to date, no such cracks have occurred. Improvements in the material have greatly retarded start of phase change. The 100-cycle tests (Section 3.1) in which the total thermal environment was much more severe than expected on the shuttle were completely successful. Post-test analysis of one specimen from these tests is included in Section 3.1.

Other areas of a lower level of concern include those means by which some surface cracking or material defects may develop; however, these potential defects (see discussion below) would be handled by proper procedures of detection and repair/refurbishment rather than resulting in orbiter failures.

The presence of significant water in LI-1500 during liftoff has been assessed. With the current LMSC system of an impervious coating, backed up with a waterproof treatment, water can occur in only small areas. To absorb water, cracks must be present after a flight and water introduced prior to the waterproof treatement. It is shown in Section 5.3 that such a condition could result in local coating loss during a mission ascent and reentry cycle. The tests performed at MSC on the LMSC gap model from Task 5.2 indicated the same results. That specimen (with unprotected sides) was sprayed with water during a test in which an equipment failure occurred. The subsequent test at reduced pressure resulted in coating loss as the specimen was

introduced into the arc-jet stream. Subsequent tests on the same model resulted in only minor degradation of the uncoated surface. This type of failure is not considered to be potentially catastrophic nor would it preclude refurbishment and reuse of the vehicle.

Manufacturing anomalies could also give rise to failures in the LI-1500 system. Of particular concern are resulting overstress conditions, if designs are not duplicated in fabrication and assembly. As shown in Section 6.1, the design of the prototype panels calls for the bondline to be discontinuous between tiles. Quality control procedures must be established and careful detail attention given in shuttle application. As discussed in Vol II, Section 3.2, stress levels could be doubled if the bond is not discontinuous.

3.4 ATTACHMENT METHODS

The present LMSC baseline utilizes bonding of LI-1500 to the various vehicle metallic surfaces. The various bonding agents and mechanical fastener schemes considered by LMSC are presented in Section 5 of Volume II. As noted, RTV-560 has been selected as the adhesive system offering the best characteristics of the commercially available adhesives.

3.4.1 Adhesive Bonding

Properties of adhesives for the various shuttle environmental conditions are not available in the literature. Therefore, LMSC has conducted some limited testing to establish critical design properties. The major design driver in establishing minimum bond thickness is shear modulus. To establish this property, shear tests were run at temperatures up to 600°F, using a double shear fixture shown in Fig. 3.4-1.

In this fixture, a bond area of 3.00-in. length by 0.50-in. width is tested on both sides of a rod having a half-inch square cross-section. To create double shear, a bar cut in the shape of a tuning fork served as the other bonding face. The stem of the tuning fork and the square rod are colinear and coincide with the axis of applied force. This is illustrated in Fig. 3.4-2. The "jaw" of the tuning fork is machined to a specific width so that when the rod is correctly centered in the jaw, the gap between the fork and the rod (to be filled with elastomer) has a carefully controlled width. The alignment and centering during bond application is maintained by a template which has pins that pass through the stems of both the fork and the rod.

For test at high temperature, holes are drilled in the fork and rod, and thermocouples are embedded in the holes to monitor the temperature at the rod or fork mid-thickness and very near the bond (0.050 to 0.060 in. away). To prevent excessive heat from the heat lamps from burning the outermost layer of bond (while attempting to heat the center), the outer (exposed) bond area is covered with heavy foil that serves to shield the bond material from the direct radiation of the lamps. The surface of the fork

HIGH TEMP BOND TEST FIXTURE AND BOND SHEAR TEST SPECIMEN

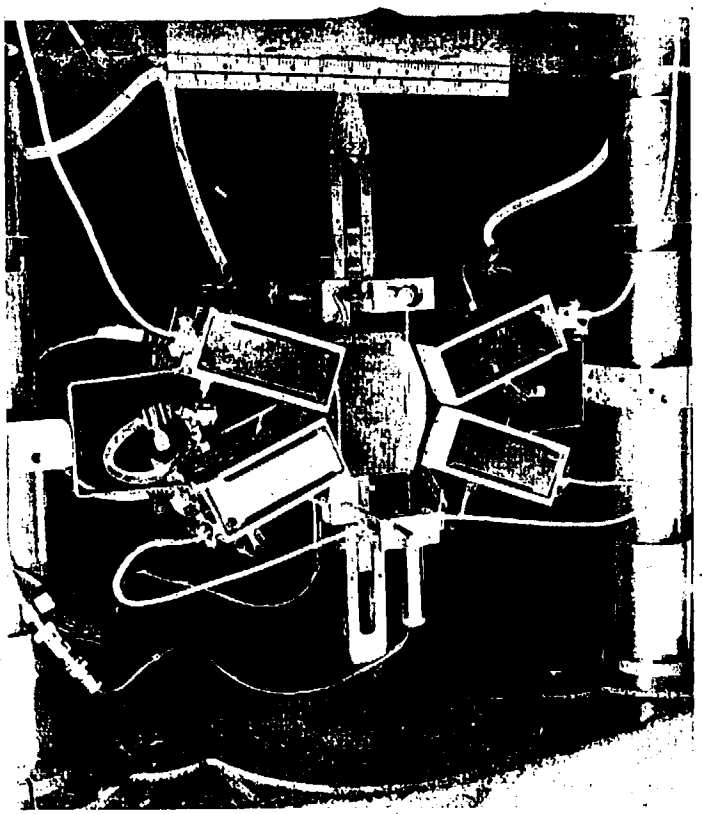

Fig. 3.4-1

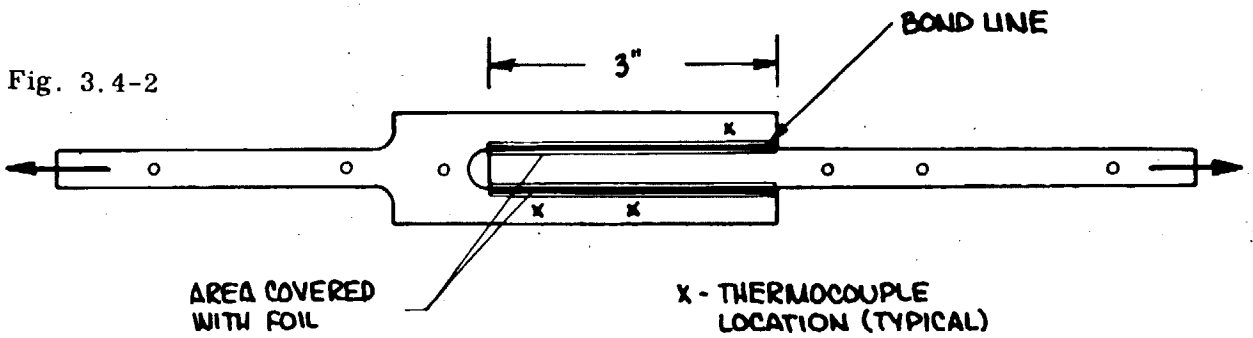

Fig. 3.4-2

and rod are coated with a black paint of high absorptivity so that the heat penetrates the fork and rod and reaches the bond through conduction. The three thermocouples indicated that at 500°F the temperature spread on the three thermocouples is within a range of 10°F during the test.

The strain was measured by two averaging deflectometers placed outside the heated zone and connected to the rod and fork by two pairs of brackets. The brackets were attached to the fork and rod (respectively) at points only 1 in. from the termination of the bond line, so that deformation of the rod and fork (especially at the low failure loads involved) is minimal. Load versus the averaged deflection was recorded on an X-Y plotter. Table 3.4-1 shows the results of the shear tests performed at 500°F and 600°F. The average shear modulus results from these tests at 500°F and 600°F are 67 psi and 21 psi respectively. Since a higher value of shear modulus is conservative in relation to the load imposed on the LI-1500, LMSC is currently using a value of 67 psi for both the 550°F flight load condition and the 600°F post-landing condition. Further, a modulus of elasticity of 200 psi has been inferred from this shear modulus by the structural mechanics relationship $E = 2(1 + \mu)G$, where Poisson's ratio, μ, equal to 0.5 is assumed.

The techniques of controlling bond line thickness and application techniques are under investigation and will be continued for ultimate use on the prototype panel.

In addition to the shear tests on RTV 560, LMSC conducted two thermogravimetric analysis (TGA) tests to determine the weight loss at temperatures up to 600°F. The tests were conducted in an air and helium environment at a heating rate of 3°C/min. The results indicated a weight loss of 2.61 percent in air and 2.58 percent in helium after heating to 600°F. At 300°F there was no recordable weight loss. Based on manufacturer's data and the results obtained at LMSC, no degradation is expected for the applications at 300°F. For the 600°F application, the 2.6 percent weight loss reported could be attributed to volatiles which are not expected to degrade the performance of the adhesive.

Table 3.4-1

RTV-560 BOND SHEAR TESTS

Bond Thickness (in.)	Specimen Number	Maximum Load at 600°F (lb)	Maximum Shear Stress at 600°F (psi)	Shear Modulus at 600°F (psi)	Shear Modulus at 500°F (psi)
0.020	A1	52	17.3	28.1	78.5
0.020	A2	38	12.7	23.8	59.4
0.030	B1	18	6.0	11.8	53.3
0.030	B2	33	11.0	17.9	84.0
0.040	C1	18	6.0	19.6	54.4
0.040	C2	34	11.3	25.8	70.0

3.4.2 Mechanical Attachment

Although LMSC has baselined bonding as the LI-1500 attachment method at this time, the use of mechanical fasteners or a combination of both may evolve to be the best method for actual shuttle application. Mechanical attachments have been considered for some time at LMSC as a method of strain isolation and were discussed in the final report for the previous contract, NAS 9-11222 (MSC-02567). Design efforts have investigated fasteners under this contract and promising concepts are reported in Vol II, Section 5. LMSC plans to continue investigations of this method of attachment. However, reliable test-proven designs must be established prior to baselining mechanical attachments.

These concepts involve two basic methods for retaining the LI-1500: (1) tap and locally densify, and (2) the use of a carrier plate bonded to the LI-1500. The use of a subpanel (Prototype Panel 1) is in essence a large carrier plate isolating the LI-1500 from primary vehicle loads. The feasibility of tapping and densifying has been proven by test, as reported in Fig. 5.2-4, Vol. II.

Attachment of the tile or carrier panel to the structure also involves two basic methods: (1) fasteners pushed into receptacles with high pull-off loads for removal, and (2) fasteners that lock by access through a small hole from the outer surface.

Although all methods appear promising, insufficient test data exist for use at this time. LMSC has fabricated a bayonet type fastener, but within the contract time span could not develop a reliable receptacle that would allow removal and reattachment from outer surface access only. This fastener is shown in Fig. 3.4-3a. Although this fastener was to be tapped into the material, the stud section could also be used on a carrier plate. To preclude thermal growth overstress problems on the LI-1500, as discussed in Section 3.2 Vol II, this fastener was made of Invar.

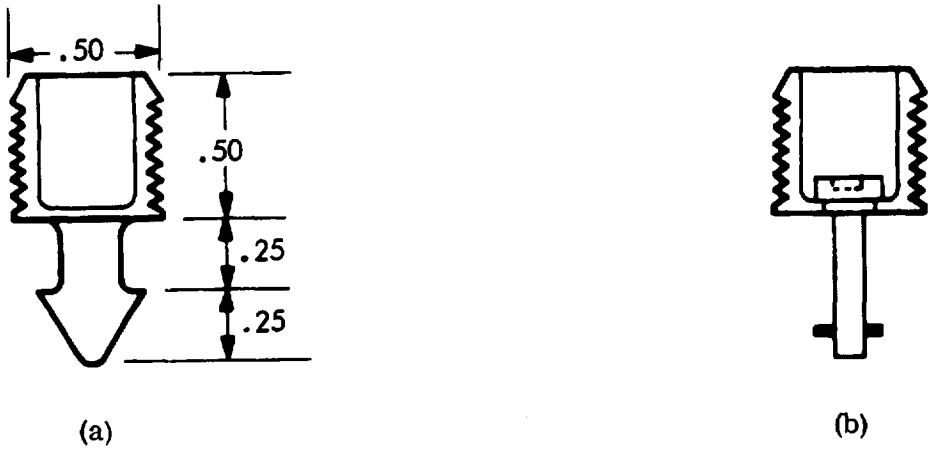

Fig. 3.4-3 Invar Fastening Devices

A second fastener was fabricated that required access from the outer surface for installation and removal. This fastener was also made of Invar and is shown in Fig. 3.4-3b. Only the threaded portion that transfers shear into the LI-1500 was fabricated. This type fastener appeared promising early in the program. However, the effect of the penetration through the coating would result in stress concentrations that could lead to coating cracking. A second problem to be faced is how to coat and/or waterproof the inside of the hole. Although a few random coating cracks over the vehicle would pick up minor weights of water following reentry, three or four unprotected holes in each tile would pick up a substantial amount of water if rain was encountered following reentry. Therefore, the concept does not appear to be feasible at this time.

3.5 NONDESTRUCTIVE EVALUATION (NDE) METHODS

The development of reliable economical NDE techniques for post-flight inspection of the LI-1500 TPS is required to qualify the system for shuttle application. LMSC has conducted in-house programs in this area to determine the feasibility of various methods of NDE. The groundrule has been established in this study that no access to the TPS backface is possible. During the past year, the following methods have been evaluated for potential use:

- Microwave
- Audible sonic ringing test
- High and low frequency ultrasonic
- Acoustic emission test
- Laser holography
- Laser vibrascope
- Infrared test (conventional and laser heat source)

Three of these methods show promise for post-flight TPS inspection: microwave, audible sonic ringing, and laser vibrascope. The microwave technique has proven useful in detecting unbonded areas (0.50 x 4.0 in.) and the presence of water in the material. The audible sonic ringing technique was developed at LMSC and shows promise in detecting cracks in the LI-1500. The laser vibrascope technique also shows promise in detecting cracks.

A separate report* on this in-house effort has been prepared. This report describes the test techniques, samples used, and results in detail for all methods evaluated. This report will be made available to NASA/MSC.

---

*Walton, R. F., "Methods for Nondestructive Evaluation (NDE) of LI-1500 Reusable Surface Insulation," LMSC-A999485, 3 Jan 1972

Section 4
PROPERTY CHARACTERIZATION

The objective of this task is to obtain detailed physical, mechanical, and thermophysical properties of LI-1500 and surface coating. The testing program has followed the Property Test Plan (LMSC-A991210) approved by NASA/MSC during the second month of the contract. This final document reports on the results and compares them with previous data.

4.1 THERMOPHYSICAL PROPERTIES

4.1.1 Specific Heat

A flooded-ice mantle drop type calorimeter was used to measure the enthalpy of the LI-1500 material, referenced to 273°K, over the temperature range from 200°F to 1800°F. The specimen was contained in an oxidized Type 316 stainless steel capsule for temperatures up to 1800°F. The specimens were heated in an air atmosphere in an alumina furnace for the measurements to 1800°F.

Enthalpy measurements were made on 12-gram specimens of the material, pulverized to obtain maximum mass for the capsule. Specimens were taken from as-fabricated LI-1500 and from LI-1500 which was thermally cycled in a 1-atmosphere air furnace for a total of 20 half-hour cycles at 2300°F. Preliminary calculations of specific heat were made, using a graphical fit of the enthalpy-temperature data. These results are shown in Fig. 4.1-1. The data are in agreement with those reported earlier (NAS 9-11222) and no significant differences were observed between the as-fabricated and the thermally cycled specimens.

VARIATION OF LI-1500 SPECIFIC HEAT WITH TEMPERATURE

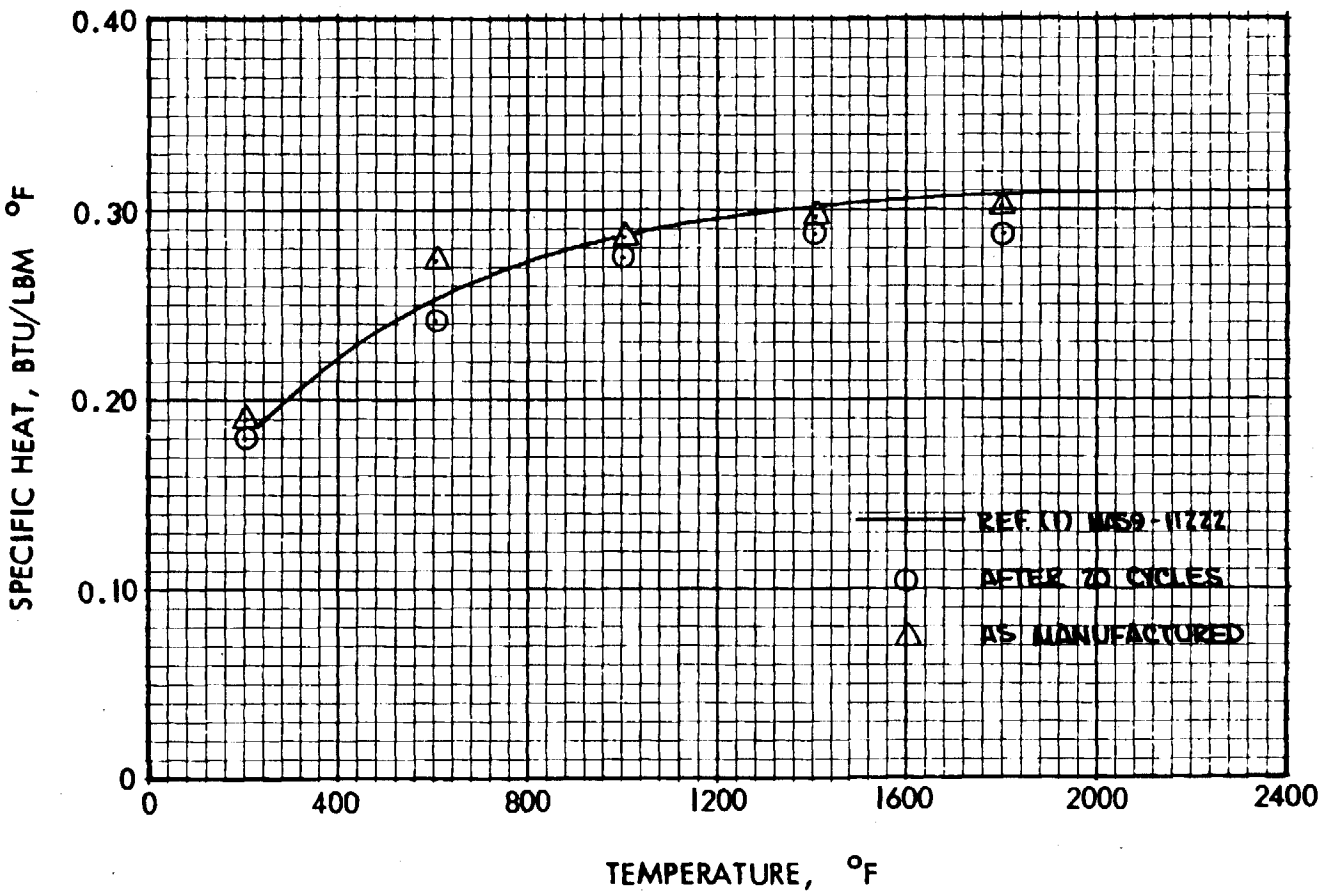

Fig. 4.1-1

DO6002

4.1.2 Thermal Expansion

Measurements of linear thermal expansion were performed in an air atmosphere over the temperature range from 70°F to 2350°F. Measurement directions were parallel and normal to the thickness direction of the as-fabricated material and material that was exposed to 20 thermal cycles of half-hour exposure to 2300°F in a 1-atmosphere air furnace. Push-rod dilatometers of two materials were used for the measurements. A fused silica dilatometer was employed up to 1650°F. This apparatus was initially calibrated against an NBS Fused Silica Standard, SRM 739, to within 5 percent over this temperature range. The specimens were heated in a furnace with a programmed temperature rate of 1.5 to 2°F/min over this temperature range. After cooling to room temperature the specimens were then placed in an alumina tube dilatometer for the temperatures above 1700°F. Dimensional changes were recorded at steady state temperatures using a calibrated dial gauge having a least count of 2×10^{-5} in. Exposure time from 1700° to 2300°F varied from 1-1/2 to 2 hours.

Three specimens were measured for both directions from the as-fabricated material. For the normal-to-thickness direction (parallel to the fiber orientation) the specimen size was 3 in. x 3/8 in. diameter rods. The specimen for the parallel-to-thickness direction (normal to the fiber orientation) was composed of two 1-1/2 in. x 3/8 in. diameter rods stacked to give an overall length of 3 in. This length was chosen to increase the measurement accuracy for low expansion material.

Specimen dimensions and pre-test exposure conditions together with post-test length and weight change data are given in Table 4.1-1. All specimens showed a negligible weight loss and a shrinkage of 0.9 to 1.4 percent. Exposure time at the highest temperature varied, and this undoubtedly had an effect on the recorded dimensional change. Also, pre- and post-test X-ray diffraction patterns were obtained to determine if the test exposure resulted in a change in crystal structure of the material. Results of the X-ray diffraction patterns for Specimens 1, 4, 20-1, and 20-4 did not reveal the presence of cristobalite or α quartz.

Thermal expansion data for Specimens 1 through 6 (pre-cycling) are shown in Fig. 4.1-2 and 4.1-3. Data for the material after exposure to 20 thermal cycles are shown in

Table 4.1-1

THERMAL EXPANSION SPECIMEN DESCRIPTIONS

Direction	Exposure Prior to Expansion Measurement	Specimen Number	Define Test Bulk		Post Test	
			Length (In.)	Density (Lb/Ft^3)	Length Change (%)	Weight Change (%) [a]
Perpendicular-to-Block Thickness (fiber orientation direction)	As Manufactured	1*	3.001	14.6	-0.9	<0.3
	As Manufactured	2	2.999	12.8	-1.0	<0.3
	As Manufactured	3	2.958	14.6	-1.0	<0.3
	After 20 thermal cycles	20-1	3.092	15.6	-0.9	<0.3
Parallel-to-Block Thickness (normal to fiber orientation)	As Manufactured	4*	2.992[b]	14.3[b]	-1.3	<0.3
	As Manufactured	5	2.990[b]	13.7[b]	-1.4	<0.4
	As Manufactured	6	2.988[b]	13.9[b]	–	<0.4
	After 20 thermal cycles	20-2	3.090[b]	15.4[b]	-1.0	<0.3

(a) Weight change may be due in part to abrasion of specimen during handling.

(b) Two specimens stacked end-to-end, density is average of two specimens.

* Pre- and post-test X-ray diffraction patterns did not reveal any phase changes.

THERMAL EXPANSION IN DIRECTION PARALLEL TO FIBER ORIENTATION

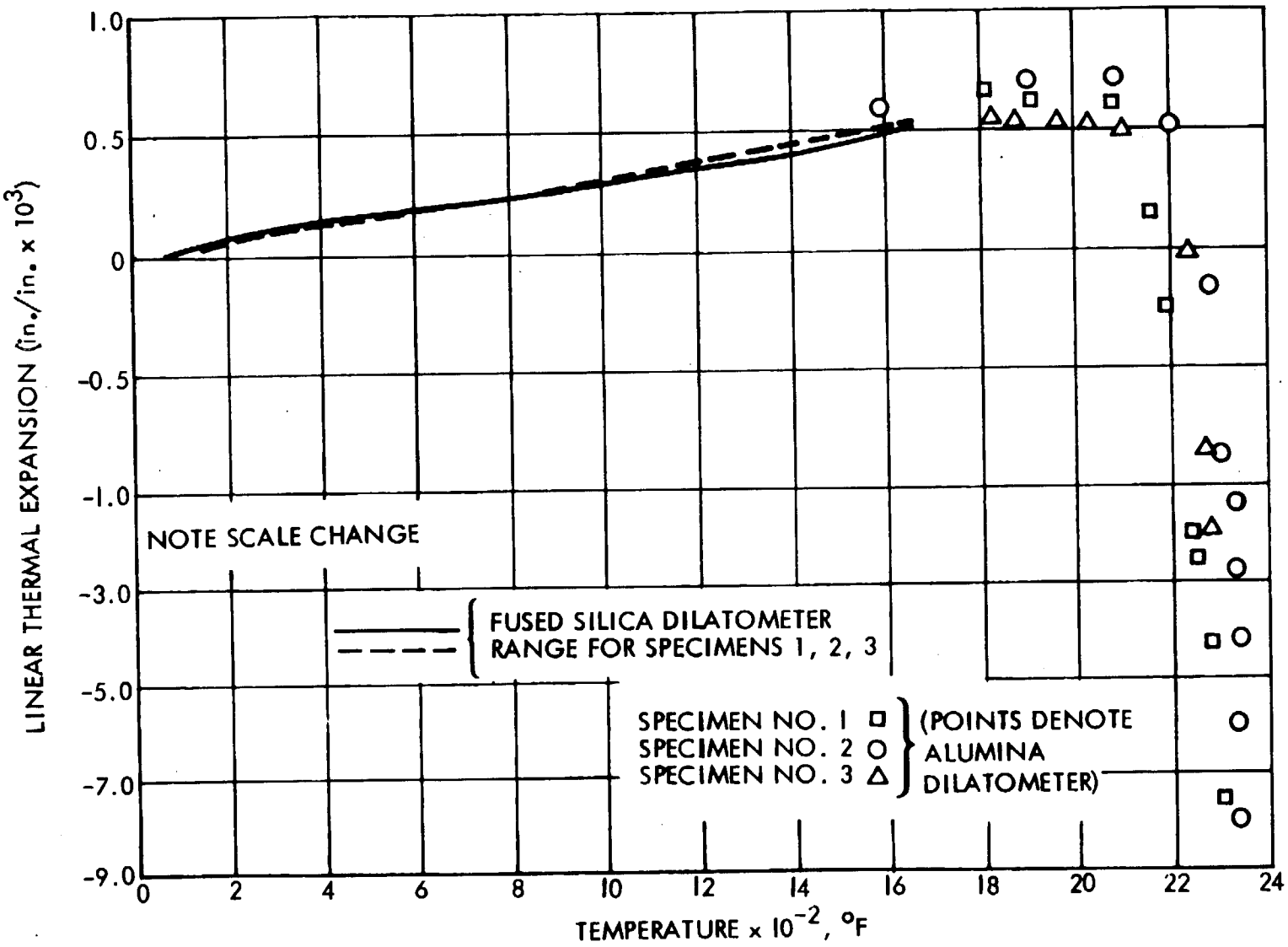

DO6118

Fig. 4.1-

LOCKHEED

THERMAL EXPANSION IN DIRECTION NORMAL TO FIBER ORIENTATION

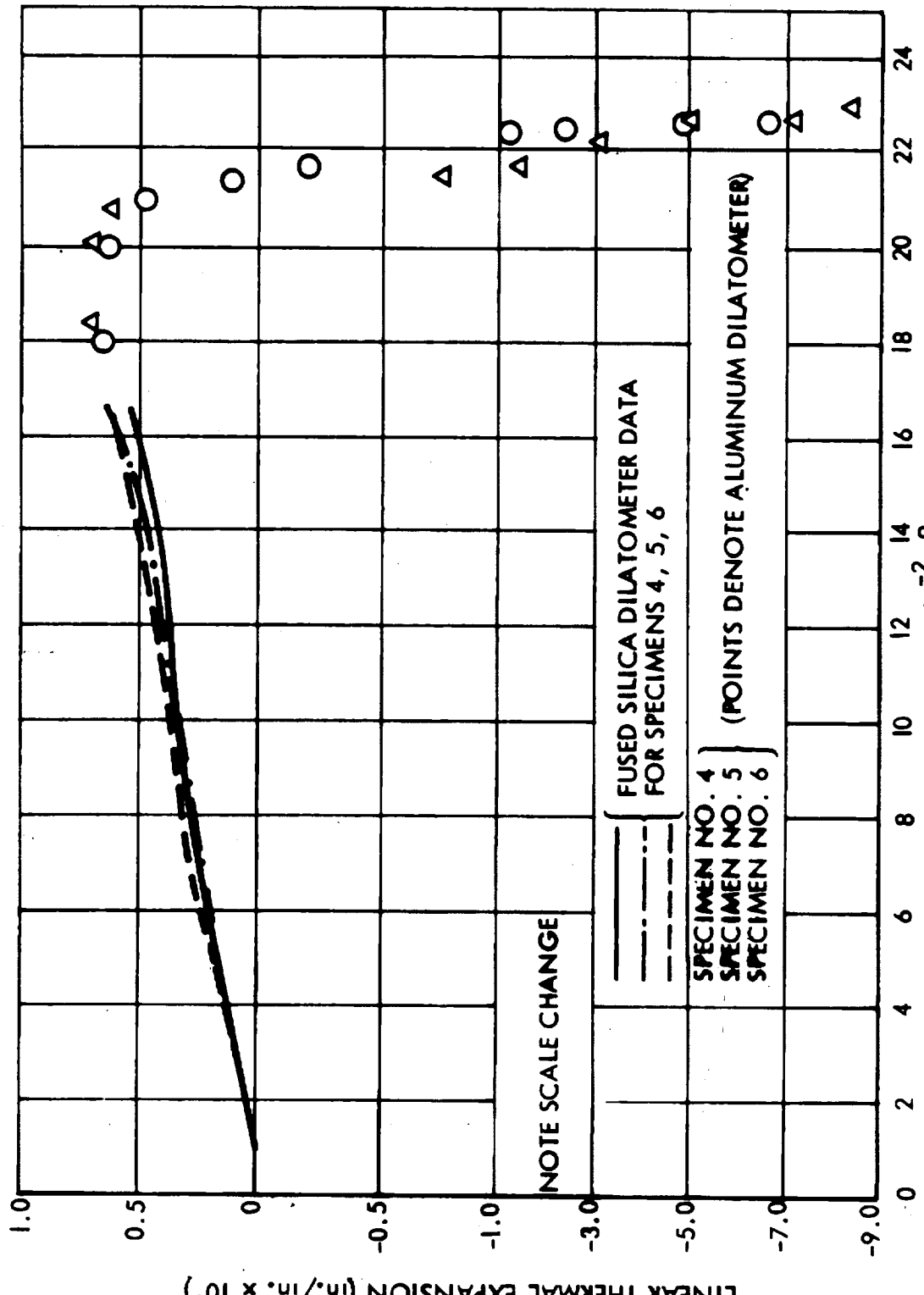

D06119

Fig. 4.1-3

Fig. 4.1-4. In all cases, the as-manufactured material started to shrink in the temperature range of 2100° to 2200°F. The post-20-cycle material showed the start of shrinkage in the 2000° to 2050°F range.

Table 4.1-2 gives a comparison of expansion at several temperatures for all of the specimens tested. The exposure to 20 thermal cycles did not have a significant effect on the expansion behavior of the material. Thermal expansion coefficients between 70° and 2000°F ranged from 3.3 to 3.6 x 10^{-7} in./in. °F for Specimens 5 and 6, and 2.8 to 3.8 x 10^{-7} in./in. °F for Specimens 1 through 3. For the post-thermal cycling specimens, expansion coefficients were 2.7 to 3.0 x 10^{-7} in./in. °F for normal and parallel to fiber orientation directions, respectively.

Comparison of the as-fabricated thermal expansion coefficients over past contracts is shown in Table 4.1-3. The thermal expansion coefficient in the fiber orientation direction has remained fairly constant for the various batches shown. The high value of expansion coefficient reported under NAS 9-11222 in the normal to fiber orientation direction is attributed to impurities in the raw fiber used to manufacture LI-1500. This situation has been remedied as evidenced by the current low values of thermal expansion coefficient.

The thermal expansion of the new surface coating (0042) which was recently brought on-line as a result of the Material Improvement Contract, NAS 9-12137, is shown in Fig. 4.1-5. The specimen consisted of two 3/8-in. diameter by 1.5-in. long cylinders of cast 0042 coating placed end-to-end to form a 3/8-in. diameter by 3.0-in. test specimen. The apparatus was discussed earlier with the data for the LI-1500 thermal expansion. The data show a decrease in expansion at temperatures near 2000-2200°F, which apparently indicates the scftening point of the coating. The thermal expansion coefficient as a function of temperature is shown in the following table.

Temp °F	α in./in. °F
70	5.6 x 10^{-7}
900	5.6 x 10^{-7}
1050	4.3 x 10^{-7}
1400	2.5 x 10^{-7}
1600	2.5 x 10^{-7}
1900	0

THERMAL EXPANSION FOR THERMALLY CYCLED SPECIMENS

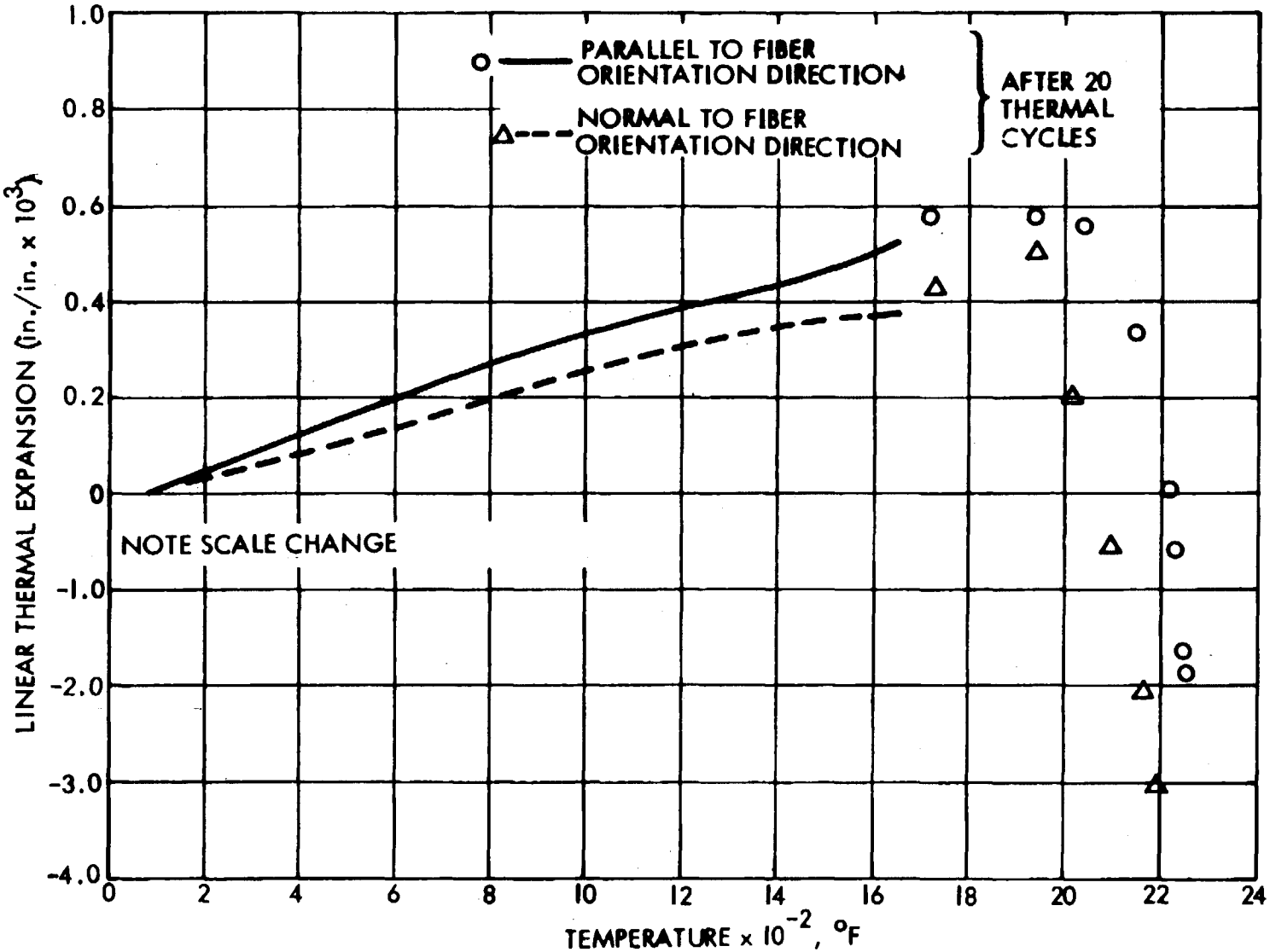

DO6124

Fig. 4.1-4

Table 4.1-2

COMPARISON OF LINEAR THERMAL EXPANSION BEFORE AND AFTER CYCLIC EXPOSURE TESTING IN PARALLEL AND NORMAL TO FIBER ORIENTATION DIRECTION

Temperature (^{o}F)	Before Cycling[a] (inch/inch)		After Cycling[b] (inch/inch)	
	Normal	Parallel	Normal	Parallel
400	9.7 to 13.5x10^{-5}	10.3 to 13.6x10^{-5}	8.6x10^{-5}	12.4x10^{-5}
650	20.1 to 25.1x10^{-5}	10.3 to 19.6x10^{-5}	15.1x10^{-5}	21.2x10^{-5}
900	30.3 to 33.8x10^{-5}	22.3 to 25.9x10^{-5}	22.5x10^{-5}	30.2x10^{-5}
1300	39.4 to 47.0x10^{-5}	37.7 to 42.3x10^{-5}	33.3x10^{-5}	41.0x10^{-5}
1650	54.6 to 62.7x10^{-5}	50.4 to 56.0x10^{-5}	37.6x10^{-5}	53.6x10^{-5}
2000	64.0 to 69.8x10^{-5}	53.0 to 73.0x10^{-5}		58x10^{-5}
2200	-40.0 to 200x10^{-5}	+52.0 to -25.0x10^{-5}		5x10^{-5}

Table 4.1-3

COMPARISON OF PAST LI-1500 THERMAL EXPANSION RESULTS

Source/Date →	LMSC 1967	SO R.I. 12-70	NAS 9-11222 2-16-71	Battelle 3-1-71	Battelle 7-1-71 (TT 14B)	NAS 9-12083 10-71
α Fiber Orientation Direction (in./in.-°F) 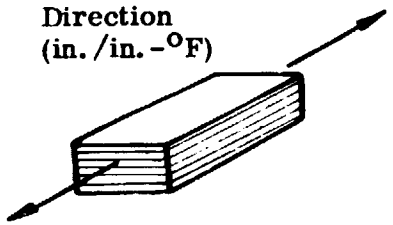	3×10^{-7}	5.1×10^{-7}	4.3×10^{-7}	$5\text{-}10 \times 10^{-7}$	$3\text{-}7 \times 10^{-7}$	$2.8\text{-}3.8 \times 10^{-7}$
α Normal to Fiber Orientation Direction (in./in.-°F) 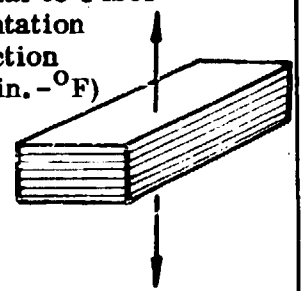	–	5.7×10^{-7}	2.7×10^{-6}	–	–	3.4×10^{-7}
Temperature Range (°F)	80-1700	80-2050	80-1700	80-1400	80-1700	80-2000

THERMAL EXPANSION OF 0042 COATING

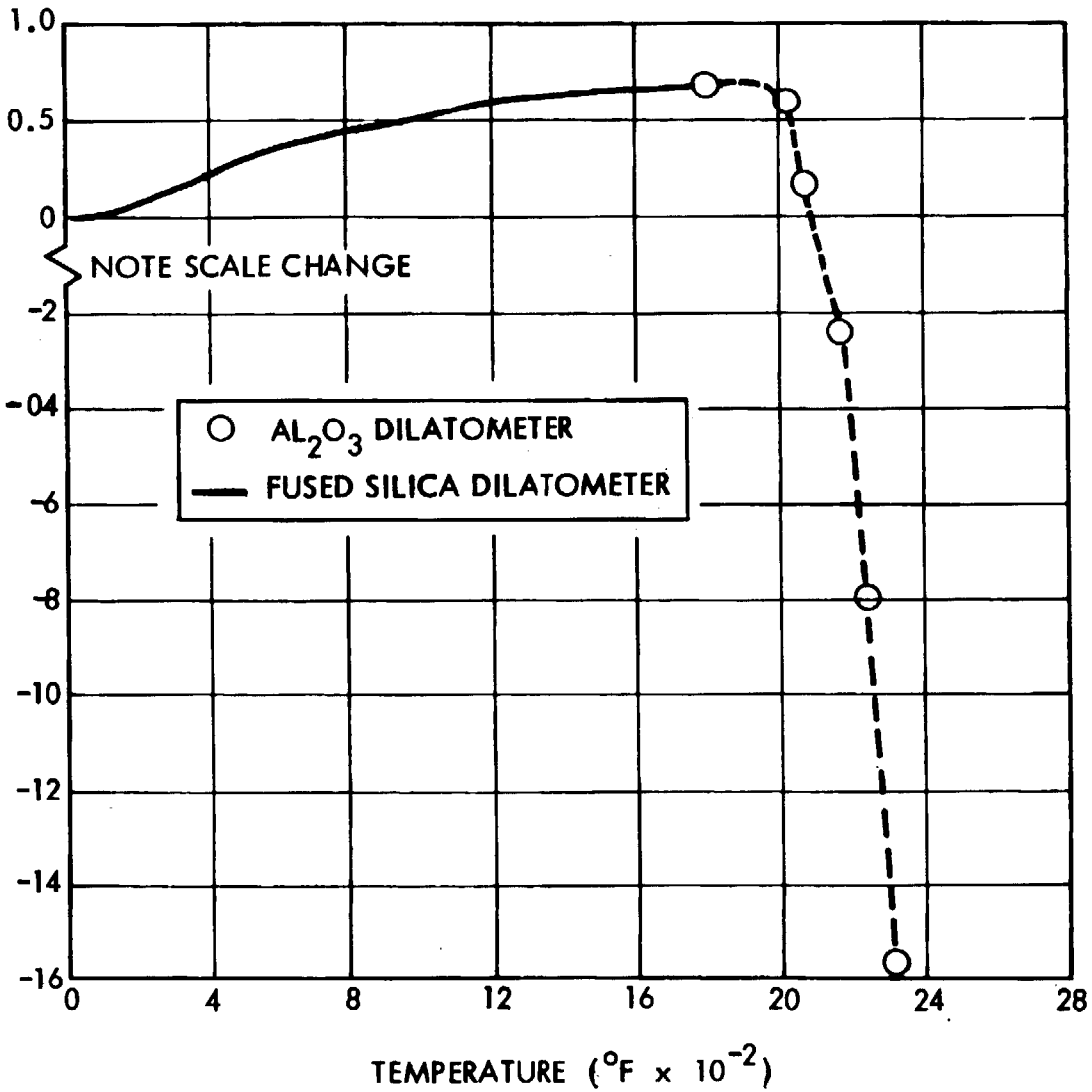

Fig. 4.1-5

The 0042 coating will be discussed further in the final report of the Material Improvement Contract.

4.1.3 Thermal Conductivity of LI-1500

To provide NASA with an independent evaluation of the thermal conductivity of LI-1500, a subcontract was let to the Southern Research Institute (So. R. I.) of Birmingham, Alabama. So. R. I. had previous experience measuring thermal conductivity of LI-1500 and Mullite under a contract from NASA/LaRC. A separate report* was issued by So. R. I.; this section summarizes the results of their tests.

So. R. I. used two pieces of equipment for the thermal conductivity measurements. At temperatures from -150 to 500°F, the tests were conducted with an ASTM C-177 guarded hot plate with a reported uncertainty of ±7 percent. At temperatures from 900 to 2000°F, the tests were conducted on a radial inflow apparatus (R.I.A.) with a reported uncertainty of +20 to -15 percent. This test equipment is described in the So. R. I. report.

The So. R. I. basic test philosophy consists of doing repeat data points on different specimens and fairing an average value through the data points, while relying heavily on the guarded hot plate results (because of lower uncertainty). LMSC agrees with the repeat data point approach – especially with low conductivity, high porosity materials like LI-1500 and especially when using small specimen thickness (0.10 in.) as in the radial inflow apparatus.

Specimens were provided to So. R. I. for tests on as-fabricated and thermally cycled material. As specified in the Property Test Plan and agreed to by NASA/MSC, the specimens were cycled at 2300°F in an oven for the equivalent time at temperature for 30 and 60 flights of an LMSC 1100-nm crossrange trajectory (RE214). This amounted to 5 and 10 hours at 2300°F. Based on the NASA/MSC perturbed temperature history for Area 2 on the delta wing orbiter (see design environment section) with about 2.5 minutes at 2300°F, the 5 and 10 hours at 2300°F corresponds to 120 and 240 flights, respectively. Hence the method of defining equivalent flights based on oven cycles is highly subjective.

*"The Thermal Conductivity of LI-1500 Rigidized Fibrous Insulation", E. D. Smyly Southern Research Institute, Jan. 18, 1972, PO EQZ6A8880F

If the equivalent flights were based on total heat, the following breakdown for the two different trajectories would result.

Reentry Trajectory	Total Heat Btu/ft^2	30 Min Oven Cycle Equivalent
LMSC RE214	16,000	2.5 Flights
NASA/MSC NAS 9-12083	26,500	1.5 Flights
30 Min Oven Cycle	~40,000	-

On a total heat basis, 10 and 20 oven cycles would amount to 25 and 50 equivalent flights based on the LMSC trajectory or 15 and 30 flights based on the NASA trajectory.

Therefore, whether the equivalent flights obtained from oven cycles are based on time at peak temperature or total heat, their meaning in terms of the actual reentry trajectory is not easily defined. For a reentry temperature history, the peak temperature occurs for a short time and the total imposed heating occurs while the surface temperature is transient from 70 to 2300°F and back to 70°F. In an oven cycle, the surface temperature is essentially constant and the total heat is imposed by a constant surface temperature.

One other consideration in oven tests is that unless the specimen is shrouded and allowed to receive energy on only one side as in the flight application, the oven specimen is usually heated from five or six sides which could result in the entire specimen being heated to 2300°F. In a flight application,the peak temperature distribution would be like that shown in Fig. 3.1-7 where for a peak surface temperature of 2500°F only the top 0.15 in. experiences temperatures above 2300°F. Hence, the oven cycle heats a larger part of the specimen to 2300°F than the flight application and results in a more severe temperature test. The thermal gradient is more severe in the flight application.

A thermal cycle consisted of placing LI-1500 in an oven preheated to 2300°F for 30 minutes. After 30 minutes, the material was removed and allowed to cool to room temperature and reinserted for a total of 10 to 20 cycles to accumulate the 5 and 10 hours at 2300°F.

Since the 2300°F during reentry occurs at very low pressure, the material used for the higher temperature tests, 900-2300°F, was cycled in a vacuum oven at a pressure of 10 mm Hg. For the low-temperature conductivity tests, -150 to 500°F, the material was cycled in an oven at a pressure of 760 mm Hg (1 atm) since, during reentry, the majority of the low temperatures within the LI-1500 occur at pressures of about 1 atm.

The thermal conductivity results for the as-fabricated and thermally cycled LI-1500 (5 and 10 hours at 2300°F) are shown in Fig. 4.1-6 and compared to the design curve from the previous contract (NAS 9-11222). The data are shown as fairings of the measured values, and the uncertainty band of ±15 percent from the design curve bounds the data at 2000°F and 760 mm Hg. Thermal cycling of the LI-1500 apparently results in a slight reduction in the thermal conductivity at high temperature for the 760 mm Hg condition and the 10-hour exposure specimens. The vacuum data indicate the 10-hour exposure specimens have slightly higher conductivity than the as-fabricated at temperatures from 1500-2000°F.

The data for the 5-hour exposure specimens are consistently lower than for the 10-hour exposure specimens but are still within the uncertainty band. Crystallography will be performed to determine if any significant changes occurred in the material. Hence, while the data indicate some reversals in thermal conductivity between the vacuum and 1 atm results, the data for all three sets of specimens are within the quoted uncertainty band.

The large difference in thermal conductivity between the vacuum and 760 mm Hg data, about a factor of 2 at 2000°F, is the primary reason for the large decrease in LI-1500 thickness (30 percent) for the flight panels discussed in Sections 2 and 6.

Figures 4.1-7, 4.1-8 and 4.1-9 show comparisons of the actual data points for the as-fabricated and thermally cycled specimens with the design curves of the previous contract. For low pressures, the data are generally in good agreement with the design curves.

COMPARISON OF DESIGN CURVES WITH RECENT THERMAL CONDUCTIVITY DATA

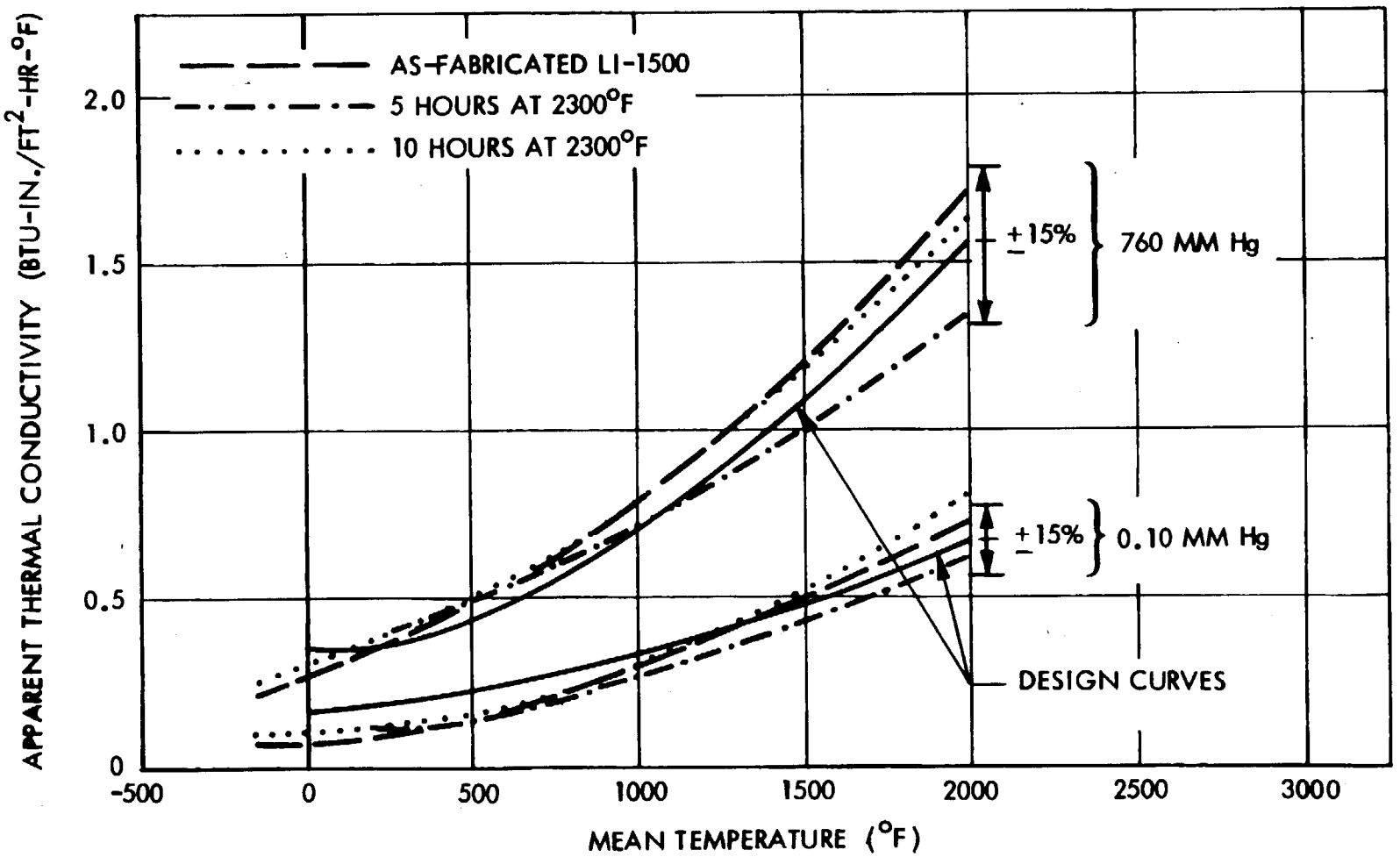

Fig. 4.1-6

COMPARISON OF DESIGN CURVES WITH THERMAL CONDUCTIVITY OF AS-FABRICATED LI-1500

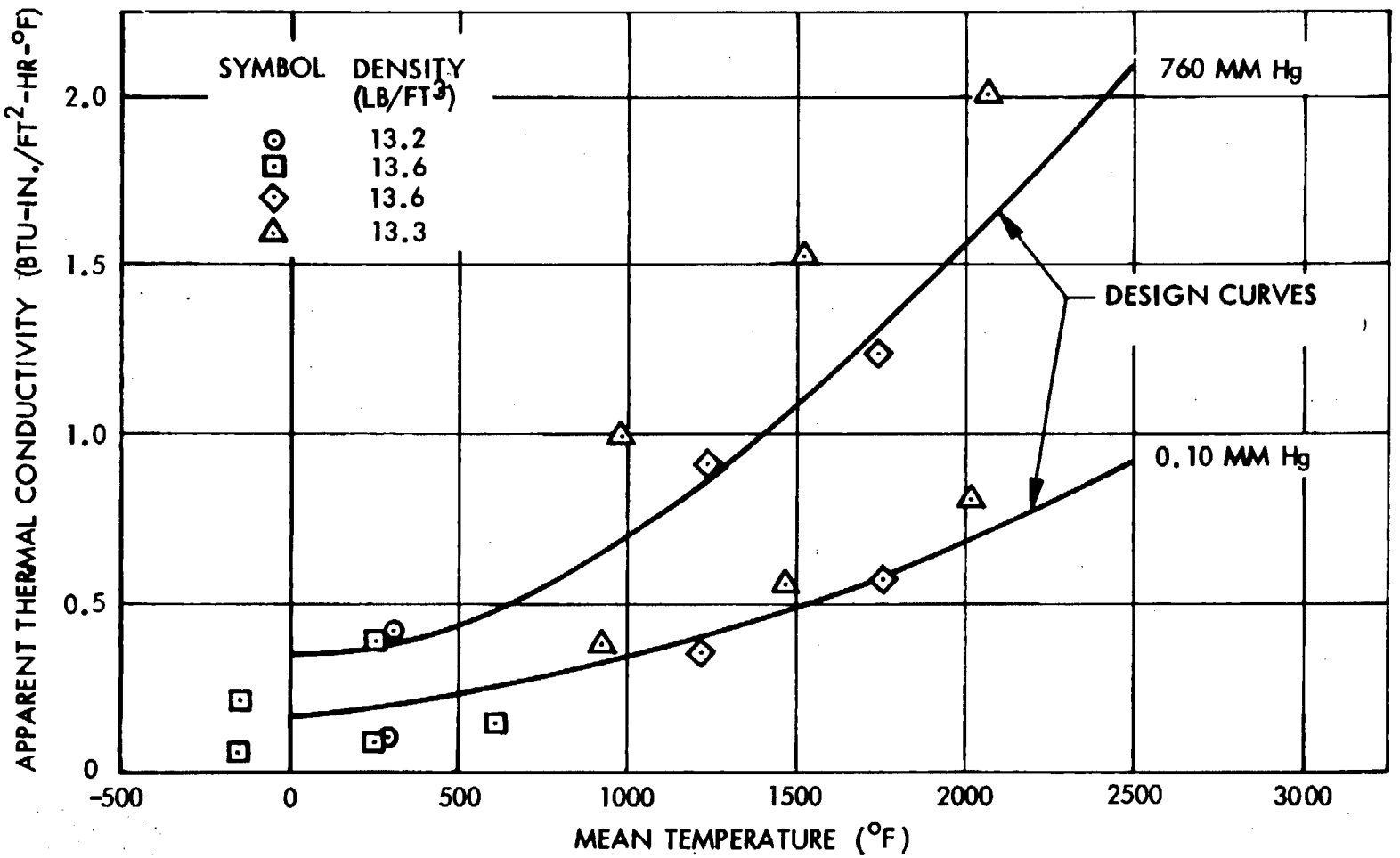

Fig. 4.1-7

COMPARISON OF DESIGN CURVES WITH THERMAL CONDUCTIVITY FOR THERMALLY CYCLED LI-1500

5 HOURS AT 2300°F

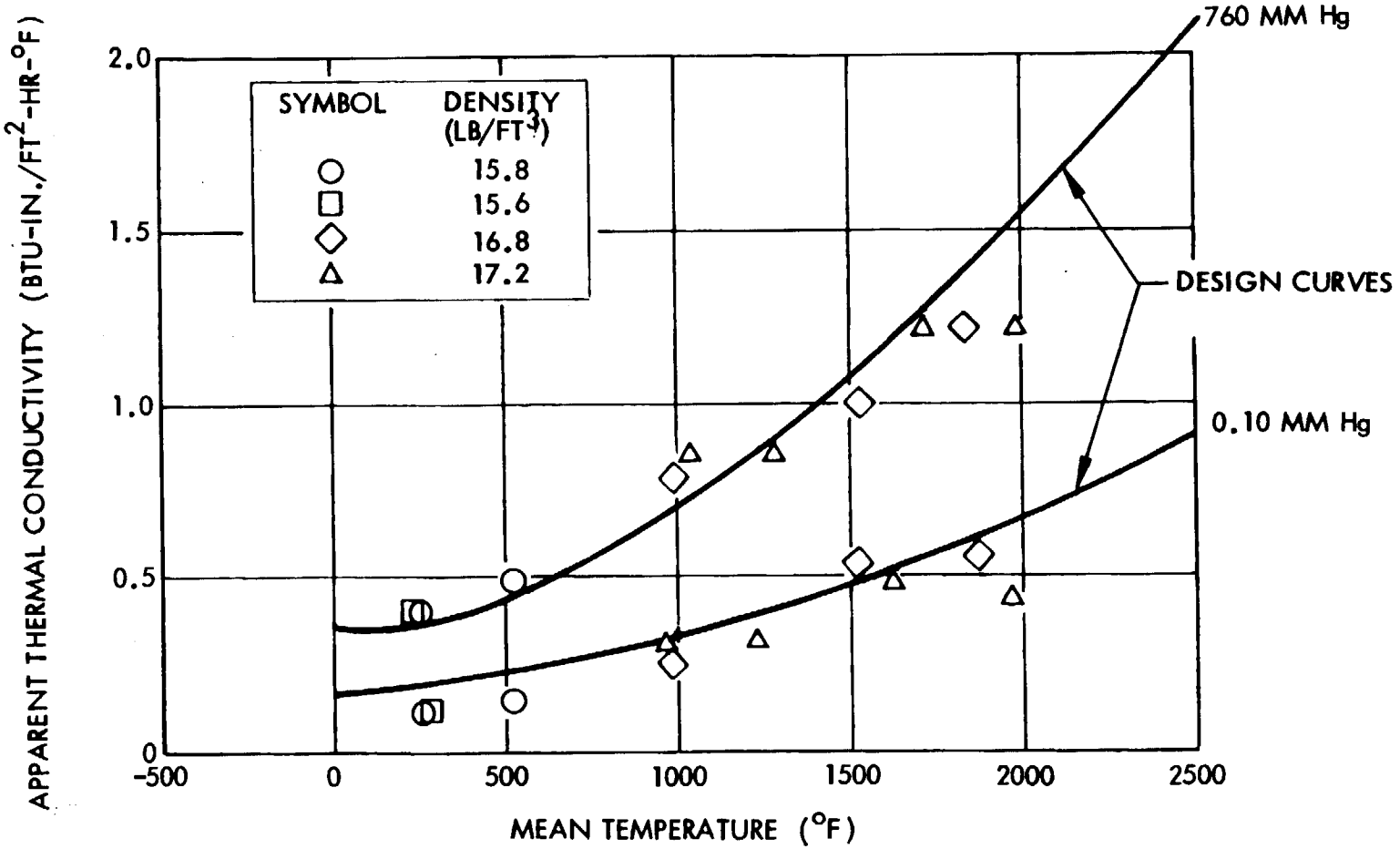

Fig. 4.1-8

COMPARISON OF DESIGN CURVES WITH THERMAL CONDUCTIVITY OF THERMALLY CYCLED LI-1500

10 HOURS AT 2300°F

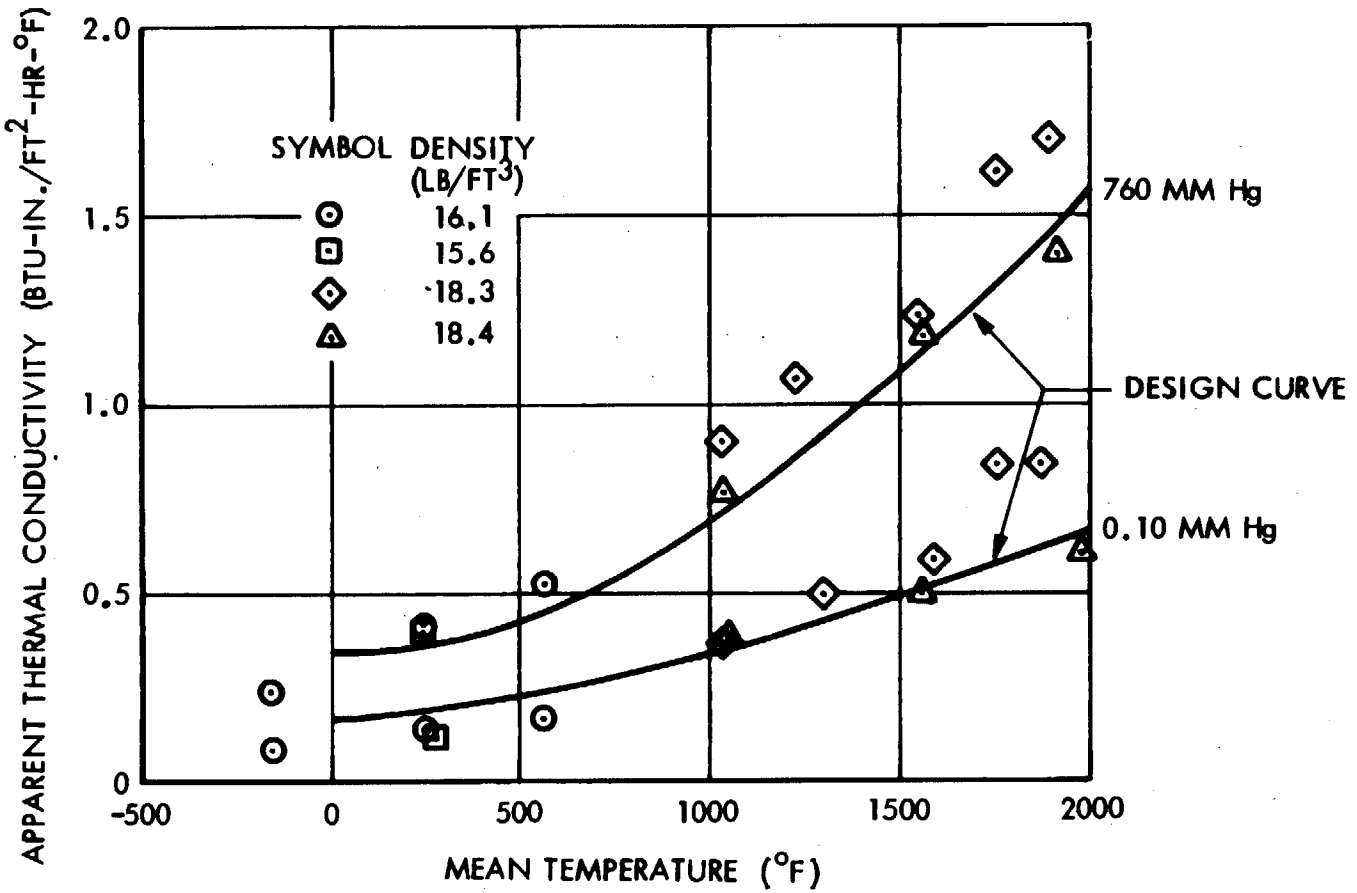

Fig. 4.1-9

At 1 atm pressure, one set of as-fabricated values is significantly above the design curve, but the data fairing as shown in Fig. 4.1-6 is within 5 to 10 percent of the design curve. The excellent agreement obtained using the design curve for the 100 cycle prediction (Figs. 3.1-7 and 3.1-9) tends to favor the design curve.

A comparison of the recently obtained data with data from other sources is shown in Fig. 4.1-10, along with the design curves. The measured spread in the data (about ±12 percent) is considered within the measuring uncertainty of the equipment and data reduction methods. Although the design curve appears low, initial correlations of 1-atm pressure radiant test data (Figs. 3.2-4 and 3.2-5) and low pressure arc jet data from NASA/ARC (Fig. 3.2-10) on LI-1500 currently favor the design curves. At both pressure levels the design curves are conservative (i.e., the calculations overpredict the measured temperatures), but more data correlations are required, especially in low pressure arc jet environments, to adequately establish design curves for the Shuttle application.

Some of the data in Fig. 4.1-10, the So.R.I. data of 11/70, was obtained on material fabricated in late 1969. Hence, even over a 2-year spread of material manufacture, the measured thermal conductivity has been relatively stable.

The variation of measured thermal conductivity with pressure for the as-fabricated LI-1500 is shown for four temperatures in Fig. 4.1-11. The data measured at 0.004 mm Hg are shown at 0.01 mm Hg, since no change in the gas conduction contribution to the total thermal conductivity is expected between these pressures.

The reduction in the apparent thermal conductivity between 760 mm Hg and 50 mm Hg is somewhat greater (22 - 30 percent) for the data shown than the reduction obtained from the design curves (12 - 18 percent). Hence, the design curves used somewhat higher thermal conductivities at pressures between 760 mm Hg and 0.10 mm Hg than the current data indicate but are conservative and are considered adequate for current design applications. The variation of thermal conductivity used for the flight panel design is shown in Fig. 4.1-12. The values at 760 mm Hg and 0.10 mm Hg are the design curves shown in Figs. 4.1-6 to 4.1-10. Tabulated values are shown in Table 4.1.4.

COMPARISON OF LI-1500 THERMAL CONDUCTIVITY DATA FROM VARIOUS SOURCES

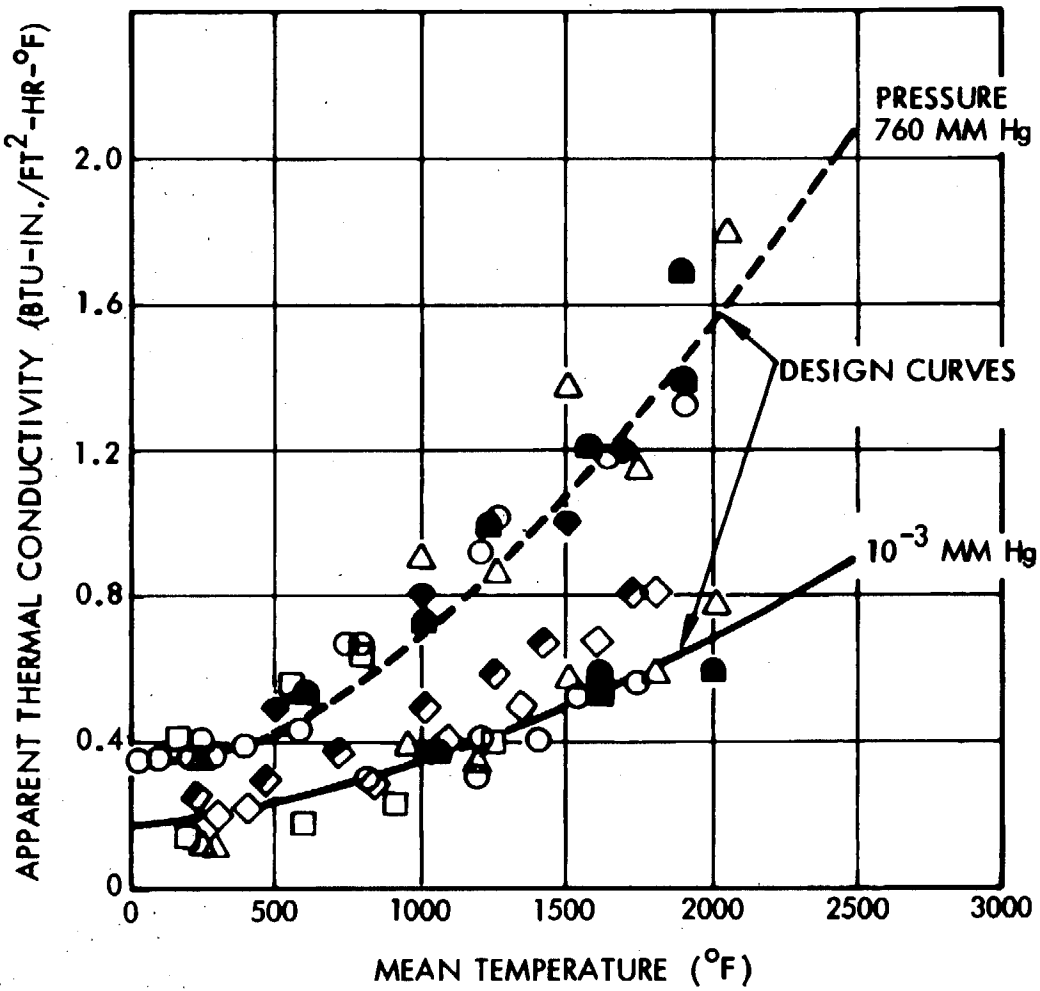

DATA SOURCE	DENSITY (LB/FT^3)
○ SO. R. I. (11/70)	
□ LMSC (12/70)	16.2
◇ BATTELLE (3/71)	15.0
◆ BATTELLE (7/71)	16.9
△ SO. R.I. (10/71)	13.8
● SO. R.I. (10/71) 10 HR AT 2300°F	18.0
◆ SO. R.I. (10/71) 5 HR AT 2300°F	17.0

Fig. 4.1-10

RECENT DATA SHOWING VARIATION OF LI-1500 THERMAL CONDUCTIVITY WITH TEMPERATURE AND PRESSURE

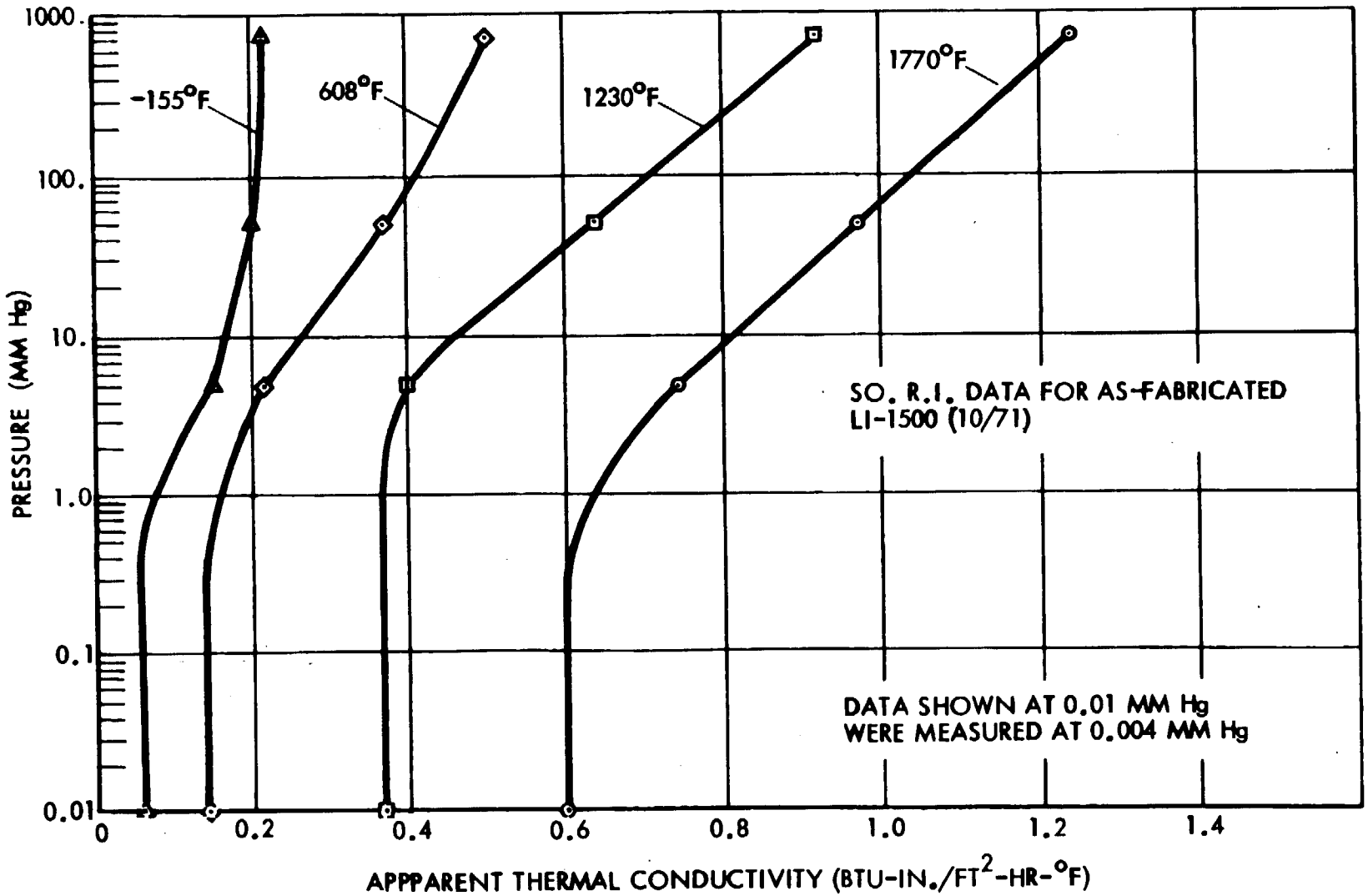

Fig. 4.1-11

DESIGN CURVES SHOWING VARIATION OF LI-1500 THERMAL CONDUCTIVITY WITH TEMPERATURE AND PRESSURE

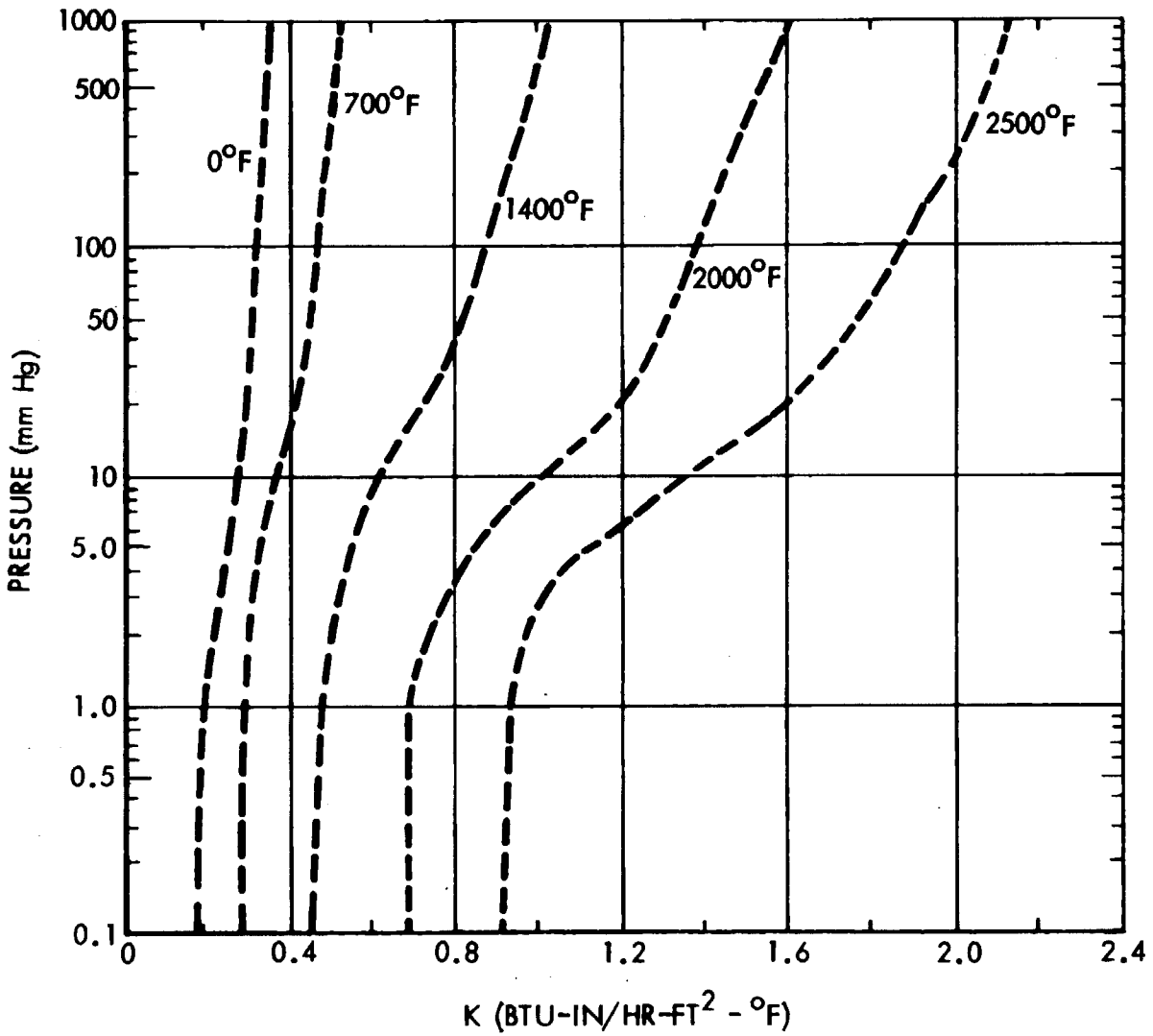

Fig. 4.1-12

Table 4.1-4

INTERIM DESIGN VALUES – THERMAL CONDUCTIVITY OF LI-1500
(Btu-in./ft^2-hr-$^\circ$F)

Temp ($^\circ$F) \ Pressure (mm Hg)	0.1	1.0	10.0	100.0	760.0
-200	0.17	0.19	0.28	0.32	0.35
0	0.21	0.23	0.31	0.34	0.37
300	0.27	0.29	0.35	0.47	0.52
700	0.45	0.47	0.60	0.90	1.00
1400	0.67	0.69	1.02	1.40	1.56
2000	0.92	0.94	1.35	1.88	2.09
2500					

4.1.4 Thermal Conductivity of 0042 Coating and RTV 560 Adhesive

A pulse technique was used to obtain thermal diffusivity and thereby measure the thermal conductivity of the 0042 coating and the RTV 560 adhesive. The data are shown in Tables 4.1-5 and 4.1-6. Since measurements were made to only 500°F, the coating conductivity values were extrapolated to higher temperatures on the basis of the coating constituents.

The technique employed for measuring the thermal diffusivity is basically that originally described by Parker*. The method consists of irradiating the front face of a disc-shaped specimen with a single pulse of energy. The specimen is located in a nearly isothermal environment, and the energy pulse is absorbed at the front face in a depth which is very small compared to specimen thickness. The time-temperature history of the rear face of the specimen is monitored with a thermocouple. Thermal diffusivity is calculated on the basis of the thickness of the specimen and the time required for the rear face temperature rise signal to reach a specified percentage of its maximum value. The estimated maximum uncertainty is ±20%.

4.1.5 Thermal Degradation

The thermal degradation tests were performed on the LI-1500 material that was eventually used for the 10- and 20-thermal cycle mechanical property tests. The material (Fiber Lot 2085) was cycled in a 1-atm air furnace with heating on five sides, according to the oven cycle shown in Fig. 4.1-13. The procedure consisted of putting the material in an oven preheated to 2300°F. The material was left in the oven for 30 min, then removed and allowed to cool in 70°F air. The time at temperature for one cycle is equivalent to three 1100 nm trajectories when following a 2300°F heating

*W. J. Parker, R. J. Jenkins, C. P. Butler, and G. L. Abbott, "Flash Method of Determining Thermal Diffusivity, Heat Capacity, and Thermal Conductivity," Journal Appl. Phys. 32 1961

Table 4.1-5

THERMAL CONDUCTIVITY OF RTV 560

TEMPERATURE ($^{\circ}R$)	CONDUCTIVITY, K (BTU-IN./FT^2-HR-$^{\circ}R$)
530	1.94
700	1.68
950	1.51

SPECIMEN DENSITY = 94 LB/FT^3

MANUFACTURER'S DATA AT 530$^{\circ}R$: 2.16 BTU-IN./FT^2-HR-$^{\circ}R$

Table 4.1-6

THERMAL CONDUCTIVITY OF 0042 COATING

TEMPERATURE (°R)	CONDUCTIVITY K (BTU-IN./FT^2-HR-°R)
460	6.48
860	6.48
1460	10.8
2460	14.2
2960	16.8

SPECIMEN DENSITY = 104 LB/FT^3

OVEN THERMAL CYCLE FOR THERMAL DEGRADATION TESTS

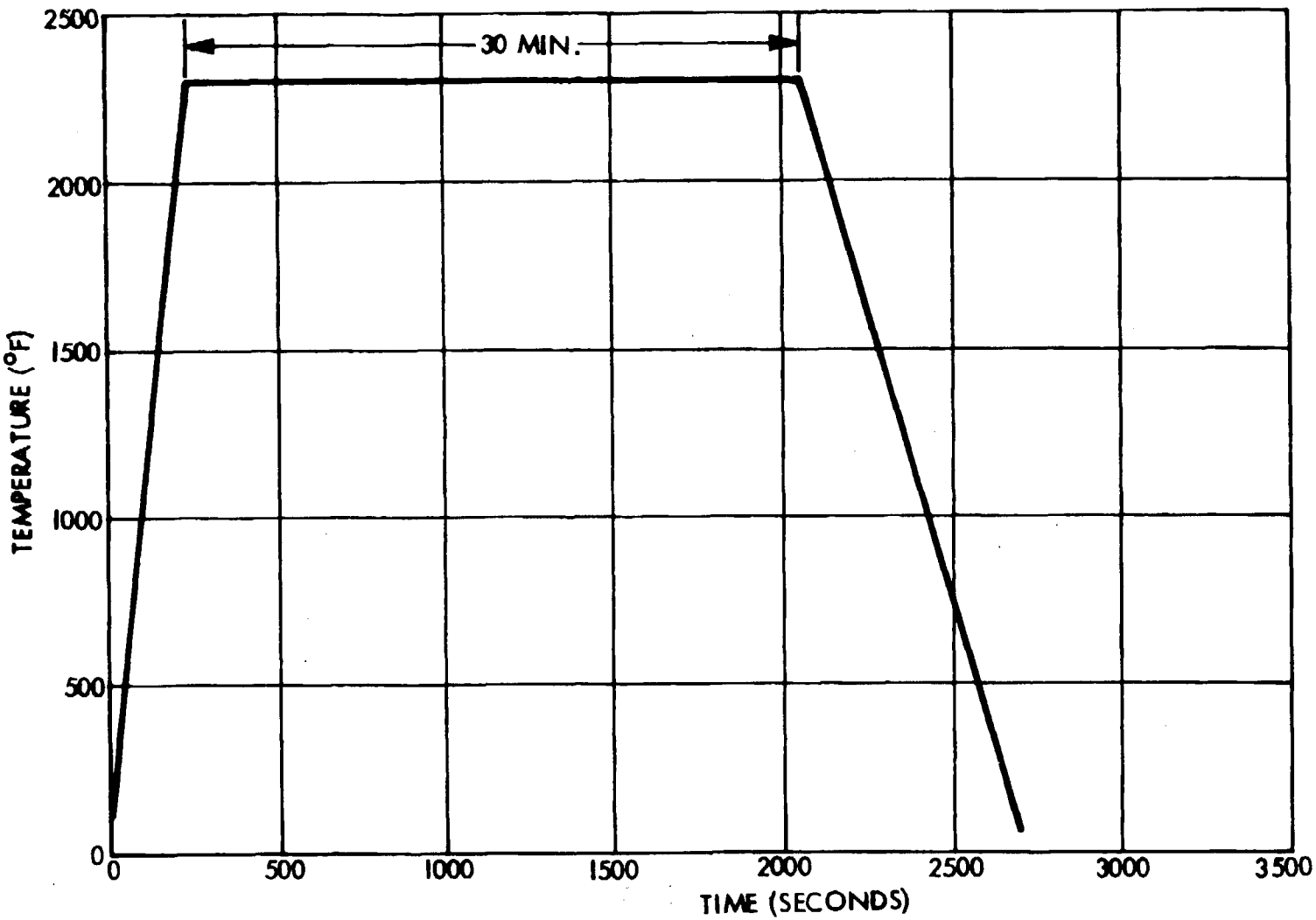

DO6129

Fig. 4.1-13

boundary as per LMSC Alternate Concept Study trajectories. The total heat (Btu/ft^2) in the oven cycle is also approximately equal to three 1100 nm trajectories.

For the NASA reentry surface temperature history shown in Section 2, which sustains $2300^{o}F$ for about 150 sec, the one 30-min (1800 sec) oven cycle is equal to about 12 flights in terms of time at temperature. Hence the 10 and 20 cycles are equivalent to 120 and 240 flights, respectively.

The density and dimensional change for the cycled material after 5 and 10 hours accumulated exposure to $2300^{o}F$ is shown in the lower part of Table 4.1-7.

The acoustic environment to which the mechanical property test specimens (uncoated) were exposed is shown in Fig. 4.1-14. The environment is based on the design conditions outlined in Section 2. During each shuttle mission, the specified design areas of the TPS would be exposed to 20 sec of an overall SPL of 159.4 db.

All test specimens listed for acoustic exposure successfully passed the acoustic test. Two additional specimens were exposed to 35 and 45 min, respectively, with no apparent degradation. These specimens were used for mechanical property tests discussed in Section 4.2.

4.1.6 Coating Emittance

Initial screening tests were performed on three coating formulations developed under the Material Improvement Contract (NAS 9-12137): $SiC/SiO_2/B_2O^{*}_3$, CoO/SiO_2, and $SiC/Cr_2O_3/SiO_2$. These tests consisted of measuring near normal spectral reflectance in the wavelength region of 0.9 to 25 microns for one sample of each coating at four nominal temperatures from $250^{o}F$ to $2000^{o}F$. All measurements were made in air at atmospheric pressure. Temperature-dependent total normal and total hemispherical emittance values were then computed from the reflectance data.

In addition, total and spectral normal emittance measurements, as a function of temperature, were performed on a sample of the coating selected for final evaluation, $SiC/SiO_2/B_2O_3$, designated 0042.

* 0042 Baseline Coating

Table 4.1-7

THERMAL DEGRADATION OF CYCLED SPECIMENS

Type of Test Specimens	Specimen I. D. No.	No. of Thermal Cycles	No. of Acoustic Cycles	Total Time (thermal)	Total Time (acoustic)
Tension	1-1 to 1-6 2-1 to 2-6	10 20	10 20	5 hours 10 hours	10 min.(1) 20 min.
Compression	3-1 to 3-5	10	10	5 hours	10 min.(2)
Shear	4-1 to 4-10	10	–	–	–
Bending	2085-1 to -4	10	10	5 hours	10 min.
Thermal Expansion		20	–	10 hours	–
Specific Heat	–	20	–	10 hours	–
Infrared Transmission	–	10 and 20	–	5 & 10 hours	–
Hard Vacuum	–	10 and 20	–	5 & 10 hours	–

All material came from fiber lot 2085

(1) One specimen exposed to 45 min. total time
(2) One specimen exposed to 35 min. total time

RESULTS AFTER THERMAL CYCLING ‡

No. of Cycles	Density ~ Lb/Ft^3		Dimensional Change		
	Before	After	Length	Width	Thickness
10*	15.0	16.1	2.0%	2.2%	2.9%
20**	15.0	16.5	3.7%	4.1%	4.3%

No weight loss was detected

*Average value for nine blocks
**Average value for four blocks

‡ The dimensional changes associated with these oven tests reflect the influence of subjecting the entire sample to 2300°F as contrasted with the 100 cycle 2500°F tests where only the outermost portion of the LI-1500 experienced these high

COMPARISON OF APPLIED ACOUSTIC TEST ENVIRONMENT WITH REQUIREMENT

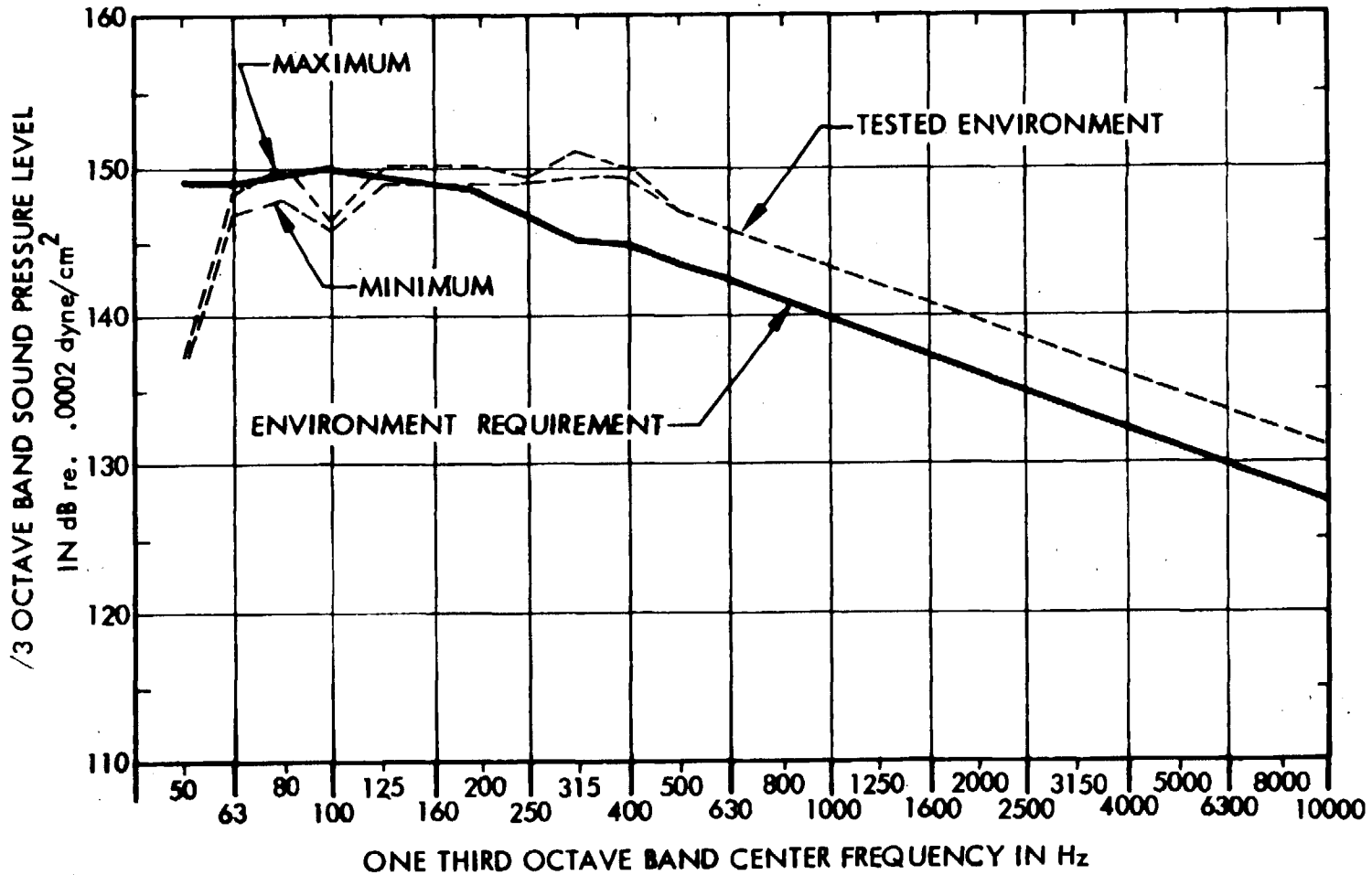

DO6128

Fig. 4.1-14

4.1.6.1 Reflectance Measurement Method. Measurements of the infrared spectral reflectance of three samples have been performed at various temperatures from ambient to 2000°F in the wavelength region 0.9 to 25 microns. These measurements were performed in the Thermophysics Laboratory at TRW Systems, Redondo Beach, California, for Lockheed Missiles & Space Co., Inc.

A paraboloid reflectometer, designed and built by TRW, was used to perform the reflectance measurements. This instrument uses two paraboloid mirrors to uniformly irradiate a sample with energy from a high-temperature diffuse black source. A chopper between the source and the first paraboloid is used to provide 13 cps alternating illumination of the sample. The detector, a vacuum thermocouple in a Perkin-Elmer Model 12C Spectrometer, and its associated ac amplifier detect only the ac or reflected energy from the sample. A gold sample is used to set the "100%" reference signal. The instrument is described in a paper presented by Newman, Luedke, and Bevans*.

The samples were cut to nominal 1/2 in. x 1 in. from the Lockheed materials for mounting in an Inconel holder. The holder was heated, using a low voltage-high current ac power supply. A chromel-alumel thermocouple was bonded to the rear surface of the samples, using Sauereisen cement.

The thermocouple readings were checked by viewing the sample with an L&N optical pyrometer. The surface temperatures as monitored with the pyrometer at the nominal 2000°F (thermocouple reading) runs indicated surface temperatures ranging from 1680°F to 1860°F. This gradient was apparently due to localized heating and variations in sample thickness. The thermocouple reading was higher due to its placement closer to the heating element. It is likely that the surface temperature during the 1470°F run was also somewhat lower than the thermocouple indication. All measurements were made with the sample backed with a black coated heating element. Samples of SiC/SiO_2/B_2O_3 and SiC/Cr_2O_3/SiO_2 were also measured at 1, 2.2, and 5 microns with a platinum backing, and no change in the reflectance data was noted, indicating that the

*B. E. Newnam, E. E. Luedke, and J. T. Bevans, "High Temperature Reflectance Measurements with the Paraboloid Reflectometer," AIAA Paper 68-25, AIAA 6th Aerospace Sciences Meeting, January 1968.

coatings were opaque. The CoO/SiO_2 specimen was destroyed during the initial test, so no transmission measurement was performed.

4.1.6.2 Results. The reflectance data for the nominal 250°F, 930°F, and 2000°F conditions are presented in Figs. 4.1-15, 4.1-16, and 4.1-17 for the three coatings. Data for 1470°F were also measured but for purposes of clarity are not shown on the curves. These data are available and will be supplied to NASA upon request.

The nominal room temperature run was actually made at 250°F due to sample heating by the source. The reflectance data for the $SiC/SiO_2/B_2O_3$ and CoO_2 coatings exhibit a relatively gray behavior in the spectral region of 0.9 to 7 microns, which would indicate that the total emittance would be nearly independent of temperature at high temperatures. The $SiC/Cr_2O_3/SiO_2$ coating showed an increase in reflectance with decreasing wavelength, which would result in a decrease in emittance with increasing temperature. In the 7- to 10-micron region, the absorption band for all coatings decreased in amplitude with increasing temperature.

Very little temperature dependence of spectral emittance was observed over the test temperature range, as shown by Table 4.1-8 for several wavelengths. The reflectance band near 9 microns, attributed to the SiO_2 constituent, decreased in magnitude and was slightly broadened at elevated temperature. Negligible transmission through the coating thicknesses examined was observed, as shown by Table 4.1-9. The backing of the coating with a blackened and then a reflective (platinum) material did not result in any significant change in reflectance.

Total normal emittance as a function of temperature was computed by integration of the spectral reflectance data for each temperature against the black body energy function for the particular temperature. These data are shown graphically in Fig. 4.1-18. Total hemispherical emittance was then computed, using the ratio of normal to hemispherical emittance for insulators given by Jakob*. These values are shown in Fig. 4.1-19.

*Max Jakob, Heat Transfer, Vol. 1, p. 52, John Wiley and Sons, Inc., 1949.

SPECTRAL REFLECTANCE FOR A BOROSILICATE COATING WITH A SILICON CARBIDE EMITTANCE AGENT – 0042

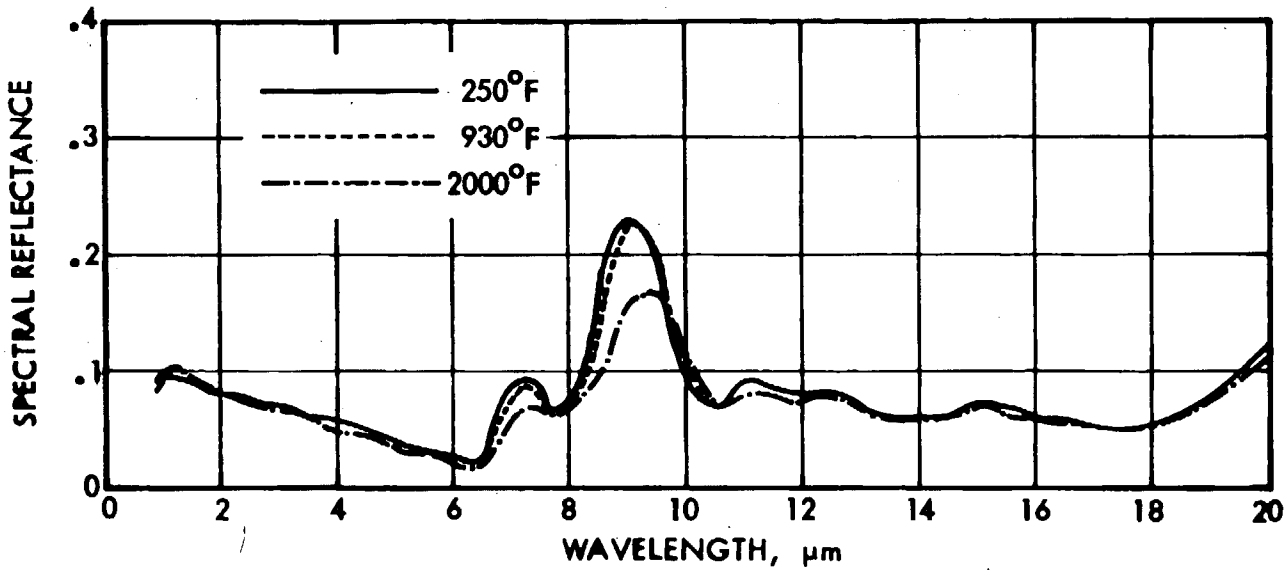

Fig. 4.1-15

SPECTRAL REFLECTANCE FOR A BOROSILICATE COATING WITH A COBALT OXIDE EMITTANCE COATING

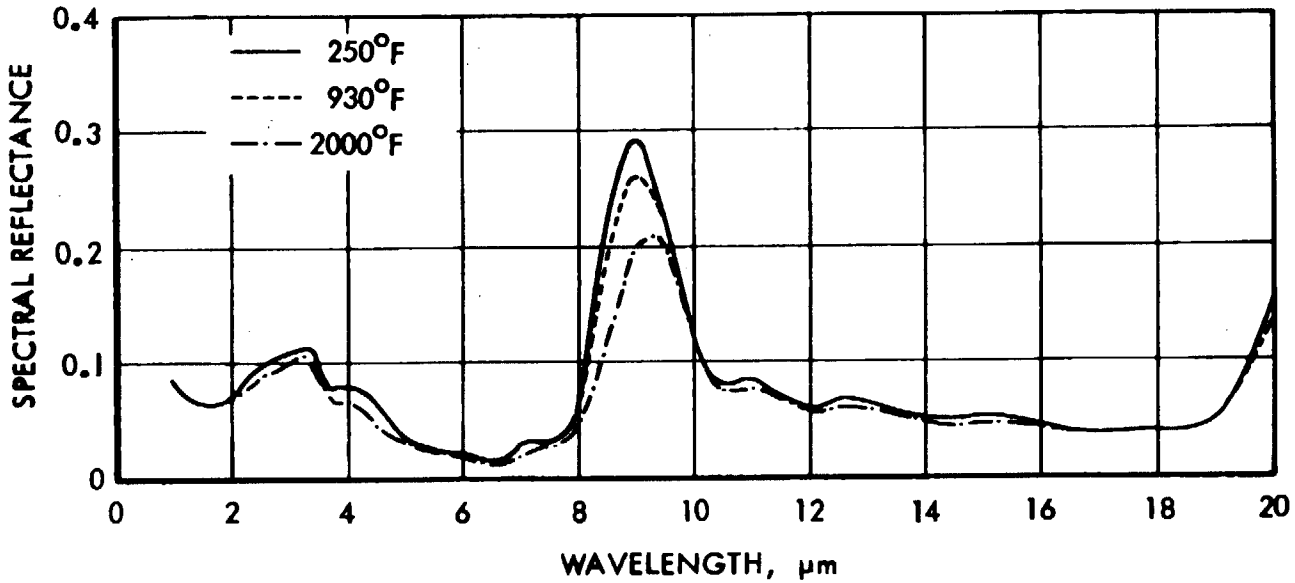

Fig. 4.1-16

SPECTRAL REFLECTANCE FOR BOROSILICATE COATING WITH SILICON CARBIDE AND CHROME OXIDE EMITTANCE AGENTS

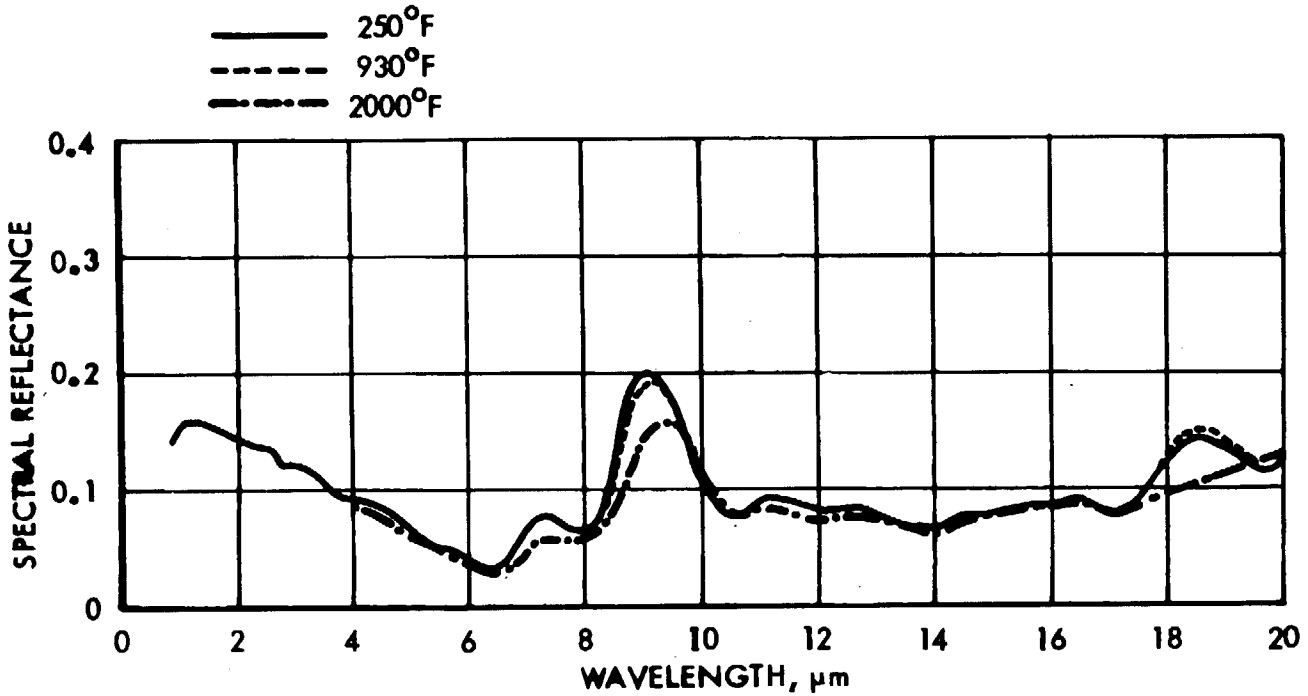

DO6127

Fig. 4.1-17

Table 4.1-8

SPECTRAL REFLECTANCE OF CANDIDATE COATINGS AS A FUNCTION OF TEMPERATURE

TEMPERATURE	$SiC/SiO_2/B_2O_3$(0042)				CoO/SiO_2				$SiC/Cr_2O_3/SiO_2$			
	REFLECTANCE AT λ											
	1μ	3μ	6μ	9μ	1μ	3μ	6μ	9μ	1μ	3μ	6μ	9μ
250°F	0.087	0.07	0.025	0.23	0.085	0.103	0.02	0.29	0.155	0.12	0.04	0.20
930°F	0.09	0.07	0.025	0.21	0.083	0.11	0.02	0.26	0.15	0.123	0.045	0.19
1470°F	0.087	0.07	0.022	0.195	0.083	0.107	0.02	0.23	0.15	0.13	0.047	0.17
2000°F	0.102	0.06	0.02	0.15	0.080	0.10	0.017	0.20	0.157	0.12	0.04	0.15

Table 4.1-9

LOCKHEED

CHANGE IN COATING REFLECTANCE WITH SPECIMEN BACKING

TEMPERATURE		$SiC/SiO_2/B_2O_3$ (0042)				$SiC/Cr_2O_3/SiO_2$			
		REFLECTANCE AT λ							
		1μ	2.2μ	3.4μ	5.0μ	1μ	2.2μ	3.4μ	5.0μ
250°F	BLACK	0.087	0.079	0.067	0.040	0.155	0.140	0.110	0.062
	PLATINUM	0.09	0.09	0.07	0.04	0.190	0.163	0.120	0.050
2000°F	BLACK	0.102	0.080	0.060	0.033	0.157	0.140	0.110	0.060
	PLATINUM	0.10	0.09	0.06	0.04	0.190	0.161	0.120	0.050

TOTAL NORMAL EMITTANCE OF CANDIDATE COATINGS AS A FUNCTION OF TEMPERATURE

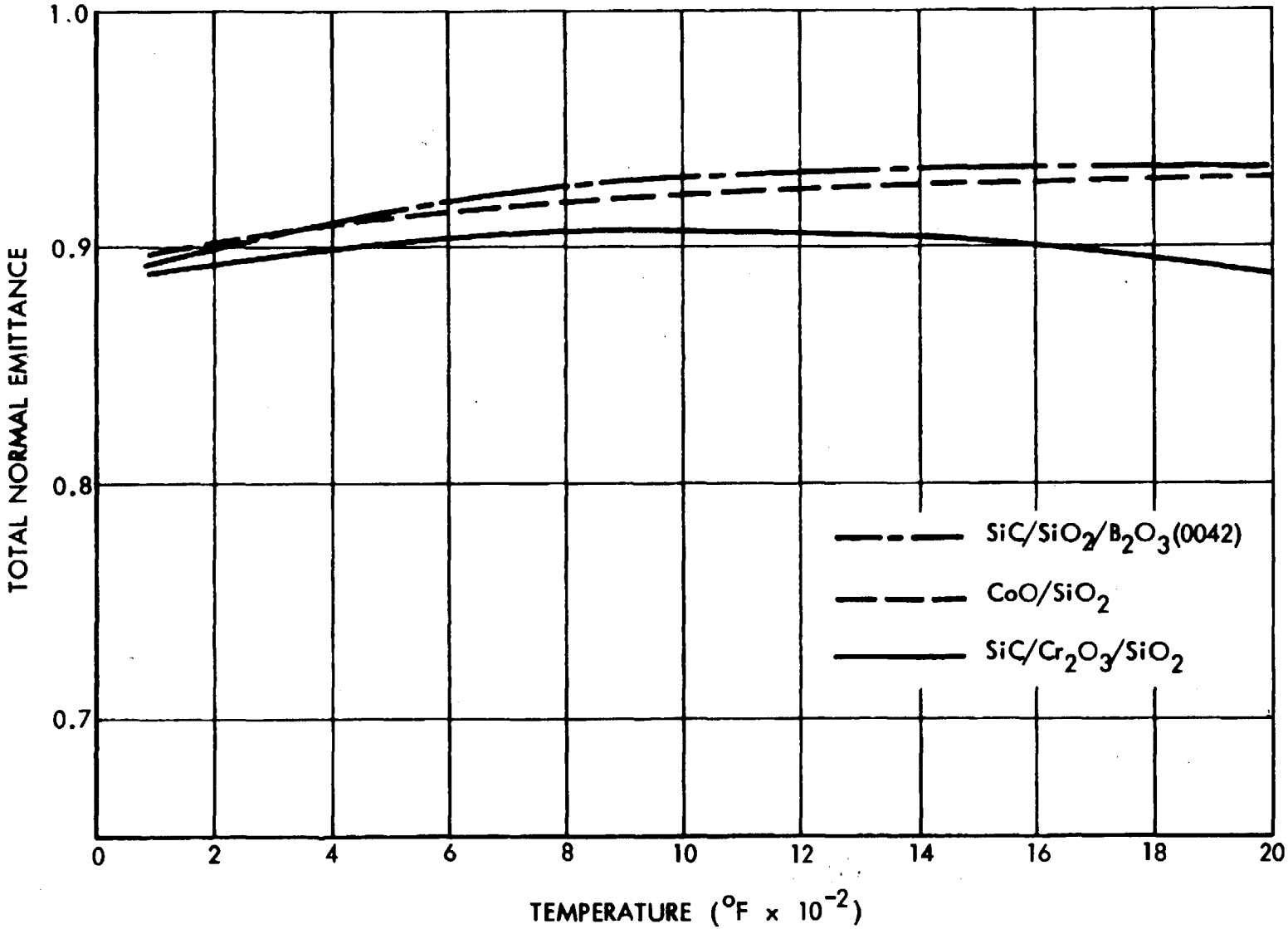

Fig. 4.1-18

TOTAL HEMISPHERICAL EMITTANCE OF CANDIDATE COATINGS AS A FUNCTION OF TEMPERATURE

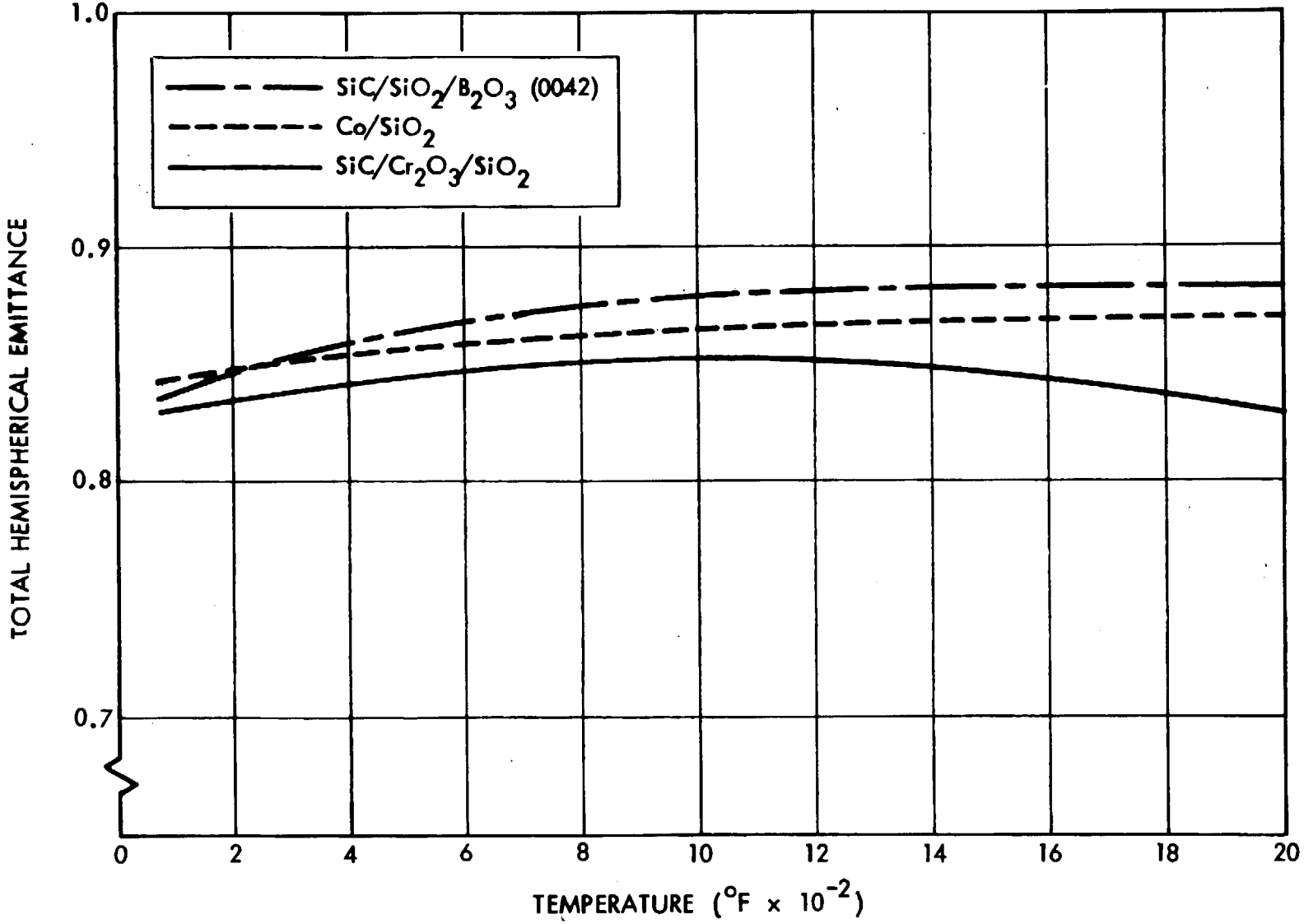

Fig. 4.1-19

4.1.7 Spectral Absorptance

The spectral absorptance of the 0042 coating, which was brought on line from the Material Improvement Contract (NAS 9-12137), was obtained for the as-fabricated coating and coating that was exposed to 20 thermal cycles (10 hours exposure at 2300°F).

Seven samples were used: four for the as-fabricated coating and three for the coating exposed to 20 thermal cycles.

The solar absorptance of each sample was determined by measuring the spectral reflectance (0.25 to 1.8 microns) under laboratory ambient conditions with a Cary Model 14 spectroreflectometer. The reflectance spectra were then integrated with respect to the solar spectrum, using a 50-point numerical integration. These specimens were then exposed to ultraviolet radiation as a specialized environmental test, and the spectral reflectance was again measured. These data, which showed very little change in solar absorptance, are reported in Section 5.3.3.

The average solar absorptance for the four as-fabricated coating samples was 0.773. The average solar absorptance for the three thermally cycled coating samples was 0.764.

The ratio of solar absorptance to hemispherical emittance (α/ϵ) at 70°F for the as-fabricated coating for a total hemispherical emittance of 0.835 was 0.93. The α/ϵ ratio for the thermally cycled specimens was 0.915.

4.2 MECHANICAL PROPERTIES

LMSC recognizes that a major area of uncertainty in RSI technology is that of correct testing methods. Hence, the property test methods and results are constantly being reviewed and new tests are being run as additional information becomes available on the behavior of LI-1500. LMSC believes that the only way to truly characterize the material is to constantly scrutinize the data in conjunction with analytical design application studies and perform any necessary additional tests.

The major effort to date has been to perform the mechanical property tests detailed in the Property Test Plan (LMSC-A991210, 30 July 1971) approved by NASA/MSC. A sketch showing the specimen sizes used for the mechanical property tests is shown in Fig. 4.2-1. The test matrix is shown in Table 4.2-1 along with average values of strength and modulus. The table lists the number of thermal cycles and time at 2300°F for the specimens that were cycled prior to testing. These specimens were also exposed to an acoustic environment simulating the ascent engine environment. The cycled specimens are also discussed under Thermal Degradation, Section 4.1.5.

The anisotropic properties of LI-1500, as indicated in the table, are due to preferred biaxial orientation of the fibers. The material supports higher stresses before fracture in the fiber orientation direction than in a direction normal to the fibers. The tensile fracture values are about 78 psi and 14 psi for the parallel and normal to fiber orientation directions, respectively. This variation in properties is accounted for in the anisotropic structural analysis performed in Task 2. The room temperature tensile fracture and elastic modulus values are essentially the same as those reported under NAS 9-11222.

The remaining parts of this section contain a detailed discussion of the test techniques and results from which the average values were obtained for each type of test. Sample calculations and stress-strain curves for various tests are included in the Appendix.

SKETCH OF MECHANICAL PROPERTY TEST SPECIMENS

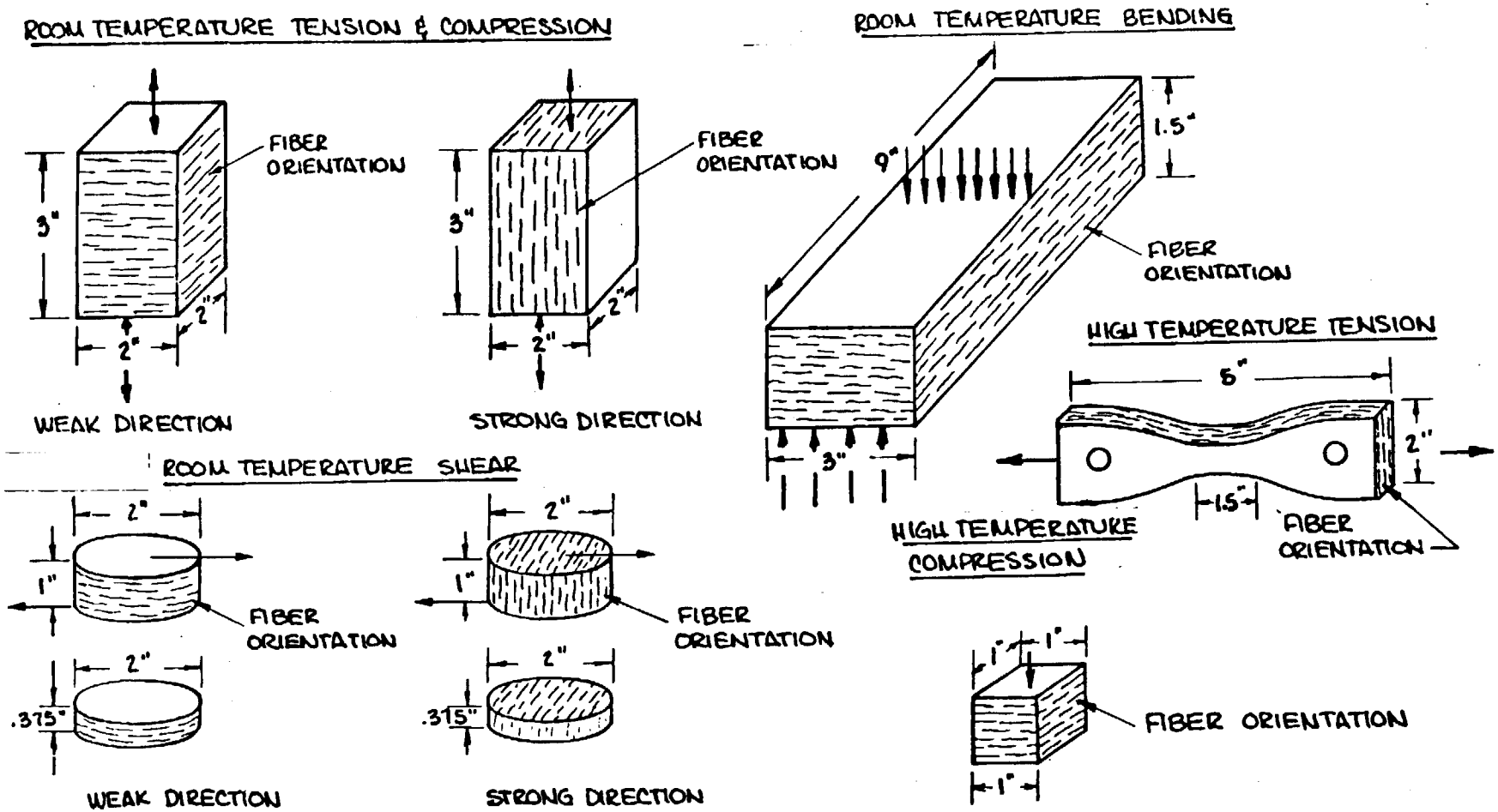

Fig. 4.2-1

Table 4.2-1

SUMMARY OF LI-1500 MECHANICAL PROPERTY TEST RESULTS

TYPE OF TEST	TEST DIRECTION	LOCATION IN BLOCK	TEMP (°F)	NUMBER OF THERMAL AND ACOUSTIC CYCLES	TIME AT 2300°F (HR)	NO. OF SPECIMENS	AVERAGE STRENGTH (LB/IN.^{2})	AVERAGE MODULUS (LB/IN.^{2})
TENSION	PARALLEL[1]	#1	RT	0		4	78	56,400
	PARALLEL	#2	RT	0		4	70	57,450
	NORMAL[2]	#1	RT	0		4	15	5,780
	NORMAL	#2	RT	0		4	14	9,518
	NORMAL	#1	RT	10	5	3	14	10,073
	PARALLEL	#1	-150	0		4	91	40,575
	PARALLEL	#1	1500	0		4	101	46,700
	PARALLEL	#1	2000	0		4	165	16,000
	PARALLEL	#1	2160*	0		4	190	
	PARALLEL	#1	RT[3]	0		3	77	60,850
	PARALLEL	#1	RT	10	5	4	47	91,300
	PARALLEL	#1	RT	20	10	4	56	89,500
COMPRESSION	PARALLEL	#1	RT	0		6	174	39,700
	NORMAL	#1	RT	0		4	42	4,070
	NORMAL	#1	2300	0		3	4	219
	PARALLEL	#1	2300	0		3	40	2,140
	PARALLEL	#1	RT	10	5	3	234	84,700
	PARALLEL (COATED)	#1	RT	0		4	167	60,300
	NORMAL	#1	RT	10	5	2	77	10,615
SHEAR	PARALLEL	#1	RT	0		2	28	6,605
	NORMAL	#1	RT	0		4	75	31,900
	PARALLEL	#1	RT	10	5	4	39	-
BENDING	PARALLEL	#1	RT	0		5	115	53,780
	PARALLEL	#1	RT	10	5	3	179	83,195
COATING (0025)	PARALLEL	-	RT	0		7	480	960,000
COATING (0042)		-	RT	0		11	2,000	1,900,000

(1) PARALLEL TO THE FIBER ORIENTATION DIRECTION
(2) NORMAL TO THE FIBER ORIENTATION DIRECTION
(3) CONTROL SPECIMENS FOR TESTS IN ELEVATED TEMPERATURE FIXTURE
* BRITTLE TO DUCTILE TRANSITION TEMPERATURE (SEE FIG. 4.2-10)

4.2.1 Room Temperature Tension Tests

Room temperature (75^{o}F) tensile tests were run on 2-in. cubes, using the fixture shown in Fig. 4.2-2. The specimen is bonded to two blocks (B), using Hysol 150 epoxy. A pair of deflectometers (D) are attached to the blocks (B) by the brackets (A). Blocks are attached to the testing machine through universal joints (U) at each end. The testing machine is a 50,000 lb SR-4 screw-driven universal testing machine.

Since the specimen fails at considerably less than full-scale of the most sensitive range on this testing machine, a more sensitive load cell is introduced between the universal joint and crosshead of the machine. With this load cell, load resolution of 0.5 percent of typical failure loads is possible.

Load and strain are recorded continuously on an X-Y plotter. System measurement accuracy is within ±1.5 percent on either the X or Y scale.

Crosshead motion of the machine is set for an approximate strain rate of 0.25 percent per minute. (It takes approximately 1 minute to load the specimens to failure.)

Universal joints are essential to ensure uniform loading, and a pair of averaging deflectometers eliminates the gross strain-measurement errors that would result from a specimen having nonuniform properties across its width.

Specimen dimensions are measured to 0.020 in. accuracy. An average of five readings is taken on each dimension.

The room temperature tension results for specimens taken from the top of a double thickness LI-1500 block are shown in Table 4.2-2. Also shown in the table is the average value obtained during the last contract, NAS 9-11222. The average values are essentially the same, considering that the test technique was a dog bone specimen and a universal test machine was used for NAS 9-11222 testing.

Room temperature tension results for specimens taken from the bottom of the LI-1500 block are shown in Table 4.2-3. Tension results for specimens exposed to

TEST FIXTURE FOR TENSILE TESTS OF LI-1500 (ROOM TEMPERATURE AND -150°F)

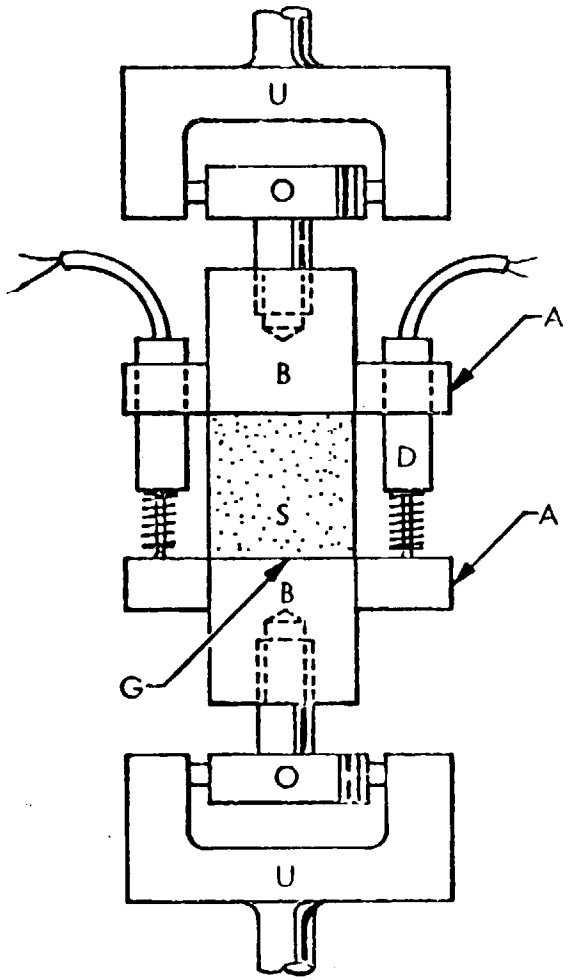

Fig. 4.2-2

Table 4.2-2

LI-1500 TENSION TESTS (UNCOATED SPECIMENS), LOCATION 1

Direction Test Temp	Specimen Number	Total Length (in.)	Test Section Width (in.)	Thickness (in.)	Weight (gm)	Test Section Area ($in.^2$)	Load (lb)	Stress (psi)	Modulus (psi)
Parallel R. T.	TT 28-1	3.00	2.00	2.00	44.3	4.00	354	88.5	61,100
R. T.	TT 28-2	3.00	2.00	2.00	44.0	4.00	260	65.0	50,500
R. T.	TT 28-3	3.00	2.00	2.00	44.2	4.00	286	71.5	60,000
R. T.	TT 28-4	3.00	2.00	2.00	44.0	4.00	342	85.5	54.000
						Average		78.0	56,400
						NAS 9-11222 avg		74.0	59,650
-150°F	TT 28-5	3.00	2.00	2.00	44.0	4.00	358	89.5	56,300
-150°F	TT 28-6	3.00	2.00	2.00	43.5	4.00	370	92.5	54,000
-150°F	TT 28-7	3.00	2.00	2.00	42.0	4.00	350	87.5	48,800
-150°F	TT 28-8	3.00	2.00	2.00	43.0	4.00	376	94.0	39,200
						Average		91.0	50,575
Normal R. T.	TT 28-41	2.00	2.00	2.00	29.0	4.00	72	18.0	5,660
R. T.	TT 28-42	2.00	2.00	2.00	29.5	4.00	55	13.8	6,130
R. T.	TT 28-43	2.00	2.00	2.00	29.0	4.00	54	13.5	6,450
R. T.	TT 28-44	2.00	2.00	2.00	29.3	4.00	51	12.8	4,890
						Average		14.5	5,780

Table 4.2-3

LI-1500 TENSION TEST (R.T.), LOCATION 2

Test Direction	Specimen Number	Length (in.)	Width (in.)	Thick-ness (in.)	Test Section Area ($in.^2$)	Load (lb)	Stress (psi)	Modulus (psi)
Normal	TT 39-1	3.00	2.00	2.00	4.00	59	14.8	9,400
	TT 39-2	3.00	2.00	2.00	4.00	50	12.5	9,150
	TT 39-3	3.00	2.00	4.00	4.00	65	16.2	9,650
	TT 39-4	3.00	2.00	2.00	4.00	50	12.5	9,870
						Average	14.0	9,518
Parallel	TT 39-6	3.00	2.00	2.00	4.00	225	56.2	67,300
	TT 39-7	3.00	2.00	2.00	4.00	363	90.8	27,600
	TT 39-8	3.00	2.00	2.00	4.00	245	61.2	66,900
	TT 39-9	3.00	2.00	2.00	4.00	286	71.5	68,000
						Average	69.9	57,450

thermal and acoustic cycles are shown in Table 4.2-4. The specimens were exposed to 2300°F for a total of 5 hours in two 2.5-hour intervals. A more detailed description of the thermal and acoustic exposures is given under Thermal Degradation, Section 4.1.

The effect of the increased tension modulus in the parallel-to-fiber orientation direction, representative of that obtained on the thermal and acoustically cycled tension specimens (89,500 lb/in.^{2}), is discussed in Volume II, Section 3.1 for the Aluminum Test Panel No. 2. The design condition analyzed was a line load of 6000 lb/in. with a 1.5 lb/in.^{2} burst pressure. These results are shown in Volume II, Table 3.1-5.

The higher tension modulus allowed the cycled layer of LI-1500 to have a modulus more compatible with the coating modulus. Hence, the calculated stresses within the cycled LI-1500 were less than those for the as-fabricated material.

For the normal-to-fiber orientation direction, the test results indicate essentially the same tensile stress and elastic modulus as the as-fabricated material.

4.2.2 High Temperature Tension Tests

The tensile properites at 1500, 2000, 2100, 2200, and 2300°F were evaluated under both static and dynamic loading conditions. Tests under static loads were conducted to establish stress-strain relationships at elevated temperatures. Dynamic tests at low strain rates, which are the normal loading tests used for determining tensile properties, were made to establish the stress for fracture.

A detailed sketch of the test specimen is shown in Fig. 4.2-3. The 2-in. long reduced section had a cross-section of 0.37 x 0.75 in. for tests at room temperature and 1500°F and a 0.27 x 0.75 in. cross-section for tests at 2000°F.

The specimens were heated to test temperature with a platinum-wound tube furnace having a 3-in. diameter by 15-in. long hot zone. Temperature within the gage section was within ±15°F of the stated test temperature. Specimens were held by pin and clevices machined from HS-25 alloy bar for tests at 1500 and 2000°F. The load train

Table 4.2-4

LI-1500 TENSION TESTS

(POST THERMAL AND ACOUSTICAL CYCLING)

NUMBER OF THERMAL AND ACOUSTICAL CYCLES	SPECIMEN NUMBER	MAXIMUM LOAD (LB)	MAXIMUM STRESS (PSI)	MODULUS (PSI)
PARALLEL 10	1-1 1-2 1-3 1-4	230 218 165 136	57.5 54.5 41.2 34.0	94,300 85,400 101,400 84,000
		AVERAGE	46.8	91,300
PARALLEL 20	2-1 2-2 2-3 2-4	274 460 114 48	68.5 115.0 28.5 12.0	102,000 61,000 86,000 109,000
		AVERAGE	56.0	89,500
NORMAL 10	1-5 1-6 2-5	36 51 83	9 13 21	10,698 9,306 10,216
		AVERAGE	14.3	10,073

TESTED PARALLEL TO FIBER ORIENTATION DIRECTION.
ALL SPECIMENS 2 x 2 x 3 IN., EXCEPT 1-5, 1-6, AND 2-5 WERE 2 x 2 x 2 IN.
TEST SECTION AREA = 4.00 $IN.^2$

PIN END LOADED TENSILE SPECIMEN

C.3

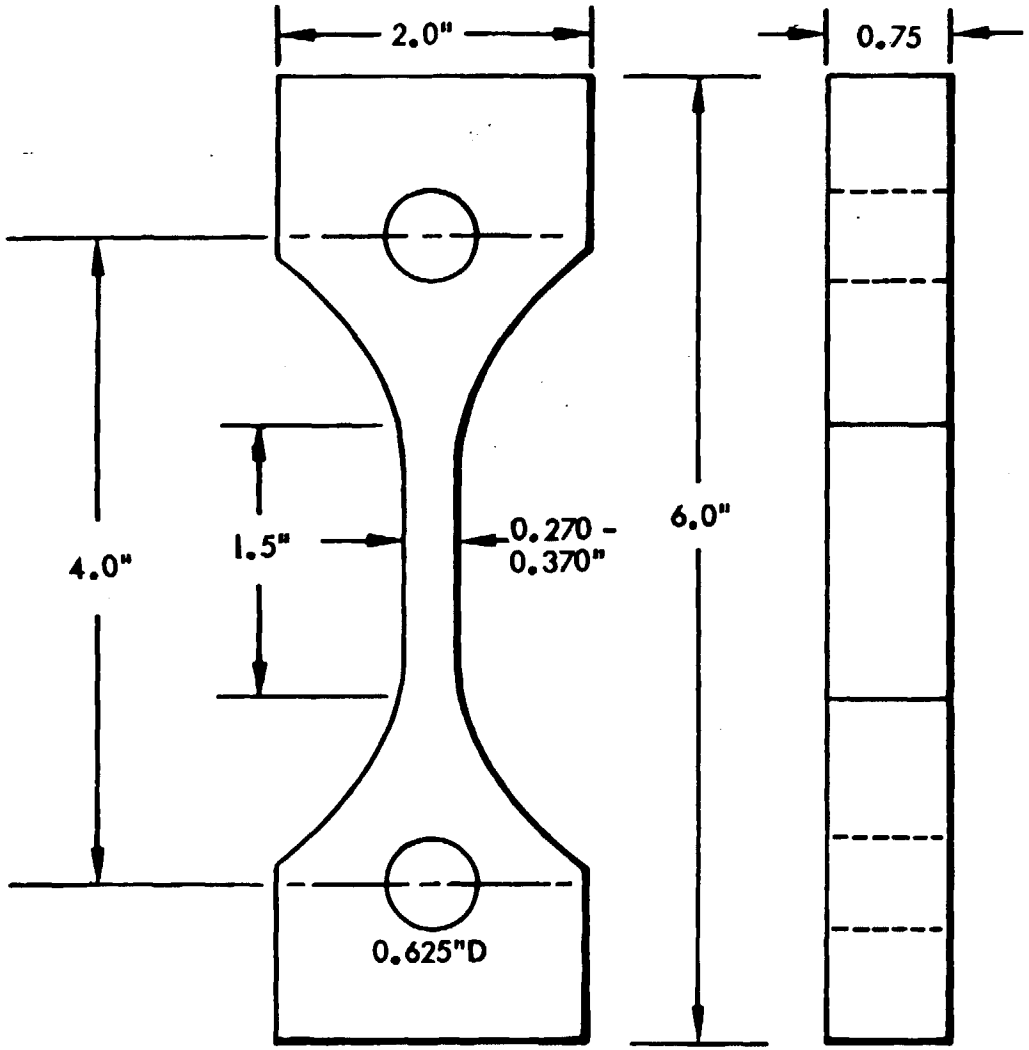

DO6087

Fig. 4.2-3

was assembled above the hot furnace as shown in Figs. 4.2-4A and 4.2-5A, and the furnace was then lifted into position with the specimen in the center of the hot zone (Figs. 4.2-4B and 4.2-5B). About 30 min. was required to stabilize at the test temperature. Prior to loading, the specimens were soaked for an additional 30 and 20 min. at 1500 and 2000°F, respectively. Temperature measurement from thermocouples imbedded in the interior of the gage section indicated the gage section reached the test temperature within 5 min. after immersion in a furnace at 2000°F.

The dynamic tensile tests were made with an Instron Model TM tensile test machine. A 50-lb load cell calibrated with certified weights was used to measure and record load. A load-time curve was plotted for each test to obtain a rough measure of gross deformation. Tests were made at a constant crosshead rate of 0.02 in./min.

Static tests were conducted in an Arcweld creep frame with the sample fixed at the upper end. Loads were applied in 2-lb increments to a pan suspended from the lower clevice (Fig. 4.2-5B). Strain within the gage section was measured optically with a platinum strip extensometer fixed to each end of the gage section. After establishing a stress-strain curve, the specimens were loaded to fracture.

The results for the room temperature, 1500°F, and 2000°F tests are shown in Table 4.2-5. The room temperature results agree well with the room temperature results on the 3 x 2 x 2 in. specimens shown in Tables 4.2-1 and 4.2-2.

The results at 1500°F reveal about a 33 percent increase in average tensile strength and about an 18 percent decrease in modulus. At 2000°F, the average tensile strength increases to 165 lb/in.^{2}, while the modulus decreases to 16,000 lb/in.^{2} from the room temperature value of 56,000 lb/in.^{2}. Hence, at elevated temperatures, the material apparently becomes more ductile and has higher tensile strength. One explanation for this trend is that at high temperatures small flaws in a brittle material have less of an effect. This is due to ductile redistribution of the stress field in the neighborhood of the flaw; i.e., alternate load paths of less intensity are created around the flaw. Hence, the load carrying capability is increased compared to that when the flaw behaves in a brittle manner.

SETUP FOR HIGH TEMPERATURE DYNAMIC TENSILE TEST

A. LOAD TRAIN ASSEMBLY

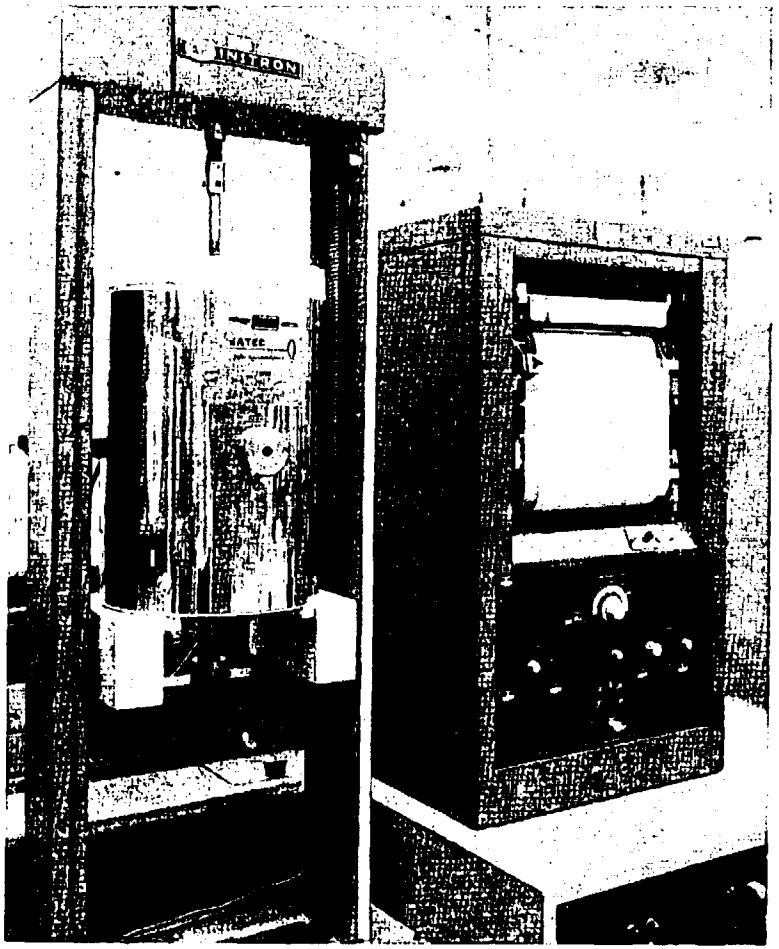

B. FURNACE IN TEST POSITION

D07120

Fig. 4.2-4

SETUP FOR HIGH TEMPERATURE STATIC LOAD TENSILE TESTS

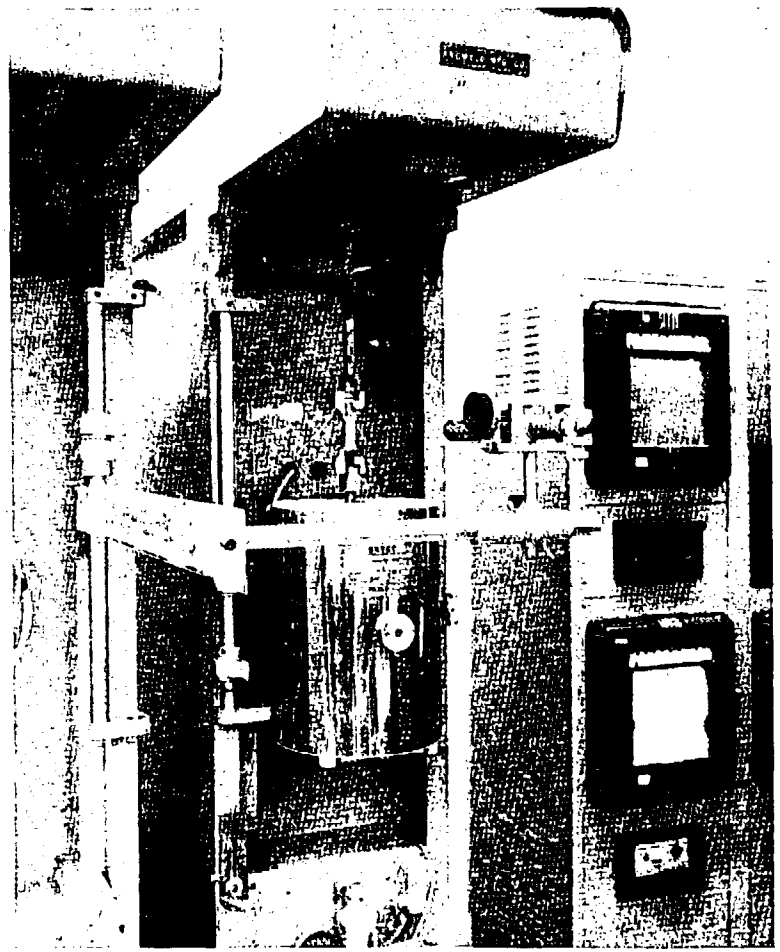

A. LOAD TRAIN ASSEMBLY

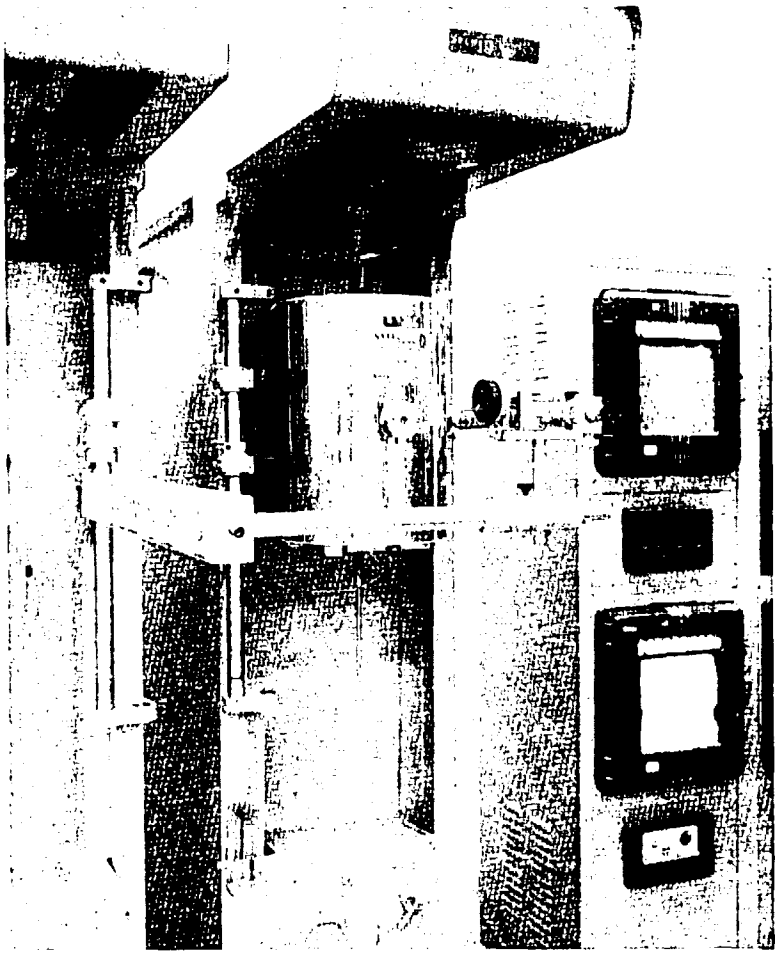

B. FURNACE IN TEST POSITION

D07121

Fig. 4.2-5

Table 4.2-5

HIGH TEMPERATURE LI-1500 TENSION TESTS (UNCOATED SPECIMENS)

TEST TEMP (°F)	SPECIMEN NUMBER	TEST SECTION WIDTH (IN.)	TEST SECTION THICKNESS (IN.)	TEST SECTION AREA (IN.^{2})	LOAD (LB)	STRESS (PSI)	MODULUS (PSI)
RT	TT441	0.450	0.75	0.364	27.2	74.7	75,500
RT	TT442	0.369	0.75	0.2765	15.0	54.2	46,200
RT	TT443	0.364	0.75	0.2655	27.0	101.6	*
				AVERAGE		76.8	60,850
1500	TT445	0.365	0.75	0.274	25.8	94.2	*
1500	TT446	0.368	0.75	0.276	27.7	100.4	*
1500	TT447	0.365	0.75	0.274	30.35	110.7	-
1500	TT448	0.371	0.75	0.278	27.35	98.3	46,700
				AVERAGE		100.9	46,700
2000	TT4410	0.365	0.75	0.274	42.5	155	*
2000	TT4412	0.365	0.75	0.274	42.9	156.5	*
2000	TT4409	0.27	0.75	0.203	33.35	164	(SEE FIG. 4.2-6)
2000	TT4413	0.27	0.75	0.203	37.35	185	-
				AVERAGE		165	16,000

* DOG BONE SPECIMEN STRENGTH TEST ONLY WITH DYNAMIC SETUP (OTHER RESULTS PERFORMED WITH STATIC SETUP)

This trend of increased tensile strength with temperature will exist until the viscosity of the material decreases to the point where the material flows easily at high temperature. At this point, the tensile strength will decrease sharply.

A preliminary stress-strain curve obtained on the static setup for test results at $1500^{\circ}F$ and $2000^{\circ}F$ is shown in Fig. 4.2-6. The increased ductility is indicated by the decrease in modulus from 46,700 $lb/in.^2$ at $1500^{\circ}F$ to 16,000 $lb/in.^2$ at $2000^{\circ}F$.

Since attempts to perform tensile tests at $2500^{\circ}F$ were unsuccessful due to specimen breakage during mounting in the load train and the extreme ductile behavior at $2500^{\circ}F$, tests were performed at 2100, 2200, and $2300^{\circ}F$ to more adequately define the material behavior above $2000^{\circ}F$. All tests were made on a 200-lb-capacity Instron test machine at a constant rate of crosshead travel as previously described. A load-deflection curve with deflection based on crosshead motion was obtained for each sample. Strength values based on initial cross-section area were calculated from loads, and elongation was measured between 1.5-in. gage marks in the reduced test section. Test data are summarized in Table 4.2-6 along with results of earlier tests shown in Table 4.2-5.

The strength of LI-1500 increases with increasing temperature to $2100^{\circ}F$. Ductility is negligible to $1500^{\circ}F$ and is very low ($\approx$ 1 percent elongation) at $2000^{\circ}F$. The measured strength values represent a brittle fracture stress in this temperature range. At $2100^{\circ}F$, the material begins to show some evidence of plastic deformation with 2 to 3 percent elongation in 1 inch at fracture. Above $2100^{\circ}F$, a major change in behavior occurs. The strength decreases rapidly with increased temperature, and ductility increases significantly. As shown in Fig. 4.2-7, very large and uniform elongations of over 150 percent are obtained at $2300^{\circ}F$. The sample tested at $2200^{\circ}F$ failed in the grip section after an increase in strain rate, and the measured elongation of 63 percent in the gage section is not the maximum that can be realized at this temperature.

The load-deflection curves for tests at 2100-$2300^{\circ}F$ are shown in Fig. 4.2-8. The most significant feature is the attainment of a steady state flow stress at 2200 and $2300^{\circ}F$. At a constant crosshead rate of 0.02 in./min, the strength increases slowly with strain and reaches a steady state value after 30-40 minutes. This represents a

HIGH TEMPERATURE STRESS - STRAIN CURVES

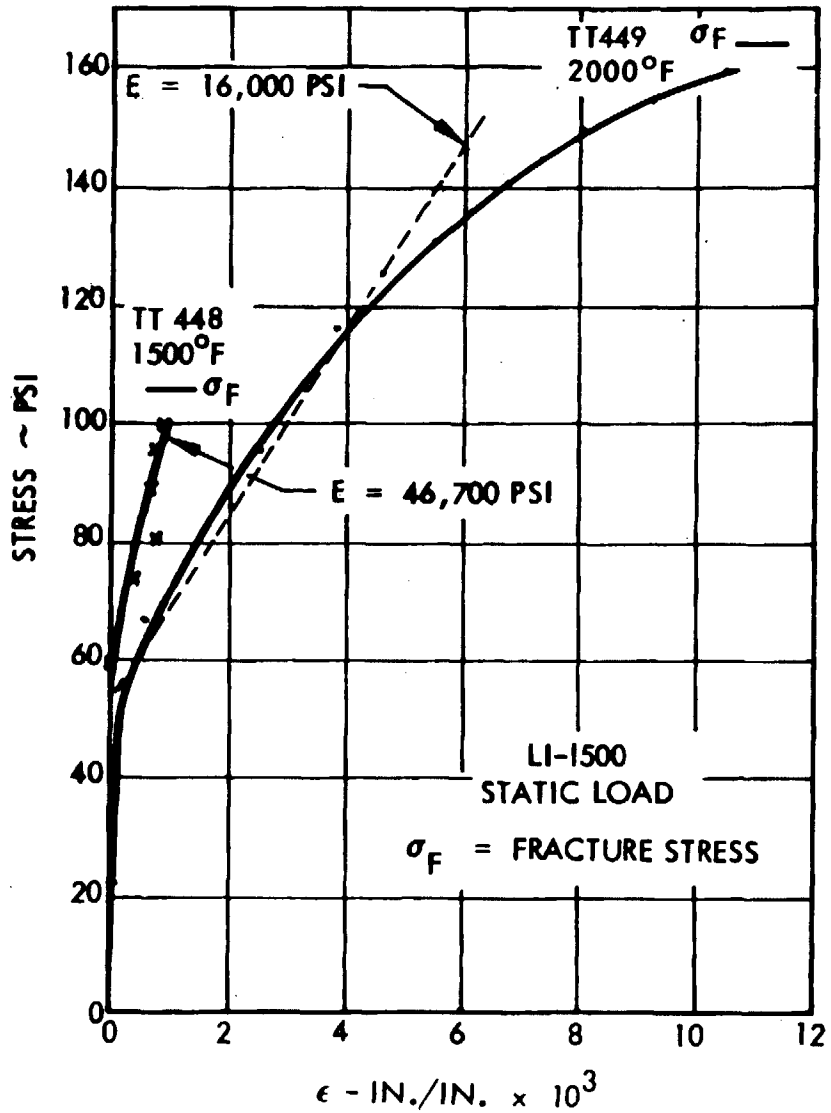

Fig. 4.2-6

Table 4.2-6

SHUTTLE

SUMMARY OF HIGH TEMPERATURE TENSILE TEST DATA

SAMPLE NUMBER	TEST TEMPERATURE (°F)	CROSSHEAD RATE (IN./MIN)	MAXIMUM FLOW STRESS(1) (PSI)	STRESS AT FRACTURE(1) (PSI)	ELONGATION IN 1-INCH (%)
TT441	75	0.02	-	75(2)	0.08
TT442	75	0.02	-	54	0.09
TT443	75	0.02	-	102	N.D.
TT445	1500	0.02	-	94	N.D.
TT446	1500	0.02	-	100	N.D.
TT447	1500	STATIC	-	110	0.04
TT448	1500	STATIC	-	98	0.09
TT4410	2000	0.02	-	156(2)	N.D.
TT4412	2000	0.02	-	155(2)	N.D.
TT449	2000	STATIC	-	164	1.04
TT4413	2000	STATIC	-	185	N.D.
TT4461	2100	0.02	-	181(2)	3.3
TT4462	2100	0.02	-	187(2)	2.5
TT4463	2200	0.02	88		
		0.05	218		
		0.10	-	285(2)	63
TT4460	2300	0.02	10.9		
		0.50	-	202	150

(1) BASED ON ORIGINAL CROSS-SECTION AREA.
(2) BROKE IN SHOULDER THROUGH PIN HOLE.

LI-1500 TENSILE TEST SAMPLES

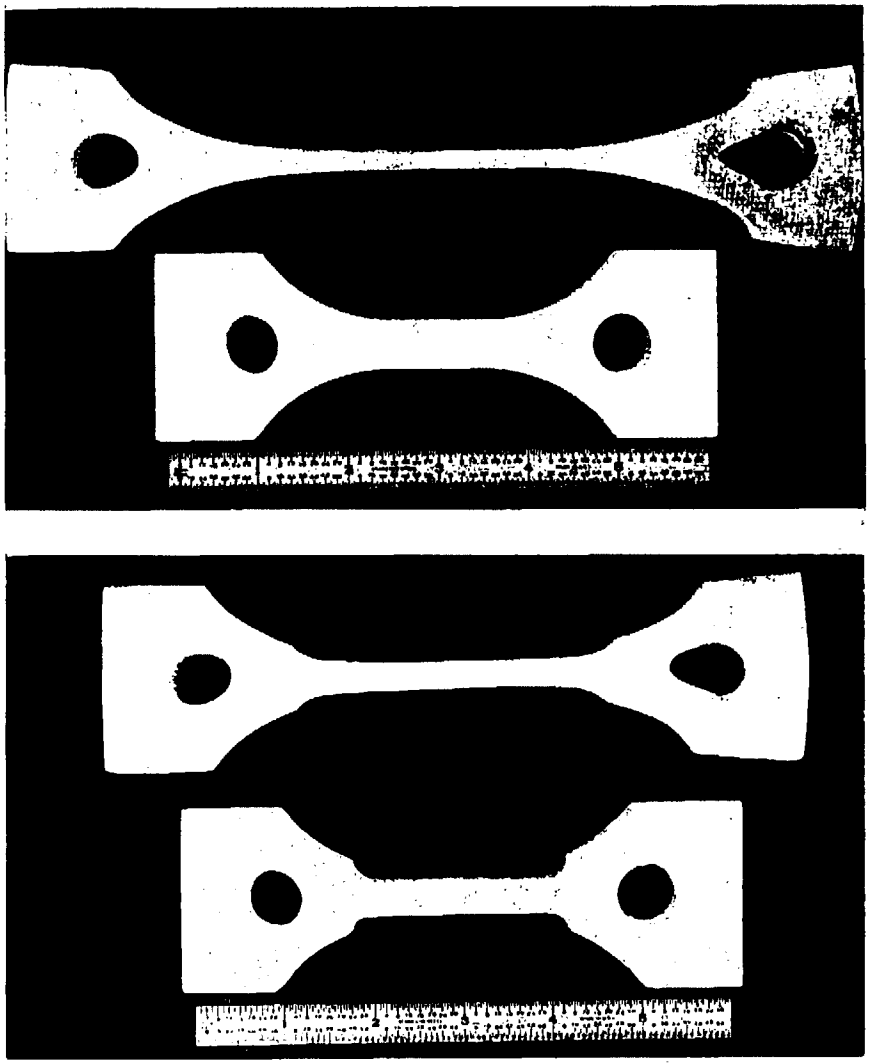

2300°F

AS RECEIVED

CROSSHEAD
RATE
0.02 IN./MIN

2200°F

2100°F

Fig. 4.2-7

EFFECT OF TEMPERATURE AND STRAIN RATE ON LOAD-DEFLECTION (TIME BASE) CURVES IN TENSION

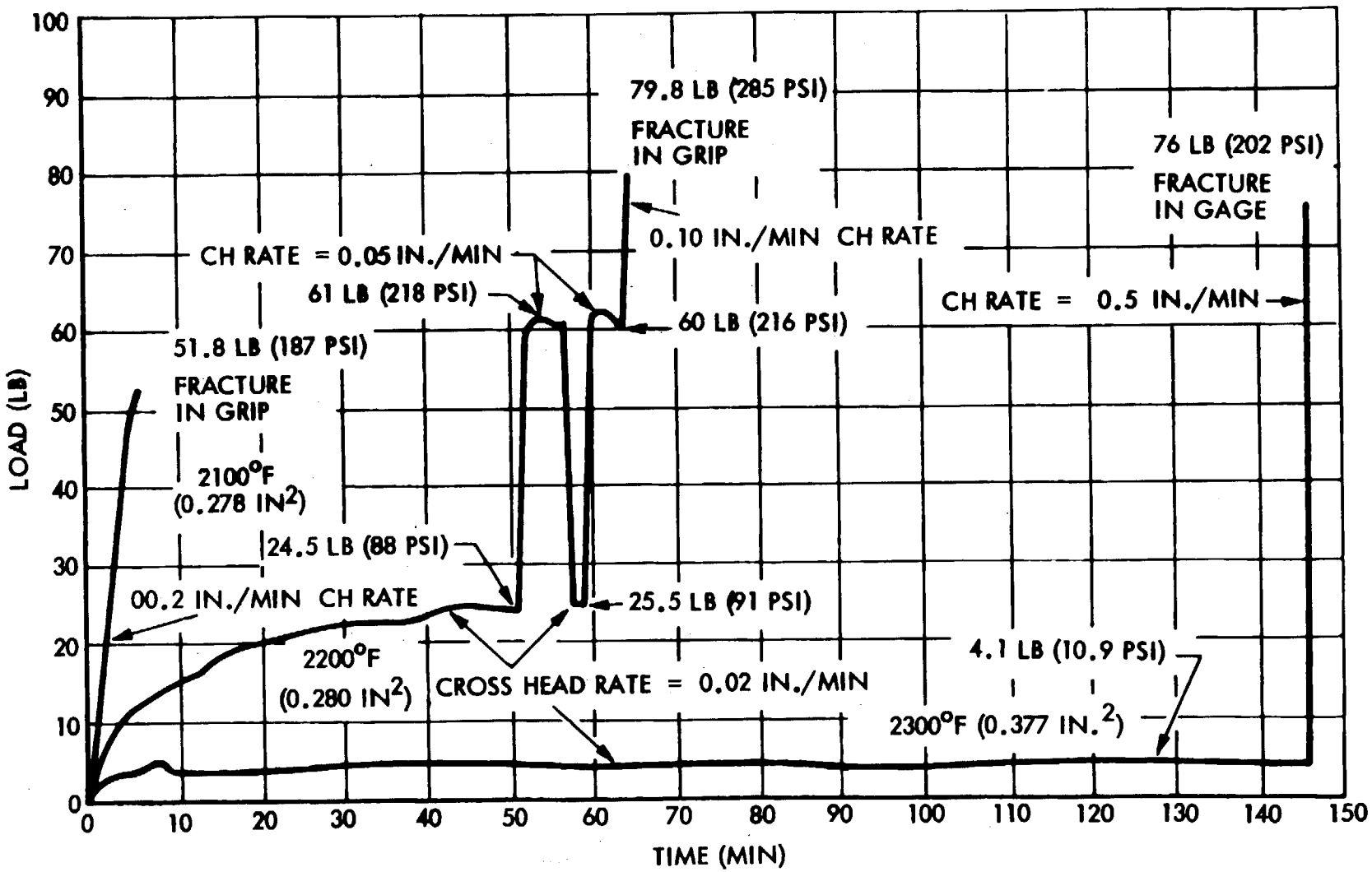

Fig. 4.2-8

total elongation of 0.6 - 0.8 in. From this point on, the material deforms plastically with no increase in stress. At 2100°F, the sample fractured in the grip section before a steady state condition was attained.

The flow stress in the ductile high temperature region is strongly dependent on temperature and strain rate. As shown in Fig. 4.2-8, a 100°F increase from 2200 to 2300°F reduces strength by a factor of 8 (from 88 to 11 psi). Slight variations in temperature during the test are reflected as variations in the load-deflection curve, with as little as 5°F change in sample temperature producing a noticeable change in load (stress). The strain rate sensitivity is also very pronounced. Increasing the strain by 2.5 (from 0.02 to 0.05 in./min) at 2200°F more than doubles the flow stress. As shown in Fig. 4.2-8, if the strain rate is reduced to the former value, the flow stress immediately decreases to the corresponding value, and no permanent change is effected. The measured strength or flow stress value, therefore, depends only on the rate of straining and temperature and is not influenced by the extent of deformation that occurs, at least for the conditions studied here. This behavior is clearly shown by the results of cycling the strain rate at 2200°F between 0.02 and 0.05 in./min (Fig. 4.2-8).

The shape of the load-deflection curves, strain rate sensitivity, and large but uniform elongation above 2100°F indicate that deformation in this region is occurring by a process analogous to viscous flow or grain boundary sliding. A log-log plot of flow stress vs crosshead rate (strain rate) reveals that the stress exponent, n , in the relation $\dot{\epsilon} = K\sigma^n$ is unity (Fig. 4.2-9). This type of behavior is characteristic of glasses at high temperature and of many plastic (long chain polymer) materials. Avery and Backofen* have shown by a simple geometric model that with a stress exponent of unity the rate of change in cross-section area, dA/dt, is independent of the cross-section area, and localized deformation or necking will not occur during straining. This type of behavior is clearly indicated for LI-1500 at 2200-2300°F (Fig. 4.2-7). It is not known if the mode of deformation involves actual deformation of the SiO_2 fibers or merely sliding between individual fibers. Considering the structure and density of LI-1500, it is postulated that sliding between the fibers may be the primary deformation mode.

*D.H. Avery and W.A. Backofen, "A Structural Basis for Superplasticity", ASM Trans. Quart., 58 (1965) 551.

STRESS DEPENDENCY OF STRAIN RATE AT TEMPERATURES IN VISCOUS FLOW REGION

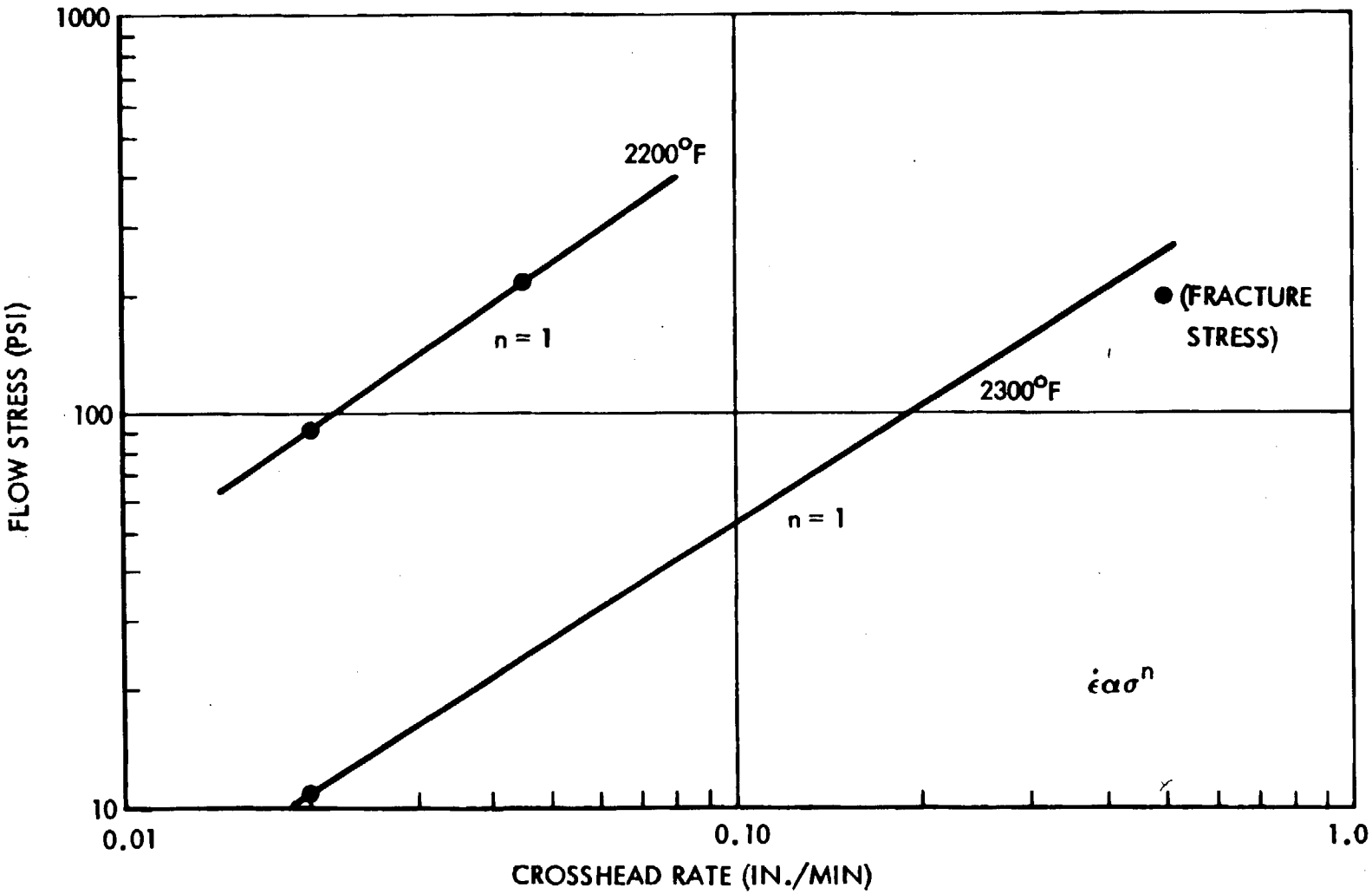

Fig. 4.2-9

The behavior of LI-1500 in tension at elevated temperatures is similar to that of many materials that have a temperature-dependent transition from ductile to brittle behavior. As temperature is decreased, the yield or flow stress increases while the fracture stress decreases. At some temperature, the two become equal and this is the limit of ductile behavior. At lower temperatures, the flow stress exceeds the fracture stress and fracture occurs with little or no deformation. This behavior is illustrated for LI-1500 in Fig. 4.2-10. The brittle fracture and ductile flow stresses are plotted as functions of temperature on a semi-log plot of stress vs reciprocal of absolute temperature. Thermally activated processes will have an exponential temperature dependency and can be plotted effectively for analysis in this manner. As shown in Fig. 4.2-10, the two curves intersect at 2160^{o}F, which is indicated to be the ductile to brittle transition temperature at a crosshead rate (strain rate) of 0.02 in./min. The maximum strength of the material is realized at this temperature and is indicated to be 190 psi for LI-1500.

The results of these tests indicate that more detailed studies are needed to fully characterize the high temperature behavior of LI-1500. A more complete knowledge of strain rate and temperature effects in both tension and compression coupled with a basic understanding of deformation and fracture modes would be very helpful in assuring the design of effective and reliable RSI panels.

4.2.3 Room Temperature Compression Tests

The compression test setup is shown in Fig. 4.2-11. All details are similar in concept to those of the tensile test, except that a spherical universal joint is used at only one end of the specimen. Accuracies, measurement procedures, and test rates are the same as for the tensile test. The test results are shown in Table 4.2-7.

For the parallel-to-fiber orientation direction, the modulus is essentially the same as obtained under NAS 9-11222, and the compressive fracture strength is slightly higher. For the normal-to-fiber orientation direction, the compressive modulus and fracture strength are essentially the same as those obtained under NAS 9-11222.

DUCTILE TO BRITTLE TRANSITION IN LI-1500

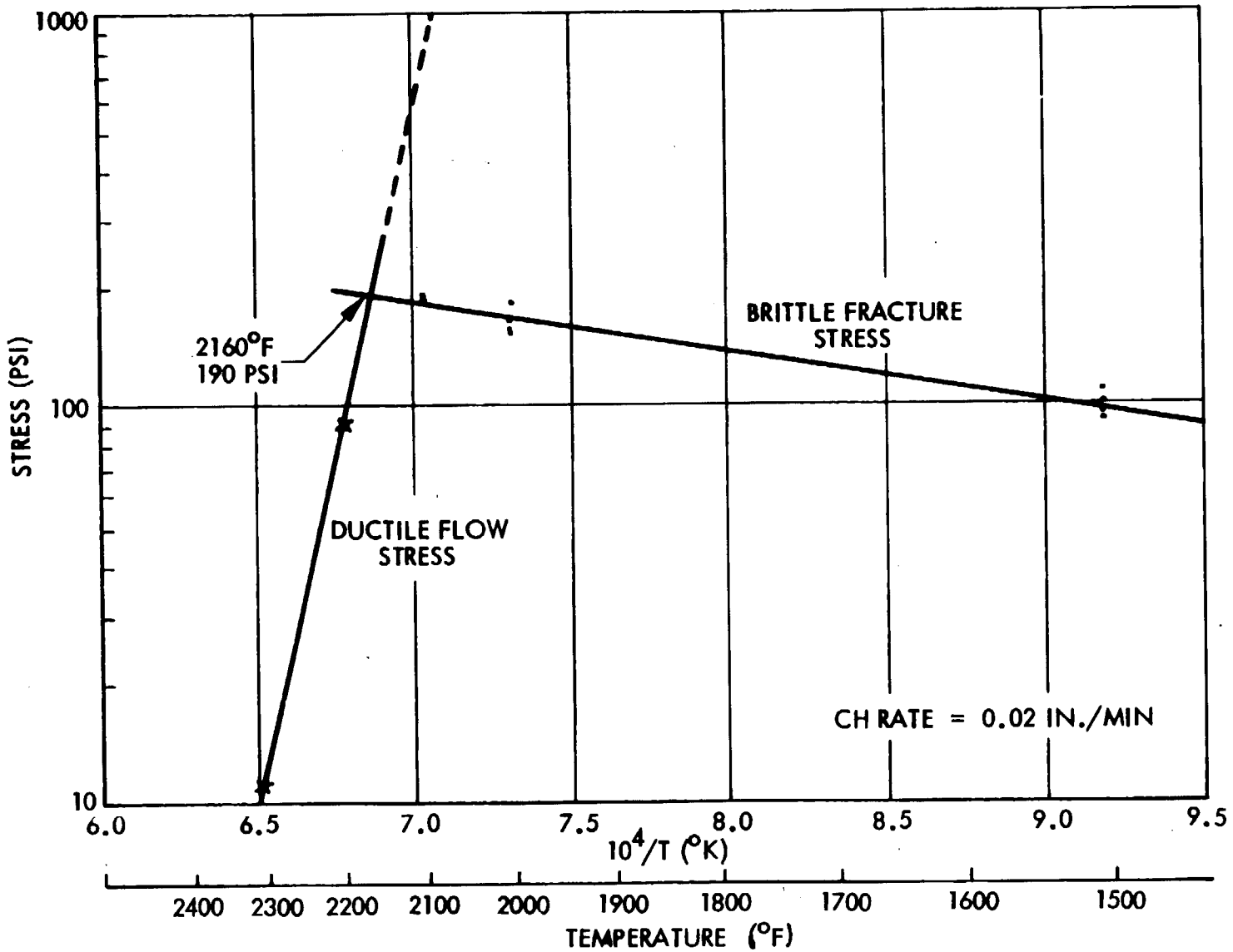

Fig. 4.2-10

TEST FIXTURE FOR COMPRESSION TESTS OF LI-1500

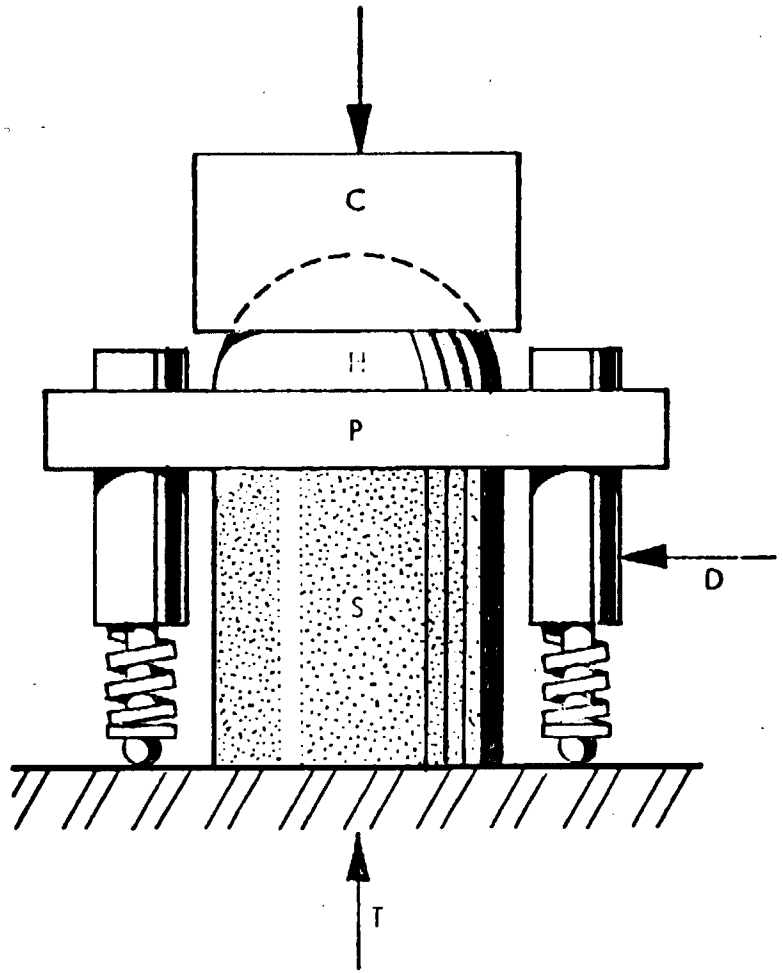

Fig. 4.2-11

Table 4.2-7

LI-1500 ROOM TEMPERATURE COMPRESSION TESTS
(Uncoated Specimens)

Direction	Specimen Number	Total Length (in.)	Test Section Width (in.)	Thickness (in.)	Weight (gm)	Test Section Area (in.)	Load (lb)	Stress (psi)	Modulus (psi)
Parallel	TT 29-1	3.00	2.00	2.00	43.5	4.00	720	180	37,800
	TT 29-2	3.05	2.05	2.08	46.0	4.26	810	190	40,000
	TT 29-3	3.00	2.00	2.05	46.0	4.10	698	170	47,000
	TT 29-4	3.05	2.05	2.05	46.0	4.20	755	180	46,500
	TT 29-19	3.00	2.05	2.05	44.5	4.20	742	177	36,100
	TT 29-20	2.00	2.05	3.00	44.0	6.15	906	148	30,800
					Average			174	39,700
					NAS 9-11222 Average			156	42,560
Normal	TT 29-5	2.05	3.00	2.00	44.0	6.00	253	42.2	5,120
	TT 29-6	2.05	3.05	2.05	44.0	6.25	268	42.9	3,620
	TT 29-7	2.05	3.00	2.00	44.0	6.00	257	44.2	4,070
	TT 29-8	2.05	3.00	2.05	44.0	6.15	242	39.4	3,470
					Average			42	4,070
					NAS 9-11222 Average			41	4,574

The test results for the thermally and acoustically cycled specimens are shown in Table 4.2-8. Both the modulus and fracture strength increased over the values for the as-fabricated material.

The results of the compression tests on specimens that were coated with LI-1500 on one 3 in. x 2 in. side are tabulated in Table 4.2-9. The average strength values are essentially the same as those obtained from the uncoated specimens, whereas the modulus is 50 percent higher.

4.2.4 High Temperature Compression Tests

High temperature compression tests were conducted at 2300°F on three 1 x 1 x 1 in. specimens in the same Instron model TM tensile test machine used for the tension tests. The specimens were placed between two 1.5-in. diameter inconel push rods with a 200-lb load capacity. The tests were made at a constant crosshead rate of 0.02 in./min. Deflection was based on crosshead motion. The specimens were heated to the test temperature (2300°F) with a platinum-wound tube furnace having a 3-in. diameter by 15-in. long hot zone. Temperature measurements were made with a thermocouple attached to the bottom of an inconel push rod.

The tests were conducted parallel and normal to the fiber orientation direction, and the results are shown in Table 4.2-10. The initial yield stresses for all cases are greater for the specimens tested parallel to the fiber orientation. The material behaved as would be expected for a material with a high porosity. Typical stress-strain curves for the specimens TT 2088-3-1 and TT 2088-3-2 are shown in Fig. 4.2-12. Although the data indicate the material is still capable of withstanding load after the initial yield stress occurs, the usefullness of the material from an engineering standpoint is lost.

4.2.5 Bend Tests

In the bend tests, a four-point loading fixture was used. The four-point loading is indicated, because it reduces the damage at the loading points by a factor of two.

Table 4.2-8

SHUTTLE

LI-1500 COMPRESSION TESTS

(POST-THERMAL AND ACOUSTICAL CYCLING)

NUMBER OF THERMAL AND ACOUSTICAL CYCLES	SPECIMEN NUMBER	MAXIMUM LOAD (LB)	MAXIMUM STRESS (PSI)	MODULUS (PSI)
PARALLEL	3-1	948	237	82,900
10	3-2	988	247	83,600
	3-3	868	217	87,700
		AVERAGE	234	84,700
NORMAL	3-4	328	82	12,465
10	3-5	288	72	8,766
		AVERAGE	77	10,615

ALL SPECIMENS 2 x 2 x 3 IN., EXCEPT 3-4, 3-5 WERE 2 x 2 x 2 IN.
TEST SECTION AREA = 4.00 $IN.^2$
TESTED IN PARALLEL AND NORMAL TO FIBER ORIENTATION DIRECTION.

Table 4.2-9

LI-1500 ROOM TEMPERATURE COMPRESSION TEST
(Coated Specimens*)

Direction	Specimen Number	Total Length (in.)	Test Section Width (in.)	Thick-ness (in.)	Weight (gm)	Test Section Area ($in.^2$)	Load (lb)	Stress (psi)	Modulus (psi)
Parallel	TT 29-10	3.00	2.00	2.00	47.5	4.00	730	182	58,900
	TT 29-11	3.00	2.00	2.00	46.0	4.00	612	153	52,100
	TT 29-12	3.00	2.00	2.00	46.5	4.00	662	164	69,300
	TT 29-14	3.00	2.00	2.00	46.0	4.00	680	170	61,000
						Average		167	60,300

*Coating on one 3 in. x 2 in. face

Table 4.2-10

HIGH TEMPERATURE LI-1500 COMPRESSION TEST RESULTS

TEST TEMP (°F)	SPECIMEN NUMBER	TEST SECTION AREA ($IN.^2$)	INITIAL YIELD			MODULUS (PSI)	MAXIMUM STRESS (1) (PSI)	STRAIN AT MAXIMUM STRESS (IN./IN.)	FINAL THICKNESS (IN.)
			LOAD (LB)	STRESS (PSI)	STRAIN (IN./IN.)				
PARALLEL									
2300	TT29-23-1	1	44	44	0.050	2553	200	0.590	0.426
2300	TT29-22-1	1	48	48	0.035	2500	200	0.612	0.393
2300	TT2088-3-1	1	29.2	29.2	0.035	1363	200	0.700	-
			AVERAGE	40	-	2140			
NORMAL									
2300	TT29-23-2	1	3	3	0.020	200	200	0.697	0.303
2300	TT29-22-2	1	7.5	7.5	0.060	238	200	0.659	0.353
2375	TT2088-3-2*	1	2	2	0.050		200	0.772	-
			AVERAGE	4	-	219			

* TEMPERATURE 2375°F, CONTROLLER ERROR.

(1) MAXIMUM STRESS ATTAINED, NO FRACTURE TO THIS POINT

HIGH TEMPERATURE COMPRESSION CURVES

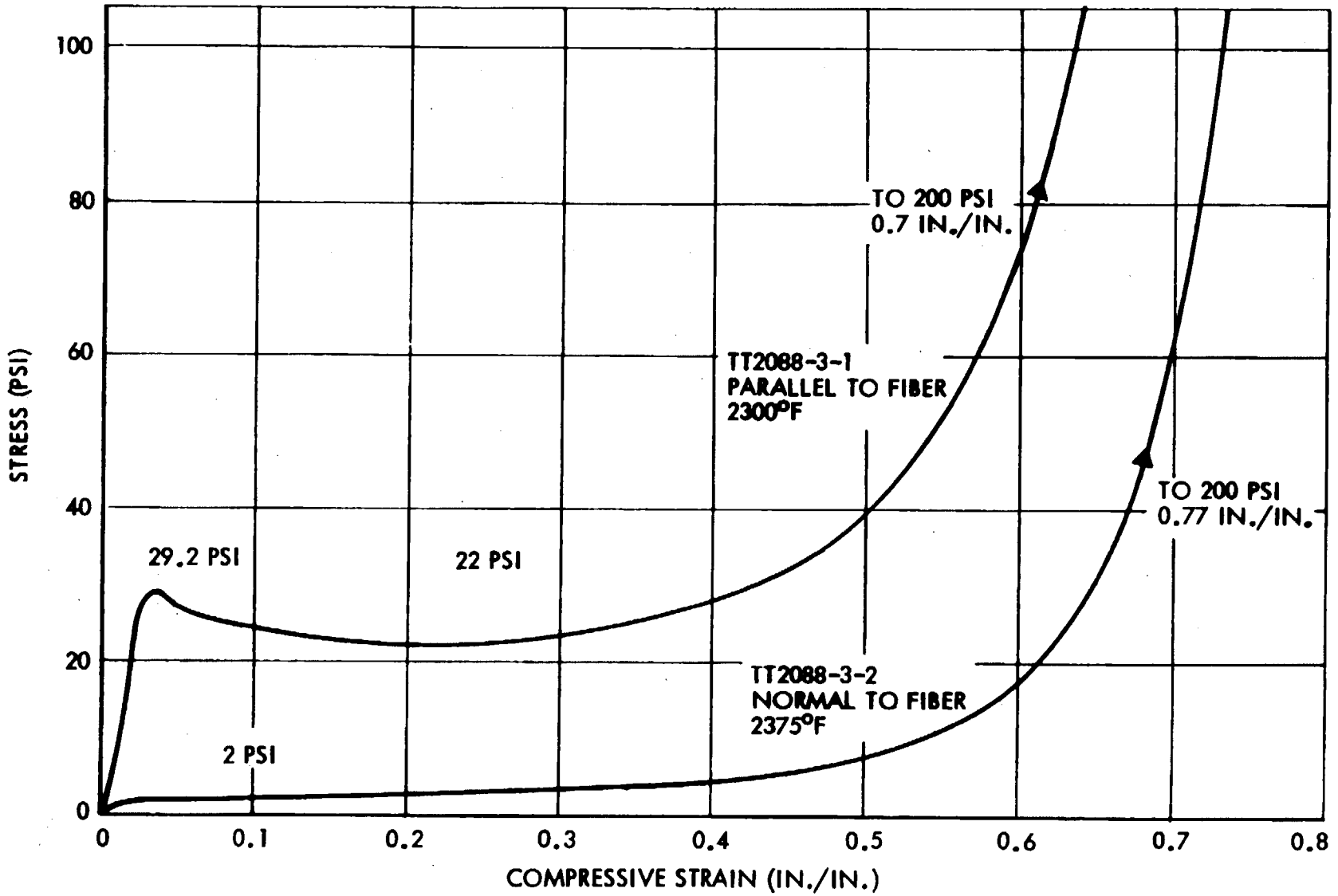

Fig. 4.2-12

As shown in Fib. 4.2-13 the two lower rollers were placed 8 in. apart with the two center loading rollers 2 in. apart and symmetrically located. Another was placed above the center to ensure load equality at these two points. One-eighth inch shims were bonded to the specimen with double-faced tape to reduce local indentation due to the rollers.

These tests were performed on an SR-4 universal screw-driven testing machine. A high-sensitivity load cell is placed between the upper-most roller and the test machine crosshead to measure failure loads that are very low compared to the machine's capacity. The loading rate is adjusted so that the specimen fails in about 1 min. of loading. This produces a loading rate of about 0.25 percent per min.

Deflection was measured by a linearly variable differential transformer placed at the specimen midspan. A small disc of 0.005 in. shim was bonded to the specimen with double-faced tape so as to present a smooth, flat, and rigid point for the deflectometer probe. On an X-Y plotter, deflection is recorded continuously versus load. System accuracy is ±1.5 percent of the maximum values being recorded. A photo of the test setup is shown in Fig. 4.2-13.

The specimen is measured to a 0.020 in. accuracy before testing, and an average of five readings is taken for each dimension. The material is assumed to have the same modulus in tension as in compression when computing the failure stress and modulus of elasticity in bending, so that values are for an average beam. The bending results for the as-fabricated specimens are shown in Table 4.2-11.

The bending results for the thermally and acoustically cycled specimens are shown in Table 4.2-12. The results indicate an increase in both the fracture stress and modulus for the cycled specimens. The 55 percent increase in fracture stress for the cycled specimens over the as-fabricated values compares favorably with the reported 50 percent increase from the Battelle tests on coated specimens.

PHOTO OF BEND TEST SPECIMEN AND LOADING FIXTURE

FLEXURE TEST

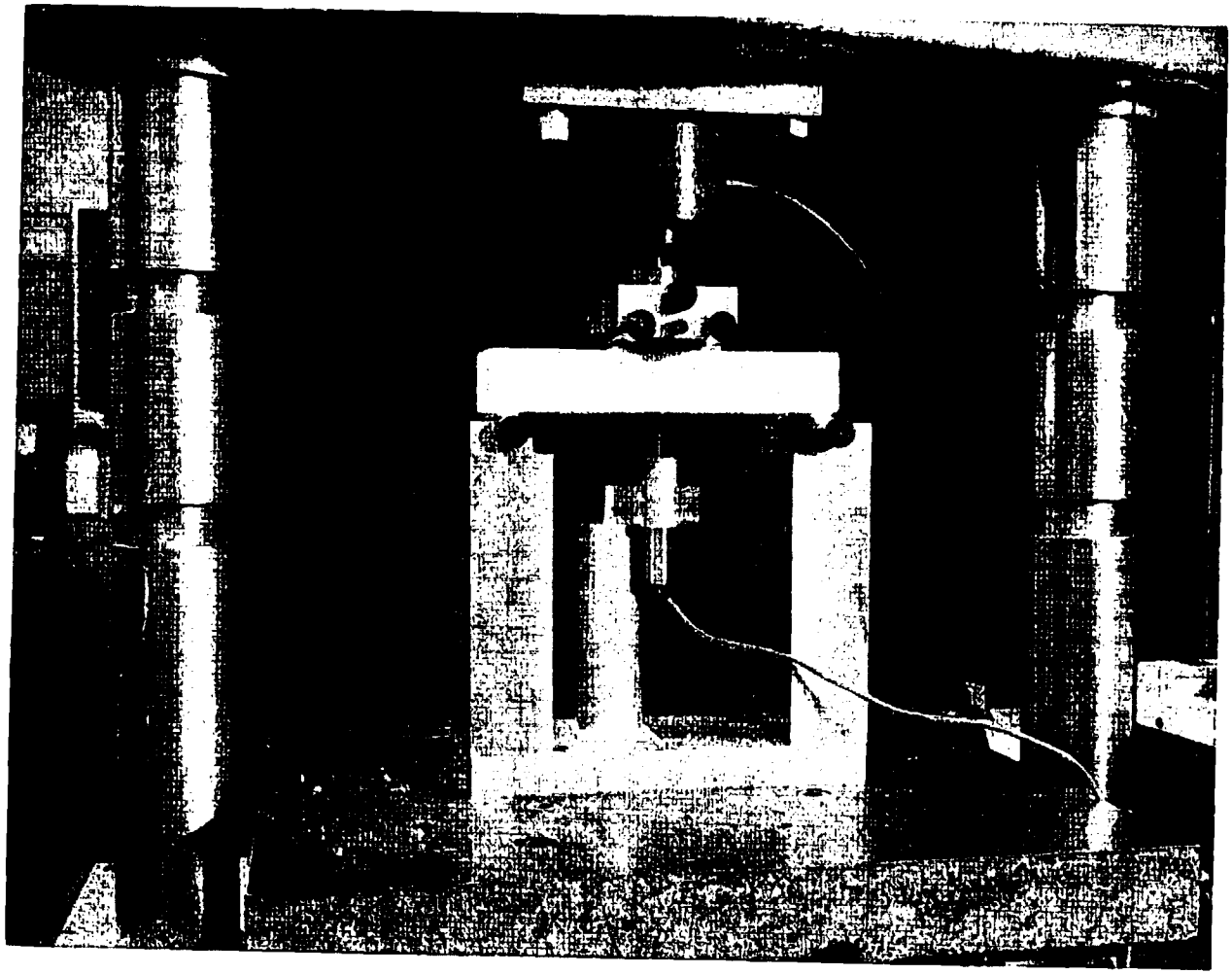

FIG. 4.2-13

Table 4.2-11

LI-1500 BENDING TESTS
(R.T., Four-Point Loading)

Specimen Number	Width (in.)	Thick-ness* (in.)	Length (in.)	Weight (gm)	Density (lb/ft^3)	Load (lb)	Deflection (in.)	Stress ($lb/in.^2$)	Modulus ($lb/in.^2$)
1	3.0	1.5	9.0	150.0	14.1	70	0.0272	93.3	29,600
2	3.0	1.5	9.0	151.5	14.2	87	0.0172	116.	58,300
3	3.0	1.5	9.0	155.0	14.6	90	0.0167	120.	62,400
4	3.0	1.5	9.0	151.0	14.2	100	0.0186	133.	62,600
5	3.0	1.5	9.0	143.5	13.5	84	0.0176	112.	56,000
Average								114.9	53,780

*Normal to fiber orientation direction

Table 4.2-12

LI-1500 BENDING TESTS

(AFTER THERMAL AND ACOUSTICAL CYCLING)

SPECIMEN NUMBER	TEST SECTION AREA ($IN.^2$)	LOAD (LB)	STRESS (PSI)	MODULUS (PSI)
1	4.5	148	197	83,046
3	4.5	110	146	78,962
4	4.5	146	194	87,576
	AVERAGE		179	83,195

TESTED IN PARALLEL TO FIBER ORIENTATION DIRECTION.
STRESS AND MODULUS BASED ON NEUTRAL AXIS AT $h/2$.

4.2.6 Disc Shear Tests

The anisotropic properties of LI-1500 are due to a layering effect known to exist in the fibers that make up the material. Although randomly oriented within these layers or planes, the fibers do not, to any appreciable extent, cross the boundaries between the layers and tie the layers together. The result is a material that tends to behave like a stack of boards or sheets that (1) can easily be deformed (pushed out of plumb) if loaded horizontally (assuming the boards are lying in a horizontal plane), but (2) is harder to deform if load is applied across the plane of boards so that a shearing force is applied to the stack. To do this, the stack of boards would have to be overhanging a loading dock. A fork lift applying upward force or a man standing on the overhanging end would be more likely to displace the whole stack rather than disrupt the relative positions of the boards.

This effect is illustrated more specifically in Figs. 4.2-14a, b, and c. In each figure, the shear force is in the X-direction, and the diagonal tension (maximum tension arising out of the shear force) force lies at 45-deg to the X-axis in the X-Z plane. Referring to Fig. 4.2-14a, note that the layers are such that the fibers lie in the X-Y plane and none come closer than 45 deg to resisting the maximum diagonal tension. Note in Fig. 4.2-14b that although the layers are now such that the fibers fall in the Y-Z plane, none come closer than 45-deg to resisting the maximum diagonal tension, which is still at 45-deg to the X-axis in the X-Z plane. In Fig. 4.2-14c, the layers are so arranged that all the fibers lie in the X-Z plane and , since they are randomly oriented in this plane, it is evident that many must be in the 45-deg direction of maximum tension, or at least close to it. This is also illustrated in Fig. 4.2-14c, where both component vectors T_Z and T_X lie in the fiber orientation plane. The result is that when specimens are tested as shown in Fig. 4.2-14c, they will show a greater shear strength and modulus.

For the most recent series of tests, a new fixture was designed that made it easier to display this significant difference between the week and strong directions of the material. The fixture used in earlier test series (see Fig. 4.2-17) was capable of showing this variation in properties, but the specimens had to be cut from a slab at least 6 in. thick, which was impractical because of excessive cost.

ORIENTATION FOR SHEAR TEST

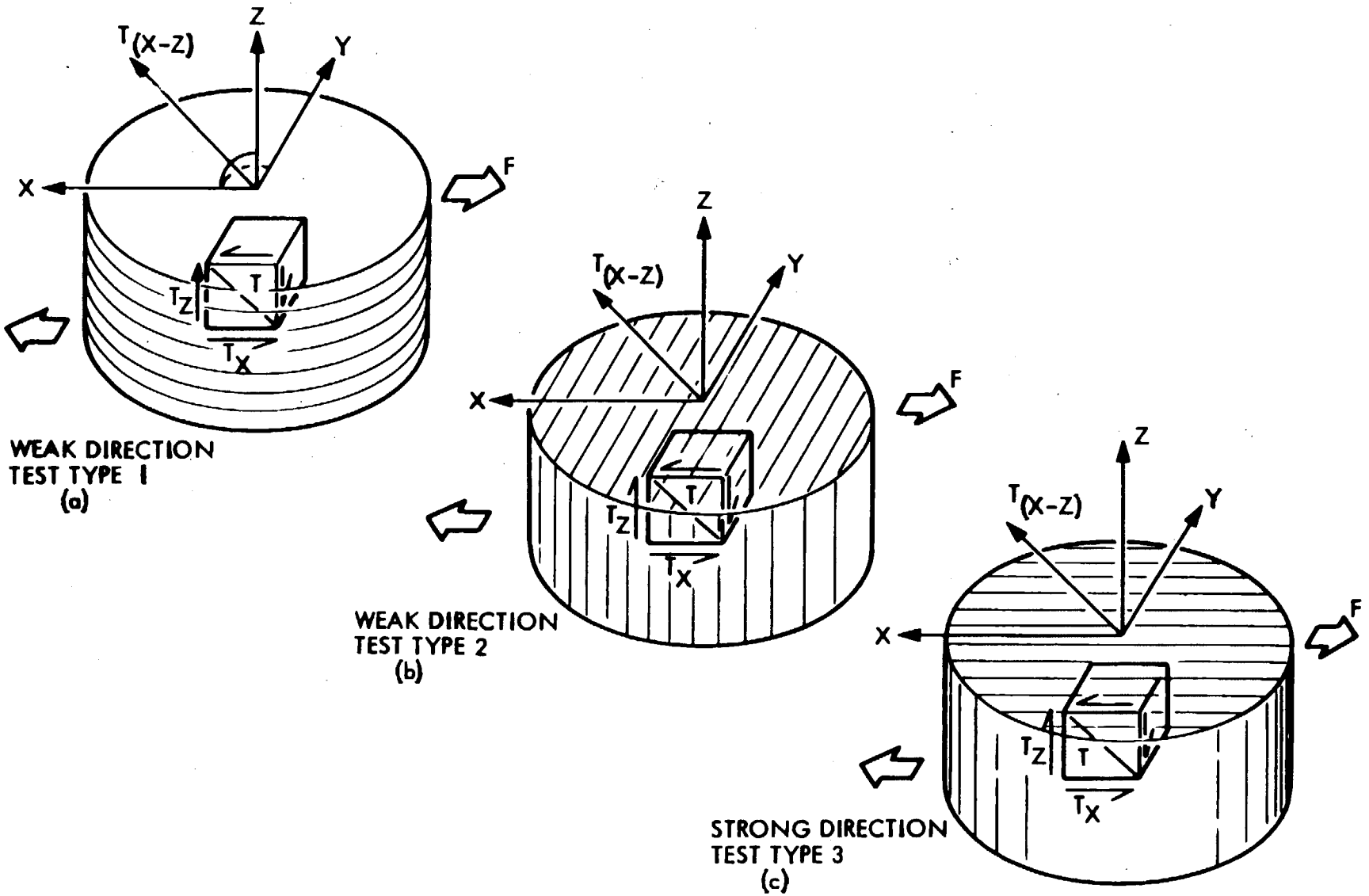

DO6078

Fig. 4.2-14

The present fixture (Fig. 4.2-15) applies a shearing motion to two specimens bonded to two bars, as shown in Fig. 4.2-16. This fixture is of a unique design, which makes it possible to apply only torsion to the assembly. At the base of the frame is a torque generator consisting of a cable wound around a drum and pulled by a hydraulic ram. A load cell is inserted into the cable between the ram and the drum so that the applied force is accurately measured. The drum is supported on high-quality bearings so that the friction is negligible. The lower plate of the specimen assembly (Fig. 4.2-16) is bolted to this drum.

The upper plate (Fig. 4.2-16) is connected to a torque-resisting head. This head has five degrees of freedom; i.e., it is free to rotate or translate about either horizontal axis by virtue of linear ball bushings mounted in gimbal configuration. In addition, the head can translate in a vertical direction (by virtue of linear ball bushings), but rotation about the vertical axis is impossible. The high-quality bearings make the five-degrees-of-freedom motion very free. In addition, the weight of the torque resisting head is "eliminated" from the specimen by suspending the head by a very soft spring and turnbuckle. The latter is adjusted until a very fine air gap exists between the upper specimen plate and the attachment plate. The spring rate of the suspension system is about 0.5 lb/in. so that gap closure induces only 0.005 lb of force to the specimen assembly, which is less than the weight of one of the plates bonded onto the LI-1500.

Deflectometers measure the relative movement of the two plates, and load (torque) is recorded versus this movement on an X-Y plotter.

Specimens required for one test are a pair of discs, each 2 in. in diameter by 1 in. in height. An additional test series was performed with specimens only 3/8-in. high. The height of the specimen is the chief shortcoming of the test method. The higher the specimen, the greater the overturning moment (see Fig. 4.2-17) and, consequently, the greater the normal forces on the end faces of the specimen. (The normal forces, as shown in Fig. 4.2-17, exist on the top and bottom face and in a distribution pattern that is unknown but self-balancing in the vertical direction.)

PHOTO OF SHEAR TEST SPECIMEN IN TEST APPARATUS

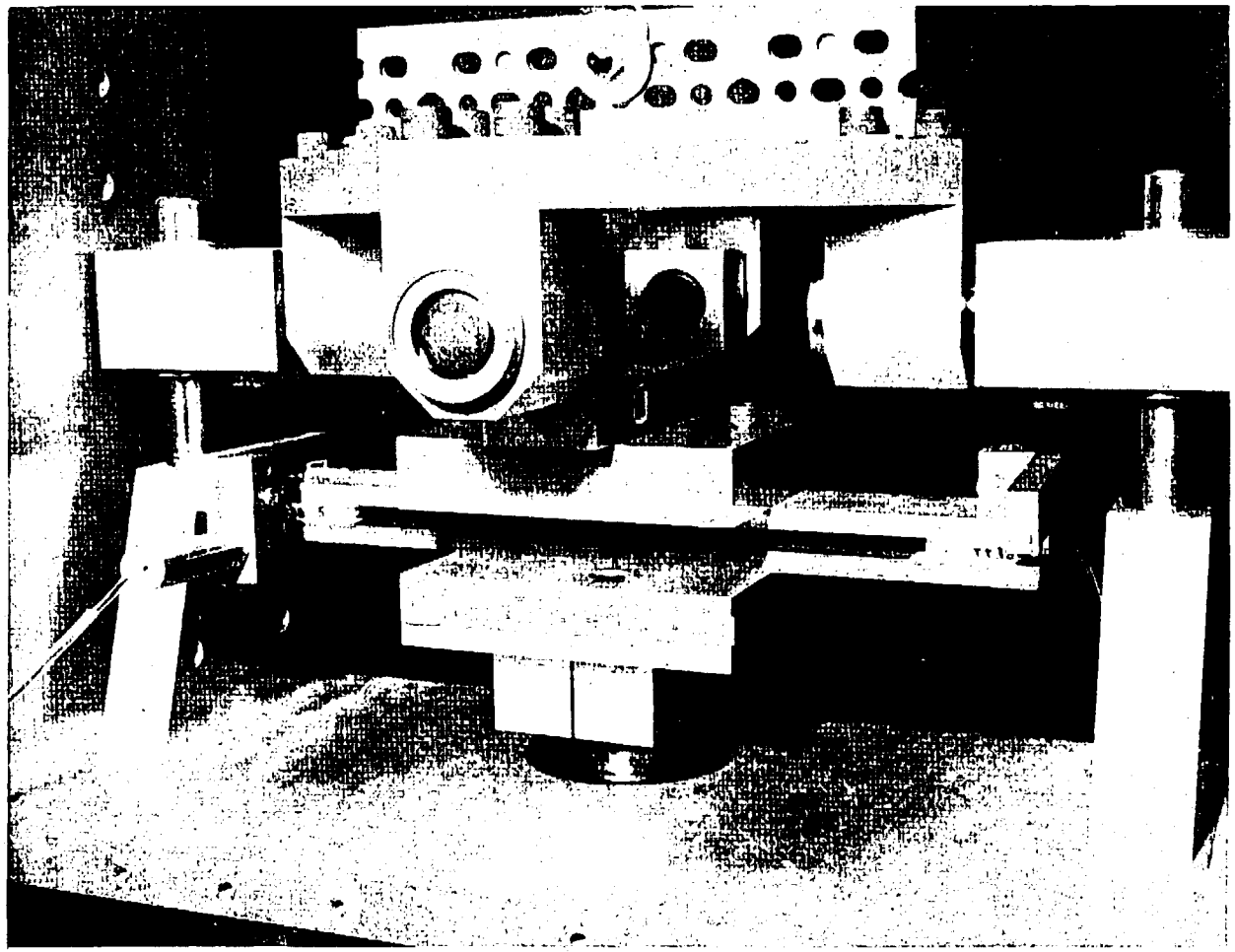

Fig. 4.2-15

SHEAR TEST SPECIMENS AND MOUNTING PLATES

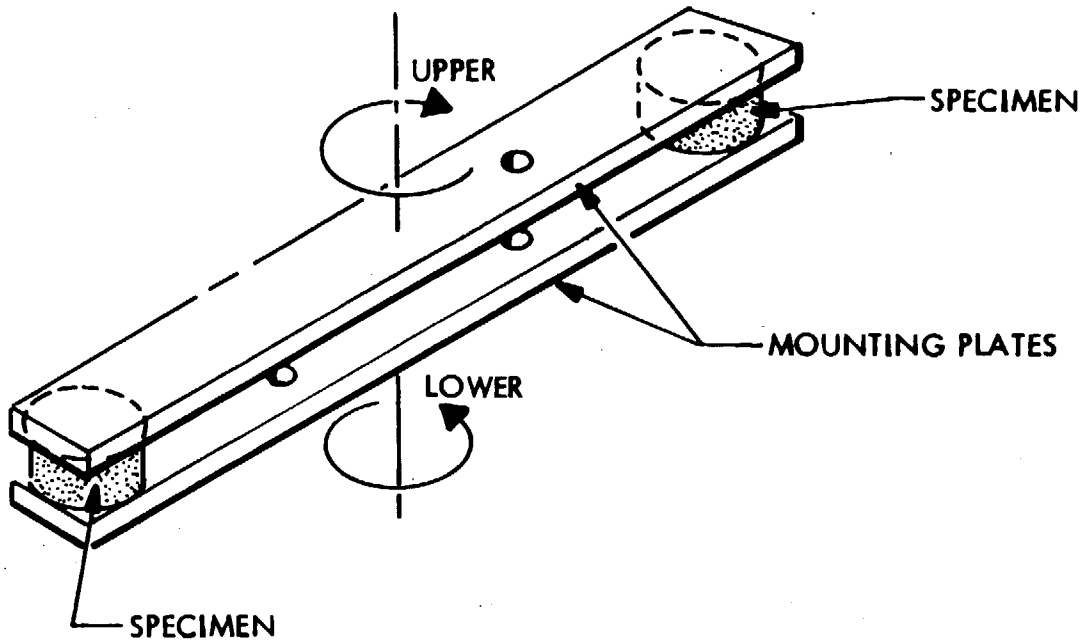

Fig. 4.2-16

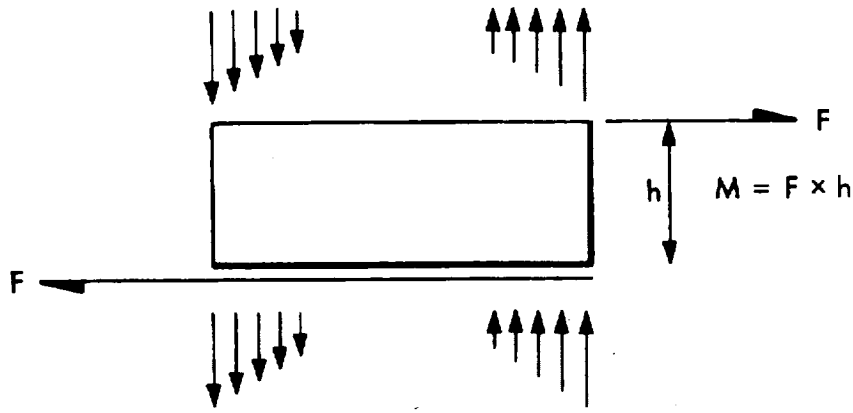

Fig. 4.2-17 Shear Test Specimen

There is no doubt that these normal forces, superimposed on the maximum diagonal tension produced by the shear, influence the results of the shear test – probably unfavorably. The only method of testing that would theoretically remove normal forces is a test on a cylindrical specimen having a relatively thin wall. Such a test would be expensive because the specimen must be large to make possible a relatively thin wall to obtain an unbiased shear test. Manufacture of a consistent specimen would be difficult.

Note that a test fixture used on an earlier series of tests, NAS 9-11222, produced somewhat stronger shear test results on a batch of material that generally showed lower strength values in all other mechanical tests. Figure 4.2-18a shows the test fixture conforming to requirements set forth by the ASTM for testing honeycomb sandwich in shear. One refinement added to the fixture is believed to cause higher shear test values; this refinement is the addition of a rim to the bonding plate, shown in Fig. 4.2-18b. This rim consists of three plates (one end plate and two triangular edge end plates) bolted to the main plates to which the specimen is bonded. Thus, the specimen is partially boxed in. In addition, bonding is used on all surfaces of the rim in contact with the specimen.

It is believed that the fixture with the rim produced higher test results because it resulted in a favorable superimposed compression field that partially cancelled the maximum diagonal tension. The effect is easier to visualize by the use of a diagram in which the box is slightly distorted (see Fig. 4.2-19). In this diagram, a tensile force

SCHEMATIC OF NAS9-11222 SHEAR TEST FIXTURE

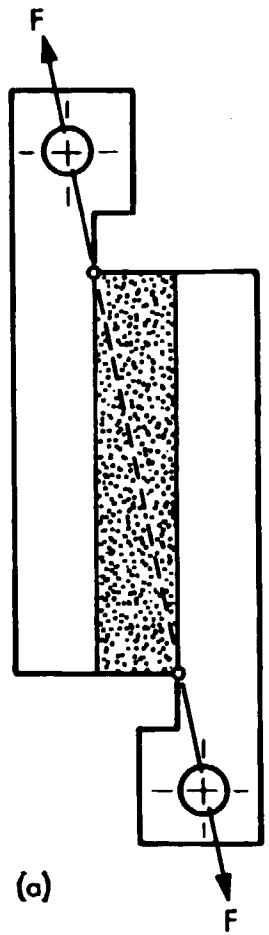

ASTM FIXTURE
(NO RIM)

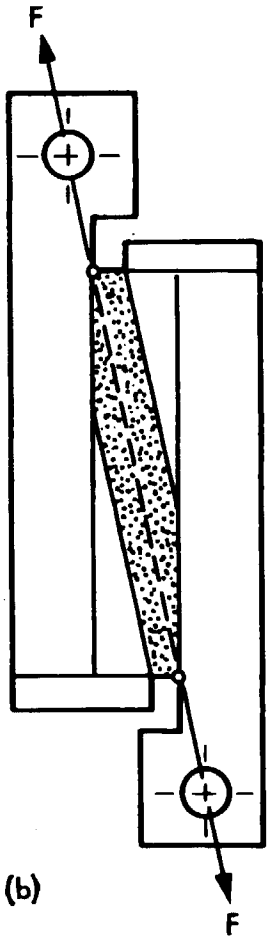

RIM ADDED TO
ASTM FIXTURE

DO6077

Fig. 4.2-18

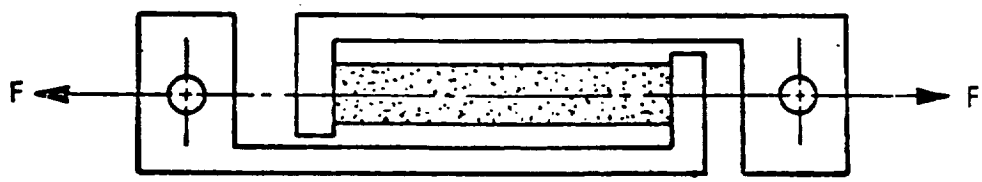

Fig. 4.2-19 Schematic of Compression Load Path

applied to the fixture results in a compressive force on the specimen. If it is remembered that the specimen is weak (i.e., has a low modulus) in shear, it is not difficult to see why an alternate load path (in this case that of a strut in compression) should carry such a disproportionately large share of the load. (Some values in the previous shear test series (NAS 9-11222) ran as much as twice the values of one weak direction in the present test series, and on the average about 25-to-30 percent higher.) The shear modulus values in the earlier test series are about 25 percent of the values reported in the present (weak-direction) series. The modulus on the early series test was obtained by measuring table motion, which explains the lower values. The present system using deflectometers placed very near the specimen is obviously much more accurate.

In the present test method, the maximum shear is calculated by multiplying the average stress by the ratio of the maximum radius to the average radius. That is, the shear force is assumed to act at the center of the 2-in. diameter specimens, but since the stress distribution varies as the distance to the center of rotation (in the case of torsion), the stress is obviously higher at the outermost point on the specimen. The shear modulus is calculated by dividing the average stress by the average strain, i.e., no prorating is performed here, since the strain must also be prorated by the same ratio.

The LI-1500 shear test results for the 2-in. -diameter x 1-in. -thick specimens are shown in Table 4.2-13. Since these values were lower than those measured during the past contract, NAS 9-11222, additional tests were performed on 2-in. -diameter x 0.375-in. -thick specimens. As discussed previously and illustrated in Fig. 4.2-17, thinner specimens tend to reduce the normal forces acting on the end faces of the specimen and tend to put the specimen in a purer state of shear. The results of the 0.375-in. -thick specimens shown in Table 4.2-14 indicate about 145 percent increase in the weak

Table 4.2-13

ROOM TEMPERATURE DISC SHEAR TESTS

Direction	Specimen Numbers	Maximum Load (lb)	Maximum Shear Stress (psi)	Maximum Shear Strain (%)	Shear Modulus (psi)
Parallel	1 and 2	118	10.0	0.391	3,970
	3 and 4	144	12.2	0.289	5,000
	5 and 6	149	12.6	0.238	6,530
	7 and 8	120	10.2	0.238	5,240
	9 and 10	130	11.0	0.306	3,690
		Average	11.0		4,890
		NAS 9-11222	16.0		1,174
Normal	14 and 15	580	49.1	0.211	28,200
	16 and 17	465	39.4	0.331	14,500
	18 and 19	493	41.8	0.216	20,600
		Average	43.0	-	21,100

All specimens - 2.00 in. diameter x 1.00 in. thick.

Table 4.2-14

ROOM TEMPERATURE SHEAR TEST RESULTS
(Torsion Tester)

Direction	Specimen Numbers	Diameter (in.)	Height (in.)	Load (lb)	Shear Stress Max ($lb/in.^2$)	Shear Modulus ($lb/in.^2$)
Parallel	111	2.00	0.375	350	29.6	6,370
	113/113	2.00	0.375	300	25.4	6,840
Average					27.5	6,605
Normal	TI 30/D113	2.00	0.375	715	60.6	32,900
	TT 38-1/-2	2.00	0.375	1,010	85.6	25,600
	TT 38-3/-4	2.00	0.375	662	56.1	25,900
	TT 38-5/-6	2.00	0.375	1,155	97.8	43,100
Average					75.0	31,900

direction (parallel-to-fiber orientation) shear values over the values obtained from the 1-in. -thick specimens. Figure 4.2-15 shows a pair of 0.375-in. thick specimens mounted in the apparatus. A 75-percent increase in the strong (normal-to-fiber orientation direction) direction shear results occurred for the 0.375-in. -thick specimens. LMSC plans to perform more shear tests in the weak direction, since the parallel shear allowable is currently a major design driver and more data points are required.

4.2.7 Tension Tests on Higher Density LI-1500

Preliminary screening tests to determine the tensile strength and tensile modulus of higher density LI-1500 were performed for the Material Improvement Contract, NAS 9-12137. These results are included here to indicate the trend in strength and modulus. Figure 4.2-20 shows the variation of tensile strength with specimen density. The average tensile strength varies from 75 to 210 lb/in.^{2} as the density increases from 15 to 59 lb/ft^3.

The variation of elastic modulus with specimen density is shown in Fig. 4.2-21. The average modulus varies from about 60,000 lb/in.^{2} to 250,000 lb/in.^{2}. Tabulated data from these tests are shown in Table 4.2-15.

4.2.8 Coating Cantilever Test

The purpose of this test is to obtain the mechanical properties of the LI-1500 surface coating alone, by applying a cantilever bending moment to a small rectangular plate specimen of the coating. From the simple relations of statics, it is possible to determine the stress and strain in the cantilever from the applied load and measured tip deflection.

As in all tests on the coating, the greatest source of error and uncertainty in the test results stems from the thickness characteristics of the coating. The coating is applied to the porous substrate in liquid form; therefore, it permeates the latter to varying degrees. In attempting to obtain a specimen of coating alone, the difficulty arises in

VARIATION OF TENSILE STRENGTH WITH LI-1500 DENSITY

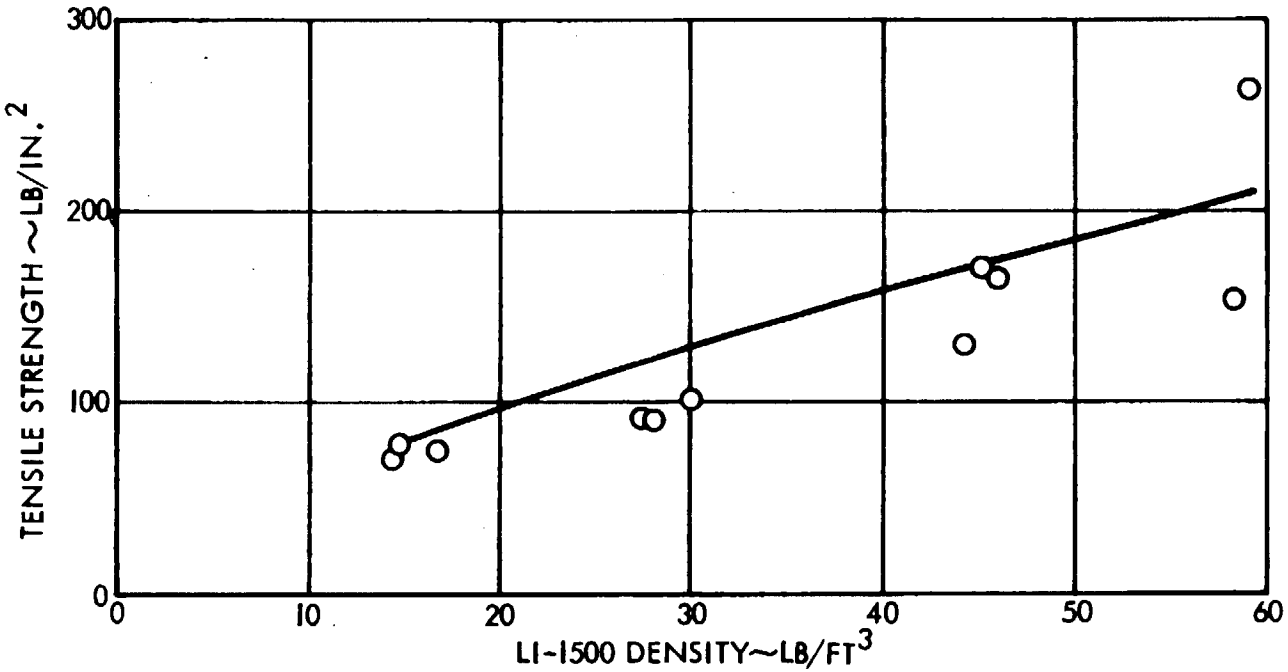

Fig. 4.2-20

LOCKHEED

VARIATION OF ELASTIC MODULUS WITH LI-1500 DENSITY

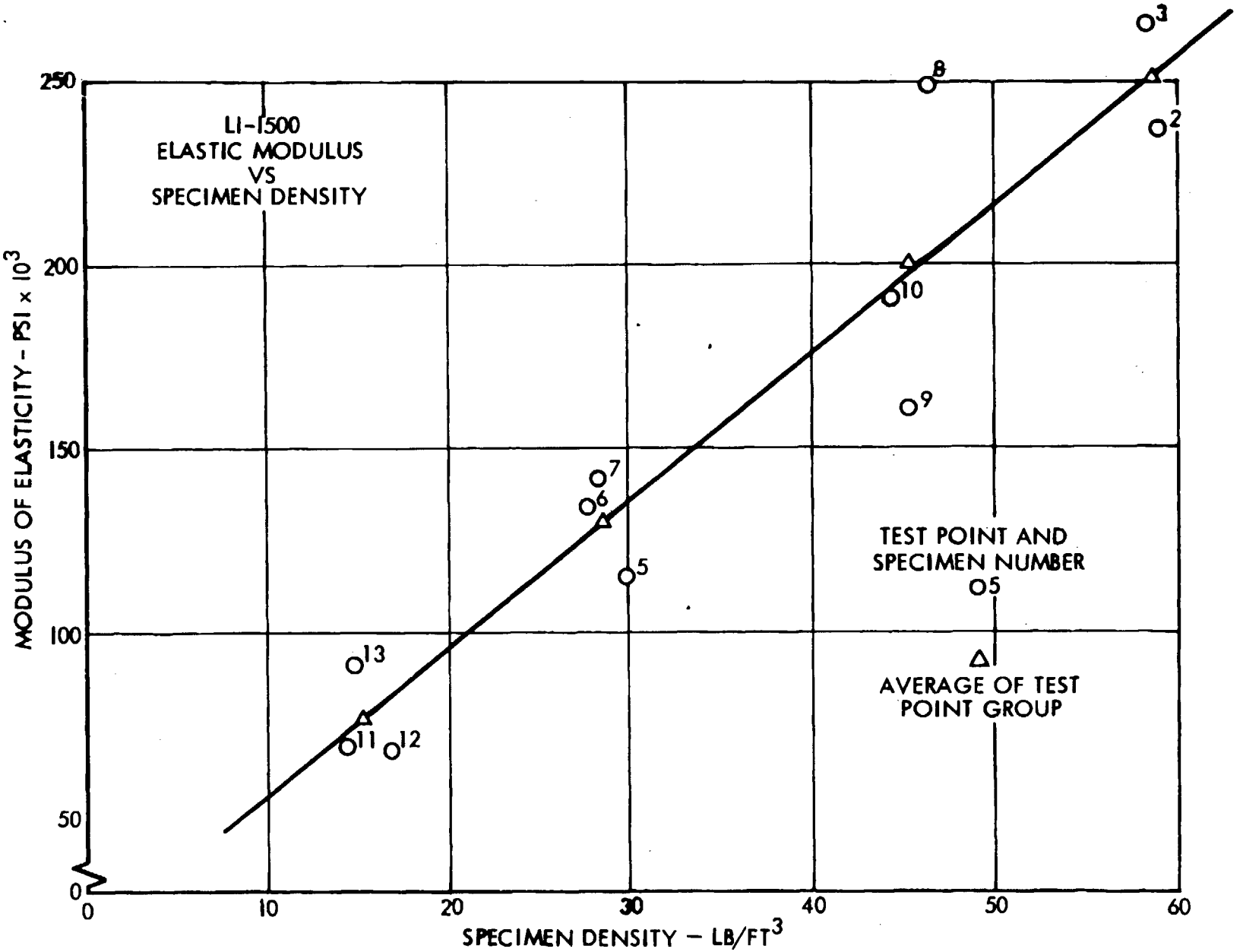

Fig. 4.2-21

DO6035

Table 4.2-15

DENSIFIED LI-1500 TENSION AND MODULUS RESULTS
(Room Temperature Tests)

Specimen Number	LI-1500 Density (lb/ft^3)	Gage Length (in.)	Test Section Width (in.)	Thick-ness (in.)	Weight (gm)	Test Section Area ($in.^2$)	Load (lb)	Stress (psi)	Modulus (psi)
2	58.9	4.00	1.51	0.24	29.5	0.362	96.0	265	238,000
3	58.3	4.00	1.50	0.27	29.0	0.405	62.8	155	267,000
8	46.3	4.03	1.50	0.20	22.0	0.300	50.4	168	250,000
9	45.2	4.00	1.49	0.20	21.0	0.298	51.0	171	161,000
10	44.4	4.05	1.50	0.20	21.0	0.294	38.4	131	192,000
5	29.8	4.00	1.50	0.20	17.0	0.300	30.4	101.0	116,000
4	28.1	4.00	1.50	0.24	16.5	0.360	32.0	88.9	142,000
6	27.6	4.00	1.58	0.24	16.0	0.380	34.8	91.6	135,500
12	16.6	4.00	1.50	0.25	8.0	0.375	28.8	74.7	68,200
13	14.7	4.00	1.50	0.20	7.0	0.300	23.2	77.3	91,900
11	14.5	4.00	1.50	0.24	7.0	0.360	26.0	72.2	69,500

deciding just where the coating boundary is located. The tendency is to have a thin layer of LI-1500 attached to the coating, since its contribution to the coating's ability to sustain load will be minor. The LI-1500 is removed by careful scraping with an Exacto knife. The final scraping is done after the specimen is bonded to an anchor block, which provides fixity in the test.

The specimen thickness is measured after the test, because the risk of specimen breakage during measurement is very high. A micrometer is used to measure the thickness to ±0.001 in. resolution, and the average of twelve readings is taken.

The LI-1500 tends to crush under the micrometer pressure, a fact that tends to make the reading (as a measure of the coating's actual thickness) somewhat more accurate than if it (the LI-1500) remained intact. The scatter in thickness readings is usually within ±0.005 in. When scatter falls outside of this range, extra readings on either side (one micrometer anvil diameter) of the high reading are taken, since high readings tend to be caused by lumps on the backface of the coating. The lumps are from intrusion of the coating into a larger than average void in the LI-1500 material. If either of the extra readings falls outside the ±0.005 in. range, the initial high reading is retained as valid. If both of the extra readings fall inside the ±0.005 in. range, the average of the extra readings is reported as a single value replacing the one that originally fell outside the ±0.005 in. range. The need for extra readings is fairly rare.

Despite these precautions, it is recognized that uncertainty remains as to the true coating thickness. Indeed, whether a true thickness does, in fact, exist is questionable, since there is probably a region (as the thickness of the specimen is traversed) where the material encountered is part coating and part base material; the thickness of this "no-man's land" probably varies from one location on the specimen to another.

This uncertainty affects the results considerably, since it has a large leverage effect in the data reduction. First, there is the physical reality that a thick layer of diluted coating represents a layer of reduced strength, which is counted as if it had full strength. Second, is the fact that in calculating the stress as a function of the applied

load, the measured thickness, t , appears as a quantity squared in the denominator of the expression for stress:

$$\sigma = \frac{6 \times P \times L}{w \times t^2}$$

where

P = applied load
L = length of the cantilever
w = width of the cantilever
t = thickness of the cantilever

Thus, P is lowered (by the diluted coating) and t is increased, resulting in a value of σ (the calculated stress) substantially reduced from its true value.

The apparatus used for the cantilever coating tests is shown schematically in Fig. 4.2-22. Photographs of the apparatus and the test specimen are shown in Figs. 4.2-23 and 4.2-24.

The specimen is attached to a fixed block (F), which is rigidly connected to the main structural frame by bolting. In the diagram, the endplate (E) is connected by the columns (labeled S) to fixed block (F). The screwjack (J) and motor are attached to an endplate as are two rods that serve to guide the linear ball bushings (B). The endplate and rods are not shown on the schematic.

The screwjack causes an assembly (T) to translate on the rods. Two transducers are attached to the translating assembly (T); one of these is a linearly variable differential transformer (D) whose probe bears against the fixed endplate, so that this transducer measures the motion of T with respect to the fixed frame. The second transducer is a thin-steel cantilever blade (C) strain gaged near its base and calibrated so that both the applied load at its tip and the deflection of its tip can be related to its electrical output.

SCHEMATIC OF COATING TEST APPARATUS

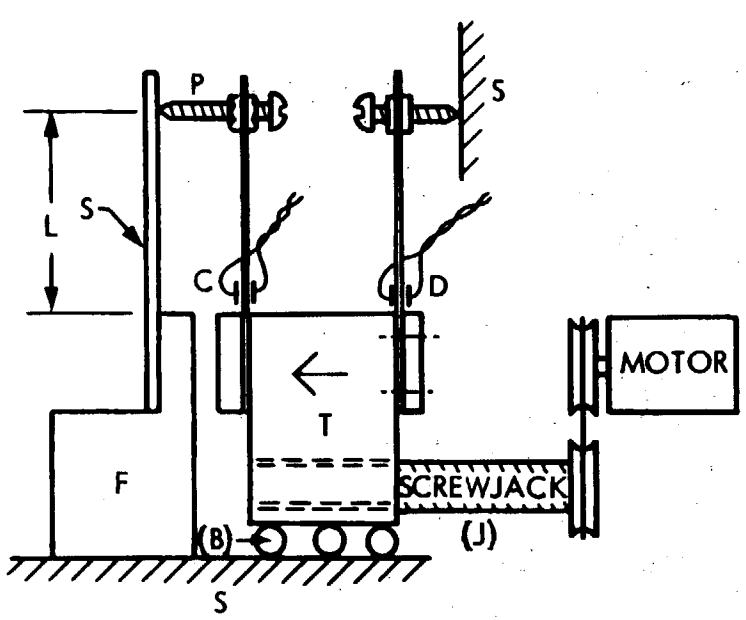

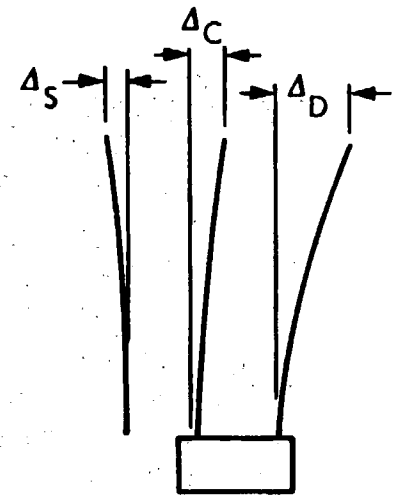

$$\Delta_S = \Delta_D - \Delta_C$$

$$M_{(SPECIMEN)} = PL \qquad \sigma = \frac{Mc}{I} \therefore \sigma = \frac{PLt}{IZ} = \frac{6PL}{bt^2}$$

$$\Delta_S = \frac{PL^3}{3EI} = \frac{ML^2}{3EI} = \frac{\sigma \times I \times L^2}{3EI \times C} = \frac{\epsilon EL^2}{3EC} = \frac{\epsilon L^2}{3C}$$

$$\epsilon = \frac{3\Delta t}{2L^2} \qquad \epsilon = 3.14 \times 10^{-5} \times \Delta \ (\Delta \text{ IN MILS}, \ \epsilon \text{ IN } \mu\epsilon \ , \ t = 0.022 \text{ IN.} \ L = 1.05 \text{ IN.})$$

$$\sigma = 64P \quad \sigma \text{ IN PSI}, \quad P \text{ IN GRAM}, \quad b = 0.45 \text{ IN.}, \quad t = 0.022 \text{ IN.}, \quad L = 1.05 \text{ IN.}$$

DO6069

Fig. 4.2-22

PRESENT COATING CANTILEVER TEST FIXTURE

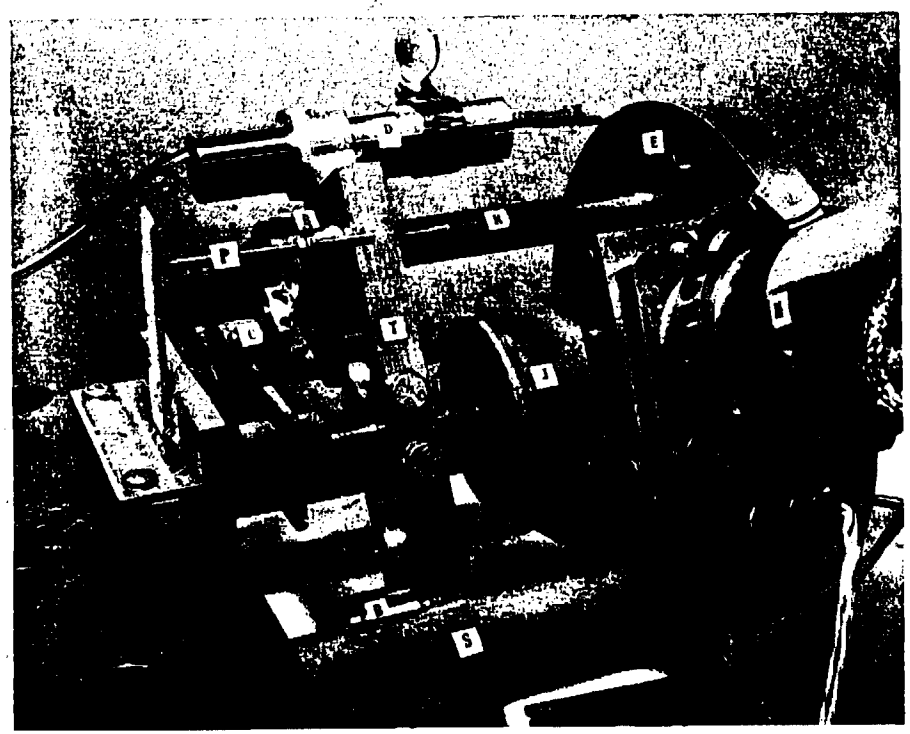

DO6079

Fig. 4.2-23

COATING CANTILEVER TEST SPECIMEN

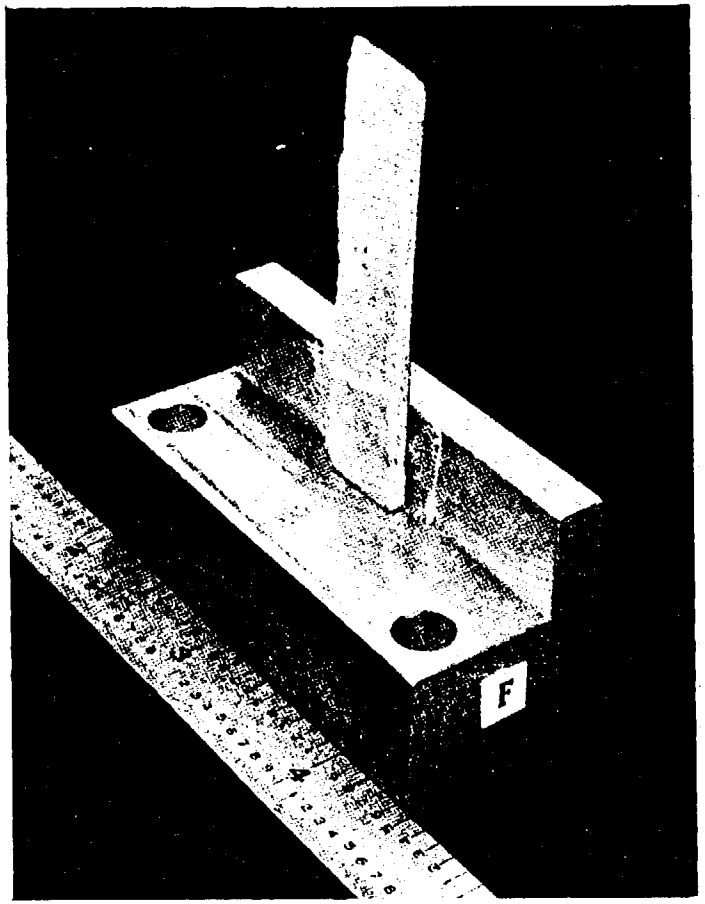

Fig. 4.2-24

The movement of the cantilever specimen tip is then the movement of T, less the movement of the cantilever tip relative to T; or the specimen tip deflection.

$$\Delta_S = \Delta_D - \Delta_C$$

In the schematic, the deflectometer (D) is represented as a second cantilever, which would, in fact, work just as well, but a linearly variable differential transformer was used instead because it was more convenient. The motor is set to drive T at a uniform speed of 0.0002 in./sec, and the two deflectometers are recorded continuously. The data are reduced by a Tymshare computer, using the following relationships:

$$\epsilon = \frac{3 \times \Delta_S \times t}{2 L^2}$$

and,

$$\sigma = \frac{6 \times P \times L}{W \times t^2}$$

where ϵ is the strain at the cantilever root, and σ the stress. All other terms were defined in the previous discussion.

The specimen is bonded to the block (F) using Duco cement and a cotton gauze scrim cloth (to improve the cement drying). A 24-hr drying time is required for the Duco cement.

Test results for seven tests on the 0025 coating are given in Table 4.2-16. Specimens for Tests 1 and 6 were cut from visibly undamaged portions of a slab that had been used in a different and unsuccessful coating test. For all other tests listed in the table, the coatings were obtained from a different specimen.

It is felt that the explanation for the extremely high modulus value for Specimen 1 is due to the fact that the coating may experience some pretest cracking due to handling or shrinkage, and that Test Specimen 1 escaped this fate. There have been other less reliable test attempts in which this higher modulus value seemed to be evident. Although

Table 4.2-16

LI-1500 COATING (0025) FLEXURE TEST

Test	Thickness (in.)	Width (in.)	Span (in.)	Maximum Stress (psi)	Average Modulus (psi x 10^6)
1	0.022	0.45	1.05	749	4.47 at σ = 498
3	0.036	0.51	1.12	720	0.397 at σ = 701
4	0.040	0.52	1.16	421	0.236 at σ = 60.5
5	0.038	0.51	1.19	134	0.077 at σ = 125
6	0.043	0.52	1.19	439	0.209 at σ = 439
7	0.035	0.47	0.78	427	0.342 at σ = 374
Average				480	0.96

these tests had to be discarded for other reasons, they indicated that the modulus was in the range from 3- to 7 million lb/in.^{2}, rather than the range well below 1 million indicated by Table 4.2-16. It is fairly safe to say that Test Specimen 4 was either damaged or had some serious but invisible manufacturing flaw, since both its strength and modulus are very low compared to the other values in the table.

It should be emphasized that the accuracies of the load and deflection measurements in the cantilever device are at least one-order-of-magnitude more refined than they need to be (relative to the accuracy with which the specimen thickness can be defined). The deflection is measured to 5μ in. precision and the load is measured to 10^{-2} gram precision. The accuracy is probably only 5- to-10 times the above quoted figures, but this is still quite acceptable when it is realized that in a typical test the tip deflects 10,000μ in. and the tip load reaches 5- to-10 grams.

4.2.9 Test Results for 0042 Coating

During the course of this contract, a new coating was developed under the Material Improvement Contract, and tension and modulus values were obtained and used for the design of the prototype panels.

The 0042 coating specimens are cut from the surface of a coated LI-1500 specimen. The test thickness of from 0.010 in. to 0.030 in. is obtained by carefully removing the LI-1500 material adjacent to the 0042 coating and measuring the coating thickness with a micrometer. Test results for eleven tests on the 0042 coating are listed in Table 4.2-17.

Based on familiarity with the test techniques and individual specimen reactions, the most realistic values for elastic modulus and ultimate stress are 1.9 x 10^6 psi and 2000 psi, respectively. The results of two pull tests on the coating resulted in an average ultimate stress of 2400 psi, which verifies the range of values obtained from the flexure tests.

Table 4.2-17

LI-1500 COATING (0042) FLEXURE TEST RESULTS

TEST	MAXIMUM STRESS (PSI)	AVERAGE MODULUS (PSI)
1	1560	0.750×10^6
2	2120	1.20×10^6
3	2600	1.93×10^6
4	2740	1.70×10^6
5	2520	2.20×10^6
6	3800	3.30×10^6
7	1420	2.00×10^6
8	2100	5.00×10^6
9	2100	1.50×10^6
10	1700	0.70×10^6
11	1500	0.70×10^6
AVERAGE	2190	1.9×10^6

ALL SPECIMENS WERE ABOUT 0.50 x 2.00 x 0.015 IN., THE THICKNESS VARIED FROM ABOUT 0.010 TO 0.032 IN.

Section 5

ENVIRONMENTAL RESPONSE BEHAVIOR

Definition of the Space Shuttle thermal protection system concept requires that the materials and design application technology be established. Demonstration of the reusability of the surface insulation TPS material, substrates, and adhesives when exposed to multiple environments requires extensive testing. The objective of this task is to demonstrate the capability of the LI-1500 RSI System to withstand the various critical environmental conditions to be encountered in shuttle operations. Under this task, LMSC has developed a comprehensive test program and has performed the required testing to simulate the critical environments encountered by the TPS for the various shuttle mission phases. The test program includes temperature and pressure tests of small TPS panels and tests of design detail models with gaps, joints, and steps, in MSC's Arc-Plasma facilities. In addition, specialized environmental tests were performed on small specimens to fully demonstrate the suitability of LI-1500 for the Space Shuttle TPS.

As noted earlier, LMSC conducted an intensive coating evaluation effort to incorporate an improved coating system into this program. Since the coating system is an integral part of the LI-1500 TPS, LMSC considered that it was desirable to incorporate the most improved coating available for these tests. As related in Section 3.1, a new coating has been baselined, the 0042 coating system. This coating was tested for 100 cycles to 2500°F, simulating a perturbed Area 2 heat pulse. Results show that the 0042 coating was intact after 100 cycles. No open cracks or coating failures were detectable. Planview shrinkage was within the accuracy of the vernier caliper measurement tools, and thickness shrinkage after 100 cycles was 1.4 percent on one panel and 3 percent on the second panel. Based on these results, all the test specimens evaluated under this task utilized this coating system. The test results are reported in the following pages. Some of the models tested under this task are shown in Fig. 5-1.

TEST SPECIMENS

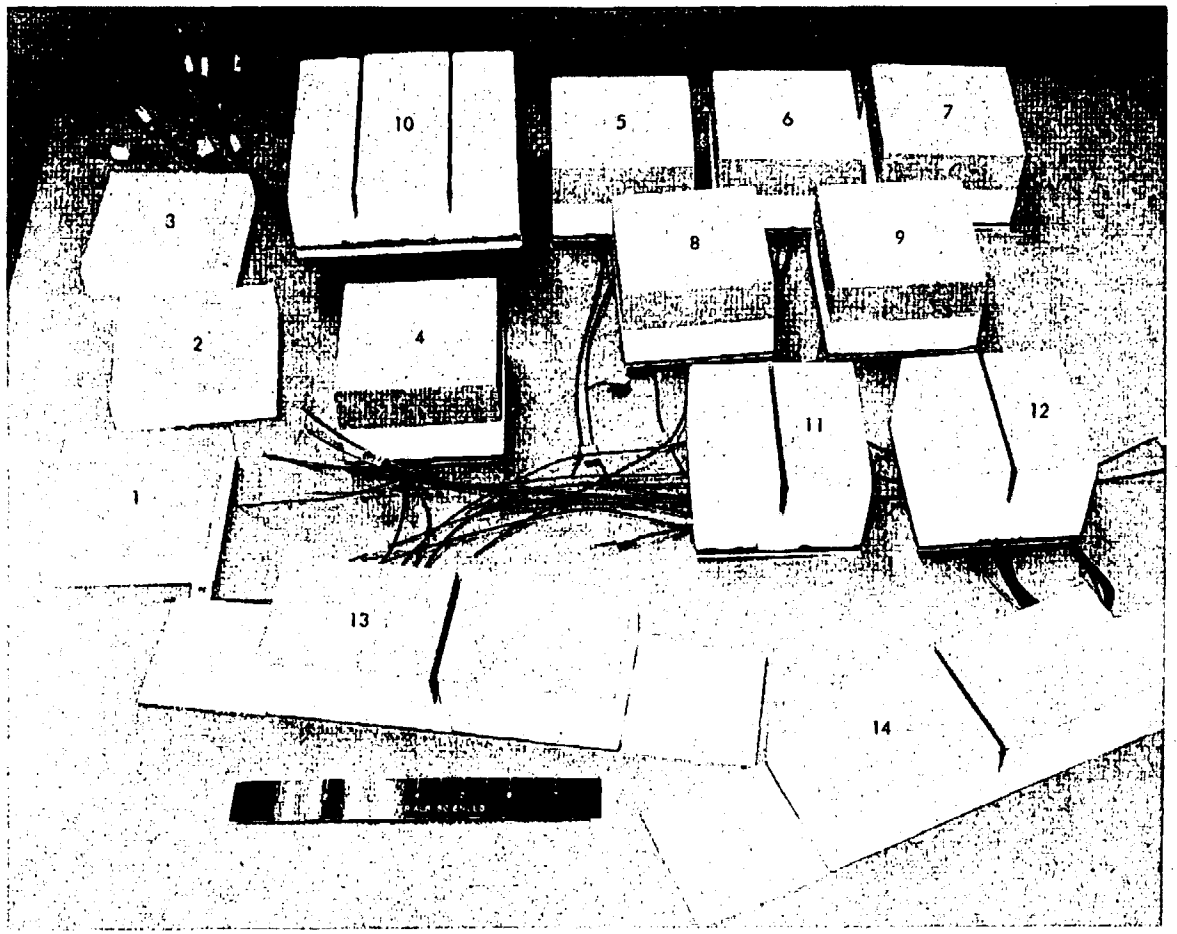

SPECIMEN NO.	SPECIMEN TEST
1	FREEZE/THAW
2	FREEZE/THAW
3	FREEZE/THAW
4	MOISTURE ABSORPTION
5	MOISTURE ABSORPTION
6	MOISTURE ABSORPTION
7	MOISTURE ABSORPTION
8	MOISTURE ABSORPTION
9	MOISTURE ABSORPTION
10	JOINT MISMATCH
11	JOINT COMPARISON
12	MOISTURE ABSORPTION
13	ANALYTICAL VERIFICATION
14	ANALYTICAL VERIFICATION

Fig. 5-1

5.1 MATERIAL/SUBSTRATE EVALUATION

The insulation material/coating system must be incorporated into a design that is compatible with the vehicle structure it protects. In addition to withstanding ambient environment conditions throughout its 100-mission operational life, the TPS design must survive the heating, acoustic pressure, pressure loading, and structurally induced loading during ascent, entry, and subsonic cruise environmental conditions. Representative structural panels and insulation tile assemblies with realistic joints and attachment methods are needed for evaluation tests. The tests are intended to demonstrate the feasibility of the LI-1500 TPS design for an equivalent 100 Space Shuttle Orbiter missions.

LMSC has fabricated a structural panel (Fig. 5.1-1) consisting of a 6 x 24-in. aluminum Z-stiffened panel (one-fourth of a regular vehicle panel) with one 6 x 12 x 2.52 in. and two 6 x 6 x 2.52-in. LI-1500 tiles bonded to the panel with a 0.090-in. thickness of RTV 560. The panel is representative of Flight Panel No. 2 discussed in Sections 2 and 6.

Tests on this panel were performed in the LMSC Radiant Heat/Vacuum Test Facility (RADVAC). This facility (Fig. 5.1-2) was developed specifically for testing LI-1500 insulated fuselage structural panels. Heat rates up to 50 Btu/ft^2-sec at the specimen surface can be achieved when operating at the lamp rated voltage. Maximum specimen size is 24 x 24 in. Differential pressure across the panel can be achieved to simulate either ascent or entry pressure histories. Up to 64 channels of data can be accommodated with the computerized data recording and processing system.

Three tests were conducted on the panel. All tests used the contract reference entry thermal environment for Area 2 of the vehicle. One test was run at reduced pressure as prescribed by the reference entry trajectory; two tests were run at 1-atm pressure. The prototype panel had no detectable degradation after the first two (1 atm) tests; however, near the end of low pressure test, a facility failure occurred that resulted in water being sprayed on the panel. The panel surface temperature at this time was about 1500°F. The only apparent change after this deviation from plan was the

LI-1500 INSULATED ALUMINUM Z-STIFFENED STRUCTURAL PANEL

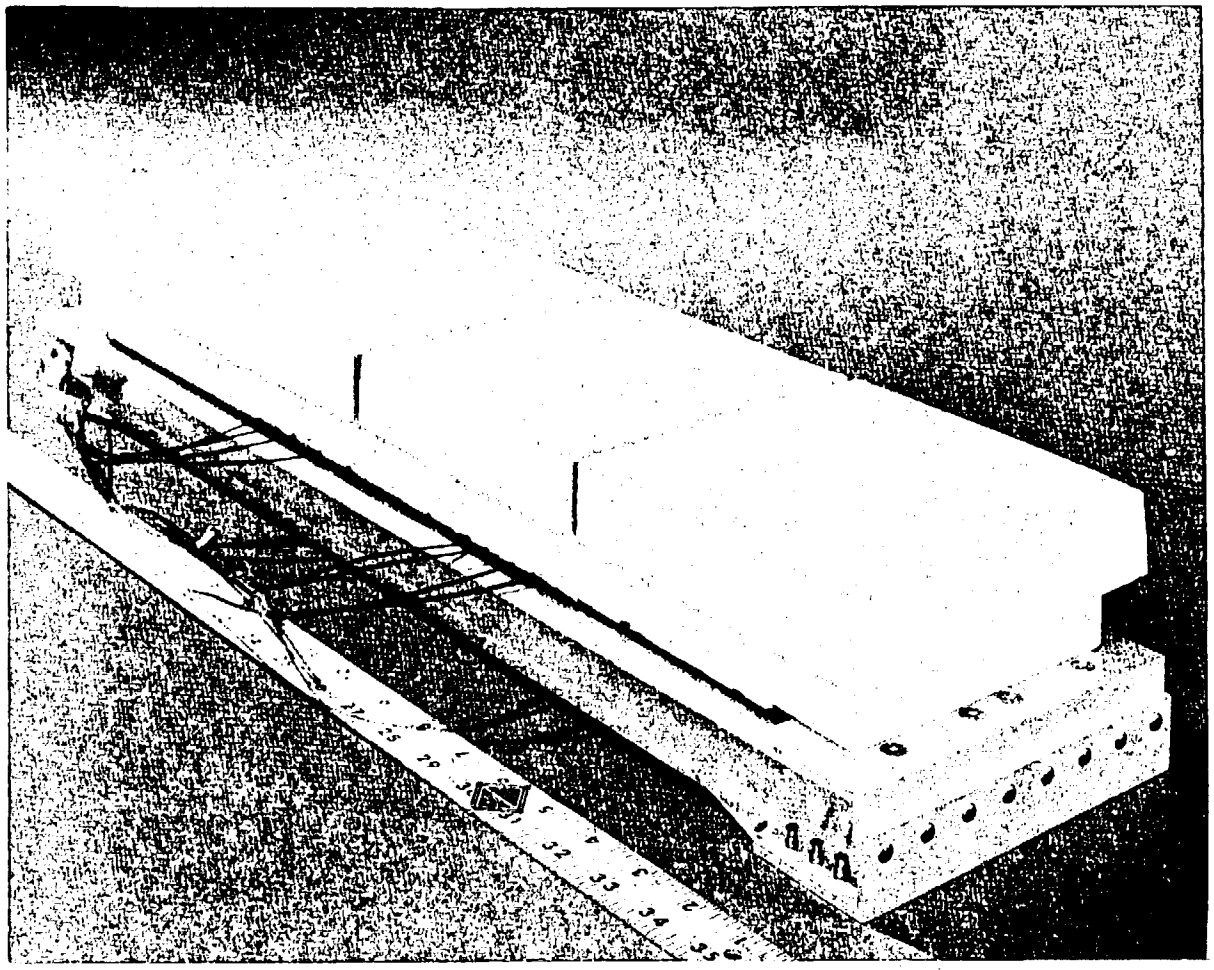

Fig. 5.1-1

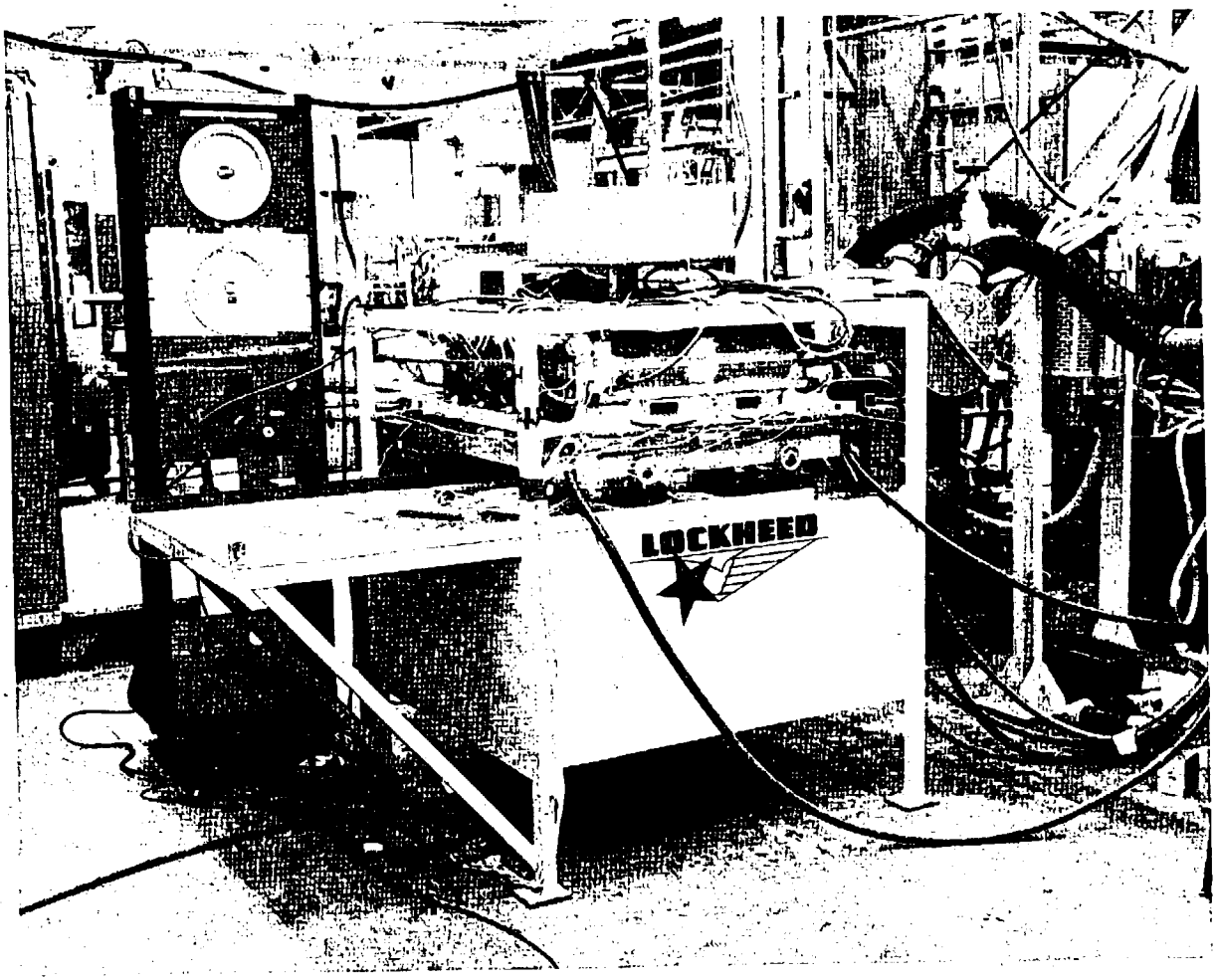

Fig. 5.1-2

appearance of shallow grooves emanating from the surface thermocouple slits, similar to those observed on the 100 cycle panels. No such grooves were discernible in the areas removed from the surface thermocouple slits.

A preliminary comparison of the predicted and measured temperatures is shown in Fig. 5.1-3 for two atmospheric pressure tests. The prediction for a 2300°F surface temperature is in reasonable agreement with but somewhat lower than, the measured data, except for the data at a depth of 2.5 in. The prediction considered an adiabatic backface for an aluminum thickness of 0.114 in.

Modifications of the test procedures will be made in an attempt to duplicate an adiabatic backface condition.

5.2 DESIGN DETAILS EVALUATION

Critical design details such as gaps, joints, and steps must be evaluated to verify the thermal/structural compatibility of the TPS design and provide data to aid in TPS performance studies. A test program* was written that utilizes small scale models of these critical design details to determine the degree to which they may cause potential heating and/or thermal stress problems. Two subscale instrumented models were designed and fabricated for the tests.

The test models are shown in Figs. 5.2-1 and 5.2-2. Dimensions and thermocouple locations are shown in Figs. 5.2-3 and 5.2-4. The joint gap and joint mismatch model designs** were modified to incorporate double-lap joints with a secondary block instead of the originally planned rectangular lap joints. In addition, the specimens have a 0.25-in layer of LI-1500 attached to the substrate backface to minimize heat leak. This is justified because of the present design criteria of an adiabatic backface assumption in sizing the LI-1500 thickness. The specimens were delivered to NASA/MSC for testing in the 10-MW arc-jet facility. The test conditions and results, when they are received from NASA/MSC, will be analyzed and made available to NASA.

* "Design Details Test Plan for Space Shuttle Thermal Protection System Development," LMSC-A991380, 1 Sep 1971

** "Monthly Technical Progress Report for Space Shuttle Thermal Protection System Development for the Month of September 1971," LMSC-A995701, 4 Oct 1971

PRELIMINARY COMPARISON OF MEASURED AND PREDICTED TEMPERATURES FOR PROTOTYPE PANEL TESTS

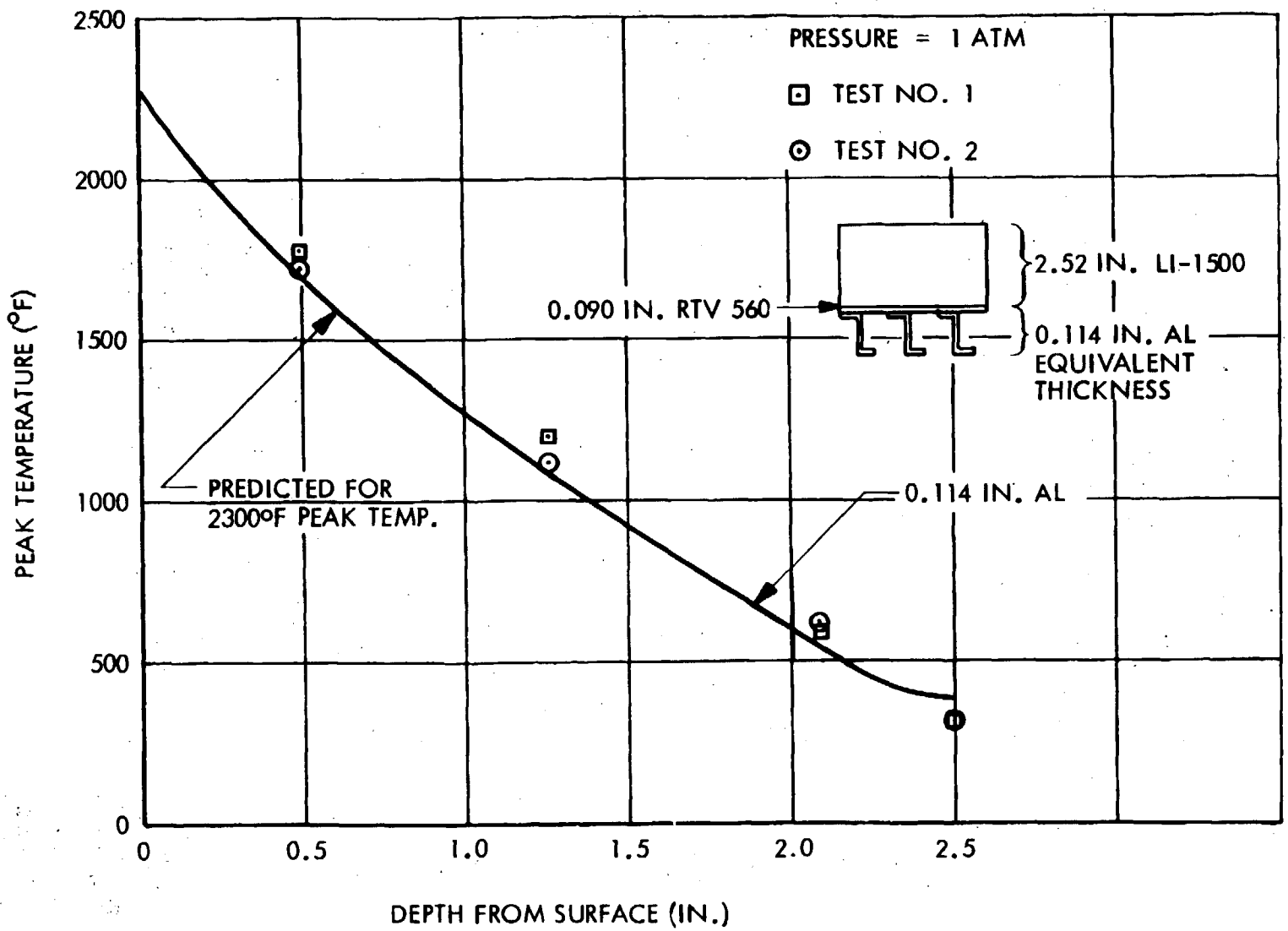

D07149 (1)

Fig. 5.1-3

LI-1500 JOINT MISMATCH MODEL

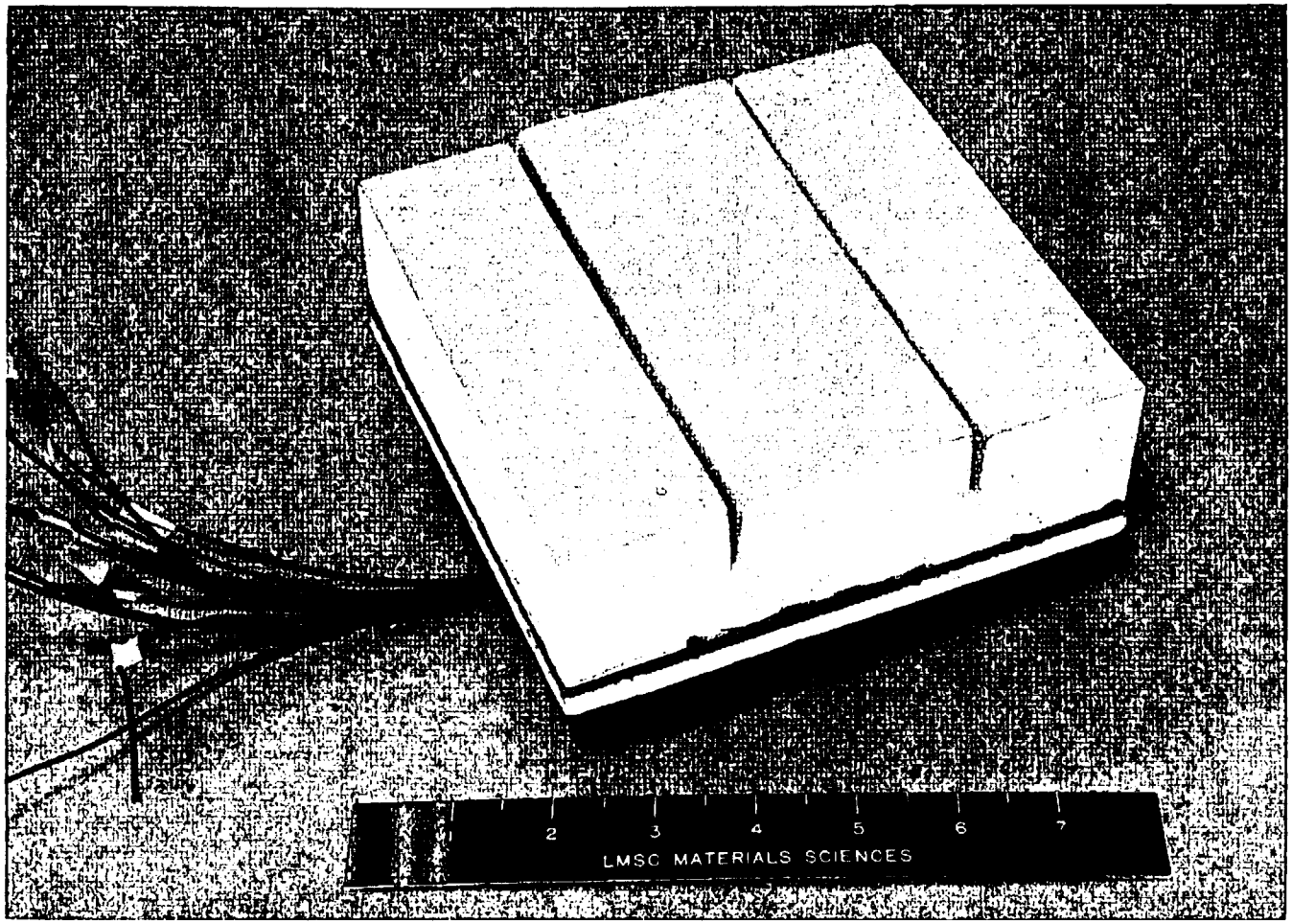

Fig. 5.2-1

LI-1500 JOINT GAP MODEL

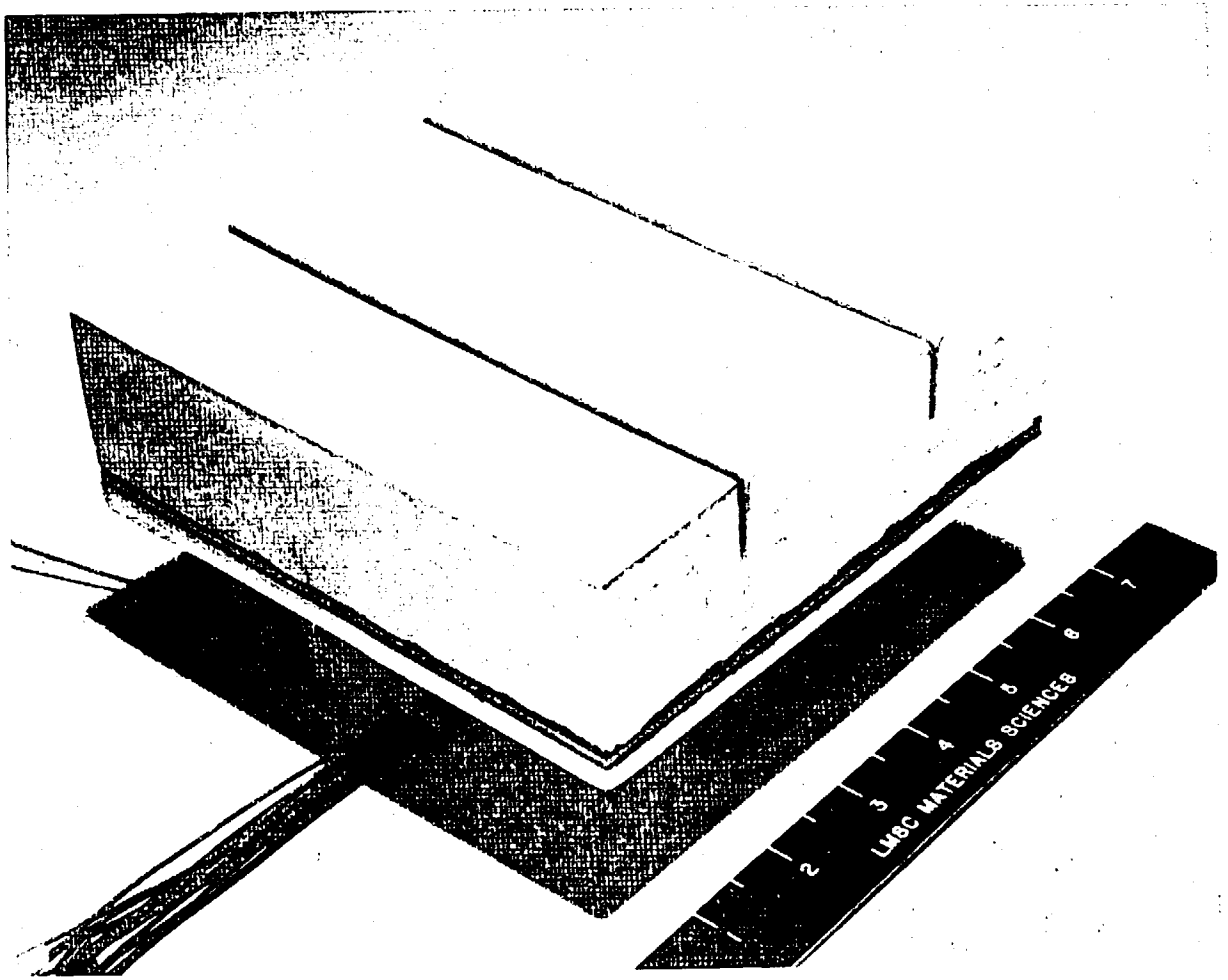

Fig. 5.2-2

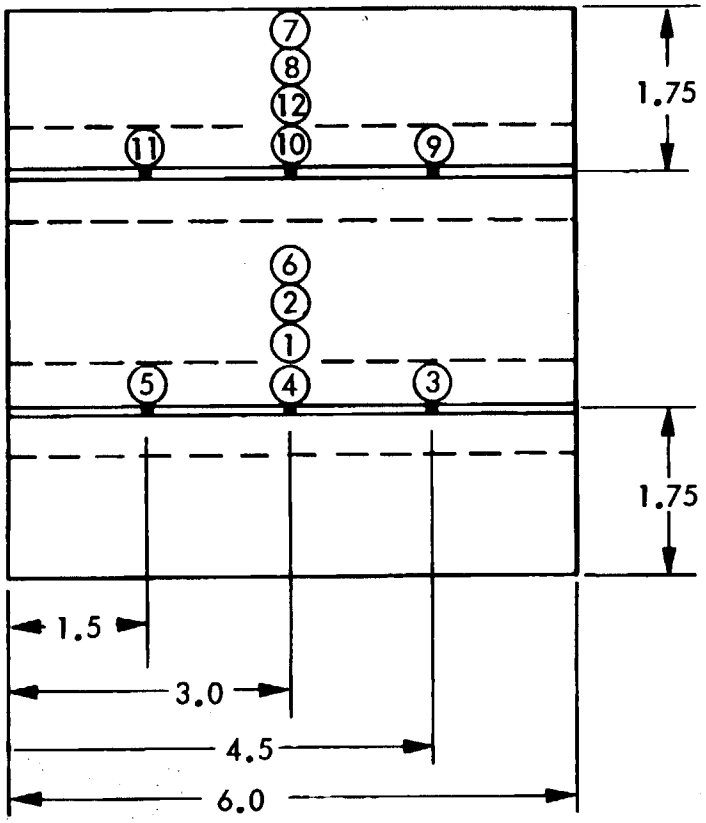

D07113

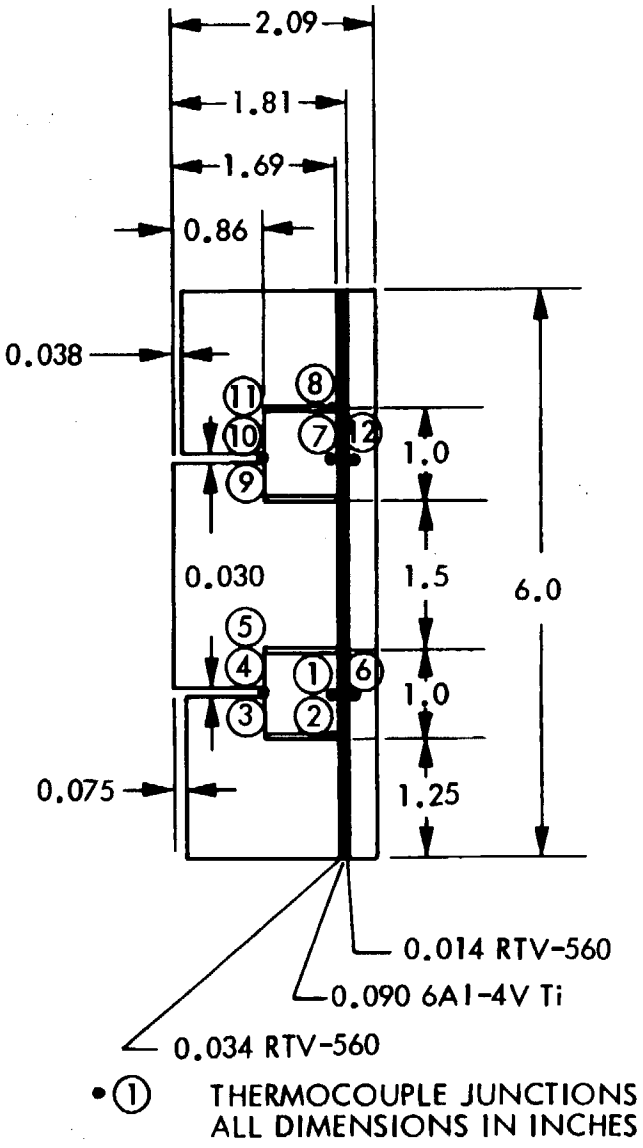

Fig. 5.2-3

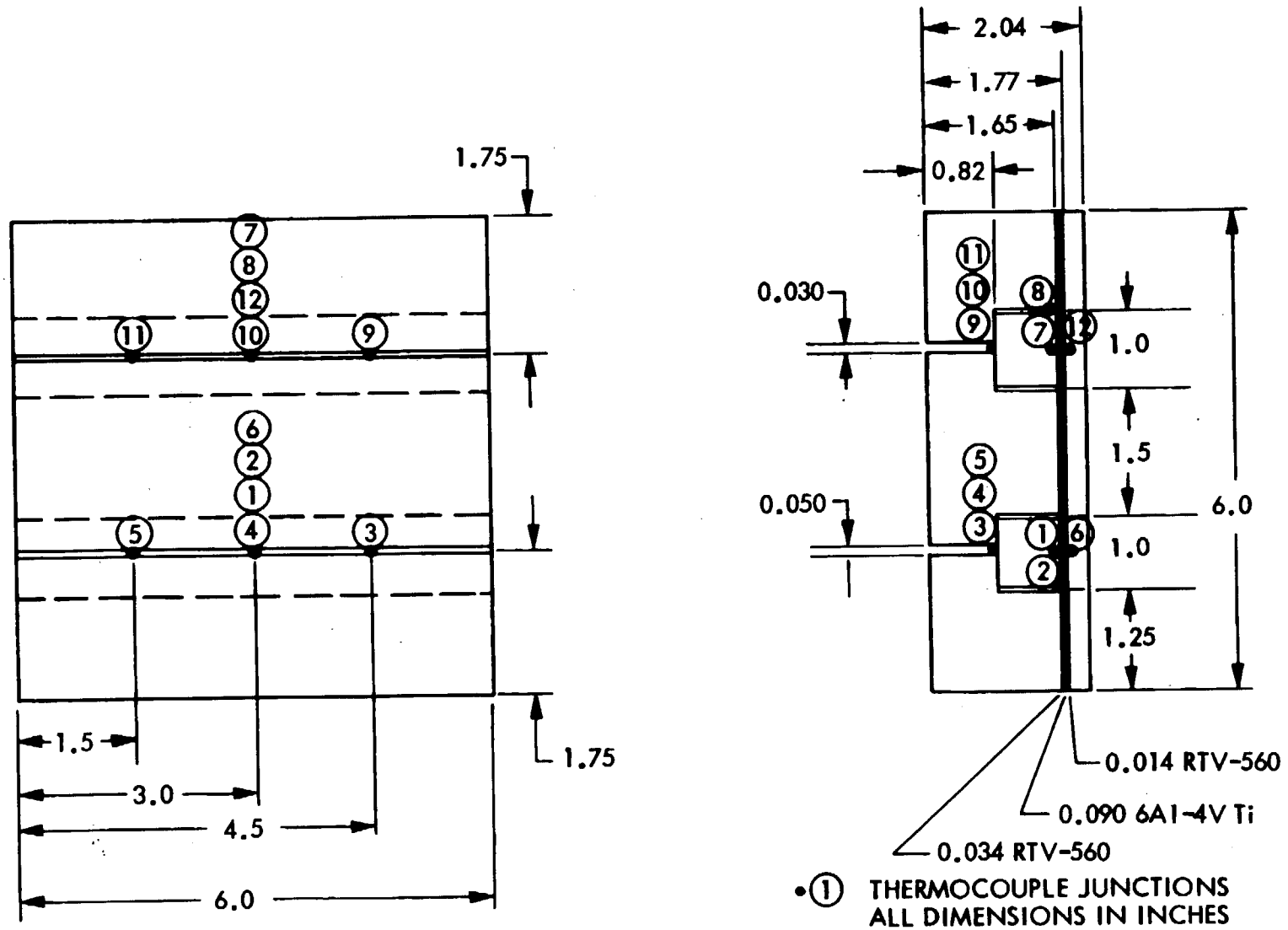
1.75
7
8
12
11
10
9
6
2
1
5
4
3
1.5
3.0
4.5
6.0
1.75
2.04
1.77
1.65
0.82
0.030
0.050
1.0
1.5
1.0
1.25
6.0
0.014 RTV-560
0.090 6A1-4V Ti
0.034 RTV-560
• (1) THERMOCOUPLE JUNCTIONS
ALL DIMENSIONS IN INCHES

Fig. 5.2-4

In addition to the above models and tests, three LI-1500 panels with different joint configurations were fabricated for evaluation in radiant heat tests. The model dimensions and thermocouple locations are shown in Fig. 5.2-5.

5.2.1 Test Results - Joint Mismatch Model

The initial joint mismatch model test series performed in the 10 MW arc-jet facility consists of three test runs each of 1080 sec duration at a surface temperature of 2300°F. Each run is at different orientation with respect to the flow. The first run, with a joint step oriented normal to the flow, was terminated at 890 sec into the test because of facility problems. The water-cooled model holder developed a leak and sprayed the test chamber with water and ice. Although the model got wet and local surface discoloration occurred (indicating a possible momentary increase in heat rate during shutdown), it appeared free of surface coating damage. The model was exposed to a heat-lamp environment overnight to dry it out, and another run was made with the same flow conditions and model orientation. Material loss was observed when the model was inserted into the flow. It appeared as if "pop-corning" occurred, probably due to expansion of water vapor within the specimen. The damage was confined primarily to the forward third of the model and was limited to the coating thickness. Two additional runs were made with the model rotated 90 and 180 degrees from the original orientation. Minor recession in the uncoated regions occurred during these runs, with no apparent thermal performance degradation.

5.2.2 Test Results - Joint Gap Model

This model was to be tested under the same conditions as the Joint Mismatch Model. During the first run, fluctuations in the flow necessitated shutting off the flow after about 540 sec of run time. Inspection of the tunnel and model showed some moisture on the model, model holder, sting, and in the nozzle. The model was subsequently removed from the holder and inspected for water absorption. No significant amount of water was present, and no model damage was observed. Apparently, the problem with the tunnel is ice formation down stream in the steam ejector system. Ice sometimes builds up to the point where the flow becomes restricted, resulting in flow breakdown. When the flow breaks down, the heat rate to the model increases

JOINT COMPARISON TEST MODELS

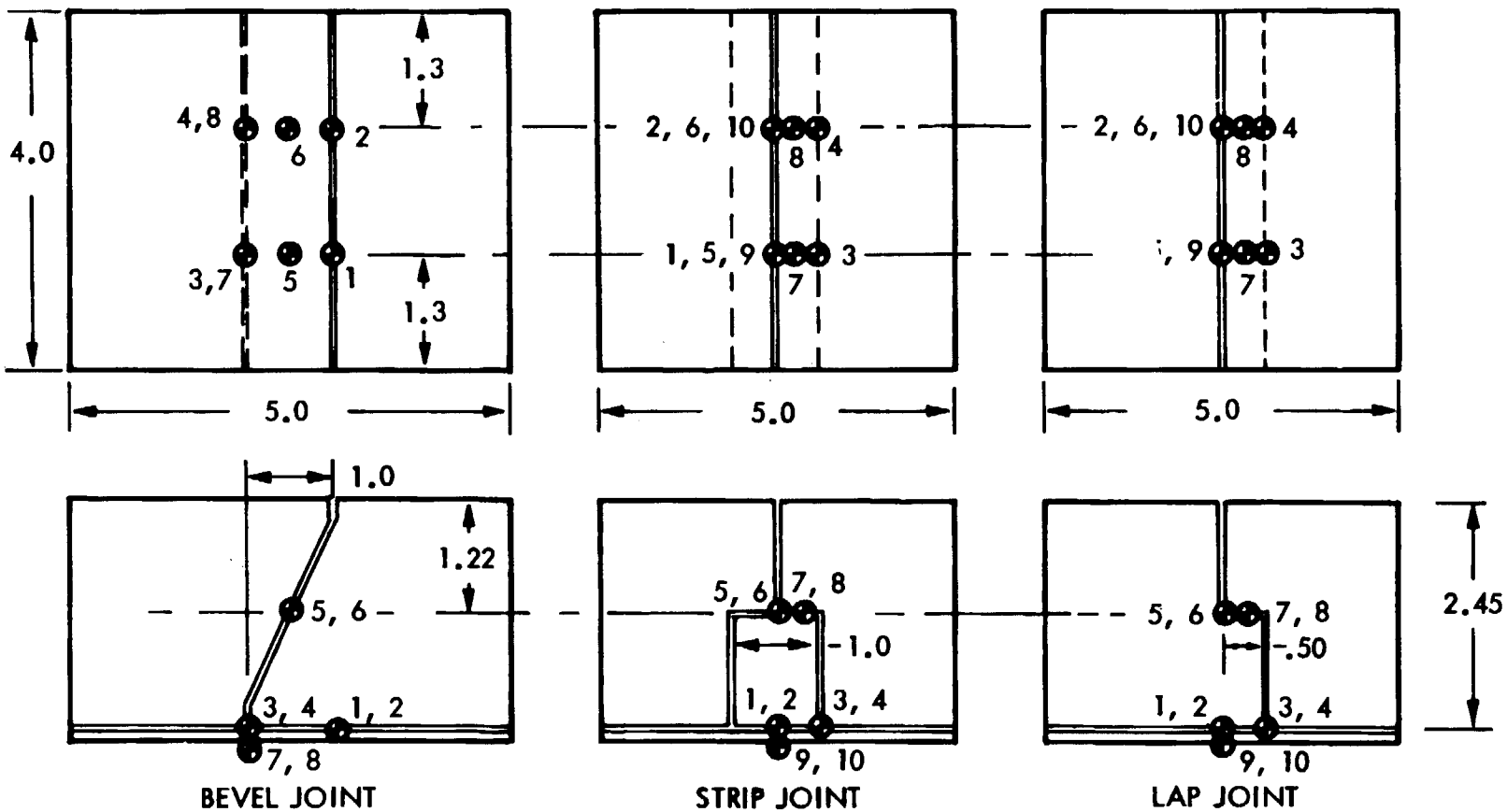

● DENOTES THERMOCOUPLE LOCATIONS
NUMBERS DENOTE T/C NUMBER
ALL DIMENSIONS IN INCHES

Fig. 5.2-5

momentarily, causing a spike in the surface temperature. The pyrometer indicated a maximum temperature of about 2700°F during a flow oscillation lasting about 2 sec. The three scheduled runs were subsequently completed. Some loss of water repellency on the surface and slight surface coating cracking were observed.

5.2.3 Joint Comparison Tests

Radiant heat tests were performed on three joint configurations specified by NASA/MSC to compare in-depth and substrate temperature responses. The three configurations were lap joint, bevel joint, and strip joint. The latter is the LMSC baseline configuration.

The test specimens consisted of 4 x 4 x 2.45 in. of LI-1500 bonded to 0.125-in. thick aluminum with 0.090-in. RTV 560 bond. The lap and strip joints were located at mid-thickness location (1.22 in.), as shown in Fig. 5.2-5. The specimens were instrumented with chromel-alumel thermocouples at the mid-thickness locations and on the substrate.

The specimens were tested in LMSC's 1-atm radiant heat facility, using the reference surface temperature history for Area 2. Five cycles to a peak surface temperature of 2300°F were performed, and the data shown in Figs. 5.2-6 and 5.2-7 are representative of all five cycles. Figure 5.2-6 shows measured mid-thickness and substrate temperature histories for the three joint configurations. Figure 5.2-7 shows measured peak temperature distributions.

The data indicate that the lap and strip joint reached about the same temperature at the mid-thickness location; the thermocouples were directly exposed to the radiant lamps and indicated a slightly higher temperature. Although the thermocouple at the mid-thickness of the bevel joint recorded a temperature 200-300°F lower than those for the lap and strip joints, the substrate for all joint configurations achieved the same maximum temperature.

TEMPERATURE RESPONSE OF VARIOUS JOINT CONFIGURATIONS TO A RADIANT HEAT TEST

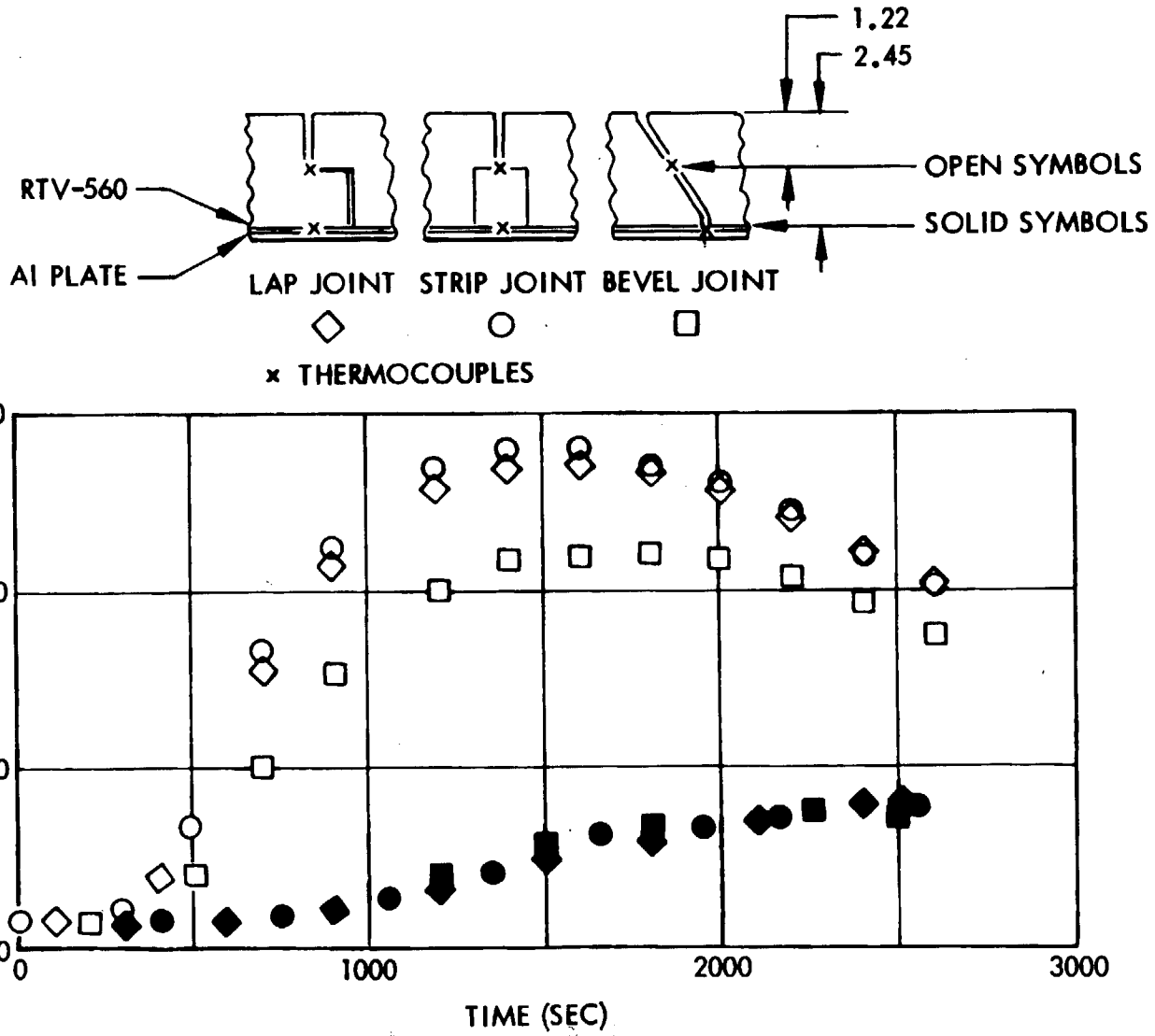

Fig. 5.2-6

COMPARISON OF MEASURED PEAK TEMPERATURES FOR THREE JOINT CONFIGURATIONS

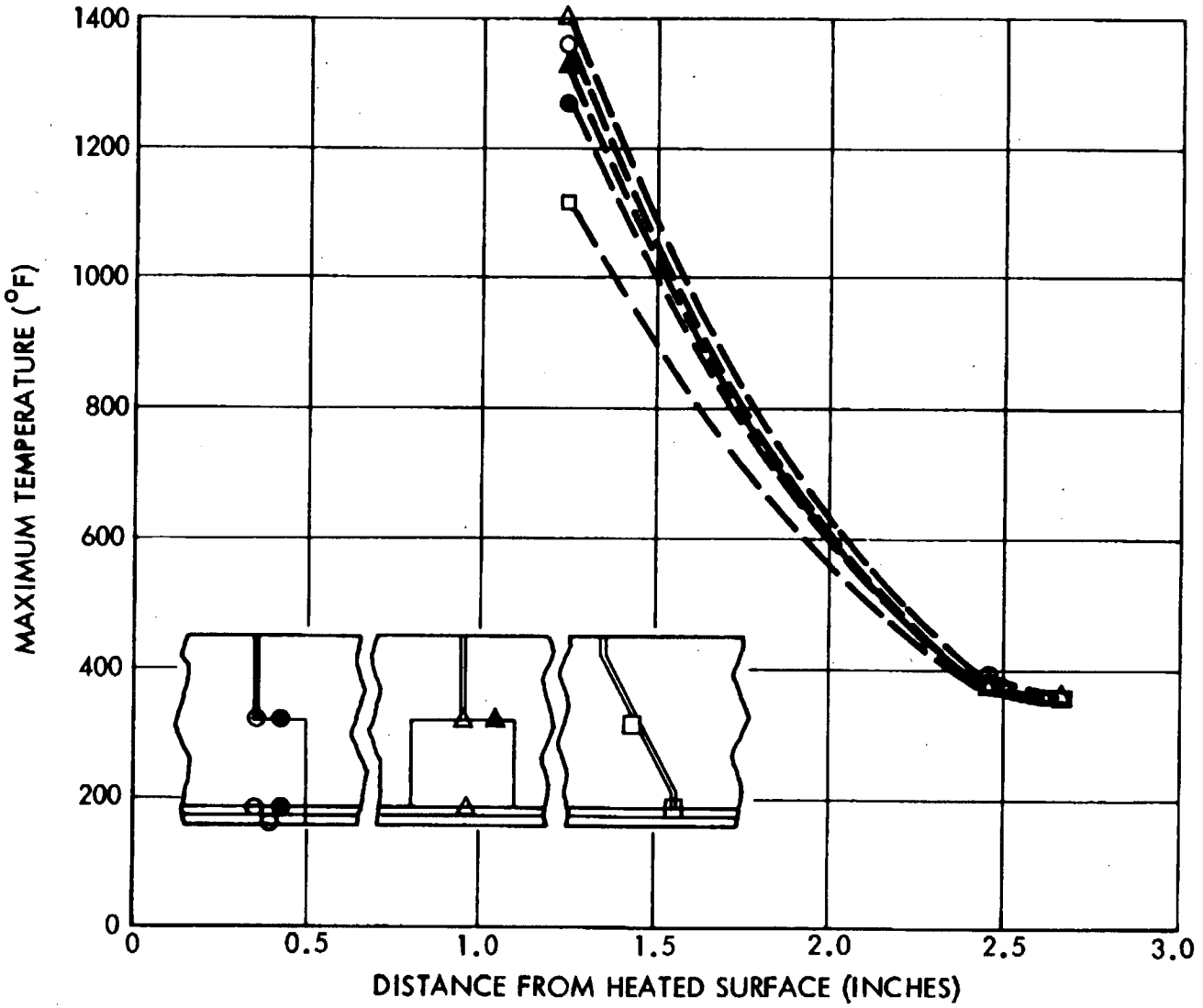

Fig. 5.2-7

In summary, the results of the test indicate no obvious thermodynamic advantage in any of the three joints with radiant heating. However, in flight application, where the LI-1500 tiles will be subjected to hot boundary layer gases during reentry, the existance of gaps extending to the substrate will probably be prohibited. Hence, the bevel type joint is undesirable and the lap or strip joint is preferable, since any gases which penetrate the joint will probably not reach the substrate. Table 5.2-1 summarizes some advantages and disadvantages of the lap, strip, and bevel joint configurations.

LMSC currently favors the strip joint approach due to its easy individual tile replacement and its inherent design feature of preventing boundary layer gases from reaching the substrate.

5.3 SPECIALIZED ENVIRONMENTAL TESTS

The effects of adverse environmental conditions on the basic RSI and surface coating must be established to allow the system service life to be predicted. The tests conducted under this subtask are intended to establish the effects of the various environmental conditions on the material and coating. In addition to the tests described in the Test Plan*, other tests are included. A brief description of the tests, an outline of the test conditions, and the test results follow.

5.3.1 Infrared Transmission

Spectral transmittance of LI-1500 and also of the coating material were determined at room temperature and a range of wavelengths. Two methods used at LMSC to measure the spectral transmittance of materials are briefly described in the following paragraphs.

*"Specialized Environmental Test Plan for Space Shuttle Thermal Protection System Development," LMSC-A991381, 1 Sep 1971

Table 5.2-1

COMPARISON OF THREE JOINTS

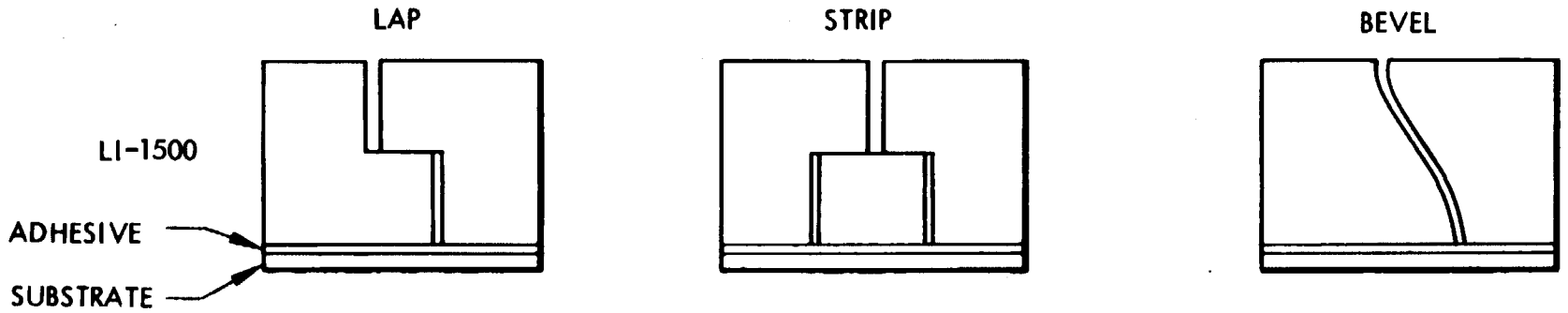

	LAP	STRIP	BEVEL
ADVANTAGES:	PREVENTS HOT BOUNDARY LAYER GASES FROM REACHING SUBSTRATE SURFACE COATING EXTENDS ONLY TO MID-DEPTH.	EASY INDIVIDUAL TILE REPLACEMENT. PREVENTS BOUNDARY LAYER GASES FROM REACHING SUBSTRATE. SURFACE COATING EXTENDS ONLY TO MID-DEPTH.	PRECLUDES LOAD TRANSFER BETWEEN TILES.
DISADVANTAGES:	MUST REMOVE FOUR TILES TO REPLACE ONE.	MANY PARTS TO MACHINE AND ASSEMBLE.	BOUNDARY LAYER GASES COULD PENETRATE GAP AND OVERHEAT SUBSTRATE. DIFFICULT TO MACHINE. SURFACE COATING MAY EXTEND DOWN SIDE TO SUBSTRATE TO ENSURE WATER PROOFING. HIGH CONDUCTIVITY SURFACE COATING PROVIDES ADDITIONAL HEAT PATH TO SUBSTRATE.

5.3.1.1 Method 1 - Total Spectral Transmittance. Measurements by this method determine the total, i.e., normal-plus-scattered radiation transmitted through a specimen into the 2π-steradian hemispherical space at the backface of the specimen. The incident radiation is monochromatic and is directed onto the specimen at a near-normal angle of incidence, i.e., perpendicular to the front face of the specimen. The irradiated area of the specimen is determined by the slit size of the monochromator and is approximately 8 mm high by 0.10 to 0.20 mm wide. The radiation source is a high-intensity 54-watt tungsten strip lamp. The source radiation is directed into a Perkin-Elmer Model 98 Monochromator with an SiO_2 prism. Monochromatic radiation of the desired wavelength between 0.35 μ and 2.5 μ is selected and directed from the monochromator exit slits to a Gier-Dunkle Model SP-210 Integrating Sphere. The integrating sphere is equipped with a transmittance-measuring attachment that permits the placement or removal of a specimen in front of the entrance port to the integrating sphere. Incident energy levels are measured with the sample in front of the entrance port. Two detectors are mounted at the rear surface of the integrating sphere: a Type 1P28 photomultiplier, for measurements at wavelengths between 0.35 μ and 0.75 μ, and a lead sulfide cell, for measurements between 0.70 μ and 2.5 μ. Both detectors collect energy from the walls of the integrating sphere, but they are shielded so they do not directly view the incident or transmitted radiation through the entrance port.

5.3.1.2 Method 2 - Spectral Normal Transmittance. Measurements by this method determine only the normal component of radiation transmitted through a specimen. For the spectral region between 0.35 μ and 2.5 μ, the same equipment described above is used; however, the sample is placed in front of the entrance slits to the monochromator instead of in front of the integrating sphere. In this case, the total white-light output of the tungsten lamp is incident on the sample at a near-normal angle of incidence. The viewing angle for the monochromator is approximately 30 milliradians; consequently, the normal transmittance of scattering samples such as LI-1500 is much lower (e.g., by a factor of 200 to 300) than the total transmittance values obtained by Method 1. For the longer wavelength IR spectral region, a 1400°F heated cavity is used as the energy source instead of the tungsten

lamp, and the vacuum thermocouple detector located inside the monochromator is used instead of the detectors associated with the integrating sphere.

The complete test matrix is shown in Table 5.3.1-1.

Table 5.3.1-1

INFRARED TRANSMISSION TEST CONDITIONS

Specimen Type	Thermal Cycles	Test Temperature (^{O}F)	Measurement Range (μ)
LI-1500	0	Ambient	1.0 to 15.0
LI-1500	20	Ambient	1.0 to 15.0
Coating	0	Ambient	1.0 to 15.0

Figure 5.3.1-1 shows room temperature data for a range of LI-1500 material thickness over a wavelength range from 0.35 to 2.5 μ. For the LI-1500 thickness proposed for the Space Shuttle (0.5 to 2.5 in.), transmission is expected to be negligible.

Normal transmission measurements are shown in Table 5.3.1-2

Table 5.3.1-2

SPECTRAL NORMAL TRANSMITTANCE OF AS-FABRICATED LI-1500

Wavelength (~ microns)	% Transmission for Various LI-1500 Thicknesses 0.043 in.	0.081 in.	0.157 in.
1.5	0.12	0.07	0.03
2.0	0.13	0.07	0.03
2.5	0.11	0.04	0.01
3.0	0.06	0.005	<0.001
4.0	0.17	0.05	0.008
5.0	0.01	0.001	<0.001
6.0	0.02	<0.001	<0.001
7.0	1.93	0.03	0.001
7.5	1.27	0.02	0.001
8.0	0.01	<0.001	<0.001
10.0	0.006	<0.001	<0.001
12.0	0.002	<0.001	<0.001
14.0	0.002	<0.001	<0.001
16.0	<0.001	<0.001	<0.001
20.0	0.01	<0.001	<0.001

TOTAL SPECTRAL TRANSMITTANCE DATA FOR THREE THICKNESSES OF LI-1500

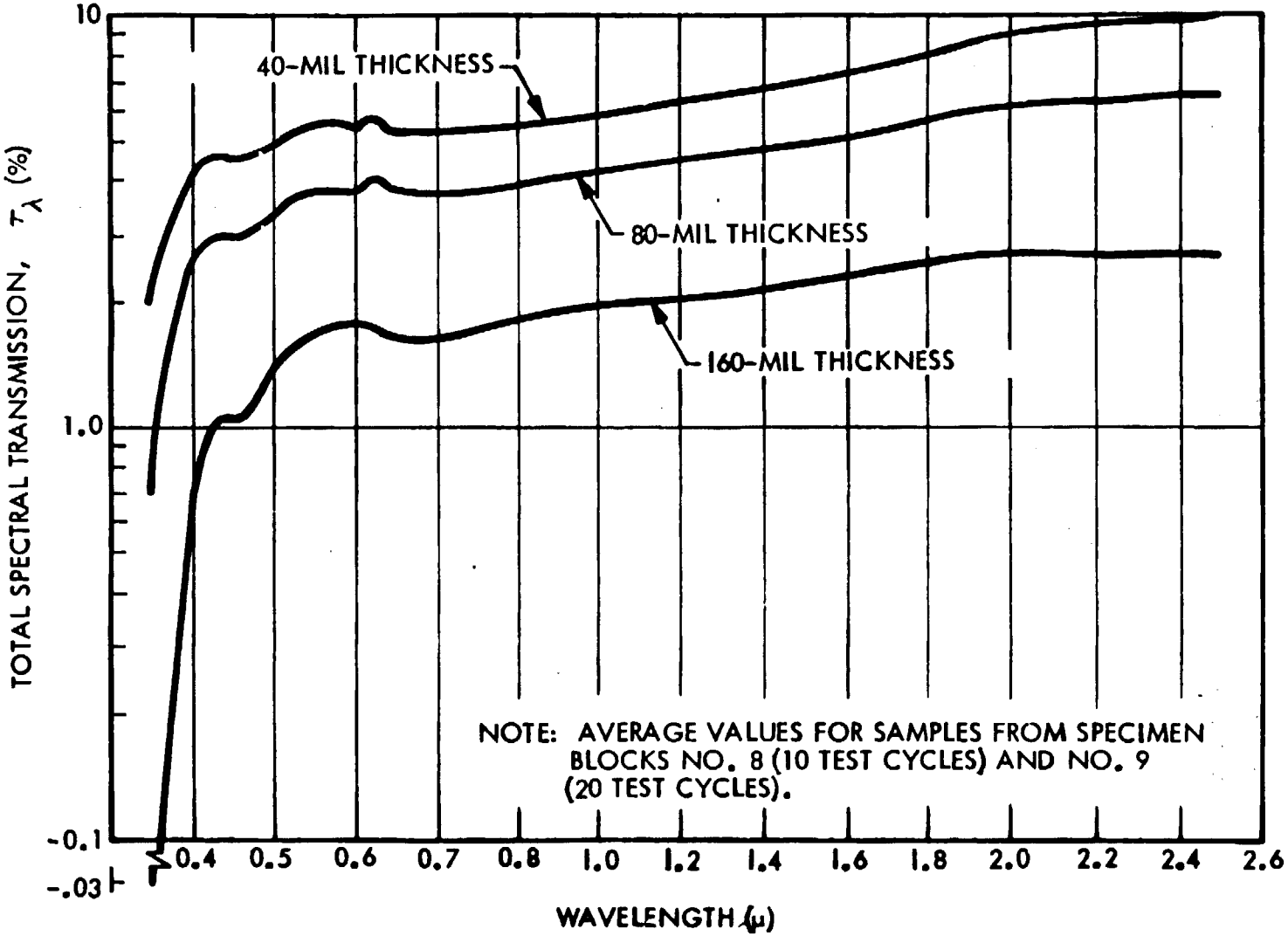

Fig. 5.3.1-1

With the exception of the transmission band at 7.5μ, the material appears to behave as an isotropic scatterer. In this band, it appears that the energy is principally transmitted in a normal direction rather than scattered hemispherically.

Post-cycling specimens (20) did not show any significant variation in the spectral transmission for 43- and 81- mil thicknesses, which was measured as compared to the as-fabricated material (Table 5.3.1-2).

The spectral normal transmission measurements on the 0042 coating ($SiC/Si0_2/B_20_3$) showed no transmission greater than 0.1 percent from 1.5 to 2.0μ.

Based on the room temperature test results, transmission is negligible for both LI-1500 and the 0042 coating. As long as the basic LI-1500 does not change, no significant change in transmission is expected at 1000^{o}F.

5.3.2 Hard Vacuum Test

A 30-day vacuum exposure test was performed to evaluate any long-term vacuum-induced effects on the dimensional stability of LI-1500 material. Two 1 x 1 x 1 in. specimens with no thermal cycles and four 2 x 2 x 2 in. specimens with 20 thermal cycles were exposed to vacuum conditions for a total duration of 30 days. Dimension and weight measurements were made initially and after 20 and 30 days of exposure. The tests were conducted in a vacuum chamber operated at a pressure of 1×10^{-6} torr and ambient temperature (75 ± 5^{o}F).

The weight measurements are shown in Table 5.3.2-1. Dimensional measurements remained constant throughout the test. No visual degradation of the material was observed.

Table 5.3.2-1
LI-1500 VACUUM EXPOSURE TEST RESULTS

Sample	Thermal Cycles	Specimen Weight (gm) Initial	After 20 days	After 30 days
1	0	21.812	21.834	21.845
2	0	21.832	21.853	21.858
3	20 (10 hrs at 2300°F)	4.240	4.240	4.240
4	20 (10 hrs at 2300°F)	4.697	4.697	4.697
5	20 (10 hrs at 2300°F)	4.512	4.512	4.512
6	20 (10 hrs at 2300°F)	4.321	4.321	4.321

The two specimens with no thermal cycles exhibited an increase in weight after vacuum exposure, whereas the thermally cycled specimens showed no weight change within the weight measurement accuracy (1 mg). Weighings were done in air at 70°F and 40-50 percent RH. The specimens were brought to atmospheric pressure with dry N_2 gas and maintained in that atmosphere until being weighed during a period of 3 to 5 min. in the laboratory environment. No reason for the weight increase was apparent from the laboratory observations. However, since the measured weight increase is very small (maximum of about 0.1 percent) it is not of concern.

Based on these test results, it may be concluded that long term exposure of LI-1500 to vacuum conditions results in no significant degradation of the material.

5.3.3 Solar Radiation Tests

Long-term exposure of the RSI to solar radiation may result in surface coating degradation with corresponding changes in the coating solar absorptance. The degree of degradation may also be a function of previous effects caused by reentry heating exposures. The following tests were performed to determine coating degradation as a function of ultraviolet exposure duration and number of reentry heating exposures.

The tests were conducted in the static ultraviolet exposure chamber, which is basically a water-cooled stainless steel bell jar 14 in. tall and 14 in. in diameter. The test specimens were mounted on a water-cooled, semicylinder copper sample holder concentric with the ultraviolet source and at a distance of 3.9 in., which resulted in nominal irradiances of 10 suns of ultraviolet energy. (A flux density of 1 sun of ultraviolet energy is defined as the flux density of extraterrestrial radiation at 1 AU from the sun, in the wavelength interval of 0.2 to 0.4μ.) At these flux densities, the LI-1500 sample temperatures were maintained between 335 and 345^{o}K for all ultraviolet tests in this chamber. Thermal contact conductance between the sample and the water-cooled copper sample holder was controlled with individual mounting frames which were pressured to the backface of the sample against the copper. Vacuum was established prior to initiation of ultraviolet exposure with cryogenic sorption roughing pumps and an electronic high vacuum pump to avoid potential oil contamination problems. The chamber pressure was typically 2×10^{-7} torr.

The source of ultraviolet energy was a 1-kw A-H6 (PEK Labs Type C) high-pressure mercury-argon capillary arc lamp. Approximately 35 percent of the lamp radiant output was in the interval 0.2 to 0.4μ. The total output of the lamp is in the interval 0.2 to 2.6μ; the lamp is water-cooled and has a quartz water jacket and velocity tube. This assembly was lowered into a quartz envelope extended into the exposure chamber from the top.

The ultraviolet intensity was monitored external to the vacuum chamber with a calibrated RCA 935 phototube in conjunction with a Corning 7-54 filter (which transmits only the near-ultraviolet output of the lamp). The output of the phototube was

automatically measured and recorded for a few minutes each hour with a recording microammeter. The intervening quartz window and 7-54 filter were periodically checked for degradation in spectral transmittance and cleaned or replaced as necessary. When desired, a Corning 0-54 filter was used to compare the intensity in the 0.2 to 0.3 μ (2000- to 3000-Å) region with that in the 0.3 to 0.4 μ (3000- to 4000-Å) region as a measure of the relative degradation of lamp output in the shorter wavelength regions.

Two sets of triplicate samples of coated LI-1500 were subjected to simulated solar ultraviolet radiation in vacuum. Set 1 consisted of samples in the uncycled condition, whereas the samples in Set 2 were previously exposed to 20 thermal cycles. The LI-1500 was cemented with silver epoxy to 0.015-in. thick aluminum discs of 1-in. diameter to provide adequate cooling during UV irradiation. The sample temperatures were monitored with a thermocouple silver-epoxied to one sample, with a radiation shield to prevent direct illumination of the thermocouple.

Solar absorptance of each sample was determined by measuring the spectral reflectance (0.25 to 1.8μ) under laboratory ambient conditions with a Cary Model 14 spectroreflectometer. The reflectance spectra were then integrated with respect to the solar spectrum using a 50-point numerical integration. Solar absorptance (α_s) was determined prior to and subsequent to 2900 equivalent sun hours (ESH) of ultraviolet exposure. In addition, for Set 1, α_s measurements were performed after 5750 equivalent sun hours.

Room temperature emittance (ϵ) measurements were performed simultaneously with the solar absorptance measurements by means of the Gier-Dunkle DB-100 portable reflectometer.

The effect of extended ultraviolet irradiation on the solar absorptance of the coated LI-1500 is shown in Table 5.3.3-1, and the effect of UV exposure on emittance is shown in Table 5.3.3-2.

Table 5.3.3-1

EFFECT OF UV EXPOSURE ON SOLAR ABSORPTANCE

SET	SAMPLE	α_S (PRETEST)	α_S (2900 ESH)	α_S (5750 ESH)	$\Delta\alpha_S$ (FINAL)
1*	1	0.774	-	-	-
	2	0.773	0.829	0.825	0.052
	3	0.775	0.831	0.818	0.043
	4	0.766	-	0.803	0.037
2**	5	0.768	0.781		0.013
	6	0.759	0.772		0.012
	7	0.761	0.777		0.016

* UNCYCLED SAMPLES
** 20 THERMAL CYCLES

Table 5.3.3-2

EFFECT OF UV EXPOSURE ON EMITTANCE

SET	SAMPLE	ϵ (PRE-TEST)	ϵ (2900 ESH)	ϵ (5750 ESH)
1*	1	0.859	0.858	0.859
	2	0.866	0.867	0.867
	3	0.862	0.862	0.861
2**	4	0.865	0.866	0.865
	5	0.856	0.856	
	6	0.864	0.862	
	7	0.865	0.866	

*UNCYCLED SAMPLES
**20 THERMAL CYCLES

From the results listed in Table 5.3.3-1, it can be seen that extended UV exposure of the uncycled coated LI-1500 causes an increase in α_s of 0.04 - 0.06. The material subjected to multiple simulated reentry cycles degrades somewhat less ($\Delta\alpha$ = 0.01 - 0.02). In all cases, however, the measured values of emittance were unchanged as a result of UV exposure.

Based on the results of these tests, it may be concluded that extended exposure to solar ultraviolet radiation will not alter the room temperature emittance of the coated LI-1500. The solar absorptance of the material appears to increase by 0.04 - 0.06 after 2900 ESH and remains essentially unchanged after an additional exposure of 2850 ESH. The material previously subjected to reentry conditions appears to degrade somewhat less ($\Delta\alpha_s$ = 0.01 - 0.02).

In either case, the change in solar absorptance is of sufficiently small magnitude to consider the effects of UV radiation negligible to the overall thermal performance of the material.

5.3.4 Freeze/Thaw Tests

Exposure of the Space Shuttle TPS to cyclic temperature conditions that would cause alternate freezing and thawing of the RSI may cause degradation of the basic material and/or coating. The material moisture content prior to freezing determines the level of internal force generated upon freezing of the moisture. In addition to the moisture content, the rates of freezing and thawing have an effect on the stress patterns generated within the RSI. The following tests were performed to determine the RSI behavior when subjected to a range of environmental conditions simulating those that may be experienced by the Space Shuttle booster.

A "worst case" approach was taken in exposing the test specimens to the various temperature conditions. Actual ambient temperature changes occur gradually, instead of abruptly as in the tests. However, this represents a most severe test

condition, and it is felt that acceptable behavior for these conditions will assure integrity for any less severe conditions. In addition, a range of thaw temperatures was chosen to determine thaw temperature level effects that may be encountered for both prelaunch and ascent conditions.

The specimens were 1 x 4 x 4 in. LI-1500 tiles coated on one 4 x 4 in. surface with the 0042 coating system. All the specimens were treated with the LI-007 silicone hydrophobic water repellant material prior to the initial test series. Each test for a particular specimen consisted of exposure to a specific moisture environment, followed by a freeze/thaw cycle. Each specimen was subjected to a series of three tests, each test being at a different thaw temperature. The test conditions are shown in Table 5.3.4-1 and the test results in Table 5.3.4-2.

Table 5.3.4-1

FREEZE/THAW TEST CONDITIONS

Specimen	Moisture Environment (% RH)	Freeze Temperature (^{o}F)	Thaw Temperature (^{o}F)		
			Cycle 1	Cycle 2	Cycle 3
TT544	50	0	Ambient	500	1,000
TT542	95	0	Ambient	500	1,000
TT541*	100	0	Ambient	500	1,000
TT453	100	0	Ambient	500	1,000

*TT541 was subjected to 2 cycles with 1000^{o}F thaw temperature.

The test procedure was as follows:

1. Exposure to indicated moisture environment for a minimum 2-hour period
2. Exposure to indicated freeze temperature for a minimum 8-hour period
3. Exposure to Cycle 1 thaw temperature for a minimum 8-hour period
   The specimen dimensions and weights were taken and visual inspection was performed prior to (1) and after (2) and (3)
4. Repetition of (1), (2) and (3) except with Cycle 2 thaw temperature conditions
5. Repetition of (1), (2) and (3) except with Cycle 3 thaw temperature conditions

Table 5.3.4-2

LI-1500 FREEZE/THAW TEST RESULTS

SPECIMEN NO.	MOISTURE ENVIRONMENT		FREEZE ENVIRONMENT		THAW ENVIRONMENT		PRE-TEST MEASUREMENTS				POST-TEST MEASUREMENTS			
	% RH	TIME (HR)	TEMP (°F)	TIME (HR)	TEMP (°F)	TIME (HR)	LENGTH (IN.)	WIDTH (IN.)	HEIGHT (IN.)	WEIGHT (GM)	LENGTH (IN.)	WIDTH (IN.)	HEIGHT (IN.)	WEIGHT (GM)
TT 544	50	2	0	14	70	8	4.030	4.032	1.000	69.9	4.030	4.030	0.999	69.4
	50	2	0	64	500	8	4.030	4.030	0.999	69.4	4.024	4.028	0.995	69.4
	50	2	0	18	1000	8	4.024	4.028	0.995	69.4	4.020	4.027	0.994	69.3
TT 542	95	2	0	8	70	8	4.030	4.038	1.003	74.0	4.025	4.033	0.995	73.9
	95	2	0	66	500	8	4.025	4.033	0.995	73.9	4.022	4.029	0.991	73.7
	95	2	0	16	1000	8	4.022	4.029	0.991	73.7	4.020	4.028	0.989	73.8
TT 541	100	3	0	12	70	8	4.032	4.025	0.997	70.6	4.022	4.013	0.994	70.7
	100	2	0	68	500	8	4.022	4.013	0.994	70.7	4.018	4.009	0.990	70.3
	100	2	0	14	1000	8	4.018	4.009	0.990	70.3	4.020	4.007	0.989	70.5

The recorded dimension and weight changes are considered negligible. No visual degradation of either the basic LI-1500 material or 0042 coating was observed.

Additional tests were performed to determine the influence of elevated temperature on the effectiveness of the water repellant material. Specimen TT541, which had been previously cycled at ambient, 500, and 1000°F thaw temperatures, was subjected to 100 percent humidity conditions, frozen, and then thawed at 1000°F. Specimen TT543, which was treated with the LI-007 silicone hydrophobic water repellant material, was tested under the same conditions to obtain a direct comparison. The test results are shown in Table 5.3.4-3. Although the untreated speciment absorbed more moisture than the treated one, the amount is considered negligible (< 1.0 percent). No visual degradation of either the basic LI-1500 material or 0042 coating was observed.

Based on these tests, it is concluded that freeze/thaw cycles, even under conditions of high humidity or rain, do not cause any degradation of LI-1500 material or 0042 coating.

5.3.5 Rain Erosion Tests

Rain conditions may be encountered by the Space Shuttle orbiter during cruise. To enable establishment of system constraints for these environmental conditions, the erosion resistance of the TPS must be determined. Since the vehicle design, and therefore its flight characteristics, has not been finalized, it was assumed that the optimum cruise velocity is 350 miles per hour and that 200 miles per hour is the minimum velocity possible to maintain altitude. The velocities, angles of attack, rain intensity, and test durations are those suggested by A. J. Meyer*. The objective of the following test program was to test coated LI-1500 material to demonstrate its ability to survive anticipated rain environmental conditions during flight.

*Meyer, Andre J., "Definition of Erosion Environment for TPS Systems, Tasks A-1 and A-25," 9 July 1971

Table 5.3.4-3

LI-1500 FREEZE/THAW TEST RESULTS

SPECIMEN NO.	MOISTURE ENVIRONMENT		FREEZE ENVIRONMENT		THAW ENVIRONMENT		MEASUREMENTS				SEQUENCE
	% RH	TIME (HR)	TEMP (°F)	TIME (HR)	TEMP (°F)	TIME (HR)	LENGTH (IN.)	WIDTH (IN.)	HEIGHT (IN.)	WEIGHT (GM)	
TT 541*	100	2	0	62	1000	8	4.018	4.009	0.993	70.2	PRE-HUMIDITY
							4.019	4.004	0.994	70.8	POST-HUMIDITY
							4.016	3.998	0.990	70.7	POST-FREEZE
							4.010	3.997	0.989	70.3	POST-THAW
TT 543**	100	2	0	62	1000	8	3.975	3.989	1.000	63.4	PRE-HUMIDITY
							3.977	3.989	1.000	63.7	POST-HUMIDITY
							3.975	3.989	1.000	63.6	POST-FREEZE
							3.980	3.989	0.999	63.3	POST-THAW

*TT 541 WAS PREVIOUSLY CYCLED TO 1000°F.

**TT 543 WAS TREATED WITH LI 007 SILICONE HYDROPHOBIC WATER REPELLANT MATERIAL BUT UNCYCLED PRIOR TO THIS TEST.

The tests were performed in the Edler Industries, Inc., High Speed Rain Erosion Test Facility located in Newport Beach, California. It is a rotary-arm type tester that subjects specimens mounted on the rotary blade to rainfall conditions of known intensity and mean volumetric drop size, while traveling at a constant velocity for a specified period of time. The following are facility specifications:

Rotor Tip Velocity	566 ±3 mph (RPM measured by Strobotac)
Rotor Blade Diameter	54 inches
Rain Nozzle Configuration	Sierracin-designed spray head
Rainfall Rate	0.7 to 1.4 in./hr
Droplet Size	1.2 to 2.0 mm (mean volumetric)

The water delivery system is unique in its high degree of accuracy of droplet size and rainfall rate. Standard methods of measurement are used, employing a sectioned water-gathering device across the specimen test area, to obtain rainfall rate and distribution in the test area and to capture representative droplets in a two-level oil-filled tray that allows for the photographing of the actual droplets superimposed upon a millimeter grid screen. These droplets are counted by category, determined by size range, and the percentage of each category is used to calculate the mean volumetric drop size. Twelve samples of droplets are taken at specific stations of the specimen traversing area.

Specimen velocity is determined by radial location on the rotary arm. All rainfall and drop size measurements are taken in the specimen test area in a static condition, i.e., without the arm being in motion. The effect of the blade motion upon these static conditions has not been specifically measured, but experimentation has indicated that blade turbulence has only slight influence on the rain conditions.

The specimen test assembly is shown in Fig. 5.3.5-1. The specimens are shown prior to testing in Fig. 5.3.5-2. The specimens are contained on all sides, except the test surface, with RTV 560 to seal the surfaces and provide a "soft" mounting to prevent high local loads on the specimen sides due to forces generated during the tests. The test conditions are shown in Table 5.3.5-1.

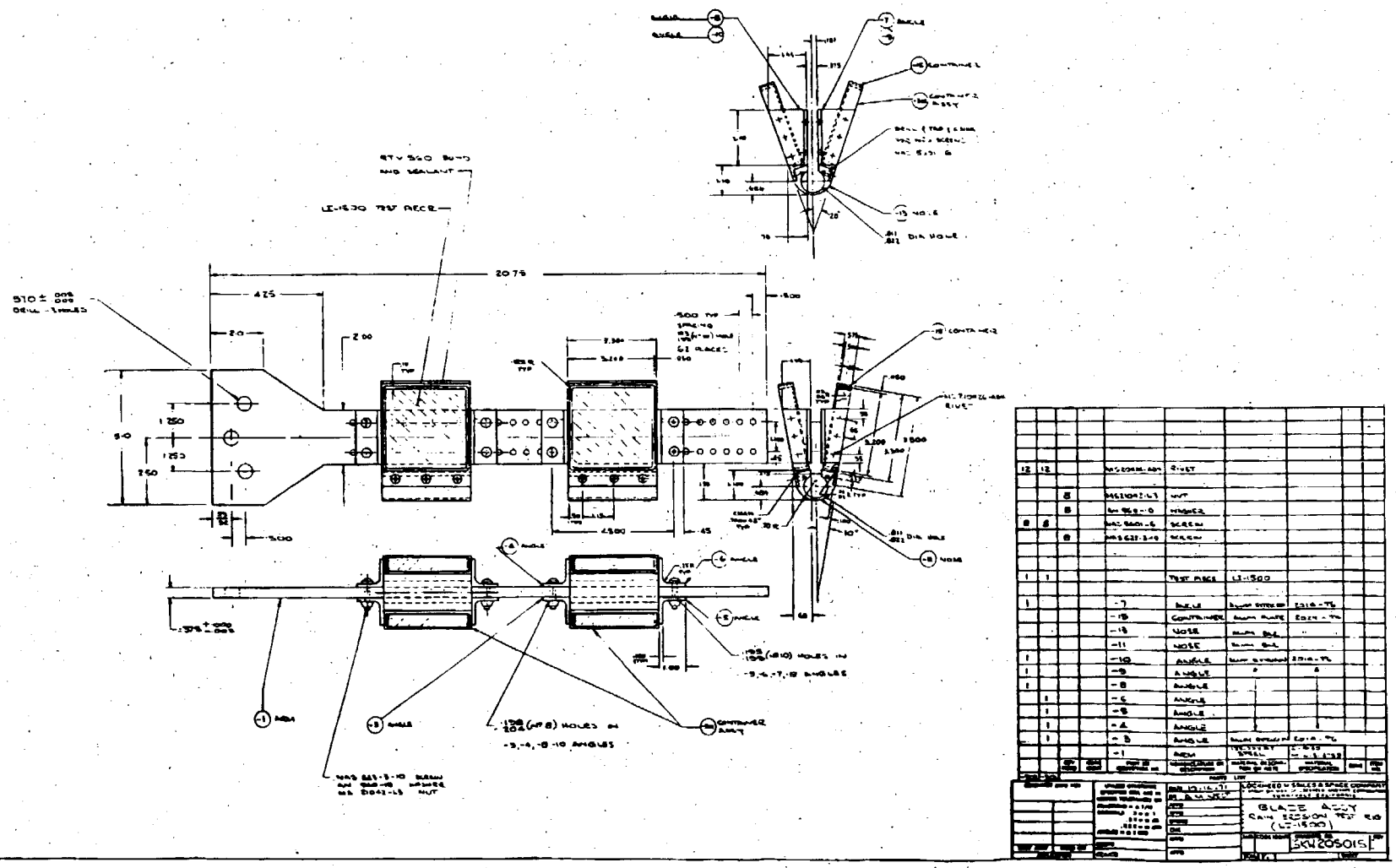

Preceding page blank

5-35

PRECEDING PAGE BLANK NOT FILMED

Fig. 5.3.5-1 Blade Assembly Rain Erosion Test Rig (LI-1500)

5-35-a

RAIN EROSION TEST SPECIMENS

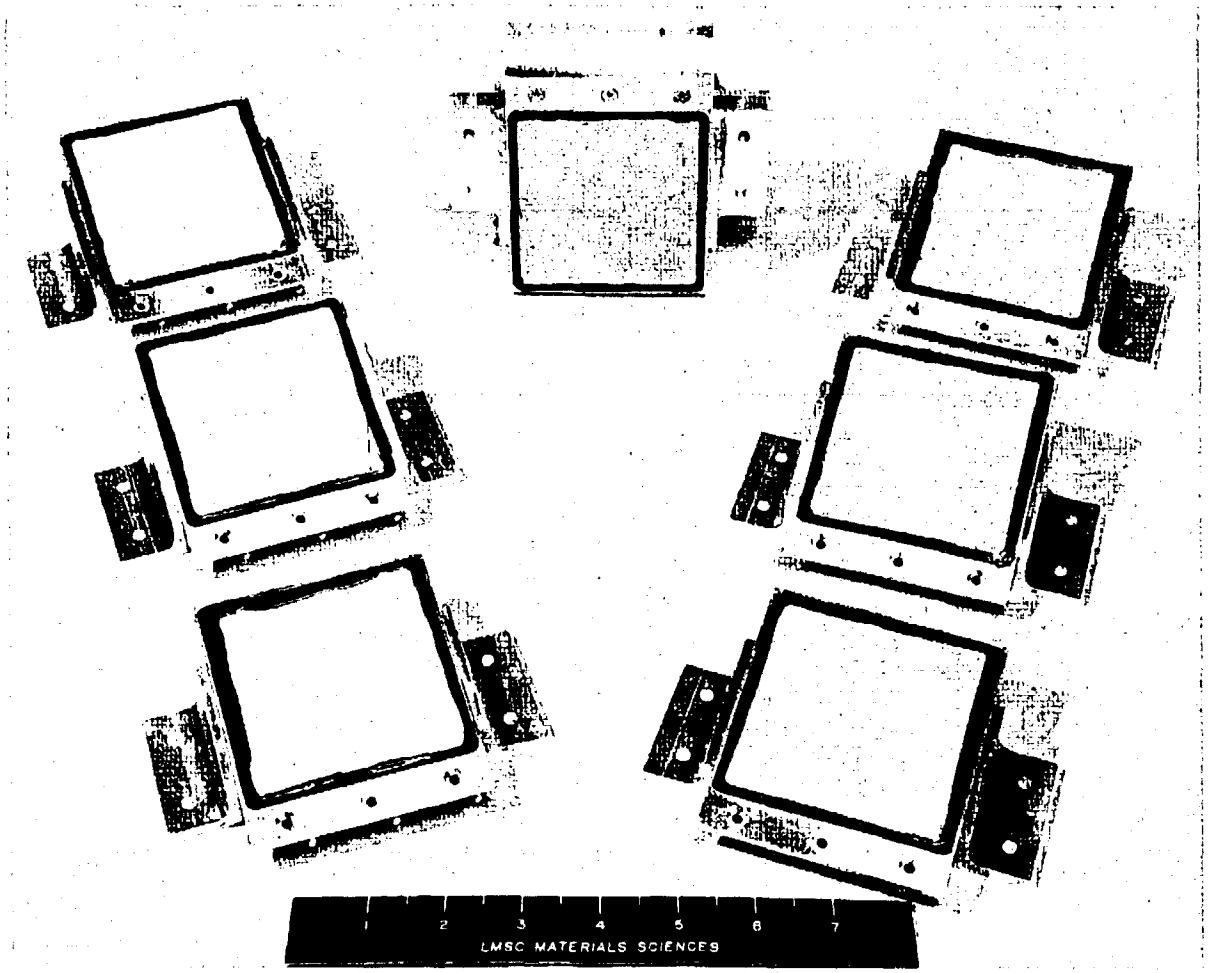

Fig. 5.3.5-2

Table 5.3.5-1

RAIN EROSION TEST CONDITIONS

Test No.	Specimen No.	Specimen Angle of Attack (deg)	Velocity (mph)	Rain Intensity (in./hr)	Test Duration (min)	Results
1	1	10	200	0	2	No change
	2	↑	↑	0	2	No change
	3	↕	↕	0	2	No change
	4	↕	↕	0	2	No change
2	1	↕	↕	1.3	5	No change
	2	↕	↕	1.3	5	No change
	3	↕	↓	1.3	5	No change
	4	↕	200	1.3	5	No change
3	1	↕	350	0	2	No change
	2	↕	↑	0	2	Coating cracked and chipped
	3	↕	↕	0	2	Coating cracked
	4	↕	↕	0	2	No change
4	1	↕	↕	1.05	5	No change
	2	↕	↕	1.05	5	No change
	3	↓	↕	1.05	5	Coating and material loss
	4	10	↕	1.05	5	No change
5	5	20	↕	0	2	No change
	6*	20	↕	0	2	Lost specimen
	7	20	↓	0	2	No change
	8	20	350	0	2	No change

*Specimen 6 had cracked coating prior to testing.

The initial test in the series was performed with Specimens 1 through 4 at 10-deg angle of attack. The test actually consisted of two 1-minute runs with no rainfall to assure mechanical integrity of the setup and to allow calibration of the specimen velocity by measurement of the rotor RPM with a stroboscope. This was necessary because changes in RPM due to drag created by the specimens had to be determined. It was found that at 200 mph the effect was negligible. The specimens sustained no degradation during the first test.

A 5-minute exposure to rain at an intensity of 1.3 in./hr was then performed (Test Number 2). Weight and thickness measurements before and after this test indicated no significant change. Visually the specimens showed no change.

The specimens were then moved to the 350 mph location and a dry run was made to obtain a stroboscope measurement of rotor RPM, which was found to be acceptable (Test Number 3). After completion of the run, it was observed that Specimen 3 had developed a surface crack and Specimen 2 had a surface crack and a chip with coating and material removal. Specimens 1 and 4 showed no change. The failures are attributed to the high mechanical loads at this test condition (~6000 g radial acceleration).

A 5-minute test with a rain intensity of 1.05 in./hr was then performed on these specimens. The coating and material on the downstream side of the crack in Specimen 3 were lost. No changes were observed in Specimens 1, 2, and 4. It is apparent from the above tests that degradation due to rain erosion at these conditions is insignificant. However, the severe mechanical loads can cause extensive degradation.

The last test in the series was a dry run performed with Specimens 5, 6, 7, and 8 mounted at 20-deg angle of attack. The specimens were located at the estimated 350 mph position on the rotor. Specimen 6 was lost during the test. This resulted in a rotor imbalance which caused excessive heating of the shaft bearing. As a result, the testing was terminated. Specimen 6 was cracked prior to this test. It was installed in the specimen holder in a cracked condition to determine the effect of rain erosion on a cracked coating. However, it is apparent that degraded specimens have difficulty surviving the mechanical loads imposed by the test facility. Therefore,

this type of information will have to be obtained under less severe load conditions.

Based on these tests, it is concluded that at 10-deg angle of attack and velocity up to 350 mph, the 0042 coating degradation due to rain erosion is insignificant. It is recommended that additional tests be conducted at 20-deg angle of attack in a facility that imposes less severe mechanical loads on the test specimens.

5.3.6 Moisture Absorption Tests

The Space Shuttle TPS may be subjected to a range of relative humidity and rain conditions either prior to or at the end of a mission. It is necessary to determine the extent to which exposure of the TPS to these conditions may influence the thermal performance and mechanical integrity of the system. Moisture present in the material during ascent or entry may increase the thermal conductivity of the material or cause internal stresses resulting in physical degradation. Since the effectiveness of the over-spray in limiting the material moisture content is of primary concern, it is necessary to determine the material behavior after exposure to moisture environments prior to and after application of an overspray. The following tests were performed to determine the RSI behavior during ascent and entry after exposure to simulated launch pad moisture environment conditions.

Seven specimens, each 4 x 4 x 2.45 in. were bonded with RTV 560 to a 0.125 in. thick aluminum plate. One of the specimens contained a typical joint; the others were monolithic tiles. The monolithic specimens were coated on the top surface and to mid-depth on each side. The joint specimen was only coated on the top surface and to mid-depth in the joint. Each specimen was subjected to a specific moisture environment, followed by a simulated ascent/entry combined heating and pressure environmental cycle. Some specimens were oversprayed before moisture environment exposure and some after. Each specimen was instrumented with two chromel-alumel thermocouples; one was bonded to the LI-1500 backface, and the other was installed by a plug at the specimen mid-point. The specimen conditions prior to exposure to ascent/entry environment conditions are shown in Table 5.3.6-1.

Table 5.3.6-1

SPECIMEN PRETEST CONDITIONS

Specimen	Configuration	Moisture Environment	Previous Thermal Cycles	Overspray
TT49 - A-1	Tile	50% RH	0	Before ME*
TT49 - A-2	Tile	50% RH	0	After ME
TT49 - B	Tile	75% RH	0	After ME
TT49 - C	Tile	95% RH	0	After ME
TT49 - D-1	Tile	Rain	5	Before ME
TT49 - D-2	Tile	Rain	5	After ME
TT49 - E	Joint	Rain	0	Before ME

* Moisture Environment

The test procedure was as follows:

1. Exposure to specified moisture environment for a minimum 2-hour period
2. Exposure to ascent/entry combined heating and pressure environmental cycle
3. Repeat (1) and (2).

Specimens A-1, D-1, and E were oversprayed prior to (1). Specimens A-2, B, C, and D-2 were oversprayed after (2). Dimensions and weights were recorded prior to (1) and after (1) and (2). Visual inspection was performed prior to (1) and after (2).

The test panels were subjected to the humidity and moisture environments outlined in Table 5.3.6-1. Post-moisture exposure weight measurements (shown in Table 5.3.6-2) indicated that moisture absorption was minimal.

Panel TT49-D2 was subjected to simulated rainfall prior to waterproofing solution application. This panel absorbed 196 grams of water.

Table 5.3.6-2

MOISTURE ABSORPTION TESTS, SPECIMEN WEIGHTS

WEIGHT (GRAMS)

PANEL NO.	ASSEMBLY WEIGHT	CYCLE NO. 1				CYCLE NO. 2		
		WEIGHT AFTER O'SPRAY	WEIGHT AFTER MOISTURE	WEIGHT AFTER O'SPRAY	WEIGHT AFTER THERMAL TEST	WEIGHT AFTER O'SPRAY	WEIGHT AFTER MOISTURE	WEIGHT AFTER THERMAL TEST
TT49-A-1	275.0	283.0	283.0	-	283.0	283.1	283.1	283.0
TT49-A-2	277.1	-	277.25	281.7*	293.6	293.7	293.7	291.9
TT49-B	281.6	-	281.6	-	281.6	▲295.85	295.85	294.2
TT49-C	264.3	-	264.5	● 280.3	280.3	280.85	280.85	278.9
TT49-D-1	277.8	282.3	282.5	-	282.1	282.3	282.5	282.1
TT49-D-2	283.2		479.1	479.2	343.95	■		
TT49-E	281.1	282.6	290.7	-	290.0	296.5	297.2	295.3

* PANEL REWORKED: REWORKED WEIGHT ~ 293.6 GM

▲ PANEL REWORKED: REWORKED WEIGHT ~ 295.2 GM

● PANEL REWORKED: REWORKED WEIGHT ~ 280.7 GM (CHIP KNOCKED FROM CORNER)

■ PANEL REMOVED FROM TESTS AND OVEN-DRIED: DRY WT ~ 282.65 GM

All panels were installed in the LMSC radiant heat/vacuum test facility and were subjected to the reference ascent and entry heat and pressure environments. The test was aborted after 1300 sec of entry heating due to a control instrumentation failure. Post-test inspection of the panels showed that panel TT49-D2 had experienced a minor coating failure. Small bits of the coating had been detached from the panel heated surface near one edge and around the coated sides. (See Fig. 5.3.6-1.) The other panels in the test fixture were undamaged.

It should be emphasized that the uncoated, unwaterproofed sides of specimen TT49-D2 were exposed to simulated rain, so that the moisture was absorbed through the sides rather than the coating. Such an exposure is admittedly unrealistic and unfair to LI-1500 but was done in the interest of gaining more information about the material.

Panel TT49-D2 was removed from the test program, and the remaining panels were tested as planned for one additional cycle. The results were the same, i.e., minimal moisture pickup, and no damage as a result of ascent and entry temperature and pressure simulation.

Temperature responses of panel midpoint and bondline thermocouples are shown in Fig. 5.3.6-2. The data are clustered closely enough that no definite effects of moisture exposure on transient temperature responses are detectable.

It may be concluded from these tests that LI-1500 should be treated with hydrophobic waterproofing compound prior to exposure to rain. However, it is standard procedure at LMSC to waterproof all LI-1500 test panels prior to release from fabrication.

The tests also show that waterproofed LI-1500 is not affected by exposure to various moisture environments; nor do subsequent simulated ascent/entry pressure and heating environments degrade the material.

5.3.7 Cold Soak Tests

Regions of the TPS may reach temperatures of -150°F while the Space Shuttle is in orbit. It must be determined whether RSI degradation will occur when the TPS experiences an entry temperature history following an initial -150°F temperature condition.

MOISTURE ABSORPTION SPECIMEN - POST TEST PHOTO

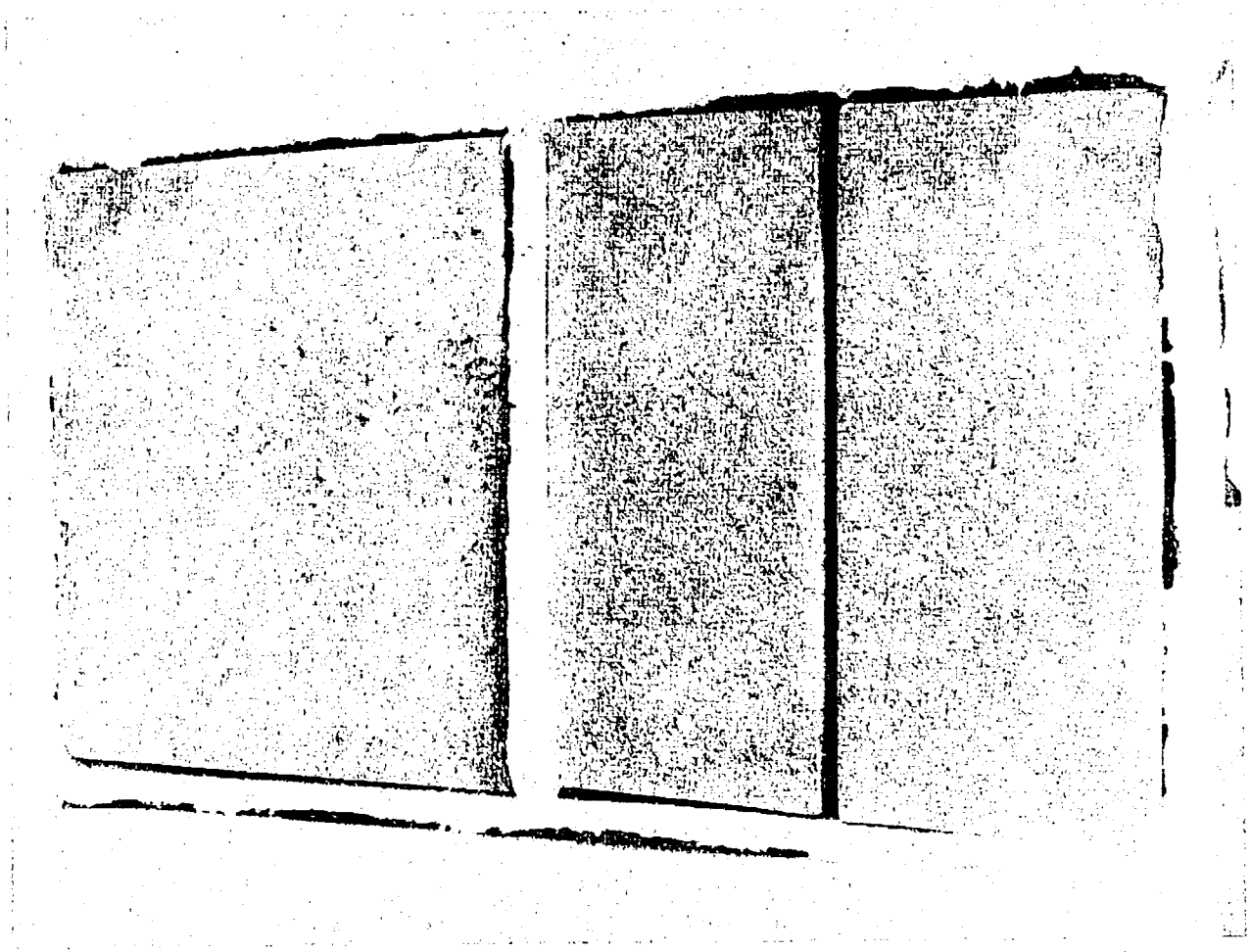

TT49-D2 TT49-E

Fig. 5.3.6-1

LI-1500 MOISTURE ABSORPTION TEST, TEMPERATURE RESPONSE

DIMENSIONS IN INCHES

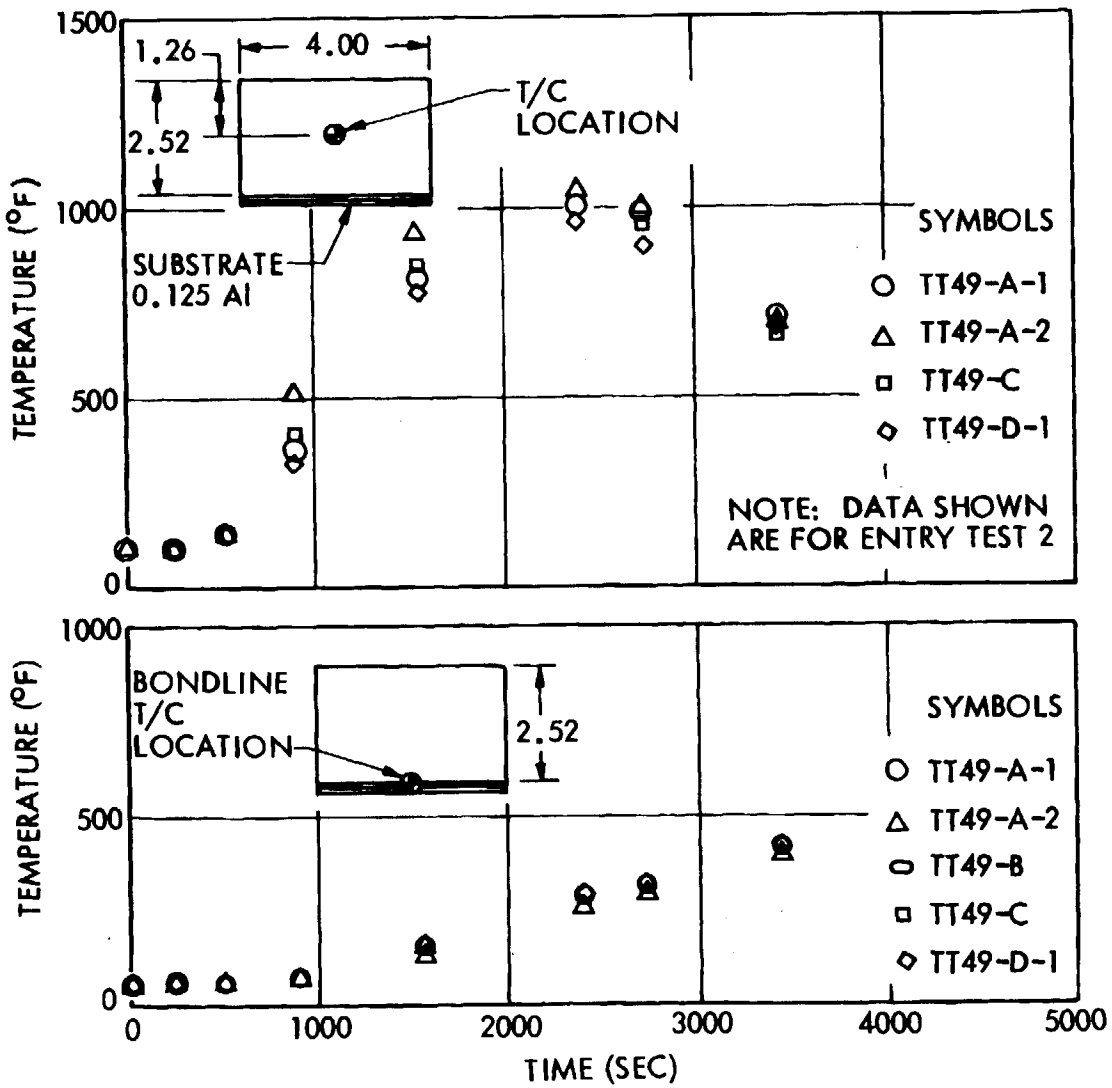

Fig. 5.3.6-2

The thermally induced stresses from severe temperature gradients within the LI-1500 will be greatest for these conditions. The following tests were performed to determine effects due to repeated temperature cycling between minimum orbit temperature and entry temperatures.

Two specimens, each 4 x 4 x 2.45 in, were bonded with RTV 560 to aluminum baseplates. The outer 4 x 4-in. surface of each specimen and the upper half of the sides was coated with the 0042 coating system. Each specimen was instrumented with three thermocouples. One was installed at the specimen midpoint, one was bonded to the LI-1500 backface, and one was bonded to the aluminum baseplate backface. The specimens were shrouded and enclosed in a plastic bag which was purged with dry N_2 during the cold soak test to prevent water condensation on the specimens. The bag was retained during handling and installation of the specimens in the radiant heat facility and then removed prior to exposing the specimens to the heating environment. The test procedure was as follows:

1. Bagging of specimens and purging with dry N_2.
2. Exposure of vacuum-bagged specimens to low-temperature environment until they reach $-150^{\circ}F$.
3. Exposure of unbagged specimens to simulated entry heating environment. (All thermocouple data were recorded during this test)
4. Repeat of (1), (2), and (3) two times.

The specimen dimensions and weights were taken, and visual inspection was performed prior to (1) and after (3).

No visual degradation or measurable change in dimensions or weights was observed. Typical measured temperature profiles are shown in Fig. 5.3.7-1. The difference in midpoint temperature is believed to be the result of excessive contact resistance between Thermocouple A and the surrounding material.

5.3.8 Temperature Overshoot Tests

Evaluation of the TPS performance when exposed to environmental conditions more severe than the design criteria is necessary to fully characterize the system. The effect of exceeding the design heating profile was examined by subjecting specimens to surface temperatures greater than the $2300^{\circ}F$ design limit.

SHUTTLE

COLD SOAK TEST DATA

(TEST NO. 2)

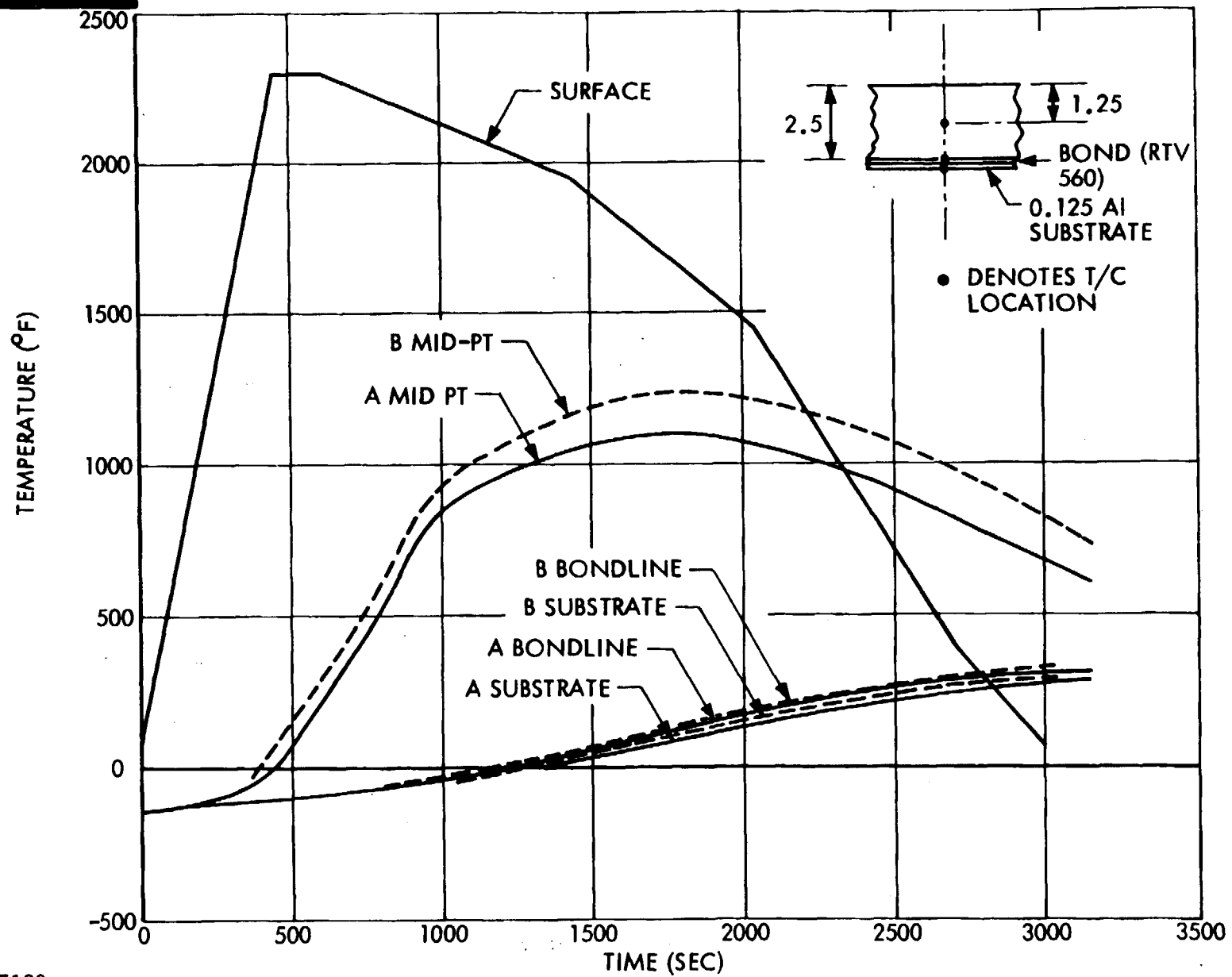

Two specimens were used for the temperature overshoot tests. Specimen 1 was a 4 x 4 x 1-in. thick, coated tile with no baseplate or instrumentation. Specimen 2 was a 4 x 4 x 2.45-in. coated tile bonded to a 0.114-in. thick aluminum plate with a 0.090-in. thickness of RTV 560 adhesive. The specimen was instrumented with two thermocouples: one on the baseplate and one at mid-depth in the LI-1500. This specimen had been used previously in the cold soak tests.

Specimen 1 experienced a series of five tests, with maximum surface temperature progressively increased from 2600 to 2950°F. The surface temperature profile is shown in Fig. 5.3.8-1. At the conclusion of the tests, small open pores were observed on the coating. No coating cracking was observed, and the water repellancy was retained.

Specimen 2 was subjected to a heat impulse that resulted in the surface temperature profile shown in Fig. 5.3.8-2. The coating remained uncracked and water repellant, although some local surface slumping was noted. Figure 5.3.8-3 shows the specimen after the test.

The effect of maximum surface temperatures greater than the design value is illustrated in Fig. 5.3.8-4. Although the 300°F maximum design temperature for the aluminum structure is exceeded (410°F for a 3000°F maximum surface temperature), the structure would remain intact and the vehicle could be landed safely.

5.3.9 THERMAL AND ACOUSTIC TEST OF FI-600

An improvement to the TPS system was made under contract NAS 9-12137 and is incorporated into the designs of the prototype panels. FI-600, a low density, flexible variant of LI-1500 was used for the seal strips in prototype panel joints. This material was exposed in an oven to 1400°F for 16 hours and then fabricated into a joint model which was subjected to an acoustic test. The acoustic environment is shown in Fig. 5.3.9-1. Total exposure duration was 30-minutes. Visual inspection of the model after test showed no observable damage or degradation of the LI-1500 or the FI-600.

TEMPERATURE OVERSHOOT PROFILE – SPECIMEN 1

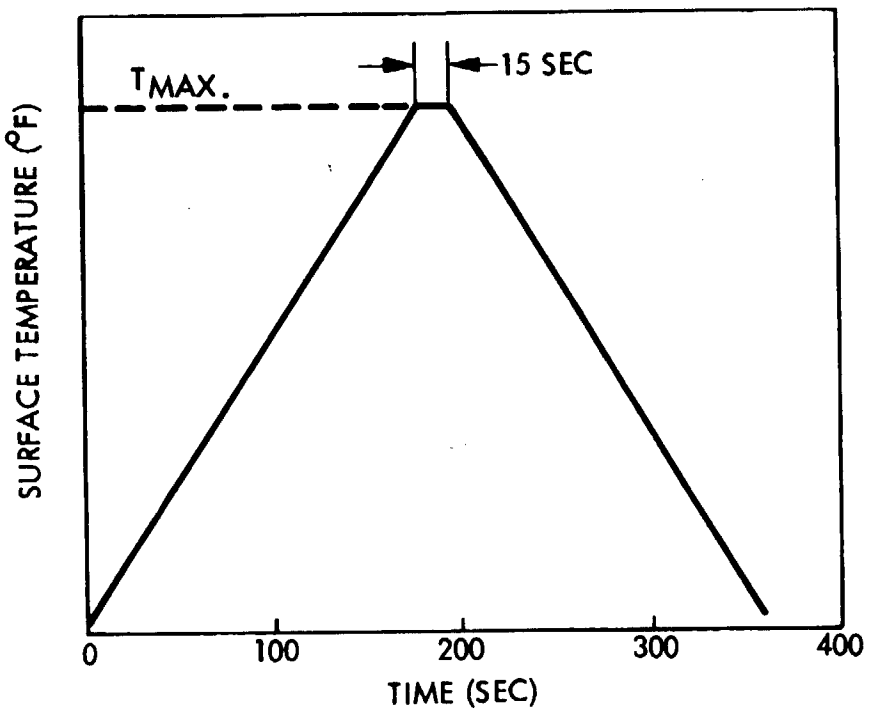

RUN	$T_{MAX.}$ (°F)
1	2600
2	2700
3	2800
4	2900
5	2950

Fig. 5.3.8-1

TEMPERATURE OVERSHOOT PROFILE – SPECIMEN 2

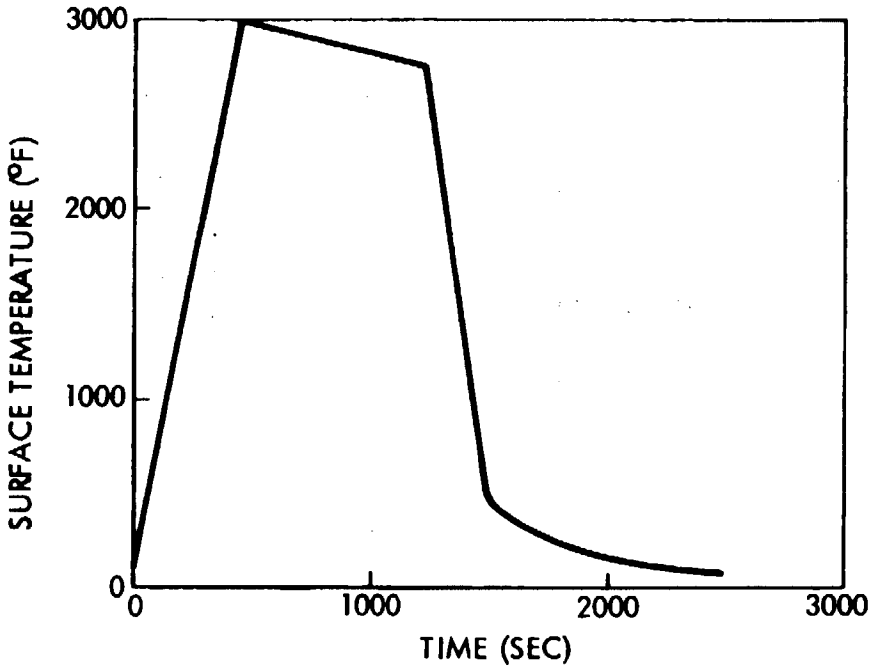

15 MINUTES ABOVE 2500 °F
16 MINUTES ABOVE 2300 °F
18 MINUTES ABOVE 2000 °F

D07128

Fig. 5.3.8-2

LI-1500 SPECIMEN AFTER 3000°F TEMPERATURE OVERSHOOT TEST

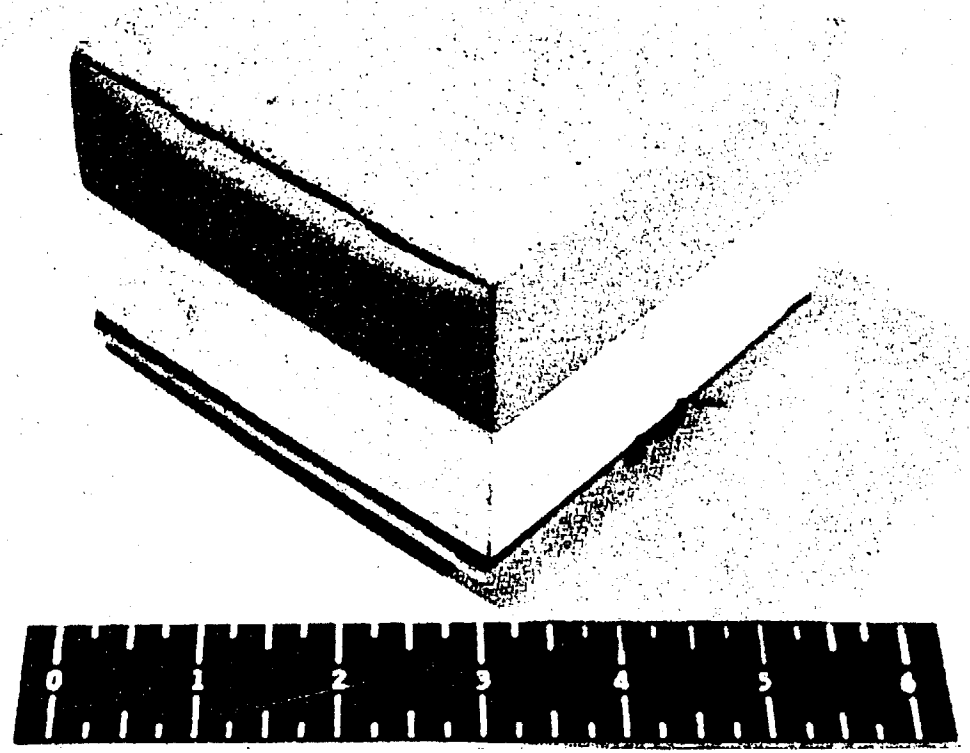

Fig. 5.3.8-3

EFFECT OF TEMPERATURE OVERSHOOT ON STRUCTURE TEMPERATURE

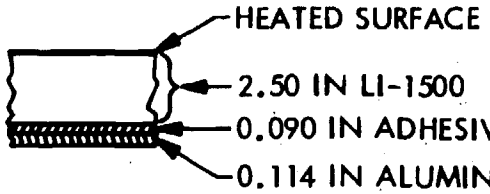

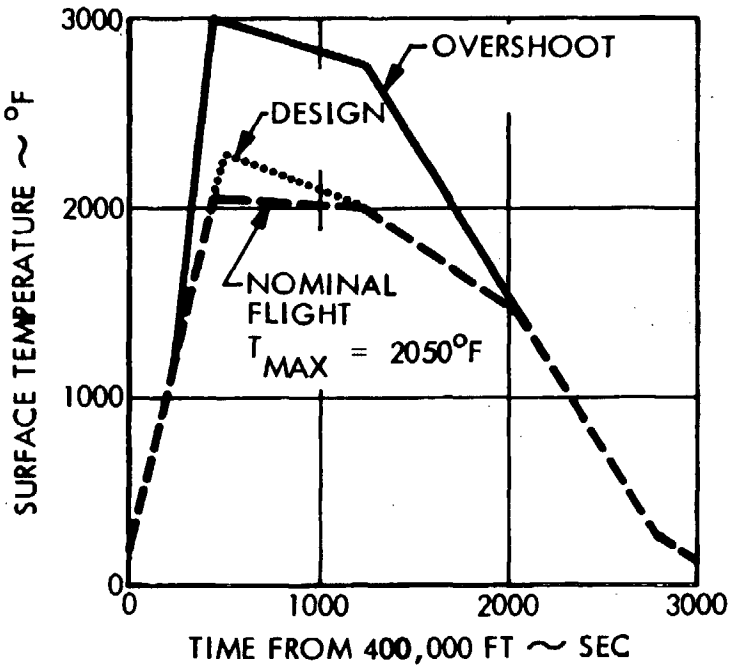

MAX SURFACE TEMP °F	STRUCTURE TEMP 30 MINUTES AFTER TD °F	STRUCTURE TEMP AT TOUCHD'N °F	TIME ABOVE 2300°F MINUTES	TIME ABOVE 2500°F MINUTES
2500	335	240	11	-
2800	385	280	20	15
3000	410	310	20	17

LI-1500 SIZED FOR T_{MAX} = 2300°F
TOUCHDOWN AT 60 MINUTES

Fig. 5.3.8-4

DO6415

COMPARISON OF APPLIED ACOUSTIC TEST ENVIRONMENT WITH REQUIREMENT

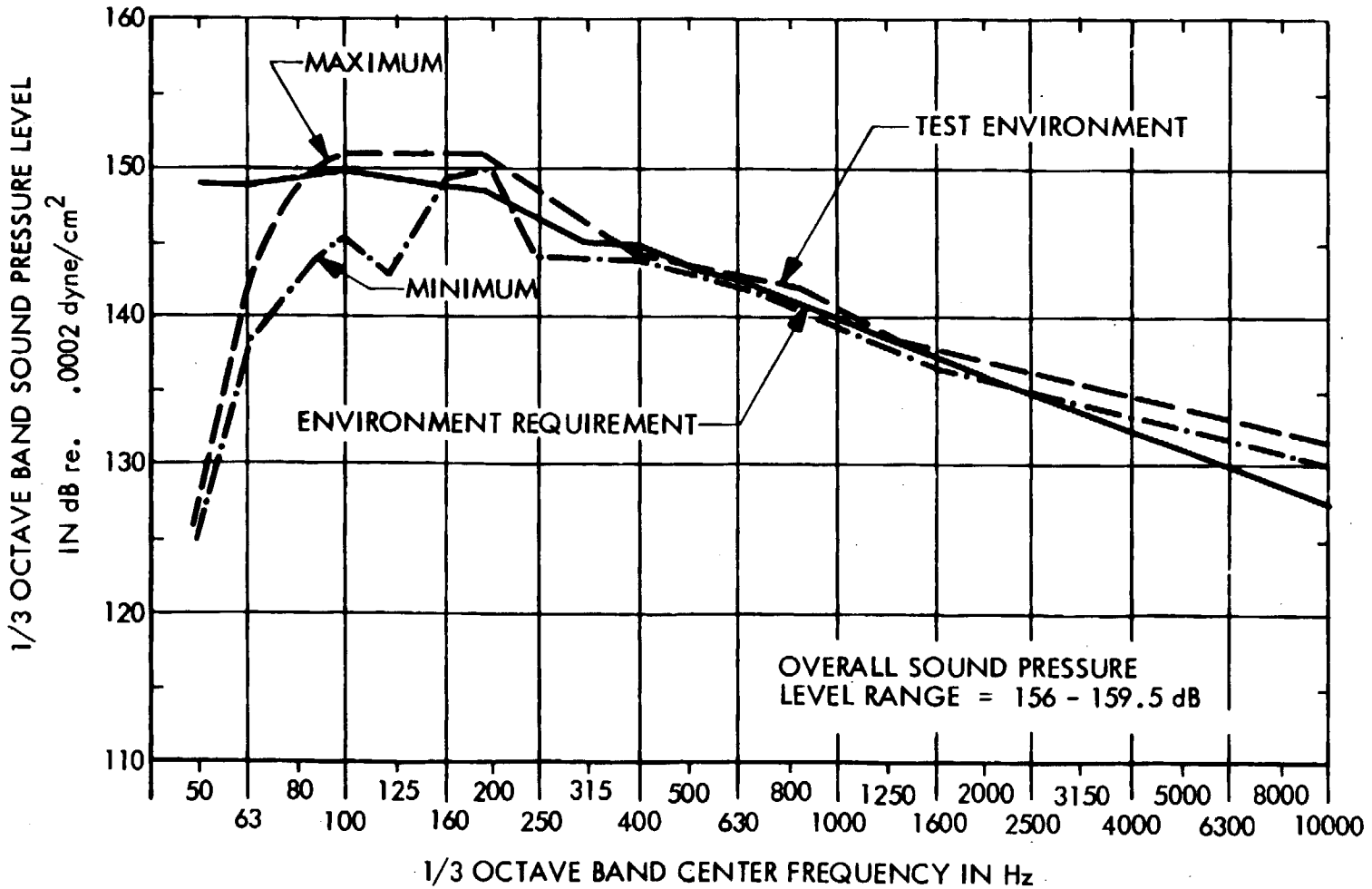

Fig. 5.3.9-1

Section 6

PROTOTYPE PANELS AND MATERIAL SPECIMENS

6.1 PROTOTYPE PANELS

LMSC has designed four prototype panels in accordance with contract requirements. Point design conditions were specified by NASA/MSC. The design effort was accomplished under Task 2.0, as negotiated and reviewed in Volume II of this report. The panels consist of a metallic structure with coated LI-1500 bonded to one side with the RTV 560 adhesive system. The original panel critical design review was scheduled for 4 October but was extended to 12 November, as discussed in Section 1. During the month of October, LMSC conducted an intensive test program on advanced coating systems; this effort culminated in a baseline coating change from 0025 to 0042. The testing of this new coating system is discussed in detail in Sections 3, 4, and 5.

Early in this program, the actual planned panel test conditions were not specified for reduced or atmospheric pressure conditions. Since LI-1500 conductivity is quite dependent on pressure (see Section 4.1), LMSC specified designs for test (1 atmosphere pressure) and flight (flight profile pressure). Prior to the review given at NASA/MSC on 4 October, eight prototype panels were designed on the basis of the 0025 coating and available test data. Based on data from all areas of testing during October, these eight panels were completely redesigned. The substrates remained essentially the same, but tile sizes and bond line thicknesses were modified. Per NASA/MSC direction, the deliverable panels are being fabricated, using LI-1500 thicknesses sized to be tested at reentry pressure levels.

Details of the prototype panels are shown in Figs. 6.1-1 through 6.1-4. The materials/applications/design areas for each panel are reviewed in Table 6.1-1. Detail design conditions, methodology, analyses, and margins of safety are given in Volume II.

Table 6.1-1

Prototype Panel Characteristics

Panel No.	Shown in Figure No.	Substrate Material	Application	Vehicle Area
1	6.1-1	Beryllium	Subpanel	2
2	6.1-2	Aluminum	Primary	2
3	6.1-3	Aluminum	Primary	1
4	6.1-4	Titanium	Primary	2

For vehicle application, the beryllium subpanel bolts directly to external vehicle frames. For testing, this panel will be bolted directly to the existing MSC differential pressure box. The primary structural panels will attach to frames for application, but will be continuous over many spans. Figure 6.1-5 shows how these units are used on the shuttle. The section to be tested is representative of a large panel between frames with end fixtures provided for testing. Figures 6.1-6a and 6.1-6b show the adapter hardware that will be provided by LMSC to tie the end plates to existing MSC test fixtures.

The LMSC finalized test plan for these panels was included in the Midterm Report as Appendix F. Some errors were discovered after this submittal and subsequently the plan was published under a separate cover (LMSC A997049). This plan specified a test sequence that included critical lift-off, ascent, orbit, reentry, and post-reentry conditions for the panels. Instrumentation locations and data acquisition requirements were also specified.

The contract originally specified that LMSC would size and apply LI-1500 to two GFE booster panels. However, these panels were not made available during the contract time span. At the direction of the NASA/MSC COR, four additional LI-1500 tiles have been furnished for evaluation in lieu of this effort.

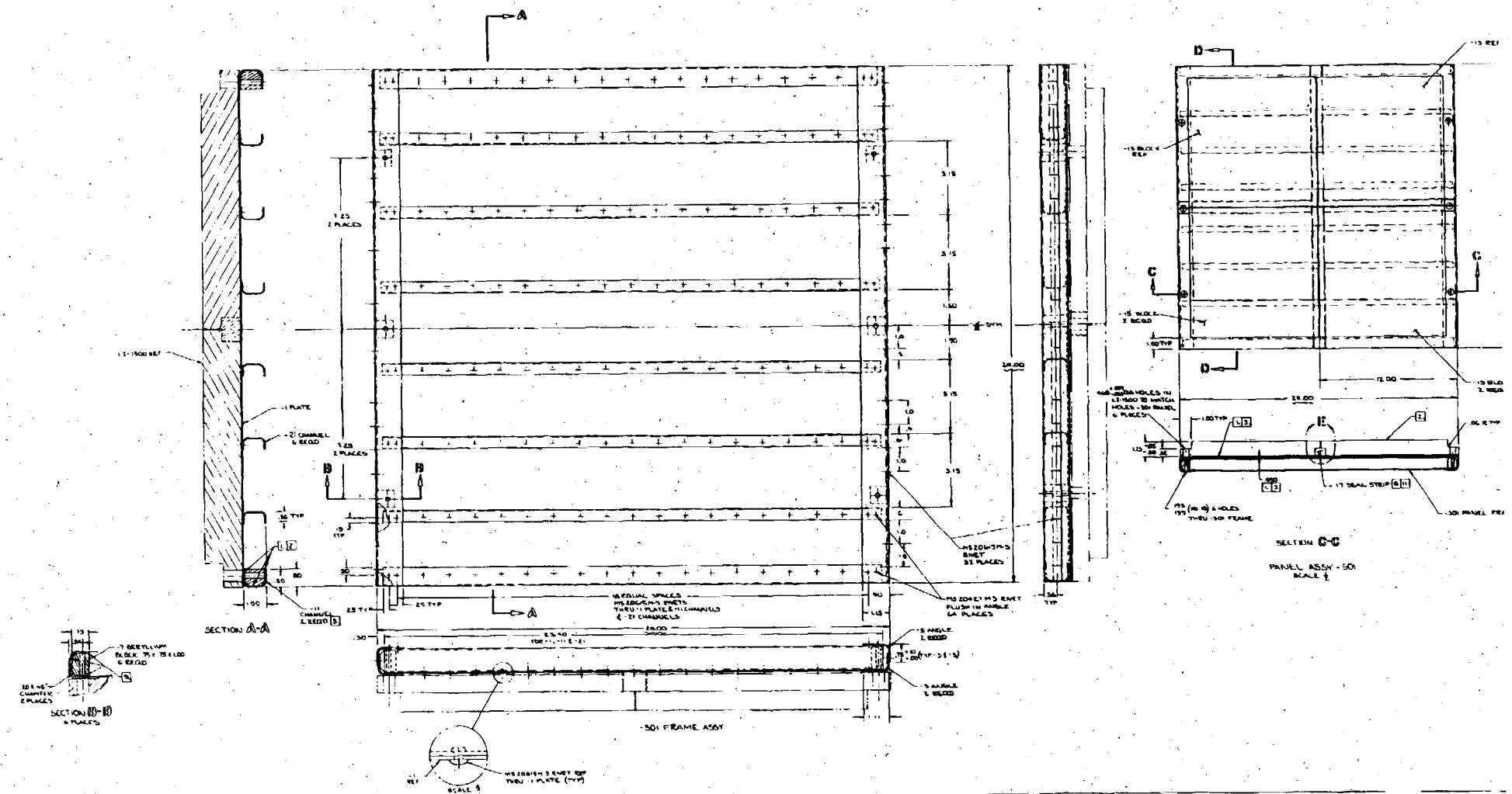
SECTION A-A
SECTION B-B
SECTION C-C
-501 FRAME ASSY
PANEL ASSY - 501

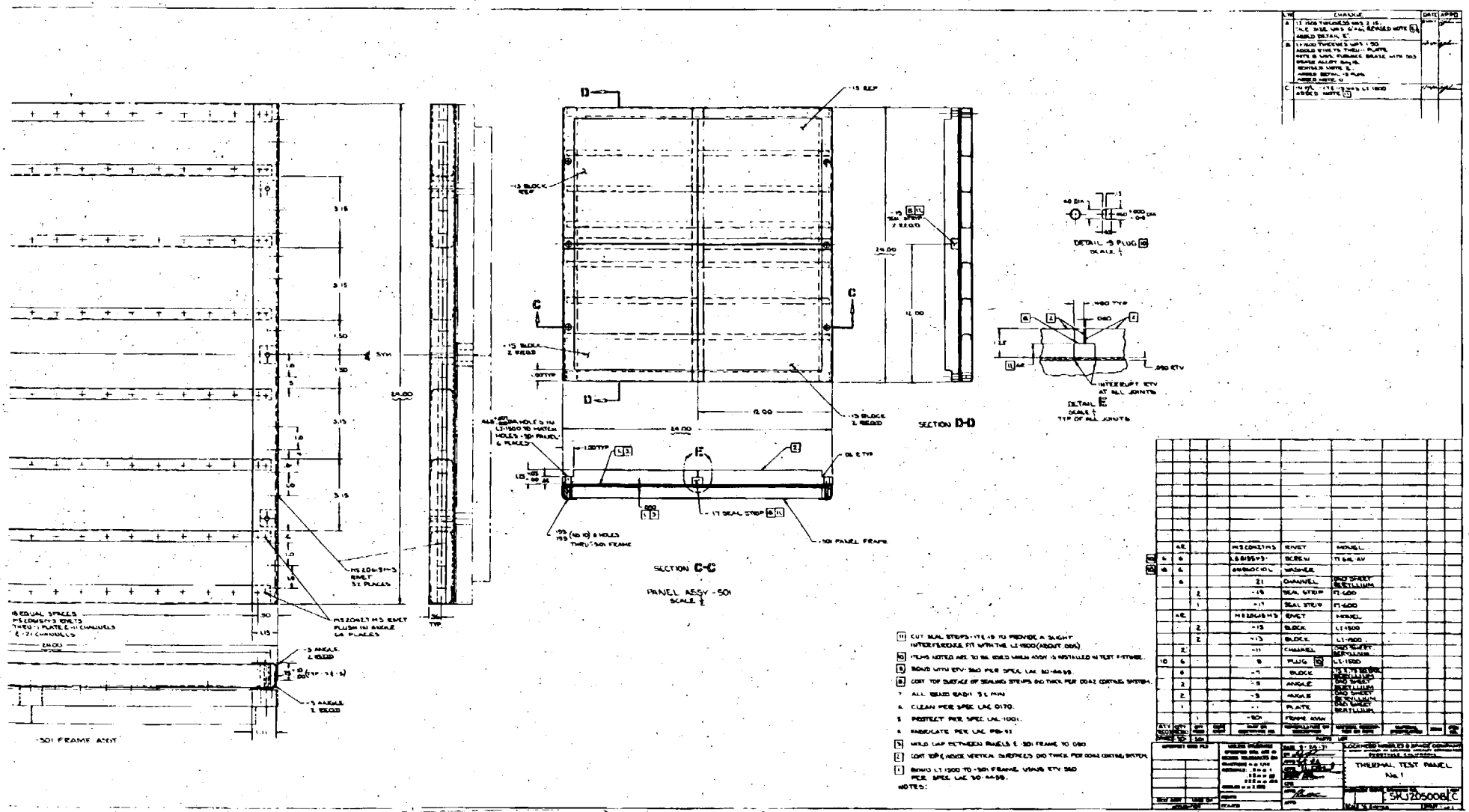

Fig. 6.1-1 Thermal Test Panel No. 1

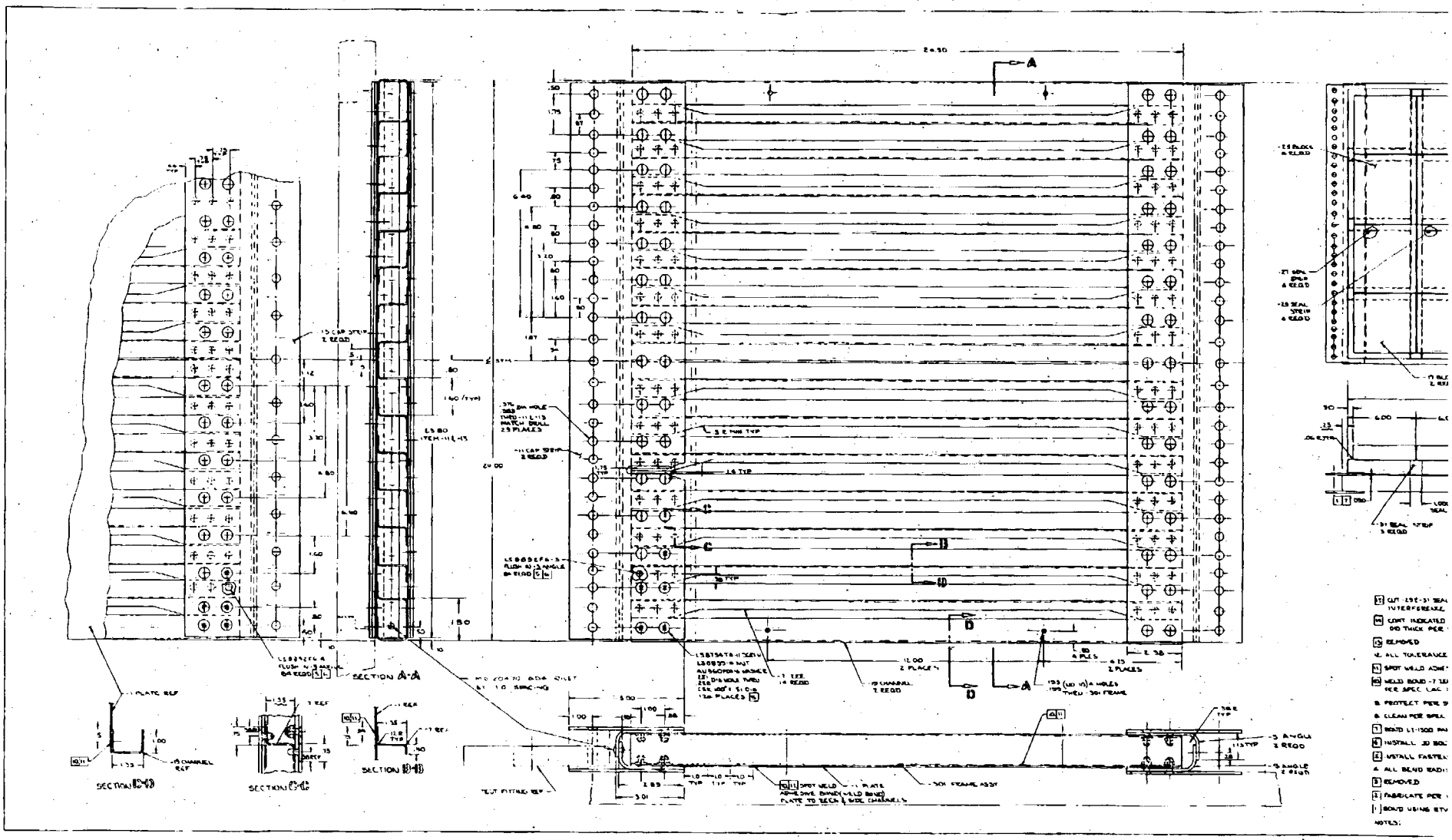

Preceding page blank

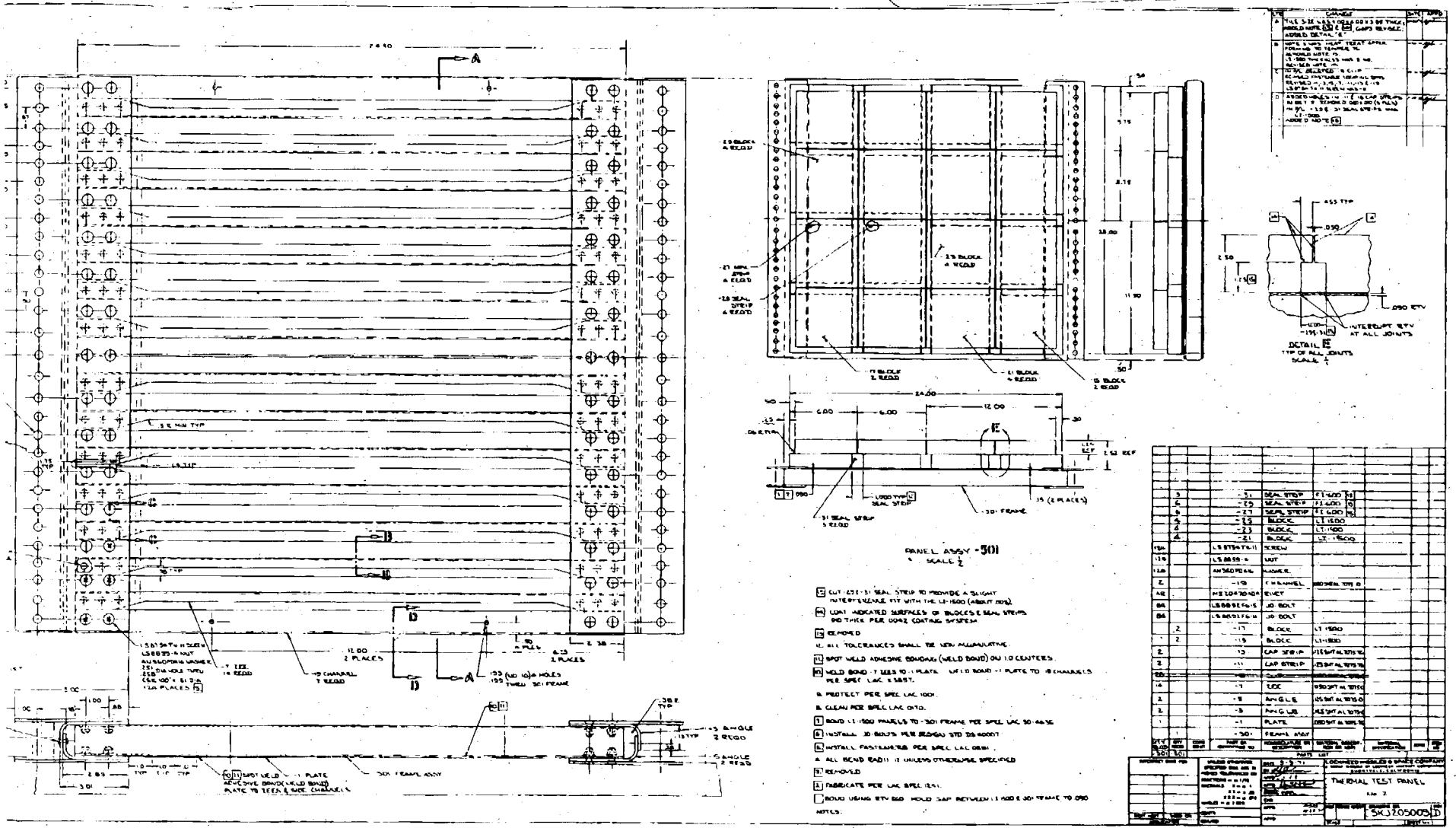

Fig. 6.1-2 Thermal Test Panel No. 2

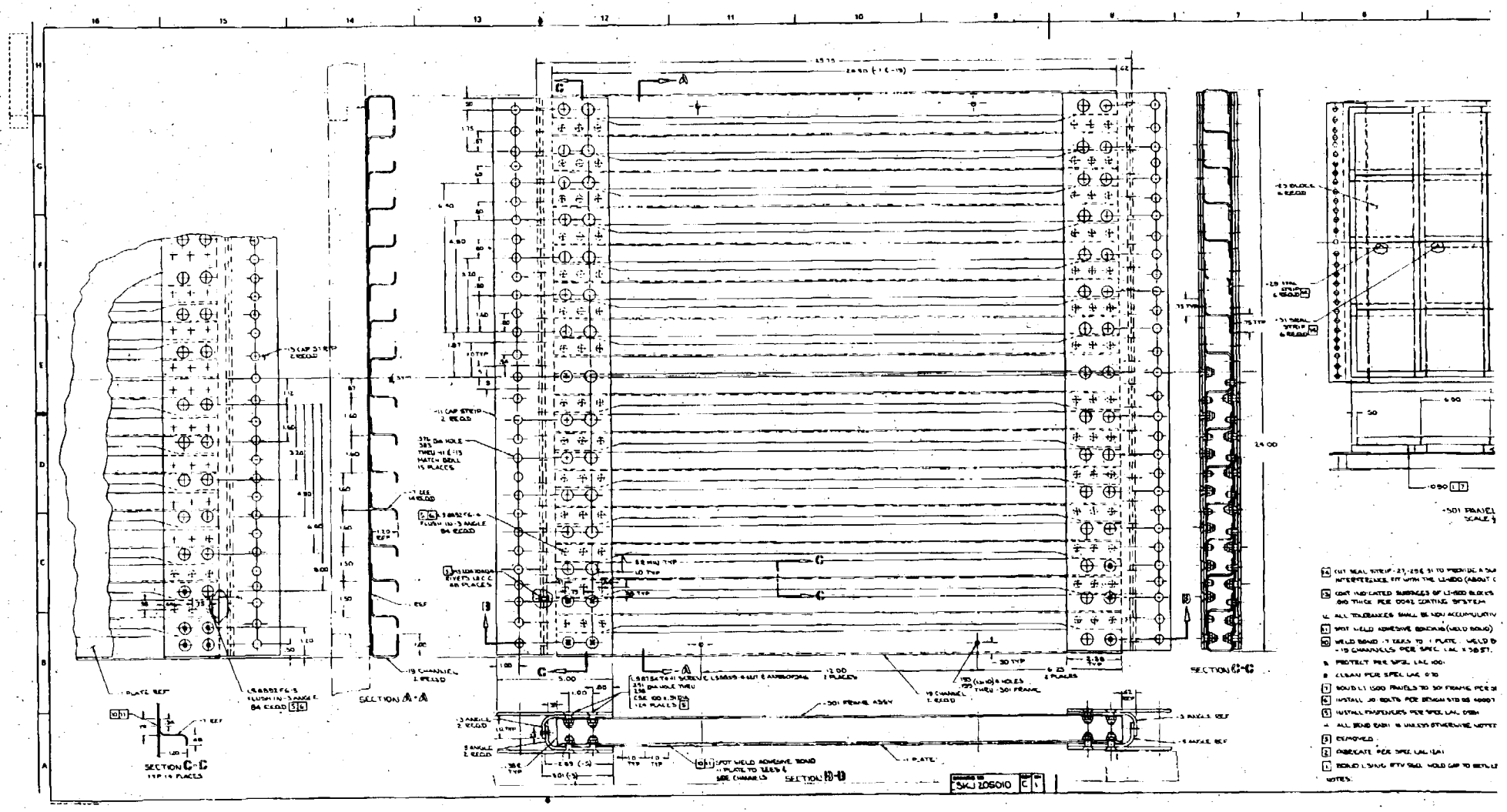

Preceding page blank 6-7

6-7.a

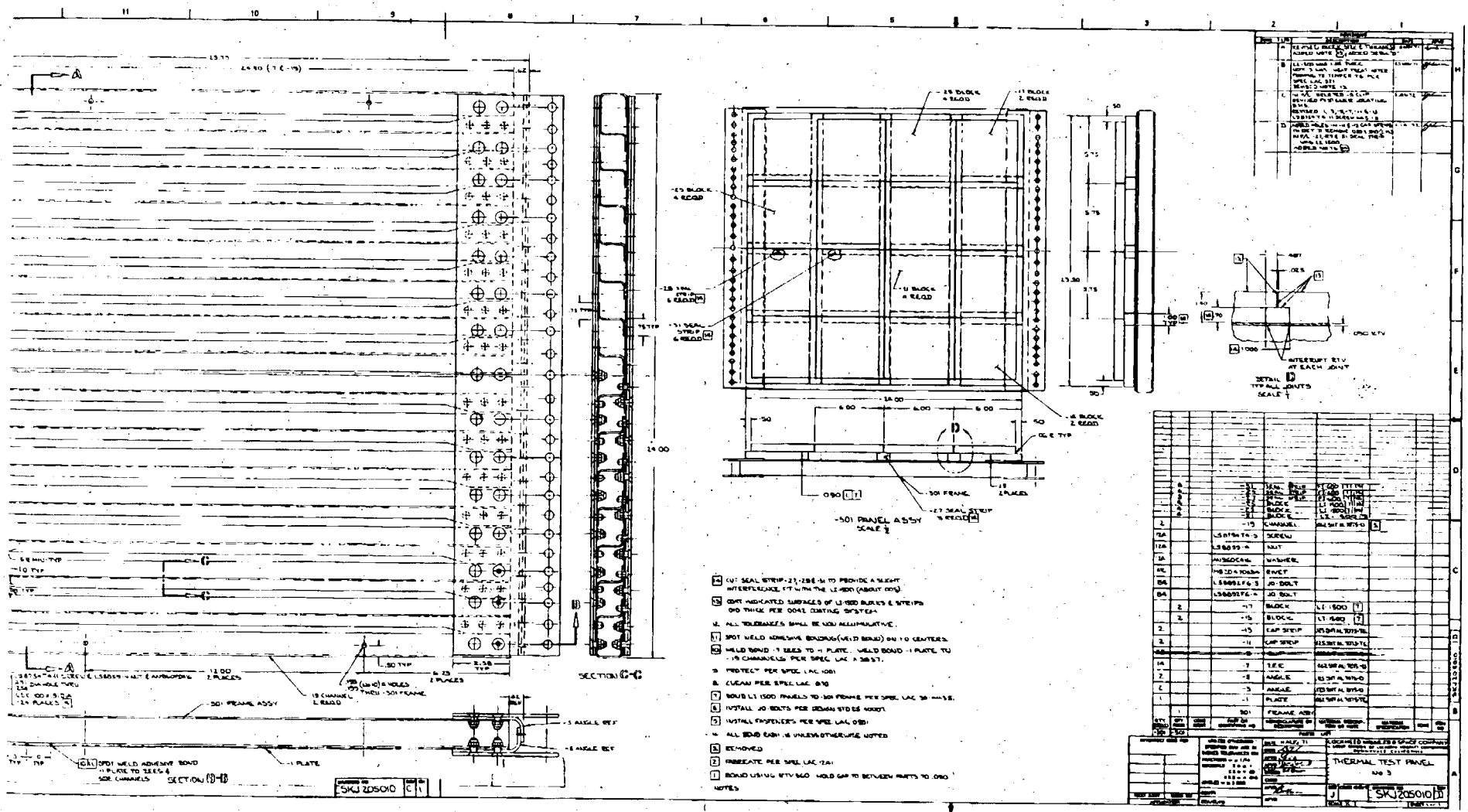

6-7-b

Fig. 6.1-3 Thermal Test Panel No. 3

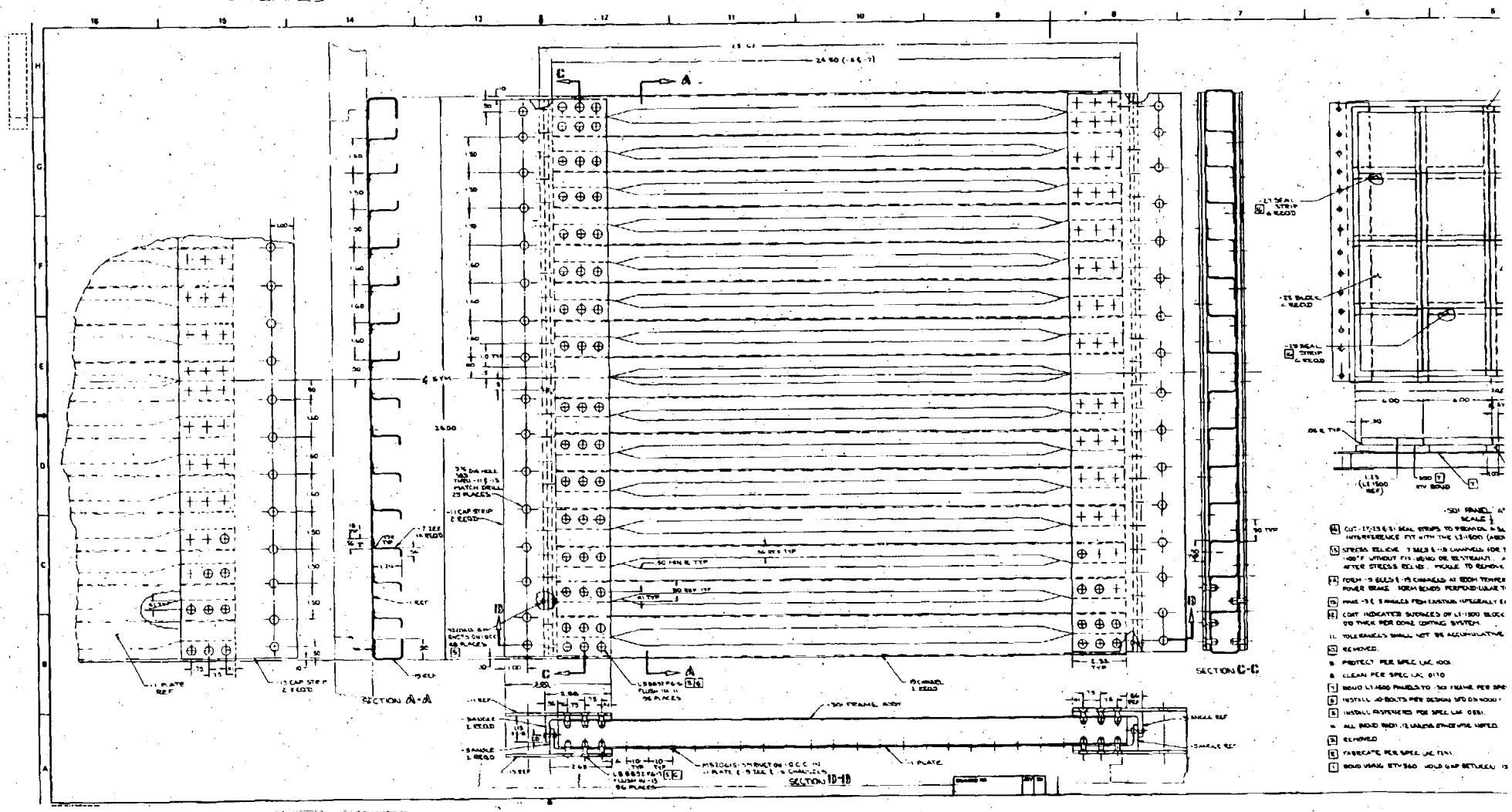

6-9-a

Preceding page blank

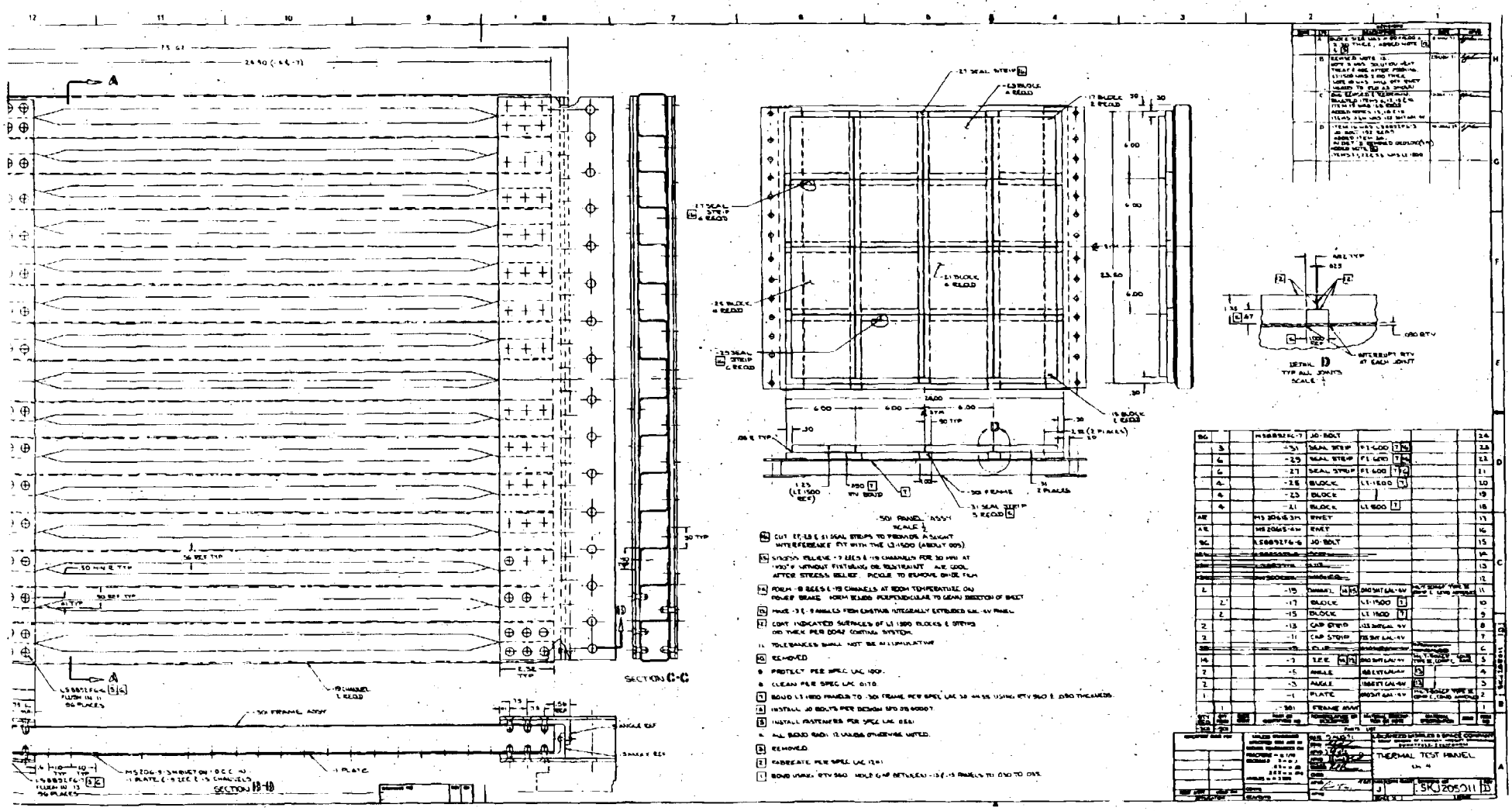

Fig. 6.1-4 Thermal Test Panel No. 4

Preceding page blank

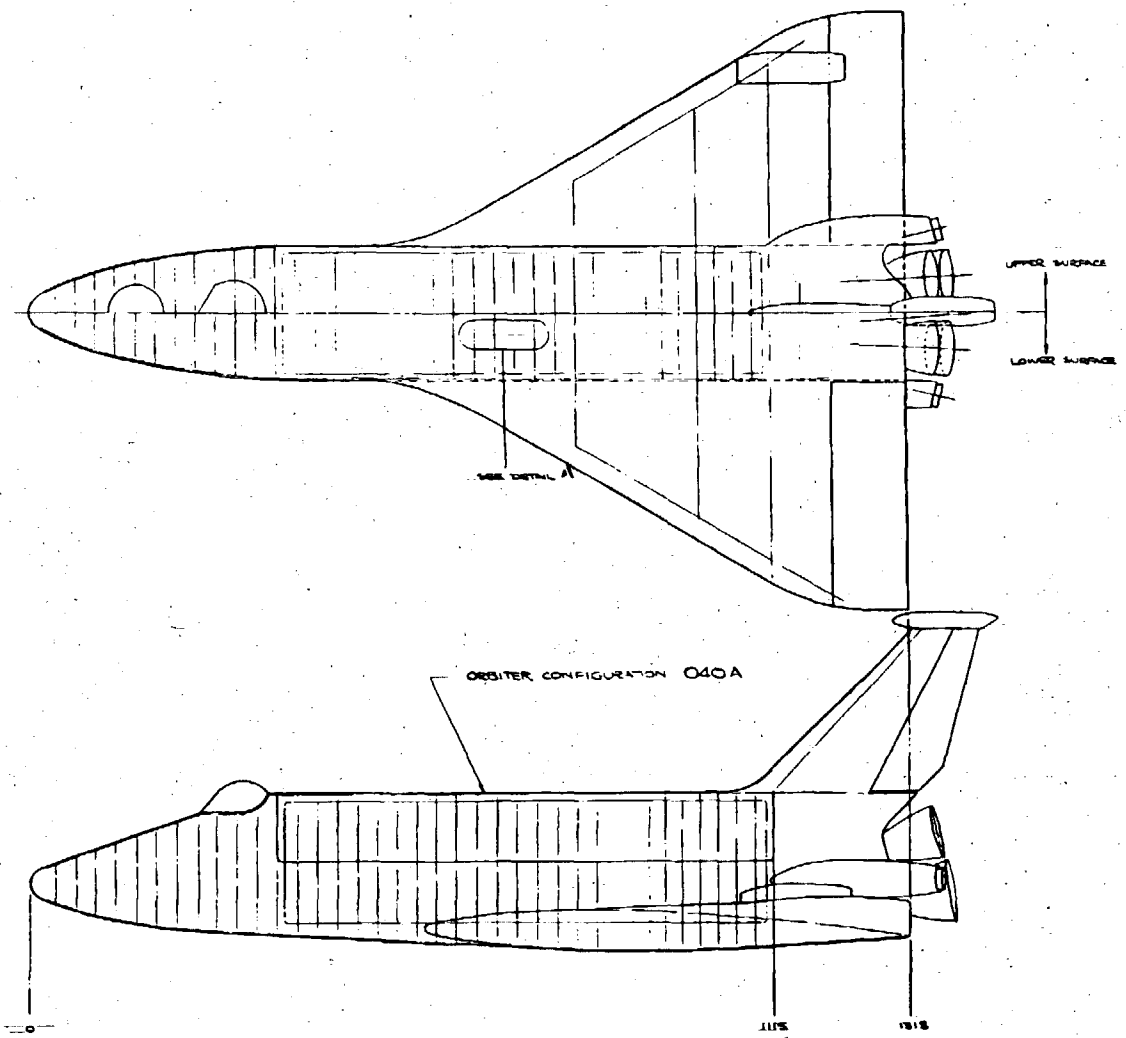

6-11

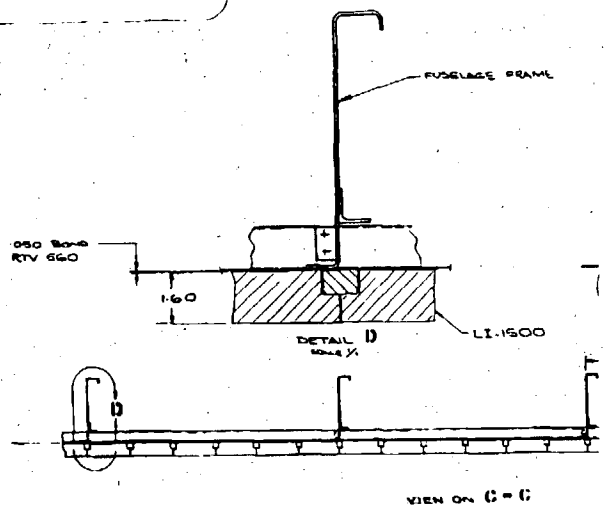

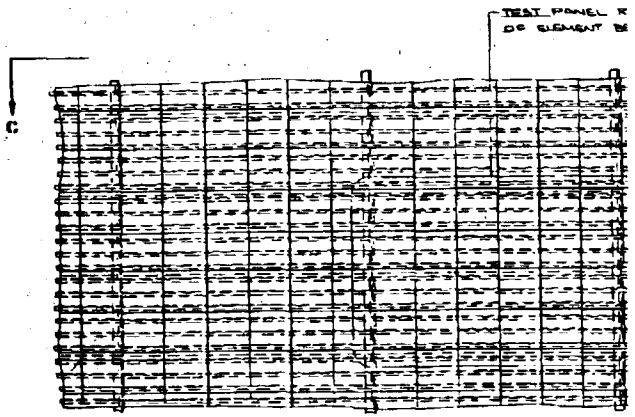

6.11-a

DETAIL A

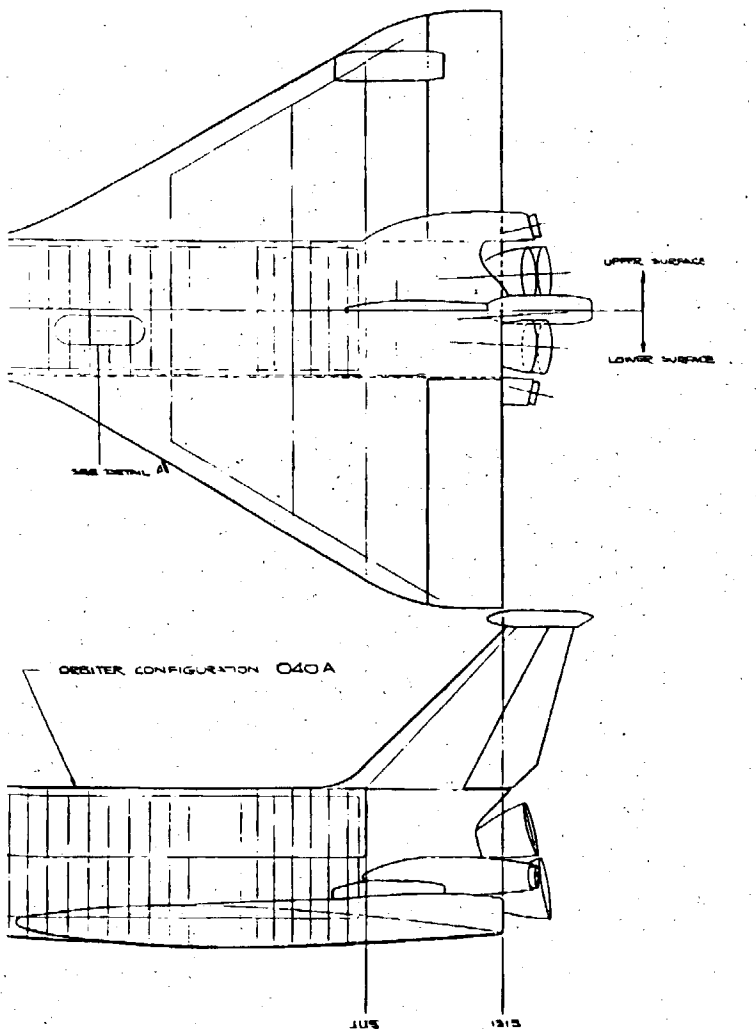

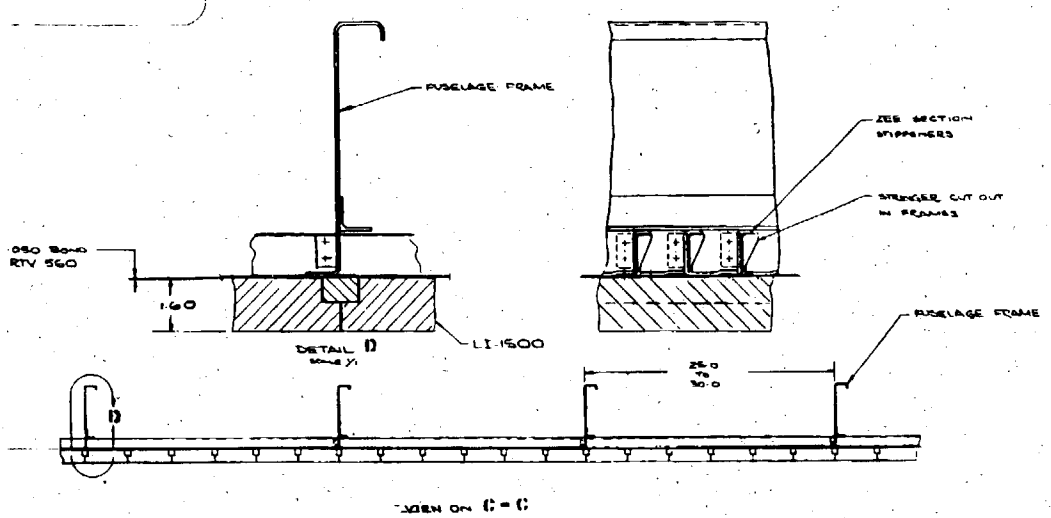

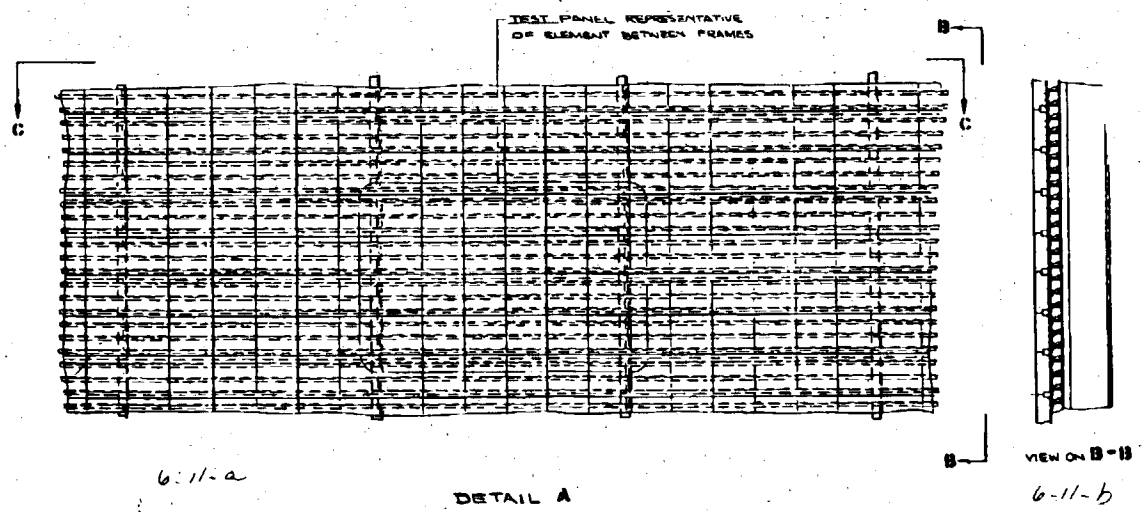

Fig. 6.1-5 Typical Application of Prototype Panels to Shuttle Vehicle

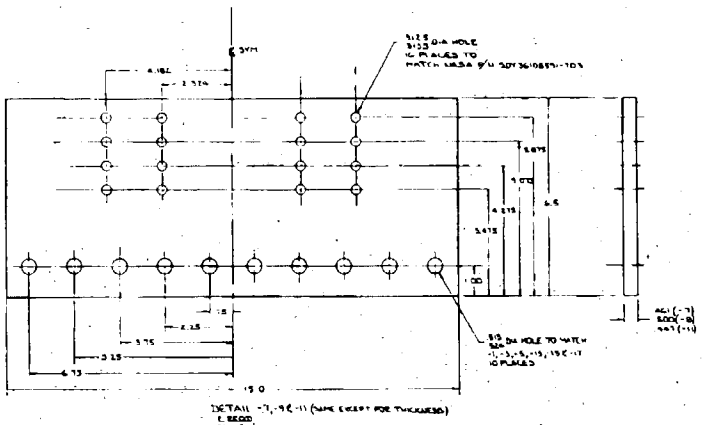

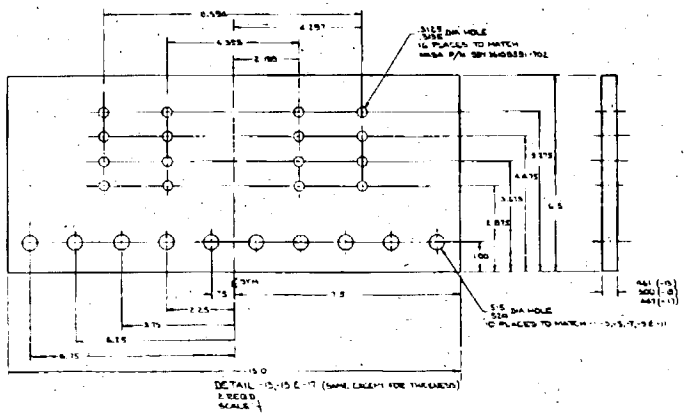

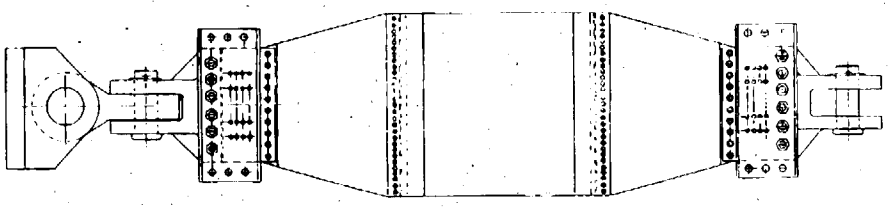

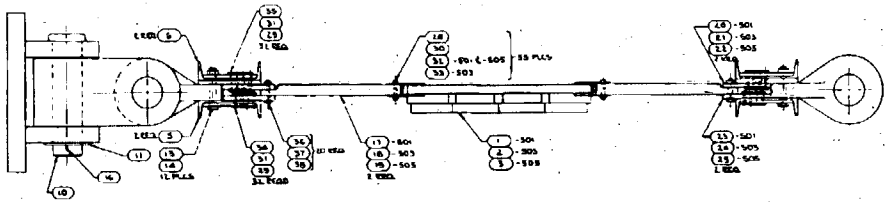

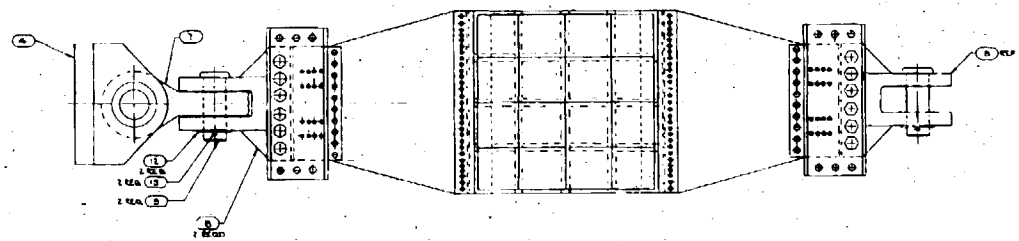

SKJ205023

Preceding page blank

6-13

6-13-a

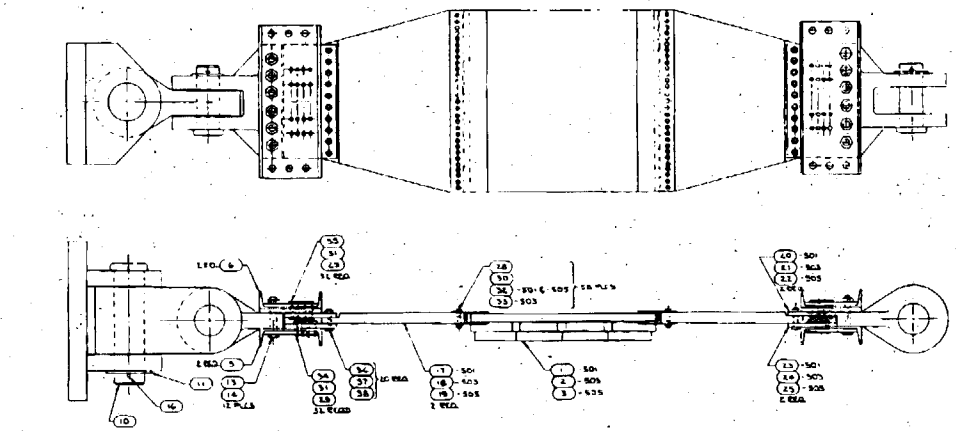

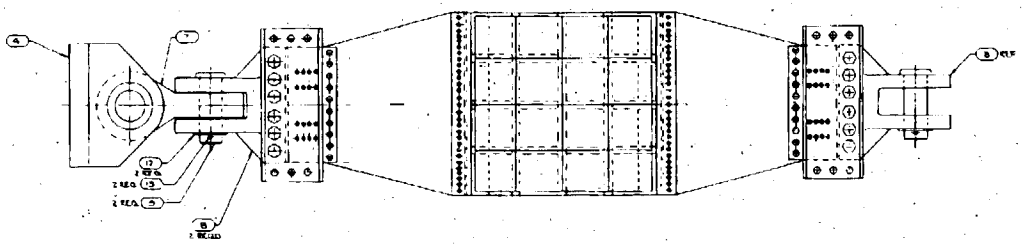

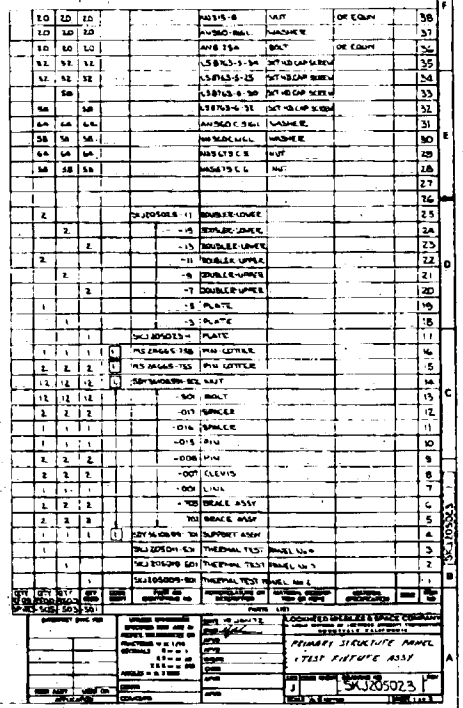

Fig. 6.1-6a Adapter Hardware for Prototype Panels

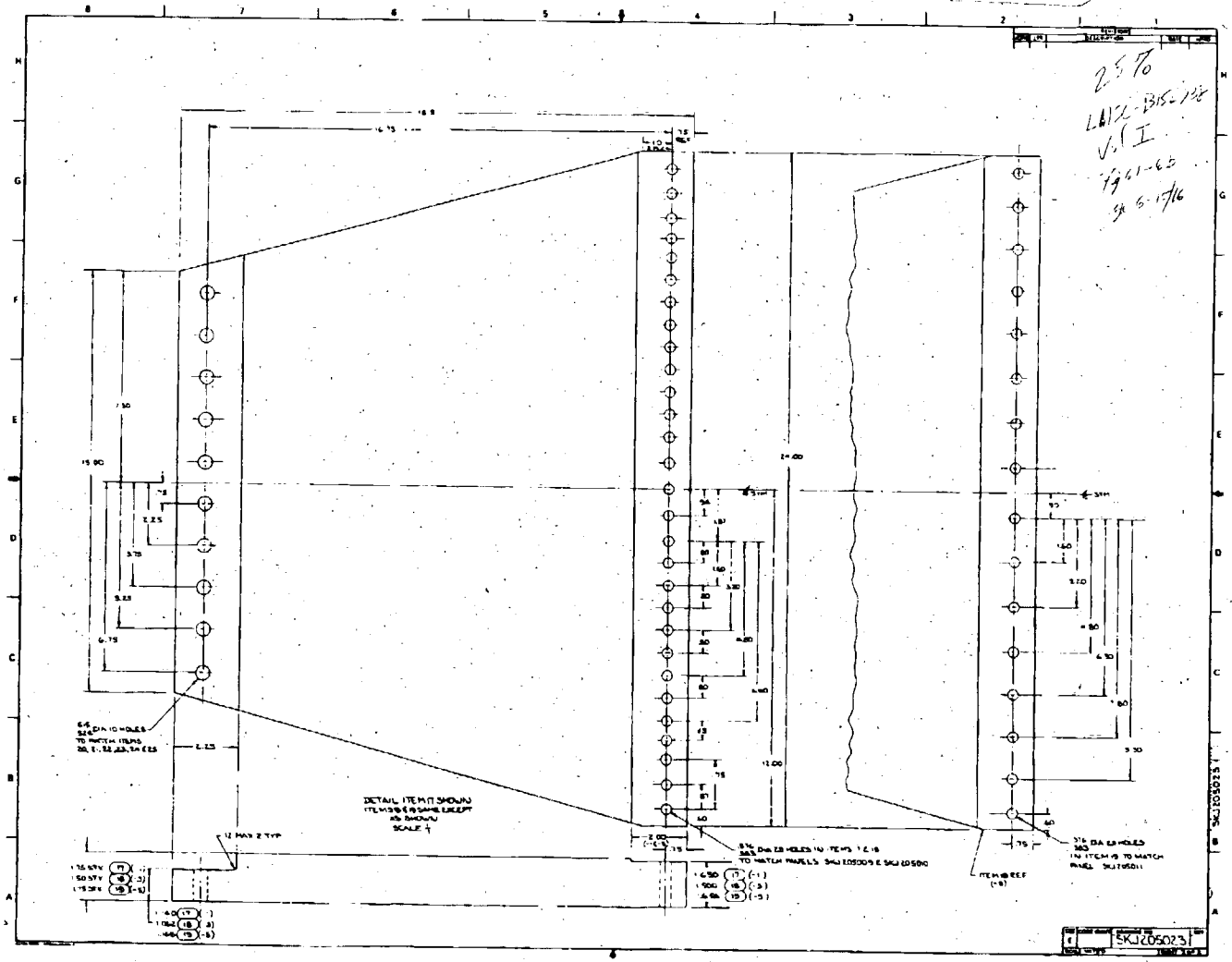

Preceding page blank

6-15

Fig. 6.1-6b Adapter Hardware for Prototype Panels

6-15a

As discussed in previous section, a new material has been introduced from the NAS 9-12137 efforts for use in the panel joints. This material has been designated FI-600 (flexible insulation -6 pcf) and consists of pure silica fibers. Representative confidence tests have been performed (Section 5.3) that resulted in the use of this material on the prototype panels. The reduced pressure conductivity closely approximates that of LI-1500, but the heat capacity is less due to the low density. Analyses have been performed that indicate increased substrate temperatures below the closure strip; the increase is less than $20^{\circ}F$ (Vol II, Section 3.2).

6.2 MATERIAL SPECIMENS

LMSC has manufactured four 12 x 12 x 2-in. LI-1500 tiles per month for each of the originally schedule months of the contract. These 24 tiles have been stored in the manufacturing facility and withdrawn to satisfy specific NASA/MSC specimen requirements. Table 6.2-1 lists the final disposition instructions received from the COR.

As noted in the preceding sections, the 0042 coating was baselined during October as the best current LI-1500 coating system. As shown in Table 6.2-1, the first deliverable specimens were shipped on 11 November. Therefore, all coated deliverables under this contract have been with the 0042 system.

A portion of the allocated tiles was lost during machining, coating, and bonding. This scrappage was due mainly to small sizes required on a portion of the deliverables and difficulties encountered in the arc-jet cylindrical specimens caused by the large number of thermocouples required. Therefore, the quantity of material used in some cases is more than the calculated volume of the deliverables.

Table 6.2-1

NAS 9-12083 DELIVERABLE MATERIAL SAMPLES

ORDER	RECEIVER	QTY	SIZE	COAT	T/Cs	TILES USED	SHIP DATE
1	MSC LeRC LaRC ARC U of W	1 ↓	12" x 12" x 2" ↓	TOP ↓	NO ↓	1.0 ↓	11/8 ↓
2	MSC MSC	12* 12*	6" x 1" x 1" 6" x 1" x 1"	5 SIDES NO	NO NO	1.0 0.5	12/3 12/3
3	MSC MSC	3 3	2" DIA x 2" 2" DIA x 2"	TOP & SIDES TOP & SIDES	NO YES	0.75 1.25	1/14
	BATTELLE	1	10" x 6" x 2"	TOP	NO	0.5	12/15
4	BATTELLE	3 1 6 3 3	12" x 12" x 2" 12" x 12" x 1" 6" x 1" x 1" 4" DIA x 2" 4" DIA x 2"	TOP ↓ TOP & SIDES TOP & SIDES	NO ↓ YES	3.0 0.5 0.25 1.0 1.25	1/15 ↓
5	MSC U of W MSFC LaRC ARC LeRC	3 1 ↓	12" x 12" x 2" ↓ 12" x 6" x 2" 12" x 6" x 2"	TOP ↓ TOP NO	NO ↓	3.0 1.0 ↓ 0.5 0.5	2/1 ↓
6	BELL	10	3.5" x 3.5" x 0.75"	TOP	NO	1.0	2/15
7	LaRC ARC	12 6 6	1" x 1" x 1" 3.5" x 3.5" x 0.875" 6" x 6" x 2"	5 SIDES 5 SIDES 5 SIDES	NO YES YES	0.25 0.50 2.0	3/1 ↓

*SIX WATERPROOF TREATMENT; SIX WITHOUT

D07155

Appendix A-1

STRESS – STRAIN CURVES

AND

EXAMPLE CALCULATIONS FOR

SECTION 4

Prepared by: B. VAN WEST	Date 10 DEC 71	LOCKHEED MISSILES & SPACE COMPANY A GROUP DIVISION OF LOCKHEED AIRCRAFT CORPORATION	Page	Temp.	Perm.
Checked by: J. A. DeRuntz	Date	Title LI-1500 MODULUS (EXAMPLE CALCULATION)	Model		
Approved by: J. A. DeRuntz	Date		Report No.		

COMPRESSION:

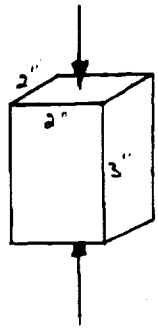

$A = 4\ in^2$. $\sigma = P/A$

Specimen TT29-1, $P_{max} = 720$ lb.

$\sigma_{max} = 720/4 = 180$ psi.

Modulus (see Fig. A4) $E_c = \frac{d\sigma}{d\epsilon} = \frac{500/4}{(9.93/3)\times 10^{-3}} = 37{,}800$ psi

---

TENSION:

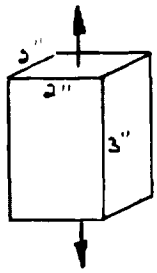

$A = 4\ in^2$. $\sigma = P/A$

Specimen TT28-4, $P_{max} = 342$ lb.

$\sigma_{max} = 342/4 = 85.5$ psi.

Modulus (see Fig. A-1) $E = \frac{d\sigma}{d\epsilon} = \frac{350/4}{(4.86/3)\times 10^{-3}} = 54{,}000$ psi

---

TENSION (High Temperature):

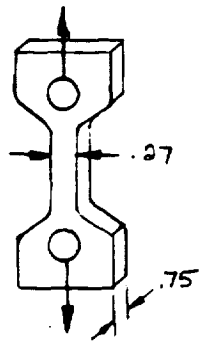

$A = .203\ in^2$. $\sigma = P/A$

Specimen TT449, $P_{max} = 33.35$ lb.

$\sigma_{max} = \frac{33.35}{.203} = 164$ psi

Modulus (see Fig. 4.2-6) $E = \frac{d\sigma}{d\epsilon} = \frac{(120-60)}{(4.2-.45)\times 10^{-3}} = 16{,}000$ psi

FORM LMSC 362 B-2

Prepared by: B. VAN WEST	Date 13 DEC 71	LOCKHEED MISSILES & SPACE COMPANY A GROUP DIVISION OF LOCKHEED AIRCRAFT CORPORATION	Page	Temp.	Perm.
Checked by: J. A. DeRuntz	Date	Title LI-1500 SHEAR MODULUS (EXAMPLE CALCULATION)	Model TPS		
Approved by: J. A. DeRuntz	Date		Report No.		

SHEAR:

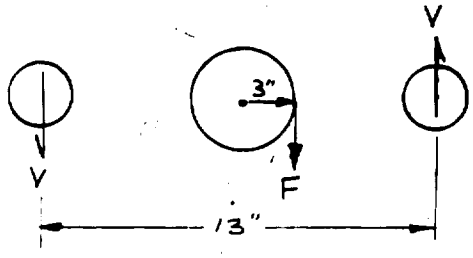

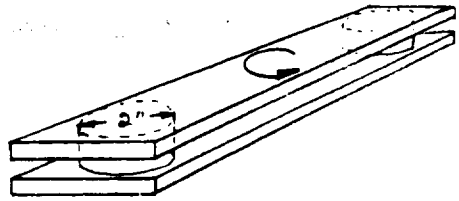

$$13V = 3F$$

$$V = \frac{3}{13}F$$

$$\gamma_{AV} = \frac{V}{A} = \frac{3/13\,F}{\pi(1)^2} = \frac{F}{13.6}$$

$$\gamma_{max} = \frac{15}{13}\gamma_{AV} = \frac{15}{13}\frac{F}{13.6} = \frac{F}{11.8}$$

Specimen 111,

dia. = 2 in., h = .375 in.

max. load F = 350 lb.

$$\gamma_{max} = \frac{350}{11.8} = 29.6 \text{ psi}.$$

Modulus (see Fig. A-8): $E_s = \frac{d\gamma_{av}}{d\delta_{av}}$ = [illegible]

= 6370 psi.

FORM LMSC 362 B-2

Prepared by: B. VAN WEST	Date 9 DEC '71	LOCKHEED MISSILES & SPACE COMPANY A GROUP DIVISION OF LOCKHEED AIRCRAFT CORPORATION	Page Temp. Perm.
Checked by: J. A. DeRuntz	Date	Title COATING (0025) MODULUS (EXAMPLE CALCULATION)	Model TPS
Approved by: J. A. DeRuntz	Date		Report No.

FROM SPECIMEN 3 CANTILEVER BENDING TEST,

$L = 1.12$ IN.
$t = .036$ IN.
$w = .51$ IN.

$$\sigma = \frac{6PL}{wt^2}$$

$$\epsilon = \frac{3\Delta t}{2L^2}$$

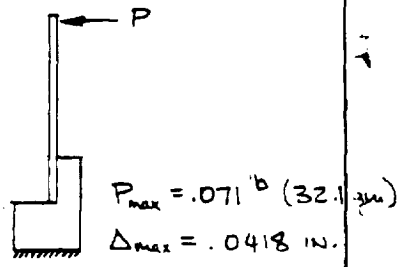

$$\sigma = \frac{(6)(.071)(1.12)}{(.51)(.036)^2} = 722 \text{ psi (max.)}$$

$$\epsilon = \frac{(3)(.0418)(.036)}{(2)(1.12)^2} = 1.8 \times 10^{-3} \text{ IN/IN. (max.)}$$

Modulus (see Fig. A-9)

$$E = \frac{d\sigma}{d\epsilon} = \frac{577-155}{(1677-515)\times 10^{-6}} = .397 \times 10^6 \text{ psi.}$$

FORM LMSC 382 B-2

LI-1500 TENSION TEST

ROOM TEMPERATURE

AVERAGE MODULUS, $E = 56{,}400$ PSI (PARALLEL)

$E = 5{,}780$ PSI (NORMAL)

AVERAGE MAX. STRESS, $\sigma = 78$ PSI (PARALLEL)

$\sigma = 14.5$ PSI (NORMAL)

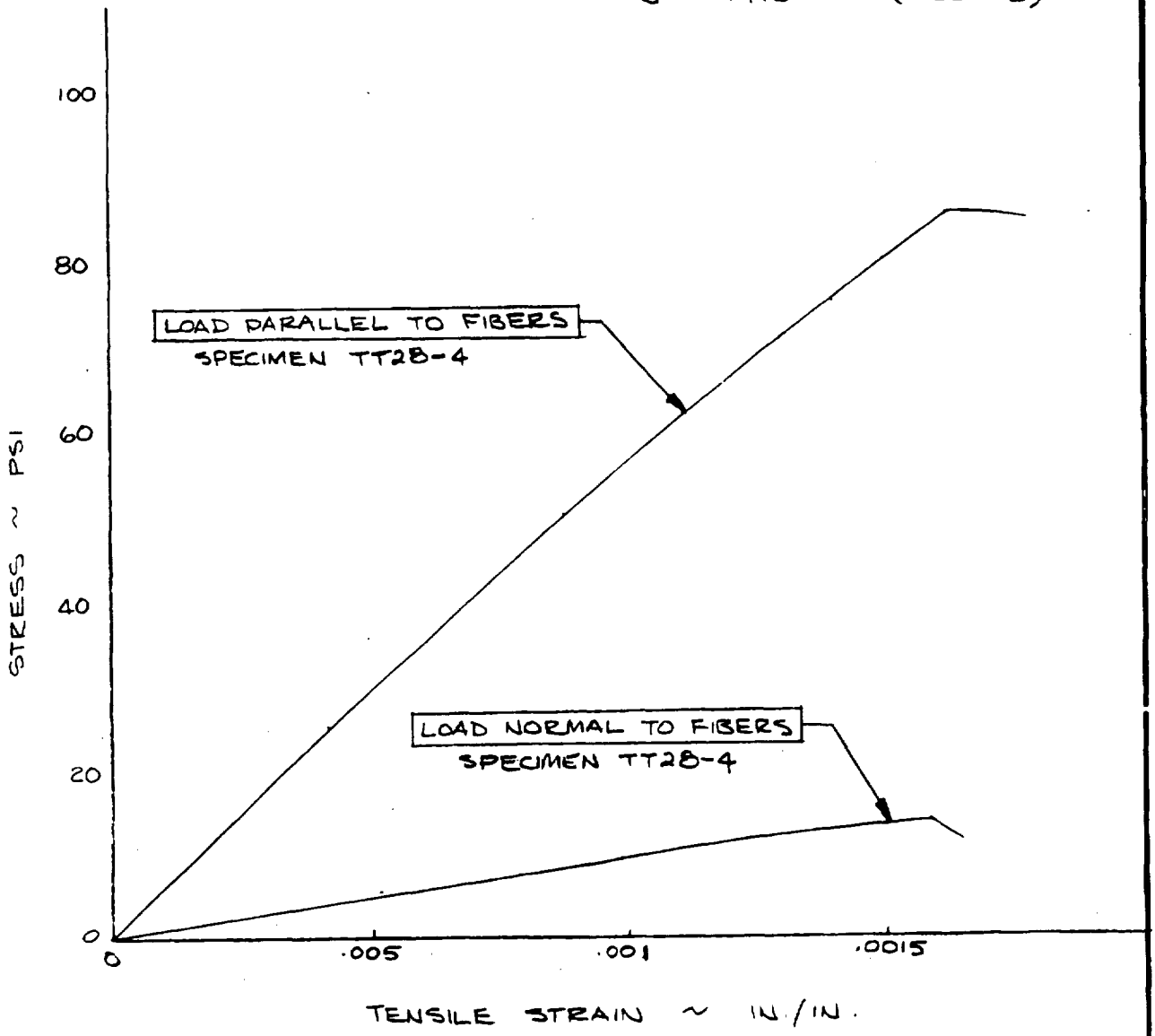

FIG. A-1 STRESS-STRAIN CURVES

LI-1500 TENSION TEST

THERMALLY & ACOUSTICALLY CYCLED SPECIMENS

AVERAGE MODULUS, E = 91,300 PSI (PARALLEL, 10 CYCLES)
E = 89,500 PSI (PARALLEL, 20 CYCLES)
E = 10,073 PSI (NORMAL)

AVERAGE MAX. STRESS, σ = 46.8 PSI (PARALLEL, 10 CYCLES)
σ = 56 PSI (PARALLEL, 20 CYCLES)
σ = 14.3 PSI (NORMAL)

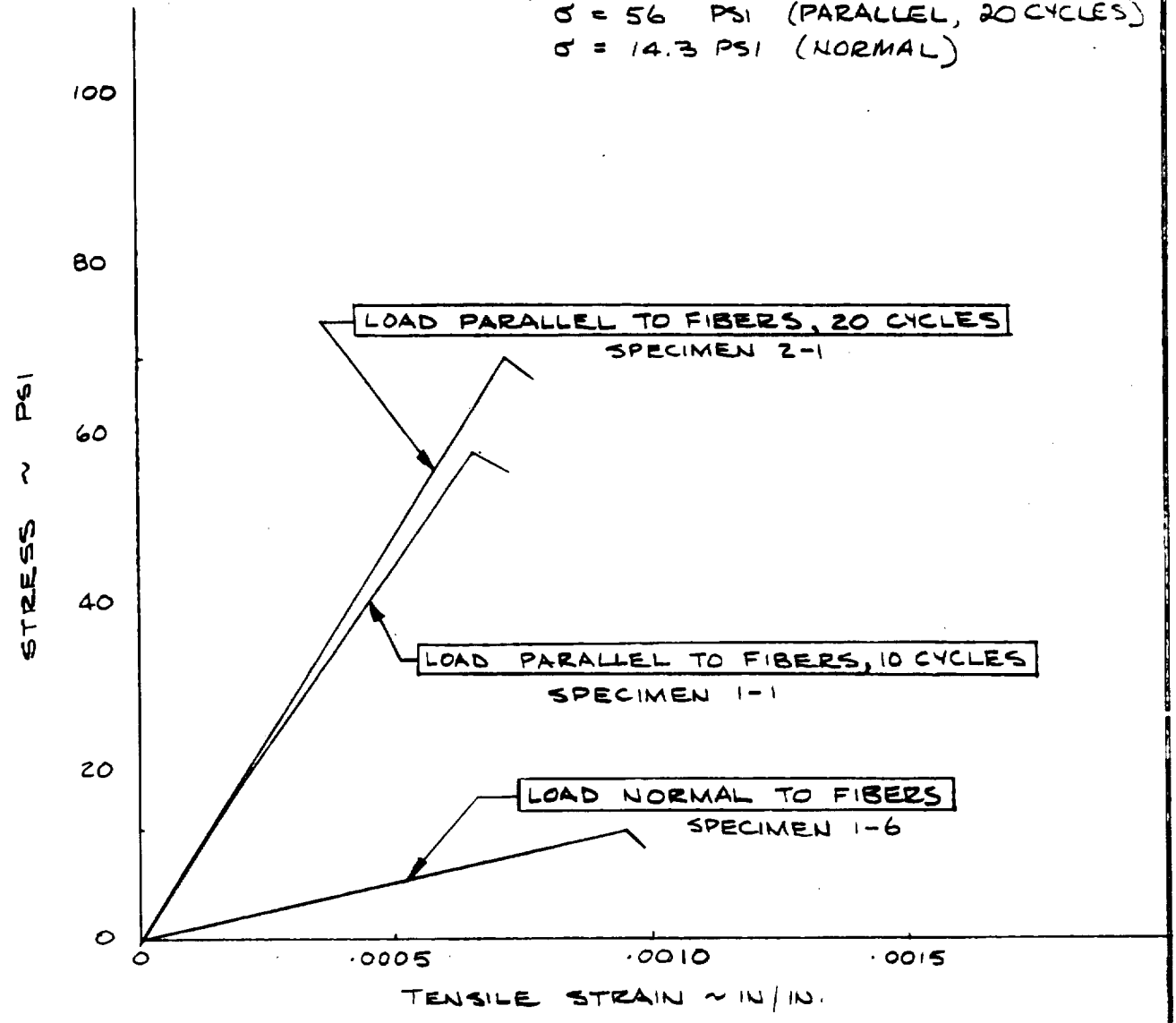

FIG. A-2 STRESS - STRAIN CURVES

LI-1500 TENSION TEST

AT -150° F

AVERAGE MODULUS, E = 49,575 PSI (PARALLEL)
AVERAGE MAX. STRESS, σ = 91 PSI (PARALLEL)

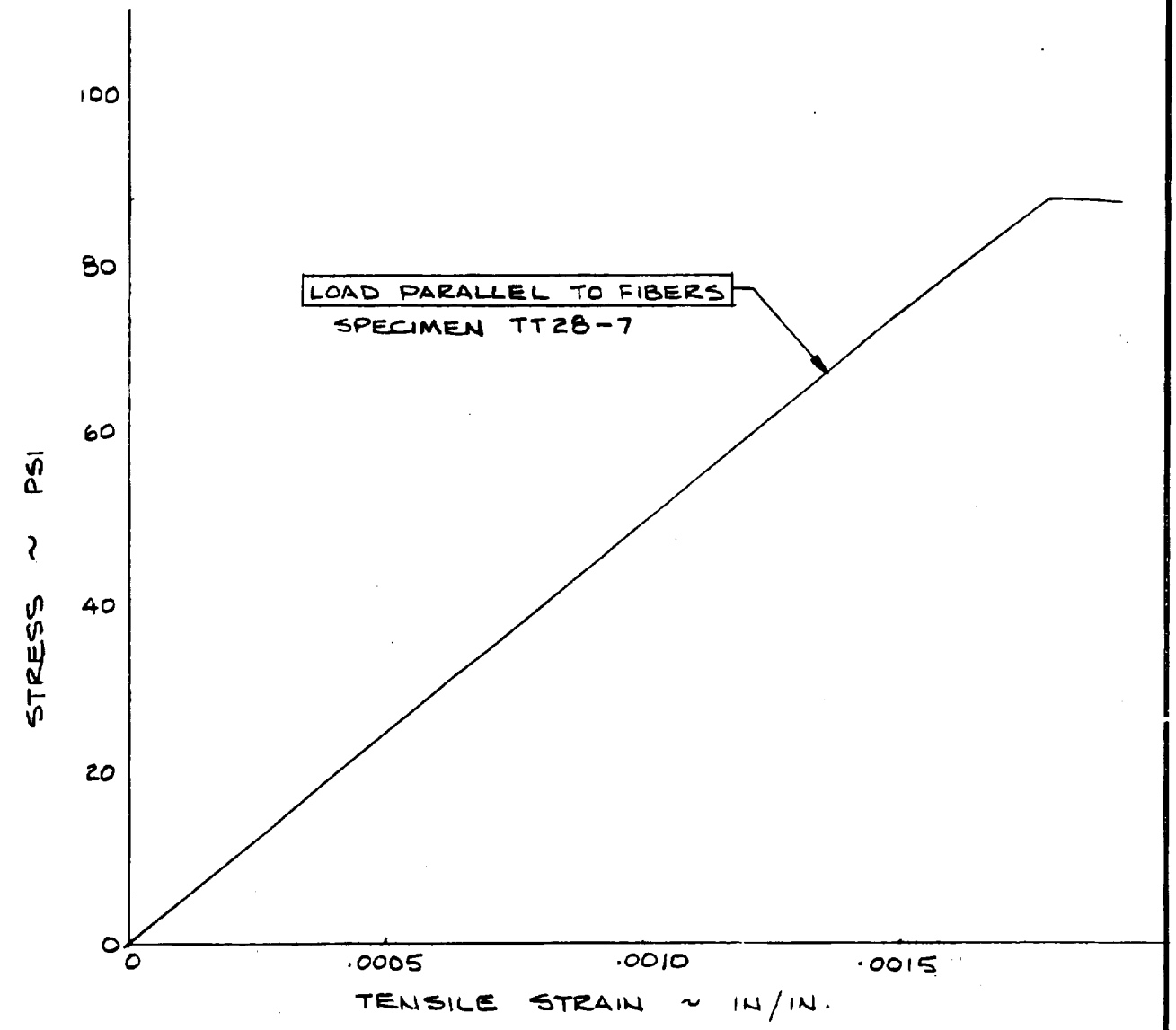

FIG A-3 STRESS - STRAIN CURVE

LI-1500 COMPRESSION TEST

ROOM TEMPERATURE

AVERAGE MODULUS, E = 39,700 PSI (PARALLEL)
E = 4,070 PSI (NORMAL)
AVERAGE MAX. STRESS, σ = 174 PSI (PARALLEL)
σ = 42 PSI

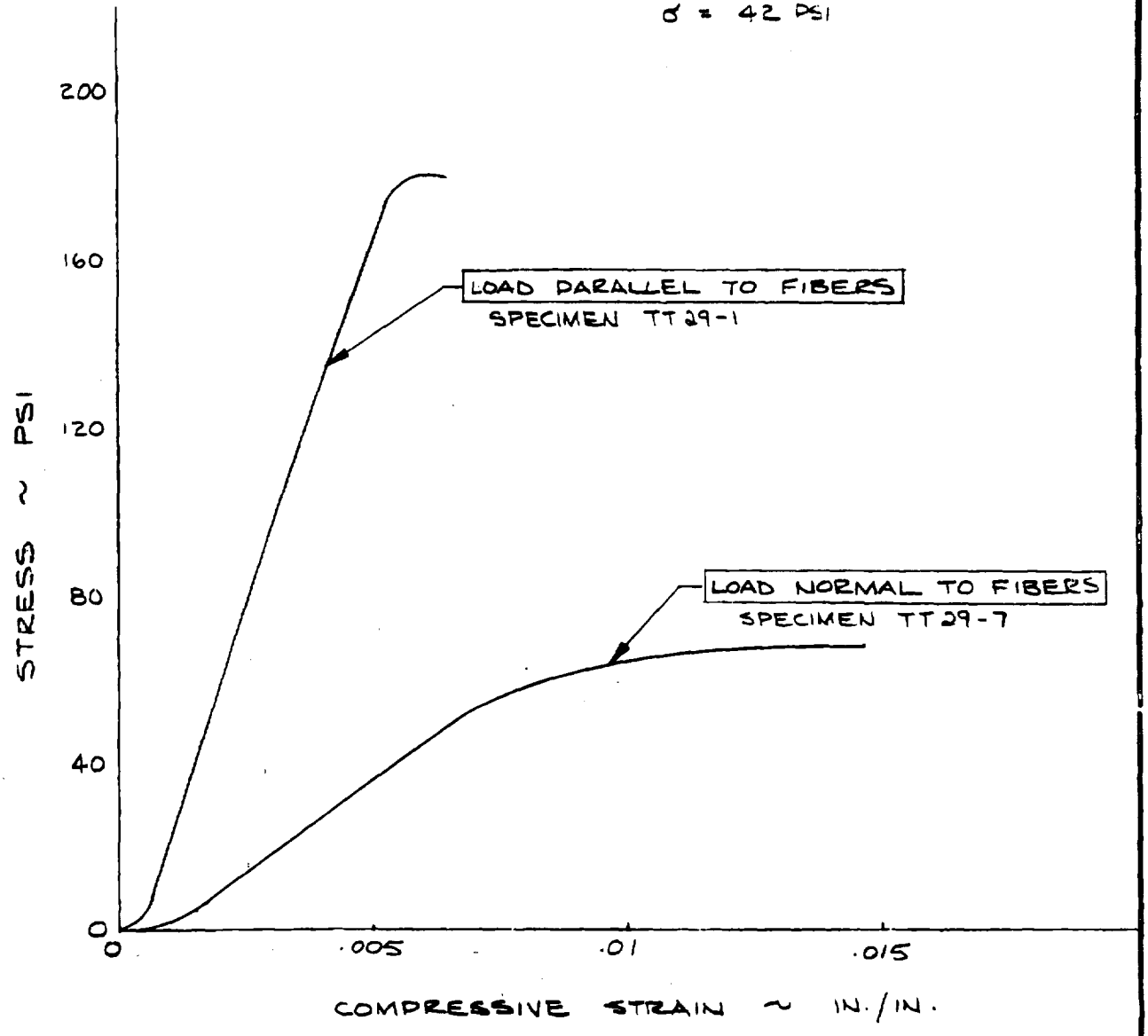

FIG. A-4 STRESS - STRAIN CURVES

LI-1500 COMPRESSION TEST

ROOM TEMPERATURE
WITH COATING ON ONE 2 x 3 IN. FACE

AVERAGE MODULUS, E = 60,300 PSI (PARALLEL)
AVERAGE MAX. STRESS, σ = 167 PSI (PARALLEL)

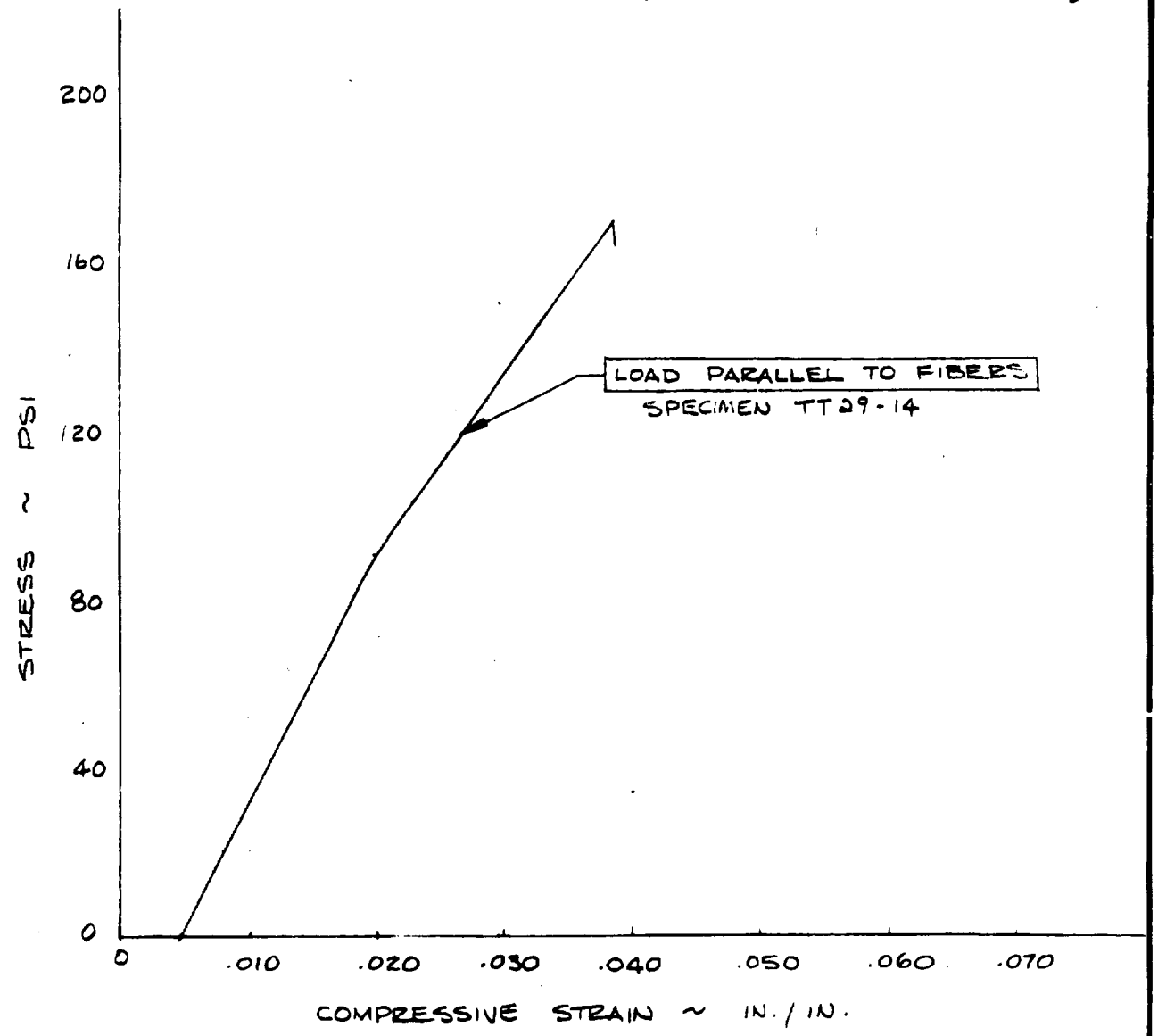

FIG. A-5 STRESS - STRAIN CURVE

LI-1500 COMPRESSION TEST

THERMALLY & ACOUSTICALLY CYCLED SPECIMENS.

AVERAGE MODULUS, E = 84,700 PSI (PARALLEL)
E = 10,615 PSI (NORMAL)
AVERAGE MAX. STRESS, σ = 234 PSI (PARALLEL)
σ = 77 PSI (NORMAL)

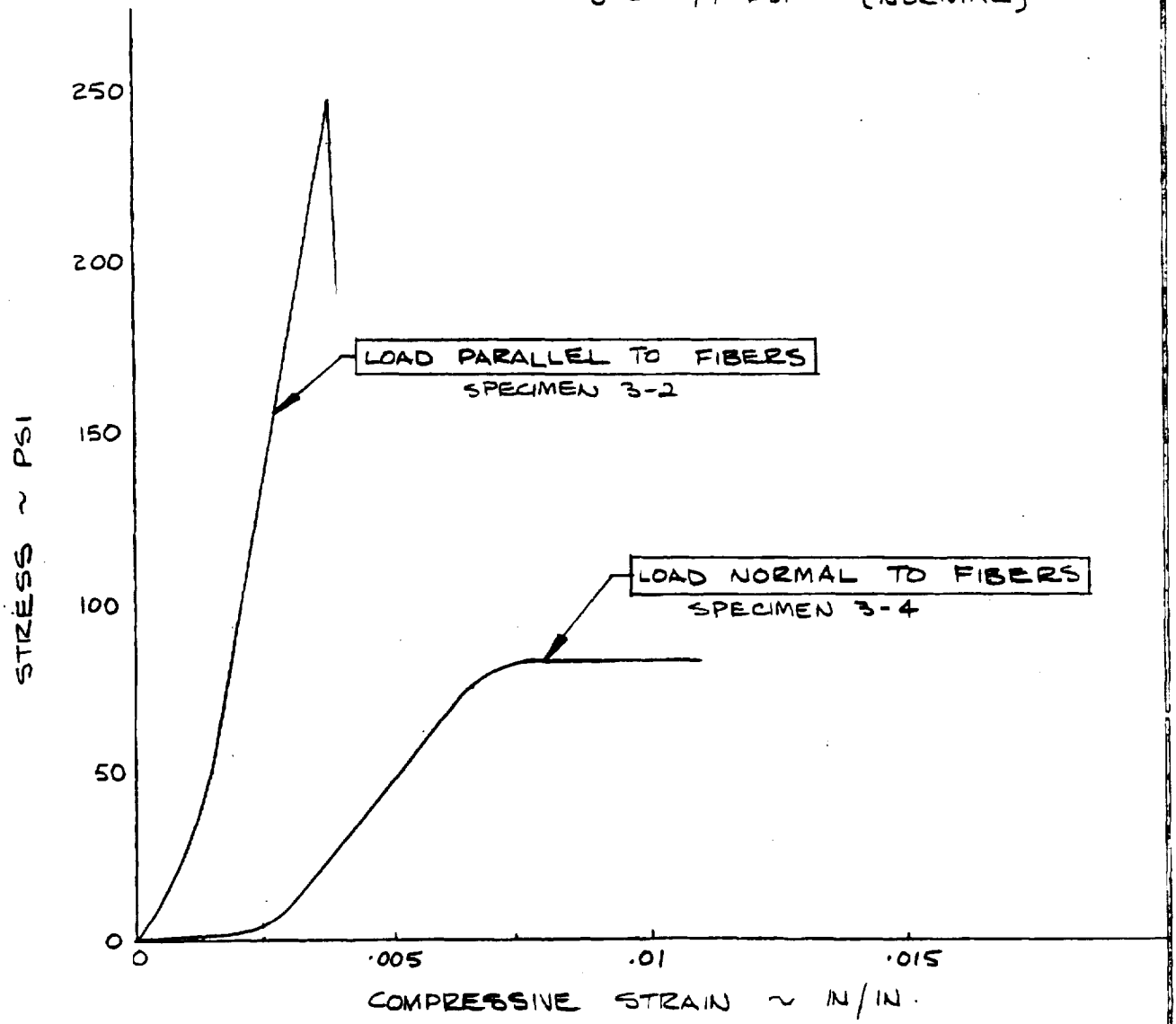

FIG. A-6 STRESS-STRAIN CURVES.

LI-1500 COMPRESSION TEST

AT 2300° F

AVERAGE MODULUS, E = 2140 PSI (PARALLEL)
E = 219 PSI (NORMAL)
AVERAGE MAX. STRESS, σ = 40 PSI (PARALLEL)
σ = 4 PSI (NORMAL)

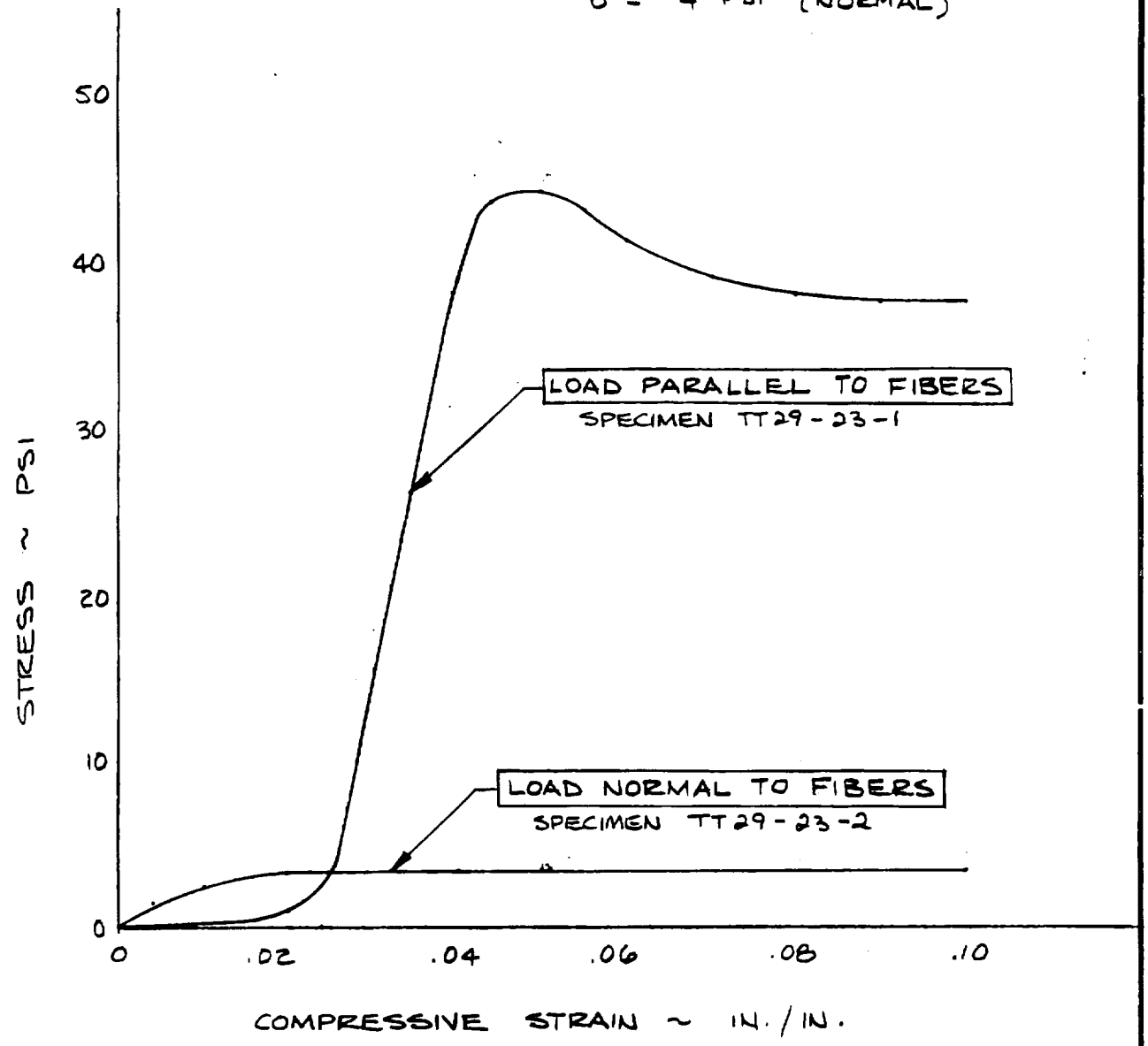

FIG. A-7 STRESS-STRAIN CURVES

LI-1500 SHEAR TEST

ROOM TEMPERATURE

AVERAGE MODULUS, $E = 31,900$ psi (PARALLEL)
$E = 6,605$ psi (NORMAL)

AVERAGE MAX. STRESS, $\tau = 75$ psi (PARALLEL)
$\tau = 87.5$ psi (NORMAL)

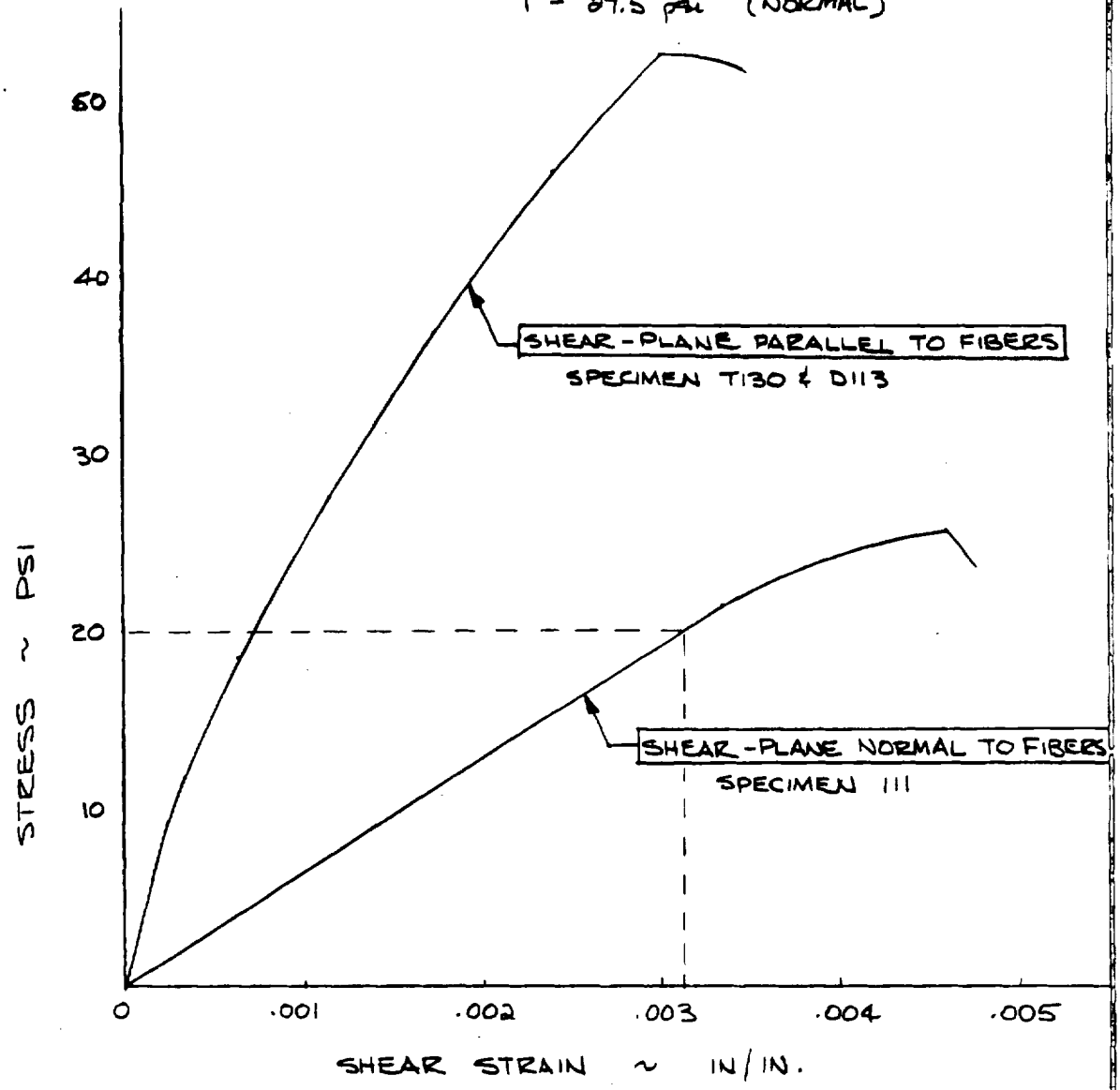

FIG. A-8 STRESS-STRAIN CURVES

COATING (0025) FLEXURE TEST

AVERAGE MODULUS, $E = 0.96 \times 10^6$ PSI.
AVERAGE MAX. STRESS, $\sigma = 480$ PSI.

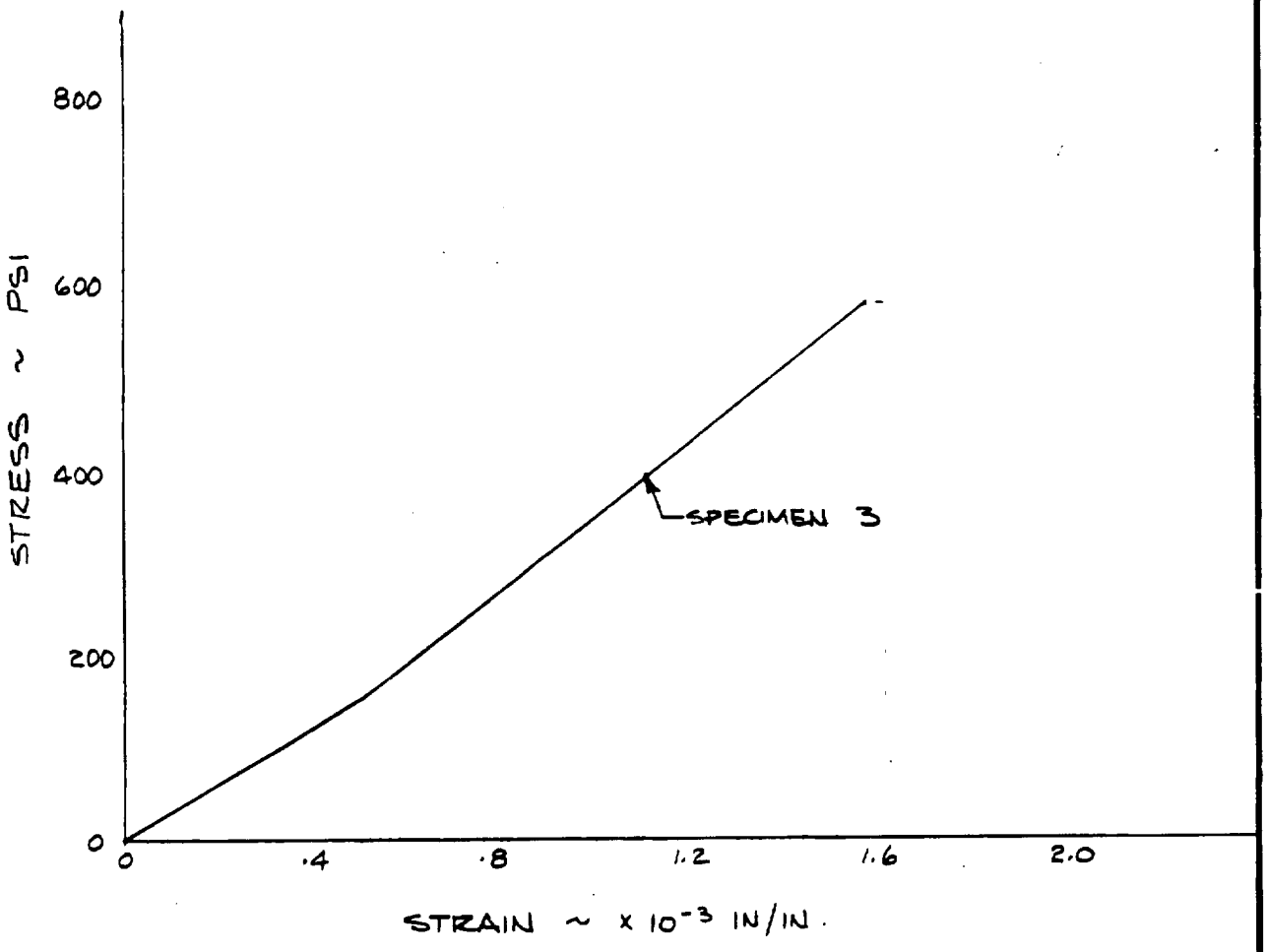

Fig. A-9 STRESS - STRAIN CURVE